

General Relativity

Volker Perlick (perlick@zarm.uni-bremen.de)

Winter Term 2020/21

Tue 12:15–13:45 (Lectures, per Zoom)

Thu 14:15–15:45 (Lectures, per Zoom)

Fri 14:15–15:45 (Tutorials, per Zoom)

Complementary Reading:

W. Rindler: “Relativity” Oxford UP (2001)

emphasis is on physical understanding

L. Hughston, P. Tod: “An Introduction to General Relativity” Cambridge UP (1990)

emphasis is on calculations

H. Stephani: “General Relativity” Cambridge University Press (1982)

good compromise between physical understanding and mathematical formalism; also available in German

C. Misner, K. Thorne, J. Wheeler: “Gravitation” Freeman (1973)

voluminous standard text-book; obviously outdated in view of experiments

N. Straumann: “General Relativity and Relativistic Astrophysics” Springer (1984)

mathematically challenging; also available in German

R. Wald: “General Relativity” University of Chicago Press (1984)

mathematically challenging

Contents

1	Historic Introduction	2
2	Special relativity	5
2.1	Special relativistic spacetime	5
2.2	Index notation	11
2.3	Lorentz transformations	12
2.4	Kinematics and dynamics of particles	15
2.5	Classical photons	22
2.6	Continuum mechanics	27
2.7	Electrodynamics	30
3	Heuristic approach to general relativity	38
4	Basic concepts of differential geometry	49
4.1	Manifolds	49
4.2	Covariant derivatives and curvature	61
4.3	Pseudo-Riemannian metrics	70
5	Foundations of general relativity	76
5.1	General-relativistic spacetimes	76
5.2	The rule of minimal coupling	80
5.3	Einstein's field equation	82
5.4	The Newtonian limit	87
6	Schwarzschild solution	90
6.1	Derivation of the Schwarzschild solution	91
6.2	Lightlike geodesics in the Schwarzschild solution	100
6.3	Timelike geodesics in the Schwarzschild solution	105
6.4	Schwarzschild black holes	112
6.5	Shadow of a Schwarzschild black hole	121
6.6	The interior Schwarzschild solution	128
7	Gravitational waves	134
7.1	The linearisation of Einstein's field equation	134
7.2	Plane-harmonic-wave solutions to the linearised field equation without sources	138
7.3	Relating gravitational waves to the source	143
7.4	The Hulse-Taylor pulsar	154
7.5	Gravitational wave detectors	157
7.6	The LIGO observations	163

1 Historic Introduction

- 1905 A. Einstein invents special relativity according to which signals cannot move at superluminal speed. This is in conflict with Newtonian gravity which predicts an action-at-a-distance. Einstein immediately sees the need for a new theory of gravity which is in agreement with the basic ideas of relativity. Formulating this new theory, which is then called general relativity, takes him 10 years.
- 1907 A. Einstein formulates the equivalence principle (“a gravitational field is equivalent to an acceleration”, “a homogeneous gravitational field is transformed away in a freely falling elevator”) which will then become a cornerstone of general relativity.
- 1908 H. Minkowski introduces a four-dimensional formulation of special relativity, combining three-dimensional space and one-dimensional time into the four-dimensional “spacetime continuum” or “spacetime” for short.
- 1915 A. Einstein presents the final formulation of general relativity with the gravitational field equation (“Einstein’s field equation”). By solving this equation approximately he can explain the anomalous perihelion precession of Mercury (43 arcseconds per century, known since U. LeVerrier, 1855) and he predicts a deflection of light by the Sun (1.7 arcseconds for a light ray grazing the surface of the Sun).
- 1916 K. Schwarzschild finds the spherically symmetric static solution of Einstein’s field equation in vacuum (“Schwarzschild solution”) which has a coordinate singularity at the “Schwarzschild radius” $r_S = 2Gm/c^2$ (G = gravitational constant, c = vacuum speed of light, m = mass of the spherically symmetric body). The same solution is found a few weeks later independently by J. Droste.
- 1916 A. Einstein predicts the existence of gravitational waves, based on the linearised field equation.
- 1919 A. Eddington verifies Einstein’s prediction of light deflection by the Sun during a Solar eclipse.
- 1922 A. Friedmann finds expanding cosmological models as solutions to Einstein’s field equation with appropriate matter models (“Friedmann solutions”).
- 1927 G. Lemaître advocates the idea that the universe began with a cosmological singularity (ironically called “big bang” by Fred Hoyle in the 1960s) and is expanding since.
- 1929 E. Hubble finds a linear relation between the redshift and the distance of galaxies (usually interpreted as a Doppler effect and, thereupon, as evidence for the expansion of the universe). The same relation was found already two years earlier by Lemaître. It is properly called the Lemaître-Hubble law.
- 1934 F. Zwicky postulates the existence of “dark matter” in order to explain the stability of galaxy clusters.
- 1937 F. Zwicky starts a longtime search for multiple images of galaxies produced by the gravitational field of intervening masses (“gravitational lens effect”).

- 1939 R. Oppenheimer and H. Snyder calculate the gravitational collapse of a spherically symmetric ball of dust.
- 1956 W. Rindler introduces the notions of “event horizons” and “particle horizons” for cosmological models.
- 1958 D. Finkelstein, M. Kruskal, G. Szekeres and C. Frønsdal explain that the singularity in the Schwarzschild solution at $r = r_S$ is an event horizon; if a spherically symmetric body has collapsed to a radius smaller than r_S , no signal can escape from the region $r < r_S$ to the region $r > r_S$. In the mid-1960s the name “black hole” is introduced for such an object; the name probably originated from John Wheeler or people around him.
- 1959 R. Pound and G. Rebka measure the gravitational redshift in a building of 22.5 m height; the prediction from general relativity is verified to within 10 %.
- 1963 R. Kerr finds a solution to Einstein’s vacuum field equation that describes a rotating black hole (“Kerr solution”).
- 1960 J. Weber starts a longtime search for gravitational waves with “resonant bar detectors”, also known as “Weber cylinders”.
- 1963 E. Gertsenshtein and V. Pustovoit suggest to use interferometers for the detection of gravitational waves. This is the idea on which the LIGO (and Virgo and GEO600 ...) detectors are based.
- 1965 A. Penzias and R. Wilson accidentally discover the cosmic background radiation which is viewed as a strong support for the big-bang hypothesis (Nobel prize 1978).
- 1965 – 1970 R. Penrose and S. Hawking prove several “singularity theorems”, thereby demonstrating that, under fairly general assumptions, solutions to Einstein’s field equations must have “singularities”. (Nobel prize for Penrose in 2020.)
- 1974 S. Hawking predicts that black holes can evaporate by emitting (“Hawking”) radiation; this is relevant only for very small black holes because for bigger black holes the time scale is enormously big. Hawking radiation has not yet been observed, but it was claimed that it was seen in analogue experiments (i.e. experiments which are described by equations which are analogous to the equations of black-hole physics).
- 1974 R. Hulse and J. Taylor observe an energy loss of the binary pulsar PSR 1913+16 which they interpret as an indirect evidence for the existence of gravitational waves (Nobel prize 1993).
- 1979 D. Walsh, R. Carswell and R. Weyman interpret the double quasar Q 0957+561 as two images of one and the same quasar, produced by the gravitational lens effect of an intervening galaxy.
- 1995 – now The centre of our Galaxy is observed with infrared telescopes. This provides clear evidence, from the motion of stars in this region, that there is a supermassive black hole of about 4 Million Solar masses at the centre of our Galaxy. (Nobel prize for A. Ghez and Reinhard Genzel 2020).

- 1998 Observations using Supernovae of Type Ia provide evidence for an accelerated expansion of our universe; this can be explained, on the basis of general relativity, if one assumes that there is not only (clumpy) “dark matter” but also (homogeneous) “dark energy” (Nobel prize for S. Perlmutter, A. Riess and B. Schmidt 2011).
- 2002 First science runs of interferometric gravitational wave detectors LIGO (USA) and GEO600 (Germany).
- 2015 First direct detection of gravitational waves by the LIGO detectors, most probably produced by a merger of two black holes that produced a single black hole of more than 60 Solar masses. During this merger process, which took less than a second, 3 Solar masses were emitted in the form of gravitational waves. This would be by far the most powerful event (power = energy/time) ever seen in the Universe (Nobel prize for R. Weiss, K. Thorne and B. Barish 2017).
- 2019 The Event Horizon Telescope Collaboration releases pictures from the centre of the galaxy M87. These pictures are believed to show the so-called “shadow” of a supermassive black hole of about 6 billion Solar masses situated there.

Most important open problems:

- explanation of dark matter and dark energy (dark energy could be explained just as the effect of a “cosmological constant”, see later in this course, but dark matter is a completely open problem);
- understanding of the singularities predicted by the theory;
- unification of general relativity and quantum theory (“quantum gravity”).

2 Special relativity

2.1 Special relativistic spacetime

The set of all events, characterised by three space coordinates and a time coordinate, is called *spacetime* (or, more fully, the *spacetime continuum*).

The spacetime of special relativity is determined by two postulates.

(P1) Special relativity principle:

There are coordinate systems, called inertial systems, in which all force-free bodies are in uniform rectilinear motion. All inertial systems have equal rights.

(P2) Principle of the constancy of the speed of light:

The vacuum speed of light has the same value c in all inertial systems (independent of the velocity of the source).

Postulate (P1) is valid also in Newtonian mechanics: It is true that Newton postulated an absolute space, but all the laws he then established showed that this absolute space would be indistinguishable from any other systems that are in uniform rectangular motion with respect to absolute space. Therefore, also in Newtonian mechanics we have a family of inertial systems which have equal rights.

For postulate (P2), in hindsight the best motivation is the Michelson-Morley experiment: Before 1905 people had thought that light is a wave phenomenon that needs a medium for propagating. This medium was called the “ether”.

Then the problem arose to determine the motion of the Earth with respect to the ether. Albert Michelson tried to detect this motion with the interferometric device named after him, first by experiments in Berlin and Potsdam, then with great effort together with Edward Morley in Cleveland in 1888: If the interferometer is being rotated, the interference pattern does not change, no relative motion of the Earth relative to the ether is observed;

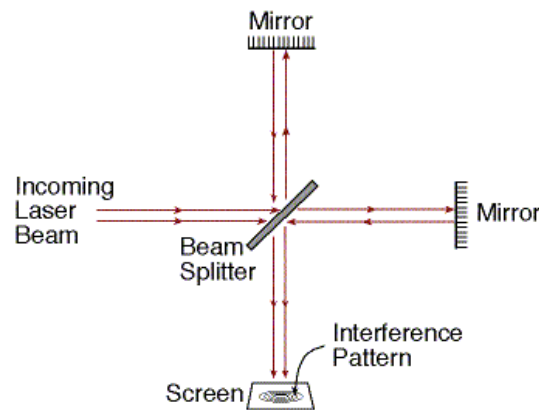


Figure 1: Michelson interferometer

On the basis of Einstein’s special relativity the answer is clear: There simply is no ether, i.e., no distinguished reference frame for the propagation of light.

Virtually any text-book on relativity gives the Michelson-Morley experiment as the main motivation for postulate (P2). Historically however, it should be noted that Einstein came to postulate (P2) by carefully investigating the invariance properties of Maxwell’s equations. The Michelson-Morley experiment played no important role for him; later, he couldn’t even remember if he knew about this experiment when he established special relativity.

It should also be mentioned that by now there are even more direct experimental verifications of the constancy of the speed of light: In the 1960s the Swiss physicist T. Alväger performed experiments where a decaying particle produced gamma quanta (light particles). Whatever the velocity of the particle was before decaying, the emitted gamma quanta always moved at the speed of light c with respect to the laboratory.

So we now accept the two postulates of special relativity. We denote the coordinates in an inertial system by $x^0 = ct$, $x^1 = x$, $x^2 = y$, $x^3 = z$. Note that we use upper indices for the coordinates. This is for being in agreement with the general rules of index positions that will be introduced later.

Every object that may be approximated as being pointlike has a “worldline”, i.e., it is characterised by a curve in spacetime that tells where the object is at any time. For a force-free body this is a straight line.

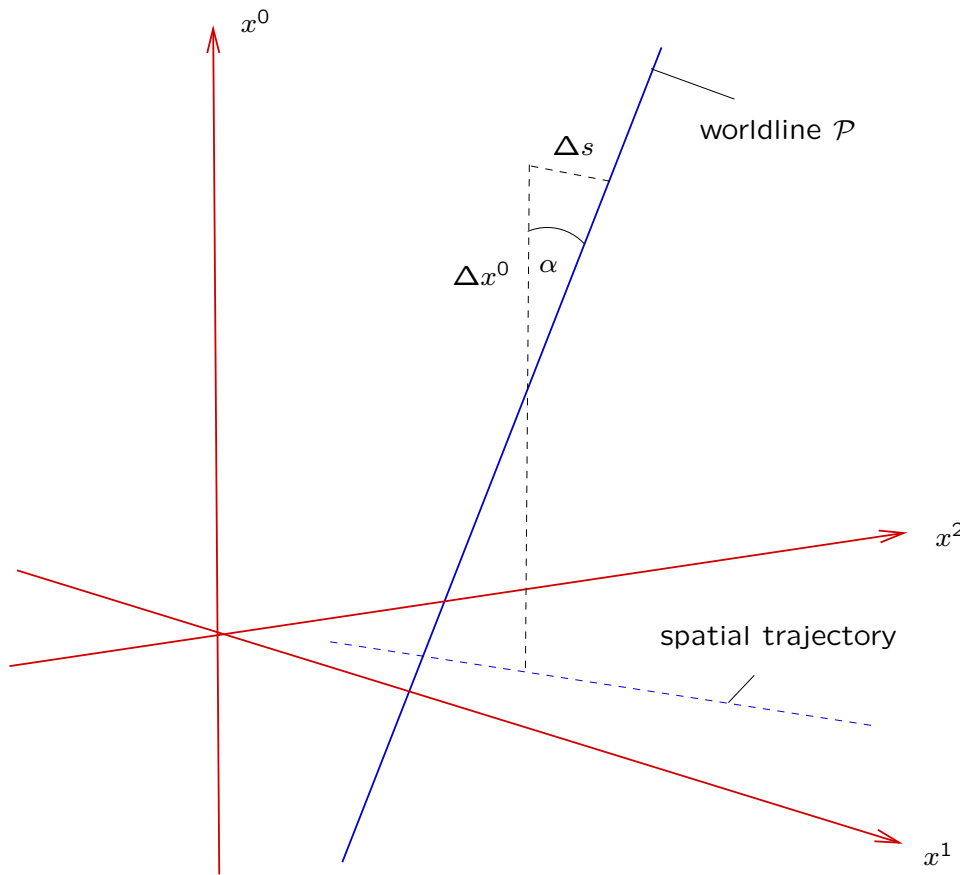


Figure 2: Worldline \mathcal{P} of a force-free body

$$\tan \alpha = \frac{\Delta s}{\Delta x^0} = \frac{\sqrt{(\Delta x^1)^2 + (\Delta x^2)^2 + (\Delta x^3)^2}}{\Delta x^0} = \frac{1}{c} \sqrt{\left(\frac{\Delta x}{\Delta t}\right)^2 + \left(\frac{\Delta y}{\Delta t}\right)^2 + \left(\frac{\Delta z}{\Delta t}\right)^2} = \frac{v}{c}$$

v and, thus, the angle α depends on the chosen inertial system.

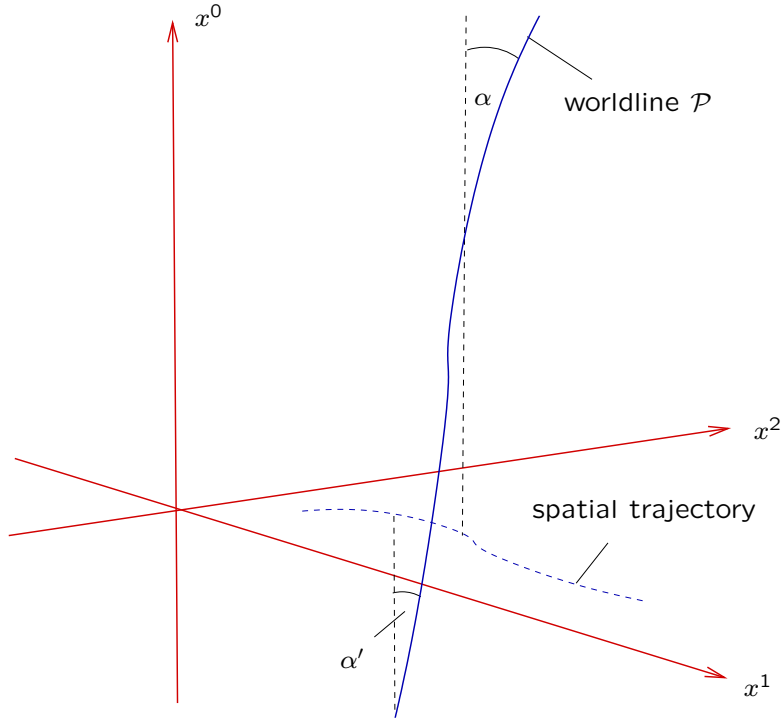


Figure 3: Worldline \mathcal{P} of an accelerated body

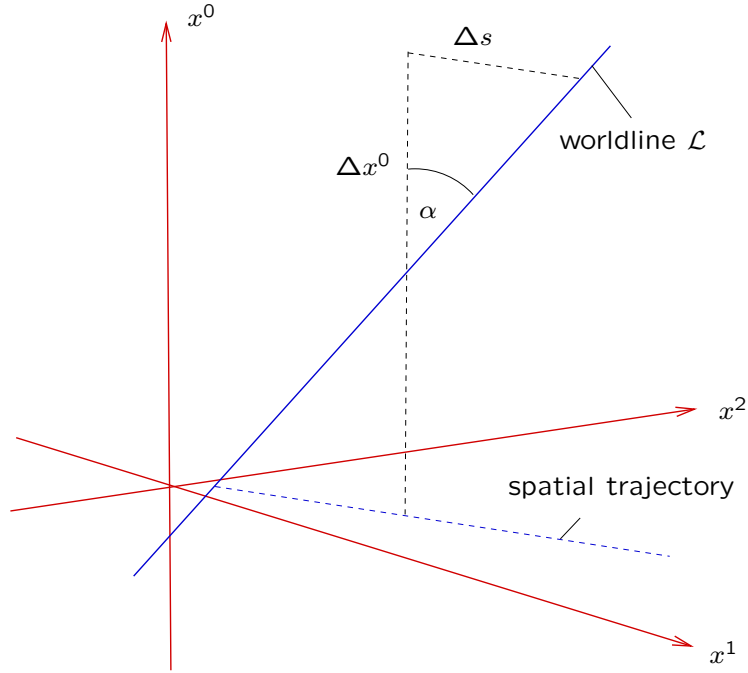


Figure 4: Worldline \mathcal{L} of a light signal

For light: $\tan \alpha = \frac{\Delta s}{\Delta x^0} = \frac{\Delta s}{c \Delta t} = \frac{v}{c} = 1$, $\alpha = 45^\circ$

In this case, the angle α is independent of the chosen inertial system.

All light signals that pass through an event A form the *light cone* of A :

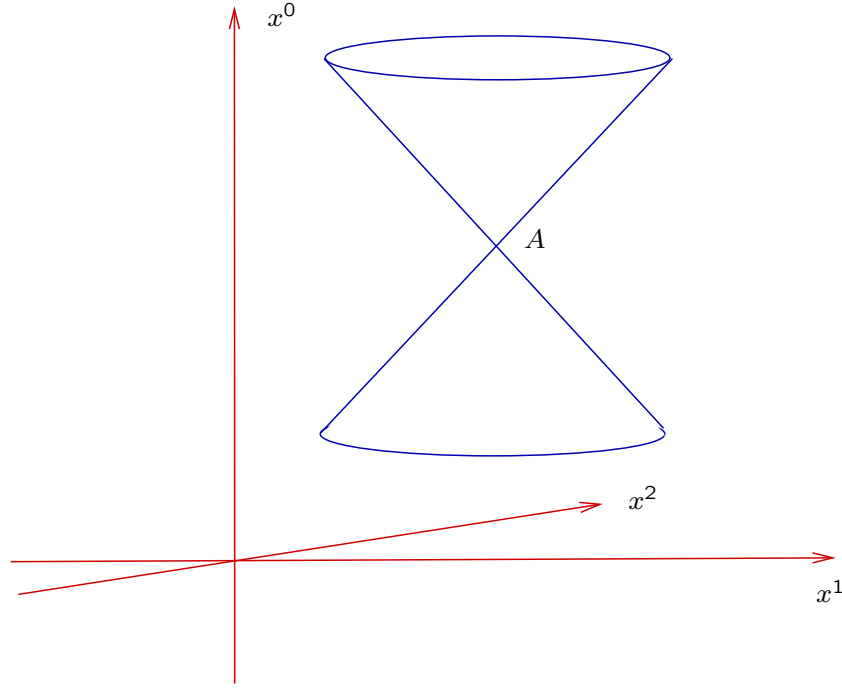


Figure 5: Light cone of the event A

In *any* inertial system, the light cone of A is given by the equation:

$$(x^0 - a^0)^2 = (x^1 - a^1)^2 + (x^2 - a^2)^2 + (x^3 - a^3)^2 \quad (1)$$

where (a^0, a^1, a^2, a^3) are the coordinates of A . The light cone of A naturally divides into a future half-cone ($a^0 < x^0$) and a past half-cone ($a^0 > x^0$).

If X is an event with coordinates (x^0, x^1, x^2, x^3) , and $X \neq A$, we say:

$$X \text{ lies } \begin{cases} \text{timelike} \\ \text{lightlike} \\ \text{spacelike} \end{cases} \text{ with respect to } A \iff -(x^0 - a^0)^2 + (x^1 - a^1)^2 + (x^2 - a^2)^2 + (x^3 - a^3)^2 \begin{cases} < 0 \\ = 0 \\ > 0 \end{cases}$$

In the first case X is in the interior of the light cone of A , in the second case it is on the boundary, and in the third case it is in the exterior. Note that the property of being timelike, lightlike or spacelike characterises events *with respect to another event*. Equivalently, it characterises vectors that connect two events.

In special relativity, simultaneity is defined with the *radar method*, also known as *Einstein's synchronisation procedure*, cf. Worksheet 1, Problem 4. The following diagrams demonstrate that simultaneity is relative.

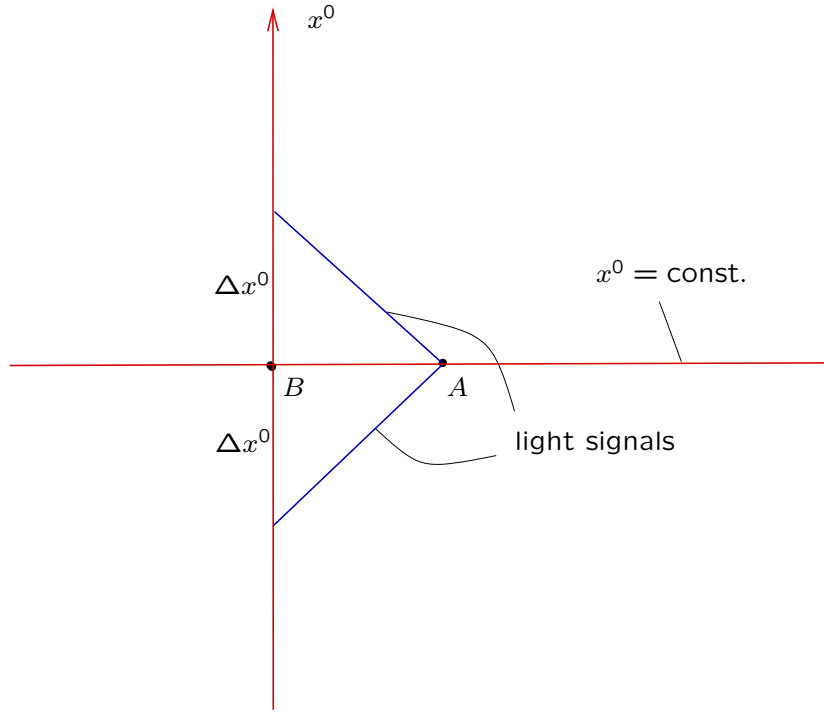


Figure 6: In the inertial system Σ , the event A is simultaneous with the event B

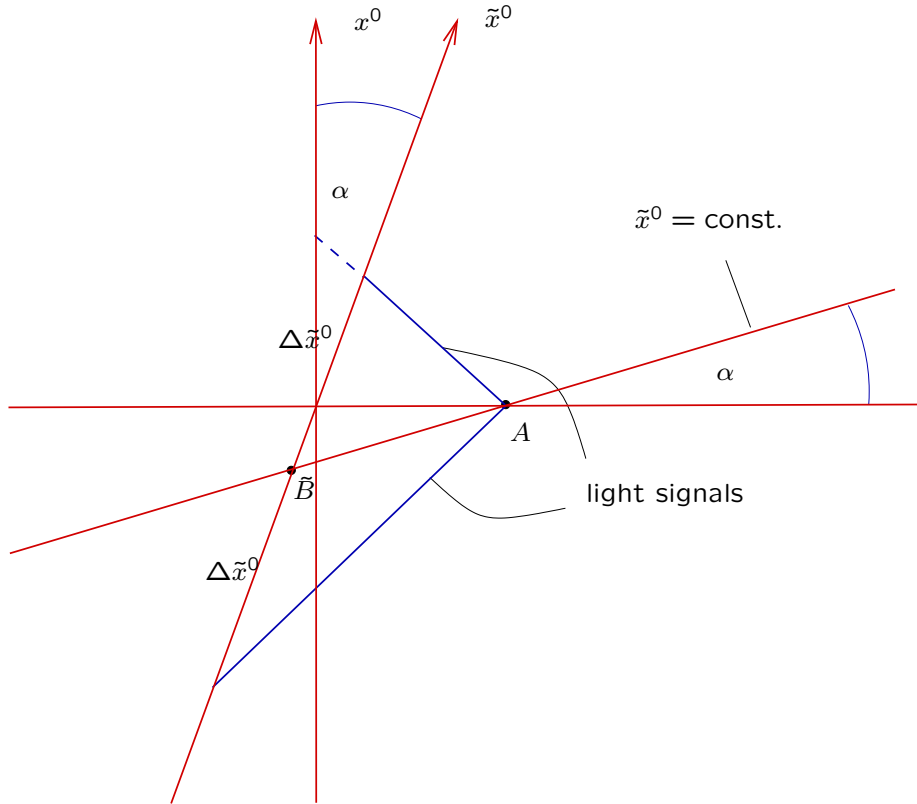


Figure 7: In the inertial system $\tilde{\Sigma}$, the event A is simultaneous with the event \tilde{B}

In Newtonian physics simultaneity is absolute and the light cones depend on the inertial system; in special relativity it is vice versa.

The relativity of simultaneity is the reason why superluminal signals are not allowed. More precisely, we will demonstrate now that the existence of superluminal signals is not compatible with causality (“the cause always precedes the effect”).

Consider the following situation.

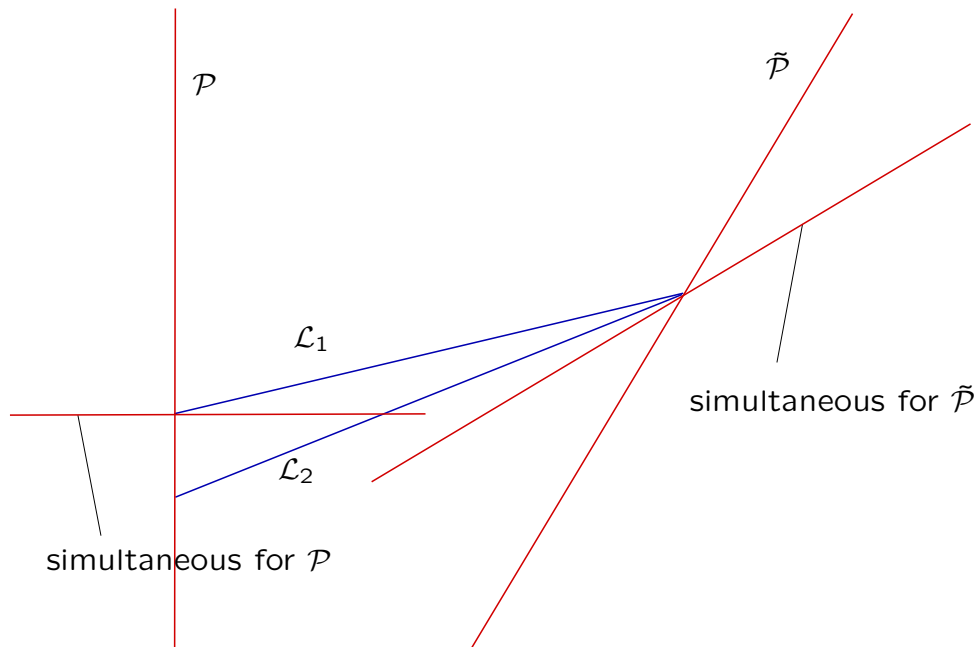


Figure 8: \mathcal{P} sends superluminal signal \mathcal{L}_1 into his future; $\tilde{\mathcal{P}}$ sends superluminal signal \mathcal{L}_2 into his future; both signals combined result in a signal from \mathcal{P} into his past

The existence of such signals would lead to paradoxa. E.g., with the help of the signals \mathcal{L}_1 and \mathcal{L}_2 , it would be possible for \mathcal{P} to kill his parents before his own birth.

In order to reconcile special relativity with causality, superluminal signals must be prohibited. A speed that is not associated with a signal, however, could be bigger than the vacuum speed of light. E.g., the bright spot produced by a laser beam can move over a screen with superluminal speed.

In 2011 it was announced that in the OPERA experiment at CERN neutrinos had been observed that moved at superluminal speed. If true, this would have been a serious problem for special (and general) relativity. However, it turned out to be a measuring mistake.

We have already said what it means that an event lies timelike, lightlike or spacelike with respect to another event. Using this terminology, we can summarise our discussion of causality in the following way. An event X can be connected with an event A by a signal if and only if X lies timelike or lightlike with respect to A . For any fixed A , the set of all such events X divides into two connected components which are called the (absolute) *future* and the (absolute) *past* of A , respectively.

2.2 Index notation

From now on, greek indices, $\mu, \nu, \sigma \dots$, take values 0,1,2,3. E.g., the coordinates (x^0, x^1, x^2, x^3) of an event in an inertial system will be denoted x^μ .

Latin indices, $i, j, k \dots$, take values 1,2,3. E.g., the spatial coordinates (x^1, x^2, x^3) of an event in an inertial system will be denoted x^i .

We define the *Minkowski metric*

$$\eta_{\mu\nu} = \begin{cases} -1 & \text{if } \mu = \nu = 0 \\ 1 & \text{if } \mu = \nu = 1, 2, 3 \\ 0 & \text{if } \mu \neq \nu \end{cases} \quad (2)$$

which can be written in matrix form as

$$(\eta_{\mu\nu}) = \text{diag}(-1, 1, 1, 1) = \begin{pmatrix} -1 & 0 & 0 & 0 \\ 0 & 1 & 0 & 0 \\ 0 & 0 & 1 & 0 \\ 0 & 0 & 0 & 1 \end{pmatrix} \quad (3)$$

(Calling $\eta_{\mu\nu}$ “the Minkowski metric” is a common abuse of notation. More pecisely, one should call $\eta_{\mu\nu}$ “the components of the Minkowski metric in an arbitrary inertial system”.)

With the help of the Minkowski metric, the equation of the light cone,

$$0 = -(\Delta x^0)^2 + (\Delta x^1)^2 + (\Delta x^2)^2 + (\Delta x^3)^2, \quad (4)$$

can be rewritten as

$$0 = \sum_{\mu=0}^3 \sum_{\nu=0}^3 \eta_{\mu\nu} \Delta x^\mu \Delta x^\nu. \quad (5)$$

From now on we adopt Einstein’s summation convention:

If a greek index, μ, ν, σ, \dots , appears twice in an expression, once as a subscript and once as a superscript, then it is to be summed over from 0 to 3. The same rule is valid for latin indices, i, j, k, \dots , but in this case the sum is only from 1 to 3.

Note that different authors use different conventions. Some of them replace our $\eta_{\mu\nu}$ with $-\eta_{\mu\nu}$, some of them use the index 4 instead of 0 for the time coordinate, some of them use latin instead of greek indices and vice versa. In some older books the imaginary unit is included into the time coordinate, $x^0 = ict$ with $i^2 = -1$, which allows to use the Kronecker delta instead of the Minkowski metric. This is no longer used as it causes confusion.

With Einstein’s summation convention the light cone equation (5) becomes $0 = \eta_{\mu\nu} \Delta x^\mu \Delta x^\nu$ and the definition of timelike, lightlike and spacelike vectors reads

$$\Delta x^\mu \text{ is } \begin{cases} \text{timelike} \\ \text{lightlike} \\ \text{spacelike} \end{cases} \iff \eta_{\mu\nu} \Delta x^\mu \Delta x^\nu \begin{cases} < 0 \\ = 0 \\ > 0 \end{cases}.$$

Later we will also use the matrix $(\eta^{\mu\nu})$, which is defined as the inverse matrix of $(\eta_{\rho\sigma})$, i.e.,

$$\eta^{\mu\nu}\eta_{\nu\sigma} = \delta_{\sigma}^{\mu}, \quad (6)$$

where δ_{σ}^{μ} is the Kronecker delta. Clearly, written as a matrix $(\eta^{\mu\nu})$ looks the same as $(\eta_{\rho\sigma})$. We will use $\eta_{\mu\nu}$ for lowering indices and $\eta^{\mu\nu}$ for raising indices, e.g.

$$v_{\mu} = \eta_{\mu\nu}v^{\nu}, \quad w^{\mu} = \eta^{\mu\nu}w_{\nu}. \quad (7)$$

2.3 Lorentz transformations

We define Lorentz transformations in the following way.

Definition: A *Lorentz transformation* is a linear transformation, $\tilde{x}^{\mu} = L^{\mu}_{\nu}x^{\nu}$, that leaves the Minkowski metric invariant, $\eta_{\mu\nu}L^{\mu}_{\rho}L^{\nu}_{\sigma} = \eta_{\rho\sigma}$.

It is easy to demonstrate that a Lorentz transformation maps an inertial system to an inertial system: What one has to prove is that a Lorentz transformation maps straight lines onto straight lines (this is necessary because of Postulate (P1)) and that it leaves the light cones invariant (this is necessary because of Postulate (P2)). The first property is obvious because Lorentz transformations are linear. The second follows from the fact that a Lorentz transformation satisfies $\Delta\tilde{x}^{\mu} = L^{\mu}_{\nu}\Delta x^{\nu}$ and thus $\eta_{\mu\nu}\Delta\tilde{x}^{\mu}\Delta\tilde{x}^{\nu} = \eta_{\rho\sigma}\Delta x^{\rho}\Delta x^{\sigma}$.

As a consequence, Postulate (P1) requires the laws of nature to be invariant under Lorentz transformations.

Lorentz transformations are not the only transformations that map inertial systems to inertial systems:

- *Poincaré transformations* (also known as *inhomogeneous Lorentz transformations*) contain an additional shift of the origin, $\tilde{x}^{\mu} = L^{\mu}_{\nu}x^{\nu} + a^{\mu}$. Then, again, straight lines are mapped onto straight lines and, as coordinate differences are unaffected by a^{μ} , we have also in this case $\eta_{\mu\nu}\Delta\tilde{x}^{\mu}\Delta\tilde{x}^{\nu} = \eta_{\rho\sigma}\Delta x^{\rho}\Delta x^{\sigma}$.
- *Weyl transformations* contain an additional multiplicative constant factor which can be interpreted as a change of (length and time) units, $\tilde{x}^{\mu} = e^k L^{\mu}_{\nu}x^{\nu} + a^{\mu}$. Also in this case straight lines are mapped onto straight lines and, as $\eta_{\mu\nu}\Delta\tilde{x}^{\mu}\Delta\tilde{x}^{\nu} = e^{2k}\eta_{\rho\sigma}\Delta x^{\rho}\Delta x^{\sigma}$, light cones are left invariant.

One can usually restrict to the case that the units and the coordinate origin are kept fixed. Then the set of all transformations that map inertial systems to inertial systems consists precisely of the Lorentz transformations. (As an aside, we mention that transformations that leave the light cones invariant, but not necessarily the straight lines, are known as *conformal transformations*. They play an important role in high-energy physics.)

We consider now two special types of Lorentz transformations.

- Spatial rotations about the x^1 -Achse:

$$\begin{pmatrix} \tilde{x}^0 \\ \tilde{x}^1 \\ \tilde{x}^2 \\ \tilde{x}^3 \end{pmatrix} = \begin{pmatrix} 1 & 0 & 0 & 0 \\ 0 & 1 & 0 & 0 \\ 0 & 0 & \cos \varphi & \sin \varphi \\ 0 & 0 & -\sin \varphi & \cos \varphi \end{pmatrix} \begin{pmatrix} x^0 \\ x^1 \\ x^2 \\ x^3 \end{pmatrix},$$

parametrised by the angle φ . These are indeed Lorentz transformation, as the following calculation demonstrates.

$$\begin{aligned} \eta_{\mu\nu} L^\mu{}_\rho L^\nu{}_\sigma x^\rho x^\sigma &= \eta_{\mu\nu} \tilde{x}^\mu \tilde{x}^\nu \\ &= -(\tilde{x}^0)^2 + (\tilde{x}^1)^2 + (\tilde{x}^2)^2 + (\tilde{x}^3)^2 \\ &= -(x^0)^2 + (x^1)^2 + (\cos \varphi x^2 + \sin \varphi x^3)^2 \\ &\quad + (-\sin \varphi x^2 + \cos \varphi x^3)^2 \\ &= -(x^0)^2 + (x^1)^2 + (x^2)^2 + (x^3)^2 = \eta_{\rho\sigma} x^\rho x^\sigma. \end{aligned}$$

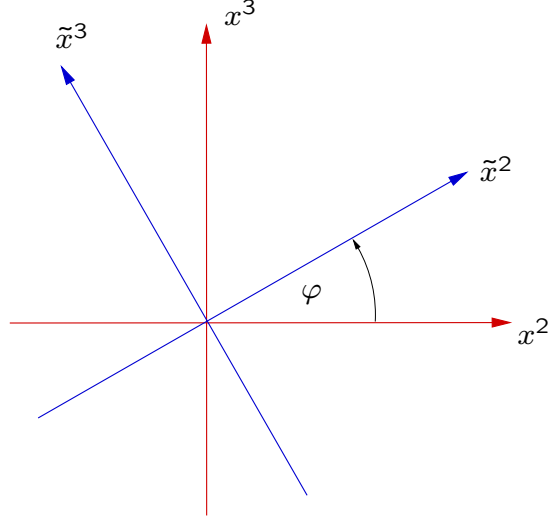


Figure 9: Spatial rotation

Analogous calculations hold for rotations about the x^2 - or the x^3 -axis.

- Boosts in x^1 -direction:

$$\begin{pmatrix} \tilde{x}^0 \\ \tilde{x}^1 \\ \tilde{x}^2 \\ \tilde{x}^3 \end{pmatrix} = \begin{pmatrix} \cosh \eta & -\sinh \eta & 0 & 0 \\ -\sinh \eta & \cosh \eta & 0 & 0 \\ 0 & 0 & 1 & 0 \\ 0 & 0 & 0 & 1 \end{pmatrix} \begin{pmatrix} x^0 \\ x^1 \\ x^2 \\ x^3 \end{pmatrix},$$

parametrised by the so-called *rapidity* η . The angle α in Fig. 10 is related to η via $\tan \alpha = \tanh \eta$.

The following calculation shows that these are, indeed, Lorentz transformation:

$$\begin{aligned} \eta_{\mu\nu} L^\mu{}_\rho L^\nu{}_\sigma x^\rho x^\sigma &= \eta_{\mu\nu} \tilde{x}^\mu \tilde{x}^\nu \\ &= -(\tilde{x}^0)^2 + (\tilde{x}^1)^2 + (\tilde{x}^2)^2 + (\tilde{x}^3)^2 \\ &= -(\cosh \eta x^0 - \sinh \eta x^1)^2 \\ &\quad + (-\sinh \eta x^0 + \cosh \eta x^1)^2 + (x^2)^2 + (x^3)^2 \\ &= -(x^0)^2 + (x^1)^2 + (x^2)^2 + (x^3)^2 = \eta_{\rho\sigma} x^\rho x^\sigma. \end{aligned}$$

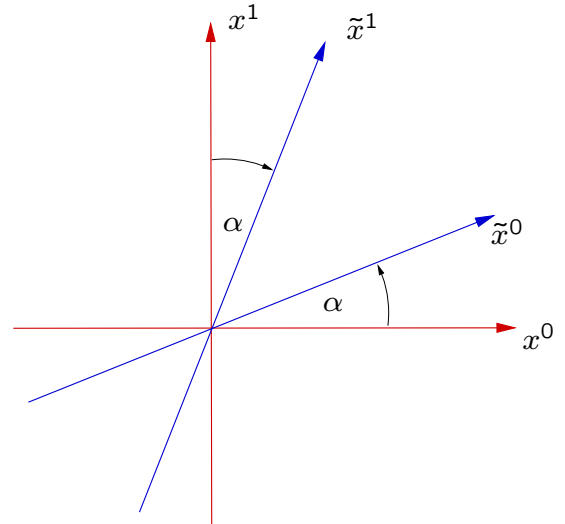


Figure 10: Lorentz boost

With $\tanh \eta = \frac{v}{c}$, which implies $\cosh \eta = \frac{1}{\sqrt{1 - \frac{v^2}{c^2}}}$ and $\sinh \eta = \frac{1}{\sqrt{1 - \frac{v^2}{c^2}}} \frac{v}{c}$, we get

the familiar form of the Lorentz transformations in one spatial dimension:

$$\tilde{x}^0 = \cosh \eta x^0 - \sinh \eta x^1 = \frac{x^0 - \frac{v}{c} x^1}{\sqrt{1 - \frac{v^2}{c^2}}}, \quad \tilde{t} = \frac{t - \frac{v}{c^2} x}{\sqrt{1 - \frac{v^2}{c^2}}} \quad (8)$$

$$\tilde{x}^1 = -\sinh \eta x^0 + \cosh \eta x^1 = \frac{-\frac{v}{c} x^0 + x^1}{\sqrt{1 - \frac{v^2}{c^2}}}, \quad \tilde{x} = \frac{x - v t}{\sqrt{1 - \frac{v^2}{c^2}}} \quad (9)$$

The limit $c \rightarrow \infty$ yields the Galileo transformation: $\tilde{t} = t$ and $\tilde{x} = x - vt$.

Analogous equations hold for boosts in x^2 - or x^3 -direction. – It is not difficult to verify that two successive boosts in different directions result in a Lorentz transformation that involves a spatial rotation; this is known as a *Thomas rotation*.

With the exception of discrete transformations (such as a reversal of a time or space axis), all Lorentz transformations can be written as combinations of spatial rotations and boosts. As there are three independent spatial rotations and three independent boosts, the Lorentz group (i.e., the set of all Lorentz transformations) is 6-dimensional. The Poincaré group is 10-dimensional, the Weyl group is 11-dimensional, and the conformal group is 15-dimensional.

The transformation formulas of coordinate differences under a boost,

$$\Delta \tilde{t} = \frac{\Delta t - \frac{v}{c^2} \Delta x}{\sqrt{1 - \frac{v^2}{c^2}}}, \quad \Delta \tilde{x} = \frac{\Delta x - v \Delta t}{\sqrt{1 - \frac{v^2}{c^2}}}, \quad (10)$$

immediately yield the familiar formulas for time dilation and length contraction.

- Time dilation:

In Σ , two events A and B occur at the same point with time difference Δt . What is their time difference $\Delta \tilde{t}$ in $\tilde{\Sigma}$?

As $\Delta x = 0$, we have

$$\Delta \tilde{t} = \frac{\Delta t}{\sqrt{1 - \frac{v^2}{c^2}}}.$$

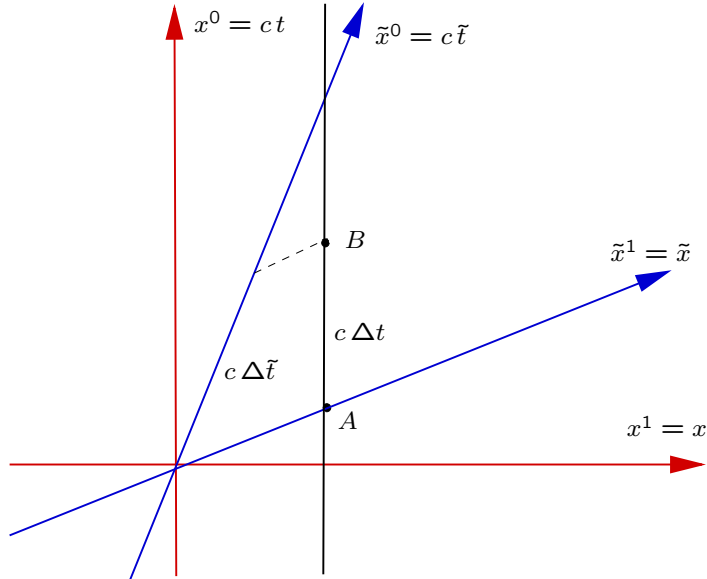


Figure 11: Time dilation

- Length contraction:

A rod is at rest in Σ , where it has length Δx . To determine its length $\Delta \tilde{x}$ in $\tilde{\Sigma}$, we have to consider events A and B that occur at the ends of the rod simultaneously in $\tilde{\Sigma}$.

As $\Delta \tilde{t} = 0$, we have $\Delta t = \frac{v}{c^2} \Delta x$ and hence

$$\Delta \tilde{x} = \Delta x \sqrt{1 - \frac{v^2}{c^2}}.$$

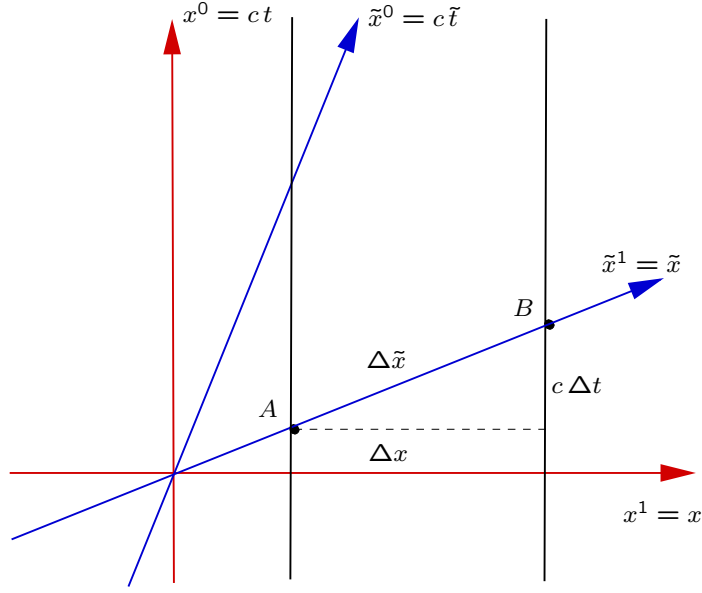


Figure 12: Length contraction

2.4 Kinematics and dynamics of particles

We require that a particle moves at subluminal speed, so its worldline $x^\mu(\tau)$ must have a timelike tangent,

$$\eta_{\mu\nu} \frac{dx^\mu(\tau)}{d\tau} \frac{dx^\nu(\tau)}{d\tau} < 0. \quad (11)$$

Note that a reparametrisation of the worldline has no influence on the motion. The parameter τ can be interpreted as the reading of a clock.

We choose the parameter such that

$$\eta_{\mu\nu} \frac{dx^\mu(\tau)}{d\tau} \frac{dx^\nu(\tau)}{d\tau} = -c^2. \quad (12)$$

Then we find in the momentary rest system,

$$\frac{dx^i}{d\tau}(\tau_0) = 0, \quad (13)$$

that along the worldline the parameters t and τ must be related in the following way.

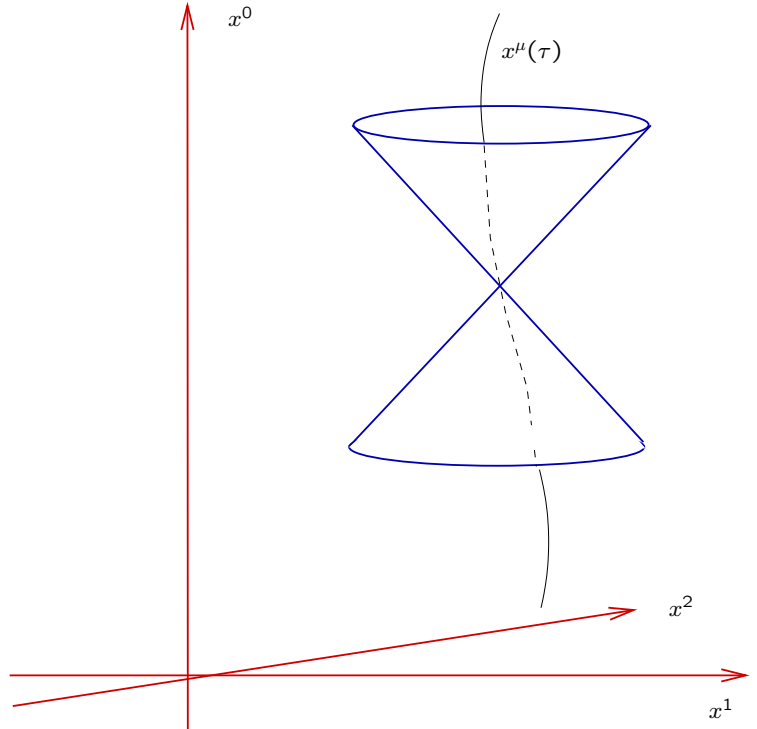


Figure 13: Worldline of a particle

$$\begin{aligned}
-c^2 &= \eta_{00} \frac{dx^0}{d\tau}(\tau_0) \frac{dx^0}{d\tau}(\tau_0) \\
&= -c^2 \left(\frac{dt}{d\tau}(\tau_0) \right)^2 \implies \\
\frac{dt}{d\tau}(\tau_0) &= 1,
\end{aligned}$$

i.e., for sufficiently short time intervals the elapsed proper time $\Delta\tau$ coincides with the elapsed coordinate time Δt in the rest system arbitrarily well. This special parameter τ is called the *proper time* of the particle, and a clock that shows proper time is called a *standard clock*. To date, all experiments are in agreement with the hypothesis that atomic clocks are standard clocks.

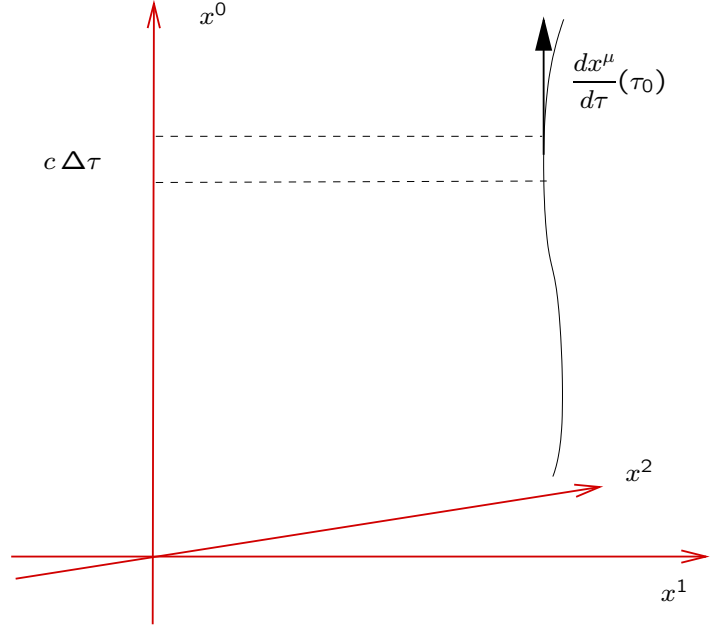


Figure 14: Proper time

Along the worldline $x^\mu(\tau)$ of a particle, we define the *four-velocity*

$$u^\mu(\tau) = \frac{dx^\mu(\tau)}{d\tau} \quad (14)$$

and the *four-acceleration*

$$a^\mu(\tau) = \frac{du^\mu(\tau)}{d\tau} = \frac{d^2x^\mu(\tau)}{d\tau^2}. \quad (15)$$

We compare the four-velocity with the ordinary (three-)velocity

$$v^i = \frac{dx^i}{dt} = \frac{dx^i}{d\tau} \frac{d\tau}{dt} = u^i \frac{d\tau}{dt}, \quad (16)$$

where t is the time coordinate in the chosen inertial system. The factor $d\tau/dt$ can be calculated from the equation that defines proper time,

$$-c^2 = \eta_{\mu\nu} \frac{dx^\mu}{d\tau} \frac{dx^\nu}{d\tau} = -\left(\frac{dx^0}{d\tau}\right)^2 + \left(\frac{dx^1}{d\tau} \frac{dt}{d\tau}\right)^2 + \left(\frac{dx^2}{d\tau} \frac{dt}{d\tau}\right)^2 + \left(\frac{dx^3}{d\tau} \frac{dt}{d\tau}\right)^2. \quad (17)$$

As $x^0 = ct$, this gives

$$-c^2 = \left(\frac{dt}{d\tau}\right)^2 \left(-c^2 + (v^1)^2 + (v^2)^2 + (v^3)^2\right). \quad (18)$$

With $v^2 = (v^1)^2 + (v^2)^2 + (v^3)^2$, we find the desired relation between proper time and coordinate time,

$$\frac{dt}{d\tau} = \frac{1}{\sqrt{1 - \frac{v^2}{c^2}}}. \quad (19)$$

As a consequence, the four-velocity can be written in matrix notation as

$$\begin{pmatrix} u^0 \\ u^1 \\ u^2 \\ u^3 \end{pmatrix} = \frac{1}{\sqrt{1 - \frac{v^2}{c^2}}} \begin{pmatrix} c \\ v^1 \\ v^2 \\ v^3 \end{pmatrix}. \quad (20)$$

It is important to keep in mind that the spatial components of the four-velocity do *not* coincide with the ordinary (three-)velocity, $u^i \neq v^i$, unless in an inertial system where the particle is at rest.

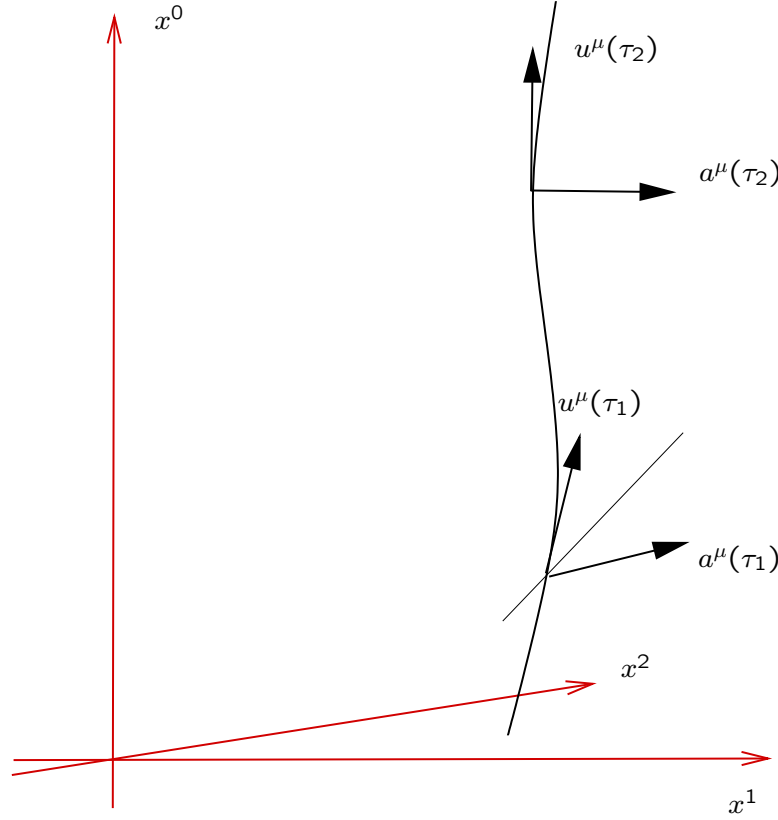


Figure 15: Four-velocity and four-acceleration of a particle

By differentiating the equation $\eta_{\mu\nu} u^\mu(\tau) u^\nu(\tau) = -c^2$ we find

$$2\eta_{\mu\nu} u^\mu(\tau) \frac{du^\nu(\tau)}{d\tau} = 0$$

and hence

$$\eta_{\mu\nu} u^\mu(\tau) a^\nu(\tau) = 0, \quad (21)$$

i.e., $a^\mu(\tau)$ and $u^\mu(\tau)$ are “perpendicular with respect to the Minkowski metric”. Geometrically this means that $a^\mu(\tau)$ lies in a (three-dimensional) hyperplane that makes the same angle with the light cone as the vector $u^\mu(\tau)$, cf. Worksheet 2.

In the momentary rest system we have $u^i(\tau_0) = 0$ and thus $-u^0(\tau_0)a^0(\tau_0) = 0$. Clearly, as the four-velocity satisfies the equation $\eta_{\mu\nu}u^\mu u^\nu = -c^2$, we must have $u^0(\tau_0) \neq 0$. This implies that in the momentary rest system $a^0(\tau) = 0$, i.e., in this inertial system $a^\mu(\tau_0)$ has only spatial components. This implies, in particular, that $a^\mu(\tau_0)$ is a spacelike vector,

$$\eta_{\mu\nu} a^\mu(\tau_0) a^\nu(\tau_0) > 0, \quad (22)$$

if it is non-zero. The equation $a^\mu = 0$ holds along the whole worldline if and only if $u^\mu = \text{constant}$. This is the case if and only if the worldline is a straight line.

Three special cases are of particular interest.

- Uniform motion in a straight line: In this case we have $a^\mu = 0$ along the whole worldline.
- Uniform motion in a circle: This case is treated in Problem 4 of Worksheet 2.
- Motion with constant acceleration in a straight line: We will now treat this case in detail, because it will be of great relevance later in connection with the equivalence principle. We assume that the motion is along the x^1 -axis, so that we can write the worldline as

$$(x^\mu(\tau)) = \begin{pmatrix} x^0(\tau) \\ x^1(\tau) \\ 0 \\ 0 \end{pmatrix} = \begin{pmatrix} c t(\tau) \\ x(\tau) \\ 0 \\ 0 \end{pmatrix}, \quad (23)$$

hence

$$(u^\mu(\tau)) = \begin{pmatrix} c dt(\tau)/d\tau \\ dx(\tau)/d\tau \\ 0 \\ 0 \end{pmatrix}, \quad (24)$$

$$(a^\mu(\tau)) = \begin{pmatrix} c d^2 t(\tau)/d\tau^2 \\ d^2 x(\tau)/d\tau^2 \\ 0 \\ 0 \end{pmatrix}. \quad (25)$$

The functions $t(\tau)$ and $x(\tau)$ have to satisfy two conditions,

$$(C1) \quad -c^2 = \eta_{\mu\nu} u^\mu(\tau) u^\nu(\tau) = -c^2 \left(\frac{dt(\tau)}{d\tau} \right)^2 + \left(\frac{dx(\tau)}{d\tau} \right)^2,$$

$$(C2) \quad a^2 = \eta_{\mu\nu} a^\mu(\tau) a^\nu(\tau) = -c^2 \left(\frac{d^2 t(\tau)}{d\tau^2} \right)^2 + \left(\frac{d^2 x(\tau)}{d\tau^2} \right)^2 \text{ with a constant } a.$$

The first condition is just the definition of proper time, the second expresses the assumption that the acceleration is constant.

Condition (C1) is automatically satisfied by the ansatz

$$\frac{1}{c} \frac{dx(\tau)}{d\tau} = \sinh(f(\tau)) , \quad \frac{dt(\tau)}{d\tau} = \cosh(f(\tau)) . \quad (26)$$

Condition (C2) requires that, in addition,

$$\frac{a^2}{c^2} = - \left(\sinh(f(\tau)) f'(\tau) \right)^2 + \left(\cosh(f(\tau)) f'(\tau) \right)^2 = f'(\tau)^2 . \quad (27)$$

Integration yields

$$f(\tau) = \pm \frac{a \tau}{c} + f(0) . \quad (28)$$

The \pm sign can be absorbed into the definition of a , i.e., we choose a positive or negative, depending on whether the acceleration is in the positive or negative x -direction. The integration constant $f(0)$ can be made to zero by choosing the zero on the dial of the standard clock appropriately. So we may assume that

$$f(\tau) = \frac{a \tau}{c} . \quad (29)$$

The equations

$$\frac{dt(\tau)}{d\tau} = \cosh\left(\frac{a \tau}{c}\right) , \quad \frac{dx(\tau)}{d\tau} = c \sinh\left(\frac{a \tau}{c}\right) \quad (30)$$

yield

$$t(\tau) = \frac{c}{a} \sinh\left(\frac{a \tau}{c}\right) + t_0 , \quad x(\tau) = \frac{c^2}{a} \cosh\left(\frac{a \tau}{c}\right) + x_0 , \quad (31)$$

hence

$$-c^2 (t(\tau) - t_0)^2 + (x(\tau) - x_0)^2 = \frac{c^4}{a^2} . \quad (32)$$

This is the equation of a hyperbola that asymptotically approaches a light cone for $\tau \rightarrow \pm \infty$, see Fig. 16. The bigger a^2 , the closer the hyperbola is to this light cone.

Observers moving on these hyperbolic worldlines, i.e., observers with constant acceleration, are known as *Rindler observers*. For these observers, there is an *event horizon*, see Problem 2 (b) of Worksheet 1. As we have already mentioned and as we will discuss in detail below, the Rindler observers are of great importance for a thorough understanding of the equivalence principle. They have also been extensively used for a discussion of quantum-field theoretical aspects of special relativity. To mention just one example, it was shown by W. Unruh that these observers see a quantum-field theoretical vacuum that is significantly different from the vacuum as seen by observers in an inertial frame; the important notion of *Unruh temperature* originates from this observation.

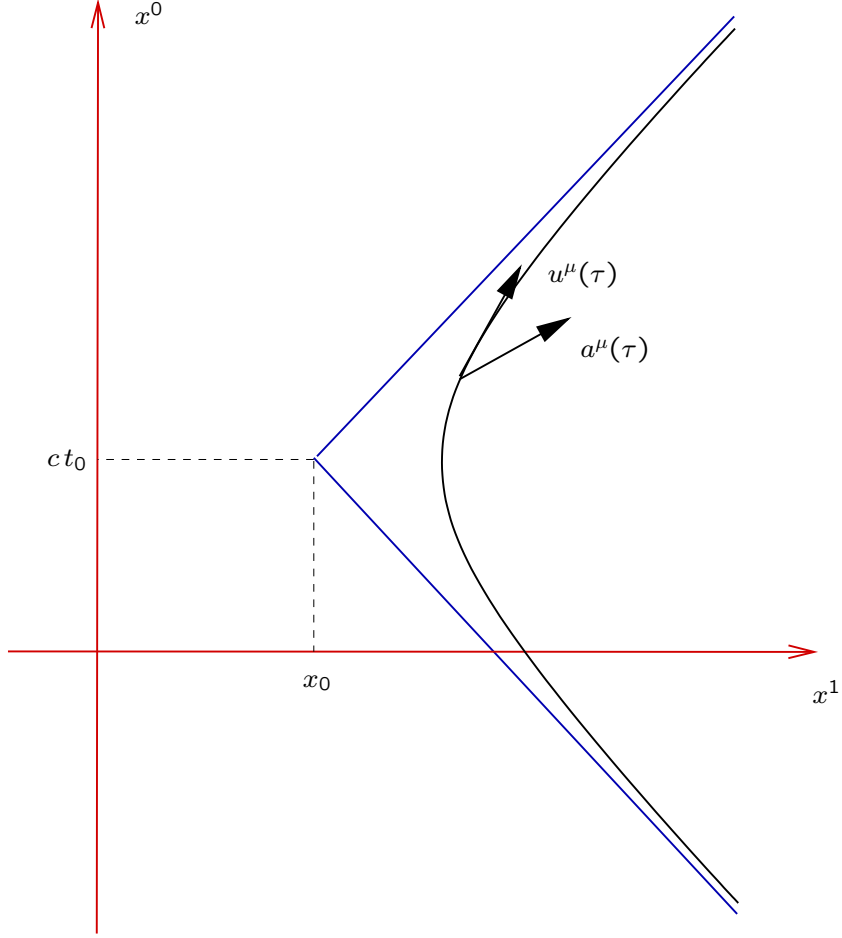


Figure 16: Worldline of an observer with constant acceleration

To each massive particle, we assign a (rest) mass $m > 0$. This is a scalar quantity that characterises the particle independently of the choice of an inertial system. A measuring prescription for the mass can be given in terms of collision experiments, see Worksheet 3.

We define the four-momentum as

$$p^\mu(\tau) = m u^\mu(\tau) . \quad (33)$$

From the definition of proper time we find the following normalisation condition for the four-momentum:

$$\eta_{\mu\nu} p^\mu(\tau) p^\nu(\tau) = m^2 \eta_{\mu\nu} u^\mu(\tau) u^\nu(\tau) = -m^2 c^2 , \quad (34)$$

i.e.

$$-(p^0)^2 + |\vec{p}|^2 = -m^2 c^2 \quad (35)$$

and hence, for future-oriented momentum four-vectors,

$$p^0 = \sqrt{m^2 c^2 + |\vec{p}|^2} . \quad (36)$$

The three spatial components of the four-momentum can be expressed in terms of the three-velocity v^i as

$$p^i(\tau) = m u^i(\tau) = \frac{m v^i(\tau)}{\sqrt{1 - \frac{v(\tau)^2}{c^2}}} = m v^i(\tau) \left(1 + \frac{v(\tau)^2}{2c^2} + \dots \right) \quad (37)$$

and its temporal component reads

$$\begin{aligned} p^0(\tau) &= m u^0(\tau) = \frac{m c}{\sqrt{1 - \frac{v(\tau)^2}{c^2}}} \quad (38) \\ &= m c \left(1 + \frac{v(\tau)^2}{2c^2} + \dots \right) \\ &= \frac{1}{c} \left(\underbrace{m c^2}_{\text{rest energy}} + \underbrace{\frac{m}{2} v(\tau)^2}_{\text{non-rel. kin. energy}} + \dots \right) \end{aligned}$$

This motivates calling $c p^0$ the (*relativistic*) *energy*,

$$\begin{aligned} E(\tau) &= c p^0(\tau) = \frac{m c^2}{\sqrt{1 - \frac{v(\tau)^2}{c^2}}} \\ &= m c^2 + \text{rel. kin. energy} . \quad (39) \end{aligned}$$

The rest energy $m c^2$ can be converted into other forms of energy, e.g. into heat. This is what happens in nuclear reactors and in atomic (fission) bombs.

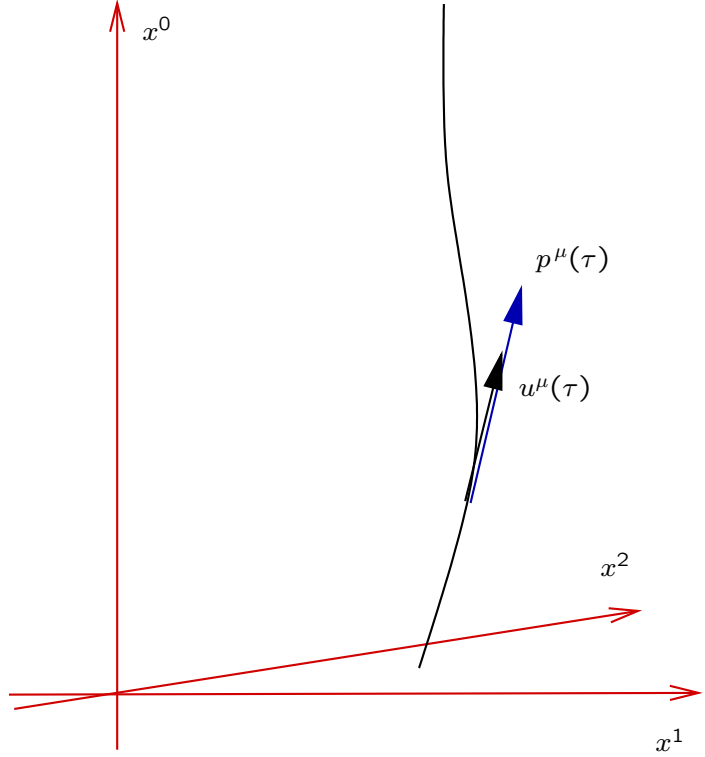


Figure 17: Four-momentum p^μ of a particle

The derivative of the four-momentum with respect to proper time gives the *four-force*

$$F^\mu(\tau) = \frac{dp^\mu(\tau)}{d\tau} . \quad (40)$$

This equation is the relativistic analogue of Newton's Second Law. If F^μ is known, it gives us a second-order differential equation for the worldline; the solution is unique up to the choice of initial conditions $x^\mu(\tau_0)$ and $u^\mu(\tau_0)$. Examples will be treated later.

Some older books use a “velocity-dependent mass” $m(v) = m/\sqrt{1 - v^2/c^2}$. We will never do this. For us, “mass” always means “rest mass”. Note, however, that the rest mass need not be constant along the worldline, i.e., that it may be a function of proper time τ . This happens, e.g., for a rocket that loses mass by way of exhausting gas. In this case the equation $F^\mu(\tau) = dp^\mu(\tau)/d\tau$ is still valid, with $p^\mu(\tau) = m(\tau)u^\mu(\tau)$.

2.5 Classical photons

In special relativity, we want to define a *classical photon* as the limiting case of a force-free particle when the (constant) speed goes to c . Such a particle may be used for modelling the free propagation of light. (“Free” means that the light is not influenced by a medium and not reflected at obstacles etc.) We deliberately speak of a “classical” photon to emphasise the obvious fact that this notion is not to be confused with the notion of a photon in the sense of quantum field theory.

We first observe that proper time, and hence the notion of a four-velocity, cannot be defined for a classical photon, because the equation

$$\frac{dt}{d\tau} = \frac{1}{\sqrt{1 - \frac{v^2}{c^2}}}$$

implies that $d\tau/dt$ goes to zero if v goes to c . (For this reason, it is occasionally said that “proper time stands still for light”.)

However, because of the equations

$$p^i = \frac{m v^i}{\sqrt{1 - \frac{v^2}{c^2}}}$$

and

$$p^0 = \frac{m c}{\sqrt{1 - \frac{v^2}{c^2}}} ,$$

a classical photon can have a finite four-momentum provided we assign to it the mass $m = 0$.

For this reason, we define a classical photon as a particle with constant lightlike four-momentum p^μ ,

$$0 = \eta_{\mu\nu} p^\mu p^\nu =$$

$$-(p^0)^2 + (p^1)^2 + (p^2)^2 + (p^3)^2 ,$$

and mass $m = 0$.

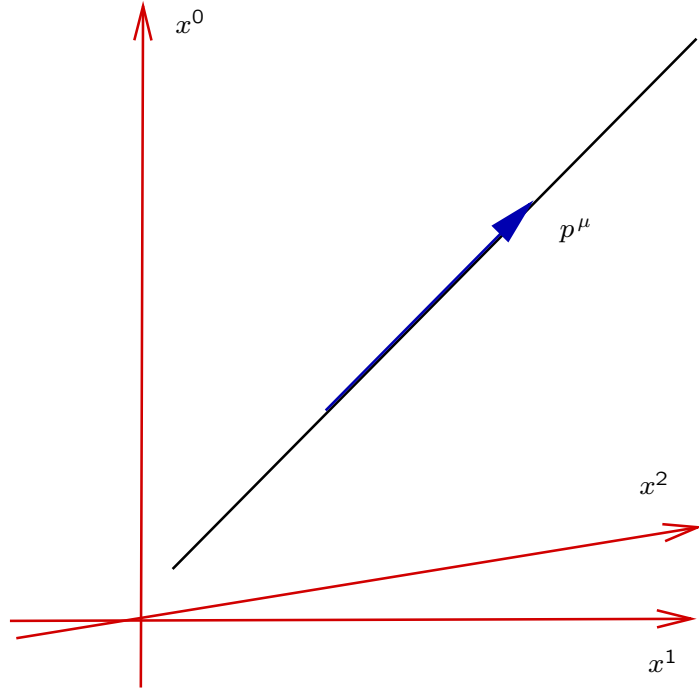


Figure 18: Four-momentum p^μ of a photon

As a consequence, the energy of a classical photon can be written in terms of its three-momentum as

$$E = c p^0 = c \sqrt{(p^1)^2 + (p^2)^2 + (p^3)^2} = c |\vec{p}| . \quad (41)$$

To illustrate the notion of a classical photon with a calculation, we will now derive the formulas for Doppler effect and aberration.

To that end, we consider an observer with constant four-velocity u^μ , and we decompose the four-momentum p^μ of a photon into components parallel and orthogonal to u^μ ,

$$p^\mu = \alpha u^\mu - \beta n^\mu \quad (42)$$

with

$$\eta_{\mu\nu} u^\mu u^\nu = -c^2, \quad (43)$$

$$\eta_{\mu\nu} u^\mu n^\nu = 0, \quad (44)$$

$$\eta_{\mu\nu} n^\mu n^\nu = 1. \quad (45)$$

We choose the coefficients α and β positive. Because of the minus sign this means that the unit vector n^μ indicates the direction from which the photon comes.

In order to determine the coefficients α and β , we calculate

$$0 = \eta_{\mu\nu} p^\mu p^\nu = \alpha^2 \underbrace{\eta_{\mu\nu} u^\mu u^\nu}_{=-c^2} - 2\alpha\beta \underbrace{\eta_{\mu\nu} u^\mu n^\nu}_{=0} + \beta^2 \underbrace{\eta_{\mu\nu} n^\mu n^\nu}_{=1} = -\alpha^2 c^2 + \beta^2.$$

As α and β are positive, we find $\beta = \alpha c$ and hence

$$p^\mu = \alpha (u^\mu - c n^\mu). \quad (46)$$

The meaning of α becomes clear if we consider the rest system of the chosen observer,

$$(u^\mu) = \begin{pmatrix} c \\ 0 \\ 0 \\ 0 \end{pmatrix}, \quad (n^\mu) = \begin{pmatrix} 0 \\ n^1 \\ n^2 \\ n^3 \end{pmatrix}. \quad (47)$$

Then we find $p^0 = \alpha c$. As p^0 is related to the energy E via $p^0 = E/c$, this implies $\alpha = E/c^2$, hence

$$p^\mu = \frac{E}{c^2} (u^\mu - c n^\mu). \quad (48)$$

For deriving the Doppler and aberration formulas, we write our decomposition with respect to two different observers:

$$p^\mu = \frac{E}{c^2} (u^\mu - c n^\mu) = \frac{\tilde{E}}{c^2} (\tilde{u}^\mu - c \tilde{n}^\mu). \quad (49)$$

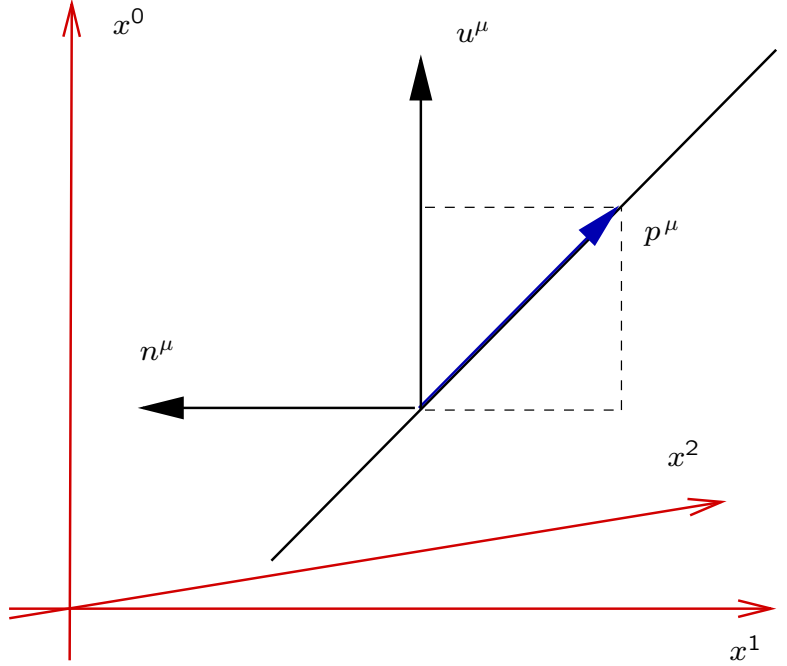


Figure 19: Decomposition of the four-momentum of a photon into spatial and temporal parts

In the rest system of the untwiddled observer, we have

$$(u^\mu) = \begin{pmatrix} c \\ 0 \\ 0 \\ 0 \end{pmatrix}, \quad (n^\mu) = \begin{pmatrix} 0 \\ n^1 \\ n^2 \\ n^3 \end{pmatrix}, \quad (\tilde{u}^\mu) = \frac{1}{\sqrt{1 - \frac{v^2}{c^2}}} \begin{pmatrix} c \\ v^1 \\ v^2 \\ v^3 \end{pmatrix}, \quad (50)$$

with v^i denoting the three-velocity of the twiddled observer in the rest system of the untwiddled one. Hence

$$\eta_{\mu\nu} p^\mu \tilde{u}^\nu = \frac{E}{c^2} \left(\underbrace{\eta_{\mu\nu} u^\mu \tilde{u}^\nu}_{= -c^2 / \sqrt{1 - \frac{v^2}{c^2}}} - c \underbrace{\eta_{\mu\nu} n^\mu \tilde{u}^\nu}_{= \vec{n} \cdot \vec{v} / \sqrt{1 - \frac{v^2}{c^2}}} \right) = \frac{\tilde{E}}{c^2} \left(\underbrace{\eta_{\mu\nu} \tilde{u}^\mu \tilde{u}^\nu}_{= -c^2} - c \underbrace{\eta_{\mu\nu} \tilde{n}^\mu \tilde{u}^\nu}_{= 0} \right),$$

which gives us the Doppler formula

$$\frac{\tilde{E}}{E} = \frac{1 + \frac{\vec{n} \cdot \vec{v}}{c}}{\sqrt{1 - \frac{v^2}{c^2}}}. \quad (51)$$

According to special relativity, there is not only a longitudinal but also a transverse Doppler effect, i.e., \tilde{E} and E are different even if \vec{n} is perpendicular to \vec{v} :

Longitudinal Doppler effekt ($\vec{n} \parallel \vec{v}$):
$$\frac{\tilde{E}}{E} = \frac{1 \pm \frac{v}{c}}{\sqrt{1 - \frac{v^2}{c^2}}} = 1 \pm \frac{v}{c} + O\left(\frac{v^2}{c^2}\right).$$

Transverse Doppler effekt ($\vec{n} \perp \vec{v}$):
$$\frac{\tilde{E}}{E} = \frac{1}{\sqrt{1 - \frac{v^2}{c^2}}} = 1 + O\left(\frac{v^2}{c^2}\right).$$

For deriving the aberration formula, we write the Doppler formula twice, once in the form just derived and then for the case that the two observers are interchanged. As in the latter case the replacements $E \mapsto \tilde{E}$, $\tilde{E} \mapsto E$, $\vec{v} \mapsto -\vec{v}$ und $\vec{n} \mapsto \vec{\tilde{n}}$ have to be made, we find

$$\frac{\tilde{E}}{E} = \frac{1 + \frac{\vec{n} \cdot \vec{v}}{c}}{\sqrt{1 - \frac{v^2}{c^2}}} \quad \text{und} \quad \frac{E}{\tilde{E}} = \frac{1 - \frac{\vec{\tilde{n}} \cdot \vec{v}}{c}}{\sqrt{1 - \frac{v^2}{c^2}}}.$$

Multiplying these two equations with each other results in

$$1 = \frac{\left(1 + \frac{\vec{n} \cdot \vec{v}}{c}\right) \left(1 - \frac{\vec{\tilde{n}} \cdot \vec{v}}{c}\right)}{1 - \frac{v^2}{c^2}}. \quad (52)$$

To get the standard formulas, we denote the angle with respect to the direction of relative motion by θ and $\tilde{\theta}$ respectively, $\vec{n} \cdot \vec{v} = v \cos \theta$ und $\vec{n} \cdot \vec{v} = v \cos \tilde{\theta}$.

This results in

$$\begin{aligned} 1 - \frac{v}{c} \cos \tilde{\theta} &= \frac{1 - \frac{v^2}{c^2}}{1 + \frac{v}{c} \cos \theta}, \\ -\frac{v}{c} \cos \tilde{\theta} &= \frac{\cancel{1} - \frac{v^2}{c^2} - \cancel{1} + \frac{v}{c} \cos \theta}{1 + \frac{v}{c} \cos \theta} \\ &= -\frac{v}{c} \frac{\left(\frac{v}{c} + \cos \theta\right)}{\left(1 + \frac{v}{c} \cos \theta\right)}, \end{aligned}$$

from which we read the aberration formula

$$\cos \tilde{\theta} = \frac{\cos \theta + \frac{v}{c}}{1 + \frac{v}{c} \cos \theta}. \quad (53)$$

With $\sin \tilde{\theta} = \sqrt{1 - \cos^2 \tilde{\theta}}$ this can be equivalently rewritten as

$$\sin \tilde{\theta} = \sqrt{1 - \frac{v^2}{c^2}} \frac{\sin \theta}{\left(1 + \frac{v}{c} \cos \theta\right)}. \quad (54)$$

Another equivalent form of the aberration formula follows if we use the trigonometric identity

$$\tan \frac{\tilde{\theta}}{2} = \frac{\sin \tilde{\theta}}{1 + \cos \tilde{\theta}}. \quad (55)$$

Then the aberration formula becomes

$$\tan \frac{\tilde{\theta}}{2} = \sqrt{\frac{c-v}{c+v}} \tan \frac{\theta}{2}. \quad (56)$$

The latter formula was found by Roger Penrose in the 1950s. It is less well known than the versions mentioned earlier. (It is rarely given in text-books. A noticeable exception is the book by W. Rindler: *Relativity*, Oxford UP (2001).) Penrose's formula is particularly instructive, see Fig. 20. As \tan is a positive and monotonically increasing function on the interval $[0, \pi/2]$, it tells us immediately the following: The faster the twiddled observer moves with respect to the untwiddled one, the more his celestial sphere is contracted in the forward direction and expanded in the backward direction. As a consequence, a rocket acts like a magnifying glass for an observer who looks out of the back window, and like a demagnifying glass for an observer who looks out of the front window. Of course, the effect is noticeable only if the speed is close to the speed of light.

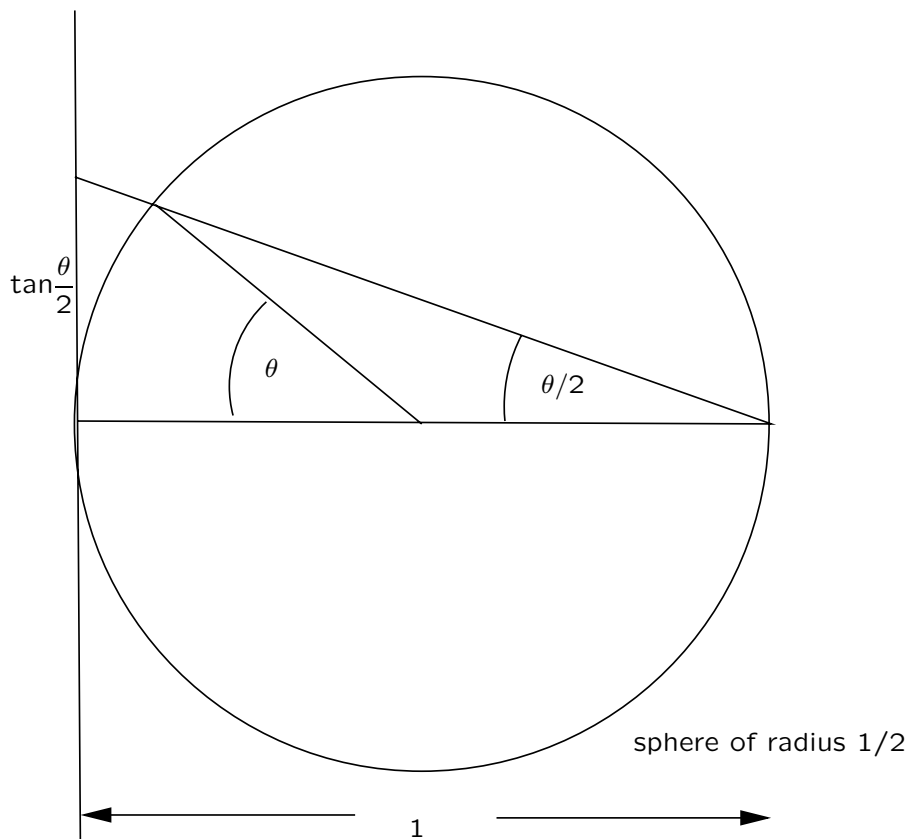


Figure 20: Illustration of Penrose's aberration formula

Aberration causes an apparent motion of stars on the sky: When the Earth goes around the Sun in one year, the stars move along an ellipse which becomes a circle for a star at the pole of the ecliptic. The correct explanation for this phenomenon was given in 1727 by James Bradley. Of course, Bradley didn't know anything about relativity. His explanation was based on a non-relativistic consideration of aberration which differs from the exact formula by omitting all terms of quadratic and higher order in v/c . The aberration of star light demonstrates in the most direct way the finiteness of the speed of light and the fact that Earth is moving with respect to the distant stars.

For an instructive visualisation of aberration see Norbert Dragon's "Relativistic flight through Stonehenge" at <https://www.itp.uni-hannover.de/435.html>.

2.6 Continuum mechanics

The motion of a material continuum (“fluid”) is described by a four-velocity field

$$U^\rho(x^0, x^1, x^2, x^3) = U^\rho(x). \quad (57)$$

We require the fluid to move at subluminal speed, $\eta_{\rho\sigma}U^\rho(x)U^\sigma(x) < 0$, so we can normalise the four-velocity according to

$$\eta_{\rho\sigma}U^\rho(x)U^\sigma(x) = -c^2. \quad (58)$$

The integral curves of $U^\mu(x)$ are called the *flow lines* of the fluid. An observer whose worldline is a flow line is called a *comoving observer*.

In any inertial system, we have

$$(U^\rho(x)) = \frac{1}{\sqrt{1 - \frac{V(x)^2}{c^2}}} \begin{pmatrix} c \\ V^1(x) \\ V^2(x) \\ V^3(x) \end{pmatrix}. \quad (59)$$

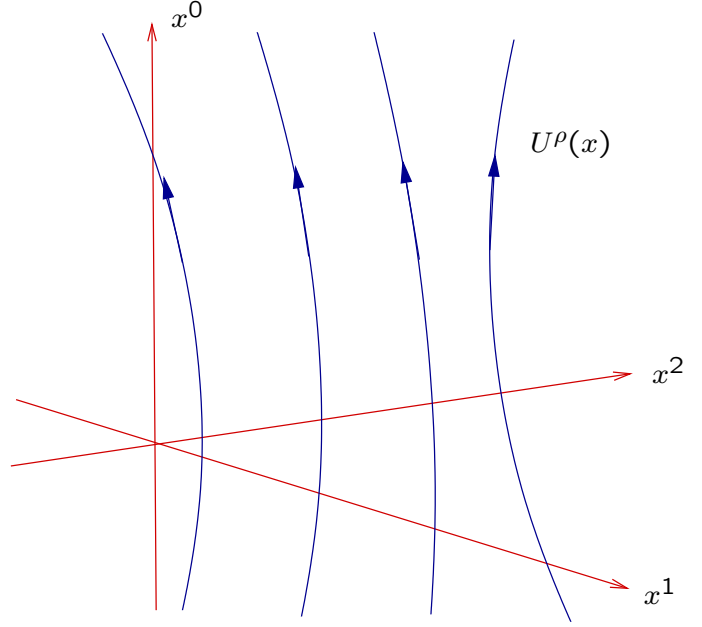


Figure 21: Four-velocity field $U^\rho(x)$ of a fluid

If we denote by u^σ the four-velocity of the observers who are at rest in the chosen inertial system, i.e.,

$$(u^\sigma) = \begin{pmatrix} c \\ 0 \\ 0 \\ 0 \end{pmatrix}, \quad (60)$$

we have

$$\eta_{\rho\sigma}U^\rho(x)u^\sigma = \frac{-c^2}{\sqrt{1 - \frac{V(x)^2}{c^2}}}. \quad (61)$$

$V^i(x)$ is the usual (three-)velocity field of the fluid in the chosen inertial system. For any one event x , we can find an inertial system such that $V^i(x) = 0$. This is called the *rest system* for the fluid at x .

We now want to introduce the *energy density* $\varepsilon(x)$ of the fluid:

$$\varepsilon(x) = \frac{\text{energy}}{\text{volume}} = \frac{\text{rest energy} + \text{kinetic energy} + \text{interaction energy}}{\text{volume}}. \quad (62)$$

As neither the energy nor the volume is a Lorentz invariant, we expect that $\varepsilon(x)$ depends on the chosen inertial system. How does $\varepsilon(x)$ depend on u^μ ?

First we consider the simplest case, namely the case where there is no interaction energy. In this case we speak of an “incoherent fluid” or a “dust”. Then the energy, recall (39), contained in a small volume around x is

$$\begin{aligned} E &= \frac{m c^2}{\sqrt{1 - \frac{V(x)^2}{c^2}}} \\ &= -m \eta_{\rho\sigma} U^\rho(x) u^\sigma, \end{aligned} \quad (63)$$

where m is the mass. Because of length contraction, the volume measured in the inertial system is

$$\begin{aligned} \text{Vol} &= \sqrt{1 - \frac{V(x)^2}{c^2}} \text{Vol}_0 \\ &= \frac{-c^2 \text{Vol}_0}{\eta_{\tau\lambda} U^\tau(x) u^\lambda}, \end{aligned} \quad (64)$$

where Vol_0 is the volume in the rest system of the fluid, see Fig. 22.

This gives the following expression for the energy density:

$$\begin{aligned} \varepsilon(x) &= \frac{E}{\text{Vol}} = \frac{m c^2}{\text{Vol}_0 \left(1 - \frac{V(x)^2}{c^2}\right)} \\ &= \frac{m \eta_{\rho\sigma} U^\rho(x) u^\sigma \eta_{\tau\lambda} U^\tau(x) u^\lambda}{\text{Vol}_0 c^2} = \frac{\mu(x)}{c^2} U_\sigma(x) U_\lambda(x) u^\sigma u^\lambda \end{aligned} \quad (65)$$

where

$$\mu(x) = \frac{m}{\text{Vol}_0} \quad (66)$$

is the mass density in the rest system. So we see that $\varepsilon(x)$ is a quadratic form in the dimensionless variable u^μ/c ,

$$\varepsilon(x) = T_{\sigma\lambda}(x) \frac{u^\sigma}{c} \frac{u^\lambda}{c} \quad (67)$$

where

$$T_{\sigma\lambda}(x) = \mu(x) U_\sigma(x) U_\lambda(x) \quad (68)$$

is the *energy-momentum tensor* field of the dust. For the time being, the $T_{\sigma\lambda}$ can be thought of as a 4×4 -matrix. In a terminology to be made precise later, they form a *second rank tensor field*.

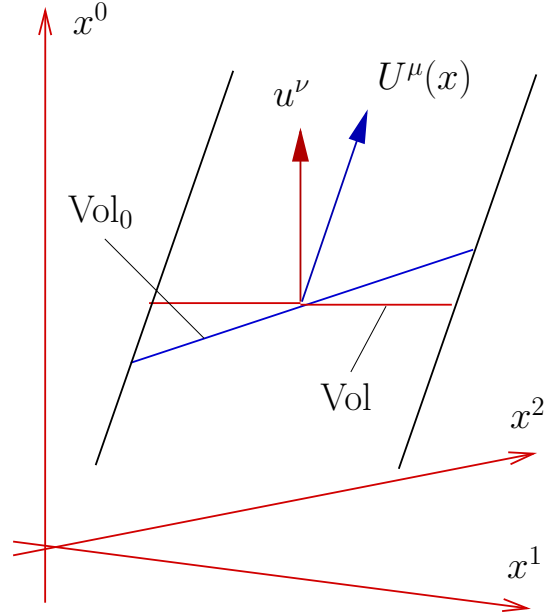


Figure 22: Transformation of the volume element

We observe the following.

- $T_{\sigma\rho}(x)$ is symmetric, $T_{\sigma\rho}(x) = T_{\rho\sigma}(x)$.
- $S^\sigma(x) = -T^{\sigma\rho}(x)u_\rho$ defines the *energy current* four-vector field of the fluid with respect to u^ν . This can be seen by decomposing it into temporal and spatial components:

$$S^0(x) = -T^{0\rho}(x)u_\rho = -\mu(x)U^0(x)U^\rho(x)u_\rho = \frac{\mu(x)c^3}{1 - \frac{V(x)^2}{c^2}} \text{ is the energy density times } c;$$

$$S^i(x) = -T^{i\rho}(x)u_\rho = -\mu(x)U^i(x)U^\rho(x)u_\rho = \frac{\mu(x)c^2}{1 - \frac{V(x)^2}{c^2}} V^i(x) \text{ is the spatial energy current.}$$

This is quite analogous to the electric current density J^σ we know from electrodynamics (see next section), just with the charge replaced by the energy.

- For a closed system (i.e., no external forces acting on the fluid), energy conservation should hold, i.e., S^σ should satisfy a continuity equation analogous to the charge conservation law $\partial_\rho J^\rho(x) = 0$,

$$0 = \partial_\rho S^\rho(x) = \partial_\rho (T^{\rho\sigma}(x)u_\sigma) = u_\sigma \partial_\rho T^{\rho\sigma}(x). \quad (69)$$

This holds in all inertial systems (i.e., for all u_σ with $u_\sigma u^\sigma = -c^2$) if and only if

$$\partial_\rho T^{\rho\sigma}(x) = 0. \quad (70)$$

The last equation is the energy conservation law the energy-momentum tensor field of a closed system has to satisfy. - If the system is not closed, $\partial_\rho T^{\rho\sigma}(x)$ gives the *force density* acting on the system.

The special form of the energy-momentum tensor field derived above holds for a dust only. More complicated matter models yield more complicated energy-momentum tensors. As a model more general than a dust, one can consider a *perfect fluid* whose energy-momentum tensor is of the following form:

$$T_{\rho\sigma}(x) = \left(\mu(x) + \frac{p(x)}{c^2} \right) U_\rho(x)U_\sigma(x) + p(x)\eta_{\rho\sigma}. \quad (71)$$

In addition to the mass density $\mu(x)$, a perfect fluid is characterised by a pressure, $p(x)$.

An energy-momentum tensor can be assigned not only to fluids but to any kind of field. E.g., there is an energy-momentum tensor for the electromagnetic field (see next section), for the Dirac field, for the Klein-Gordon field, etc. As the defining property of the energy-momentum tensor we view the fact that

$$\varepsilon(x) = T_{\rho\sigma}(x) \frac{u^\rho}{c} \frac{u^\sigma}{c} \quad (72)$$

gives the energy density measured at x by an observer with four-velocity u^ρ . As a possible antisymmetric part of $T_{\rho\sigma}(x)$ gives no contribution to the right-hand side, we require $T_{\rho\sigma}(x) = T_{\sigma\rho}(x)$. A “physically reasonable” energy-momentum tensor should satisfy the following conditions in addition.

- $T_{\rho\sigma}(x)u^\rho u^\sigma \geq 0$ for all timelike u^ρ , i.e., the energy density must not be negative (“weak energy condition”),
- $S^\rho(x) = -T^{\rho\sigma}(x)u_\sigma$ is non-spacelike for all timelike u^ρ , i.e. the energy current must not be superluminal (“dominant energy condition”).

More systematically, the energy-momentum tensor of a field can be derived from the Lagrange formalism (if the field theory under consideration admits a Lagrangian formulation). We will not pursue this approach here, but we mention that then the energy-momentum tensor may have an antisymmetric part, $T_{\rho\sigma} \neq T_{\sigma\rho}$. This is true, e.g., for spin fluids.

2.7 Electrodynamics

Maxwell’s equations, if written in traditional three-vector notation, read

$$(MI) : \quad \nabla \cdot \vec{B} = 0, \quad \nabla \times \vec{E} + \partial_t \vec{B} = \vec{0}, \quad (73)$$

$$(MII) : \quad \nabla \cdot \vec{D} = \rho, \quad \nabla \times \vec{H} - \partial_t \vec{D} = \vec{J}. \quad (74)$$

Following Gustav Mie and Arnold Sommerfeld, we call (\vec{E}, \vec{B}) the *field strengths* and (\vec{D}, \vec{H}) the *excitations*. (Unfortunately, it is still not uncommon to call \vec{H} the “magnetic field strength”. This is confusing because \vec{E} and \vec{B} produce the Lorentz force onto a charged particle, not \vec{E} and \vec{H} .) To give a determined system, Maxwell’s equations must be supplemented with constitutive relations that relate (\vec{E}, \vec{B}) to (\vec{D}, \vec{H}) . The constitutive relations characterise the medium. In vacuum they read

$$\vec{D} = \varepsilon_0 \vec{E}, \quad \vec{B} = \mu_0 \vec{H} \quad (75)$$

with constants of Nature ε_0 and μ_0 that satisfy the *Maxwell relation*

$$\sqrt{\varepsilon_0 \mu_0} = 1/c. \quad (76)$$

We will now recall the well-known fact that, even in the case without sources ($\rho = 0$ and $\vec{J} = \vec{0}$) and in vacuum ($\vec{D} = \varepsilon_0 \vec{E}$ and $\vec{B} = \mu_0 \vec{H}$), Maxwell’s equations are not invariant under Galilean transformations. The most instructive way of demonstrating this fact is by deriving the wave equations for \vec{E} and \vec{B} . From the “bac-cab-rule” for the ∇ operator we find

$$\nabla \times (\nabla \times \vec{E}) = \nabla(\nabla \cdot \vec{E}) - \Delta \vec{E} \quad \Longrightarrow \quad -\nabla \times (\partial_t \vec{B}) = \varepsilon_0 \nabla(\nabla \cdot \vec{D}) - \Delta \vec{E} \quad (77)$$

$$\Longrightarrow \quad -\partial_t(\nabla \times \vec{B}) = \vec{0} - \Delta \vec{E} \quad \Longrightarrow \quad \mu_0 \partial_t(\nabla \times \vec{H}) = \Delta \vec{E} \quad (78)$$

$$\Longrightarrow \quad \mu_0 \partial_t^2 \vec{D} = \Delta \vec{E} \quad \Longrightarrow \quad \mu_0 \varepsilon_0 \partial_t^2 \vec{E} = \Delta \vec{E} \quad (79)$$

and thus

$$\square \vec{E} := \Delta \vec{E} - \frac{1}{c^2} \partial_t^2 \vec{E} = \vec{0} \quad \text{with} \quad c = \frac{1}{\sqrt{\mu_0 \varepsilon_0}}. \quad (80)$$

Analogously, one shows that $\square \vec{B} = \vec{0}$. This demonstrates that, in the coordinate system in which Maxwell's equations hold, there are wave-like solutions for \vec{E} and \vec{B} that propagate in all spatial directions with speed c . If we now apply a Galilean transformation (e.g. in the x -direction, i.e., $\tilde{t} = t$, $\tilde{x} = x + vt$, $\tilde{y} = y$, $\tilde{z} = z$) to such a solution, it is obvious that the wave in the new coordinate system travels with different speeds in different directions, so it cannot be a solution of the wave equation in the new coordinates. But then, as the wave equation was derived from Maxwell's equations, it cannot be a solution of Maxwell's equations. This line of reasoning demonstrates the following: If one assumes that, according to pre-relativistic physics, inertial systems are related by a Galilean transformation, then the source-free vacuum Maxwell equations can hold only in one distinguished inertial system; this was called the “Ether system”. As the Earth rotates around the Sun, one would expect a motion of the Earth relative to the Ether. However, all attempts of detecting this relative motion, most notably the Michelson-Morley experiment, showed no result.

We will now demonstrate that Maxwell's (vacuum) equations without any modifications (i.e., without any “relativistic corrections”) are invariant under Lorentz transformations. According to special relativity they hold, indeed, in *any* inertial system. The Ether system could not be detected for the simple reason that it does not exist.

For a relativistic (4-dimensional) description of the electromagnetic field strengths we combine the three components of the vector field $\vec{E} = (E^1, E^2, E^3)$ and the three components of the vector field $\vec{B} = (B^1, B^2, B^3)$ into a 4×4 matrix (or, using a language that will be made precise later, into a “second rank tensor”):

$$(F^{\mu\nu}) = \begin{pmatrix} 0 & -E^1/c & -E^2/c & -E^3/c \\ E^1/c & 0 & -B^3 & B^2 \\ E^2/c & B^3 & 0 & -B^1 \\ E^3/c & -B^2 & B^1 & 0 \end{pmatrix}. \quad (81)$$

An analogous construction is made with the three components of the vector field $\vec{D} = (D^1, D^2, D^3)$ and the three components of the vector field $\vec{H} = (H^1, H^2, H^3)$:

$$(G^{\mu\nu}) = \begin{pmatrix} 0 & -cD^1 & -cD^2 & -cD^3 \\ cD^1 & 0 & -H^3 & H^2 \\ cD^2 & H^3 & 0 & -H^1 \\ cD^3 & -H^2 & H^1 & 0 \end{pmatrix}. \quad (82)$$

Note the antisymmetry of $F^{\mu\nu}$ and $G^{\mu\nu}$,

$$F^{\mu\nu} = -F^{\nu\mu}, \quad G^{\mu\nu} = -G^{\nu\mu}. \quad (83)$$

The charge density ρ and the current density $\vec{J} = (J^1, J^2, J^3)$ are being merged into a column vector with four components:

$$(J^\mu) = \begin{pmatrix} c\rho \\ J^1 \\ J^2 \\ J^3 \end{pmatrix}. \quad (84)$$

Recall our rule that greek indices will be raised and lowered with the help of the Minkowski metric, e.g.

$$F^\mu{}_\rho = F^{\mu\nu}\eta_{\nu\rho} = -F^{\nu\mu}\eta_{\nu\rho} = -F_\rho{}^\mu, \quad (85)$$

$$F_{\rho\sigma} = F^{\mu\nu}\eta_{\mu\rho}\eta_{\nu\sigma} = -F^{\nu\mu}\eta_{\mu\rho}\eta_{\nu\sigma} = -F_{\sigma\rho}. \quad (86)$$

In matrix form, we have e.g.

$$(F_{\mu\nu}) = \begin{pmatrix} 0 & E^1/c & E^2/c & E^3/c \\ -E^1/c & 0 & -B^3 & B^2 \\ -E^2/c & B^3 & 0 & -B^1 \\ -E^3/c & -B^2 & B^1 & 0 \end{pmatrix}. \quad (87)$$

This allows to rewrite Maxwell's equations in the following compact form:

$$(\text{MI}) : \quad \partial_\mu F_{\nu\sigma} + \partial_\nu F_{\sigma\mu} + \partial_\sigma F_{\mu\nu} = 0, \quad (88)$$

$$(\text{MII}) : \quad \partial_\mu G^{\mu\rho} = J^\rho. \quad (89)$$

Proof:

$$\begin{aligned} (\text{MI}) : \quad \partial_1 F_{23} + \partial_2 F_{31} + \partial_3 F_{12} = 0 & \iff -\partial_1 B^1 - \partial_2 B^2 - \partial_3 B^3 = 0 \\ \partial_0 F_{12} + \partial_1 F_{20} + \partial_2 F_{01} = 0 & \iff -\frac{1}{c} \partial_t B^3 - \partial_1 \frac{E^2}{c} + \partial_2 \frac{E^1}{c} = 0 \\ \partial_0 F_{23} + \partial_2 F_{30} + \partial_3 F_{02} = 0 & \iff -\frac{1}{c} \partial_t B^1 - \partial_2 \frac{E^3}{c} + \partial_3 \frac{E^2}{c} = 0 \\ \partial_0 F_{31} + \partial_3 F_{10} + \partial_1 F_{03} = 0 & \iff -\frac{1}{c} \partial_t B^2 - \partial_3 \frac{E^1}{c} + \partial_1 \frac{E^3}{c} = 0 \\ (\text{MII}): \quad \partial_1 G^{10} + \partial_2 G^{20} + \partial_3 G^{30} = J^0 & \iff c \partial_1 D^1 + c \partial_2 D^2 + c \partial_3 D^3 = c \rho \\ \partial_0 G^{01} + \partial_2 G^{21} + \partial_3 G^{31} = J^1 & \iff -\frac{1}{c} \partial_t (c D^1) + \partial_2 H^3 - \partial_3 H^2 = J^1 \\ \partial_0 G^{02} + \partial_1 G^{12} + \partial_3 G^{32} = J^2 & \iff -\frac{1}{c} \partial_t (c D^2) + \partial_3 H^1 - \partial_1 H^3 = J^2 \\ \partial_0 G^{03} + \partial_1 G^{13} + \partial_2 G^{23} = J^3 & \iff -\frac{1}{c} \partial_t (c D^3) + \partial_1 H^2 - \partial_2 H^1 = J^3 \end{aligned}$$

Remarks:

- (i) $F^{\mu\nu}$ and $G^{\mu\nu}$ have to be related by *constitutive relations* that specify the medium. For vacuum, which is the simplest medium, the constitutive relations read

$$G^{\mu\nu} = \frac{1}{\mu_0} F^{\mu\nu}, \quad (90)$$

where μ_0 = permeability of the vacuum, ε_0 = permittivity of the vacuum, $\mu_0 \varepsilon_0 = c^{-2}$. Decomposing into $0i$ -components and into ij -components reproduces, indeed, the traditional form of the vacuum constitutive relations,

$$\vec{D} = \varepsilon_0 \vec{E} , \quad \vec{H} = \frac{1}{\mu_0} \vec{B} . \quad (91)$$

(ii) From (MII) we find the law of charge conservation:

$$\partial_\nu J^\nu = \underbrace{\partial_\nu \partial_\mu G^{\mu\nu}}_{=\partial_\mu \partial_\nu} = \partial_\mu \partial_\nu \underbrace{G^{\mu\nu}}_{=-G^{\nu\mu}} = -\partial_\mu \partial_\nu G^{\nu\mu} = -\partial_\nu \partial_\mu G^{\mu\nu} = -\partial_\nu J^\nu , \quad (92)$$

hence

$$\partial_\nu J^\nu = 0 . \quad (93)$$

This is the continuity equation in index notation. The traditional form is recovered by writing spatial and temporal parts separately,

$$0 = \partial_\nu J^\nu = \partial_0 J^0 + \partial_i J^i = \frac{1}{c} \partial_t(\rho) + \nabla \cdot \vec{J} = \partial_t \rho + \nabla \cdot \vec{J} . \quad (94)$$

(iii) (MI) can be written more concisely with the help of the so-called epsilon symbol $\epsilon^{\mu\nu\rho\sigma}$ which is defined by the following two properties: (E1) $\epsilon^{\mu\nu\rho\sigma}$ is totally antisymmetric; (E2) $\epsilon^{0123} = 1$. This is equivalent to saying that $\epsilon^{\mu\nu\rho\sigma}$ equals 1 if $(\mu\nu\rho\sigma)$ is an even permutation of (0123), it equals -1 if $(\mu\nu\rho\sigma)$ is an odd permutation of (0123), and it equals 0 if two indices are equal. With the help of the epsilon symbol, (MI) reads

$$\epsilon^{\mu\nu\rho\sigma} \partial_\nu F_{\rho\sigma} = 0 . \quad (95)$$

We will now demonstrate that Maxwell's equations are, indeed, invariant under Lorentz transformations

$$\tilde{x}^\mu = L^\mu{}_\nu x^\nu , \quad \eta_{\mu\rho} L^\mu{}_\nu L^\rho{}_\sigma = \eta_{\nu\sigma} . \quad (96)$$

We first calculate with the help of the chain rule

$$\partial_\nu = \frac{\partial}{\partial x^\nu} = \frac{\partial \tilde{x}^\mu}{\partial x^\nu} \frac{\partial}{\partial \tilde{x}^\mu} = L^\mu{}_\nu \tilde{\partial}_\mu . \quad (97)$$

If we denote the inverse matrix by L^{-1} , i.e.

$$L^\mu{}_\nu (L^{-1})^\nu{}_\sigma = \delta^\mu_\sigma = (L^{-1})^\mu{}_\tau L^\tau{}_\sigma , \quad (98)$$

this results in

$$\tilde{\partial}_\sigma = (L^{-1})^\nu{}_\sigma \partial_\nu . \quad (99)$$

We require the transformation behaviour

$$\tilde{F}^{\mu\nu} = L^\mu{}_\rho L^\nu{}_\sigma F^{\rho\sigma} , \quad \tilde{G}^{\mu\nu} = L^\mu{}_\rho L^\nu{}_\sigma G^{\rho\sigma} , \quad \tilde{J}^\mu = L^\mu{}_\rho J^\rho , \quad (100)$$

from which we can calculate the transformation behaviour of $F_{\mu\nu}$,

$$\tilde{F}_{\mu\nu} = \eta_{\mu\tau} \eta_{\nu\sigma} \tilde{F}^{\tau\sigma} = \eta_{\mu\tau} \eta_{\nu\sigma} L^\tau{}_\rho L^\sigma{}_\lambda F^{\rho\lambda} \quad \big| \quad L^\mu{}_\alpha L^\nu{}_\beta ,$$

$$L^\mu{}_\alpha L^\nu{}_\beta \tilde{F}_{\mu\nu} = \eta_{\alpha\rho} \eta_{\beta\lambda} F^{\rho\lambda} = F_{\alpha\beta} \quad | \quad (L^{-1})^\alpha{}_\kappa (L^{-1})^\beta{}_\gamma ,$$

$$\tilde{F}_{\kappa\gamma} = (L^{-1})^\alpha{}_\kappa (L^{-1})^\beta{}_\gamma F_{\alpha\beta} . \quad (101)$$

By an analogous calculation one finds the transformation behaviour for the mixed components,

$$\tilde{F}_\kappa{}^\lambda = (L^{-1})^\alpha{}_\kappa L^\lambda{}_\beta F_\alpha{}^\beta . \quad (102)$$

As a rule, upper indices transform with $L^\mu{}_\nu$ and lower indices transform with $(L^{-1})^\alpha{}_\beta$. It is now easy to verify the invariance of Maxwell's equations:

(MI): Assume that $0 = \partial_\mu F_{\nu\sigma} + \partial_\nu F_{\sigma\mu} + \partial_\sigma F_{\mu\nu}$ holds. By multiplying this equation with $(L^{-1})^\mu{}_\rho (L^{-1})^\nu{}_\beta (L^{-1})^\sigma{}_\gamma$ we find:

$$0 = \tilde{\partial}_\alpha \tilde{F}_{\beta\gamma} + \tilde{\partial}_\beta \tilde{F}_{\gamma\alpha} + \tilde{\partial}_\gamma \tilde{F}_{\alpha\beta} .$$

(MII): Assume that $J^\nu = \partial_\rho G^{\rho\nu}$ holds. By multiplying this equation with $L^\mu{}_\nu$ we find

$$\tilde{J}^\mu = L^\mu{}_\nu \partial_\rho G^{\rho\nu} = L^\mu{}_\nu \partial_\sigma G^{\rho\nu} \delta_\rho^\sigma = L^\mu{}_\nu \partial_\sigma G^{\rho\nu} (L^{-1})^\sigma{}_\tau L^\tau{}_\rho = \tilde{\partial}_\tau \tilde{G}^{\tau\mu} .$$

Note that we have only used that $(L^\rho{}_\mu)$ is invertible, but not that it preserves the Minkowski metric. Hence, the Maxwell equations (MI) and (MII) are even invariant under *arbitrary* linear transformations, not just under Lorentz transformations, when written in terms of $F_{\mu\nu}$ (lower indices) and $G^{\mu\nu}$ (upper indices).

We now consider the vacuum constitutive law. If we write this, again, in terms of $F_{\mu\nu}$ (lower indices) and $G^{\mu\nu}$ (upper indices), we see that we need the Minkowski metric,

$$F_{\rho\sigma} = \mu_0 G^{\mu\nu} \eta_{\mu\rho} \eta_{\nu\sigma} . \quad (103)$$

To demonstrate that this equation is invariant under Lorentz transformations, we assume that it holds in the untwiddled coordinates and find

$$\tilde{F}_{\tau\kappa} = (L^{-1})^\rho{}_\tau (L^{-1})^\sigma{}_\kappa F_{\rho\sigma} = (L^{-1})^\rho{}_\tau (L^{-1})^\sigma{}_\kappa \mu_0 G^{\mu\nu} \eta_{\mu\rho} \eta_{\nu\sigma} .$$

Now we use that $(L^\mu{}_\nu)$ is a Lorentz transformation,

$$\eta_{\mu\rho} = \eta_{\alpha\beta} L^\alpha{}_\mu L^\beta{}_\rho , \quad \eta_{\nu\sigma} = \eta_{\gamma\lambda} L^\gamma{}_\nu L^\lambda{}_\sigma ,$$

which results in

$$\tilde{F}_{\tau\kappa} = \mu_0 \delta_\tau^\beta \delta_\kappa^\lambda G^{\mu\nu} \eta_{\alpha\beta} \eta_{\gamma\lambda} L^\alpha{}_\mu L^\gamma{}_\nu = \mu_0 G^{\mu\nu} \eta_{\alpha\tau} \eta_{\gamma\kappa} L^\alpha{}_\mu L^\gamma{}_\nu = \mu_0 \tilde{G}^{\alpha\gamma} \eta_{\alpha\tau} \eta_{\gamma\kappa} .$$

This demonstrates that Maxwell's equations in vacuum are invariant under Lorentz transformations (but not under arbitrary linear coordinate transformations). As any two inertial systems are related by a Lorentz transformation (once we have fixed the origin and the units), according to special relativity Maxwell's vacuum equations hold in any inertial system if they hold in one inertial system. There is no distinguished "Ether system".

We will now calculate the tranformation behaviour of \vec{E} and \vec{B} for a boost

$$(L^\mu{}_\rho) = \begin{pmatrix} \cosh \eta & -\sinh \eta & 0 & 0 \\ -\sinh \eta & \cosh \eta & 0 & 0 \\ 0 & 0 & 1 & 0 \\ 0 & 0 & 0 & 1 \end{pmatrix}, \quad \tanh \eta = \frac{v}{c}. \quad (104)$$

To that end we write the equation $\tilde{F}^{\mu\nu} = L^\mu{}_\rho L^\nu{}_\sigma F^{\rho\sigma}$ in matrix form:

$$\begin{pmatrix} 0 & -\tilde{E}^1/c & -\tilde{E}^2/c & -\tilde{E}^3/c \\ \tilde{E}^1/c & 0 & -\tilde{B}^3 & \tilde{B}^2 \\ \tilde{E}^2/c & \tilde{B}^3 & 0 & -\tilde{B}^1 \\ \tilde{E}^3/c & -\tilde{B}^2 & \tilde{B}^1 & 0 \end{pmatrix} =$$

$$\begin{pmatrix} \cosh \eta & -\sinh \eta & 0 & 0 \\ -\sinh \eta & \cosh \eta & 0 & 0 \\ 0 & 0 & 1 & 0 \\ 0 & 0 & 0 & 1 \end{pmatrix} \begin{pmatrix} 0 & -E^1/c & -E^2/c & -E^3/c \\ E^1/c & 0 & -B^3 & B^2 \\ E^2/c & B^3 & 0 & -B^1 \\ E^3/c & -B^2 & B^1 & 0 \end{pmatrix} \begin{pmatrix} \cosh \eta & -\sinh \eta & 0 & 0 \\ -\sinh \eta & \cosh \eta & 0 & 0 \\ 0 & 0 & 1 & 0 \\ 0 & 0 & 0 & 1 \end{pmatrix} =$$

$$\begin{pmatrix} \cosh \eta & -\sinh \eta & 0 & 0 \\ -\sinh \eta & \cosh \eta & 0 & 0 \\ 0 & 0 & 1 & 0 \\ 0 & 0 & 0 & 1 \end{pmatrix} \begin{pmatrix} \sinh \eta \frac{E^1}{c} & -\cosh \eta \frac{E^1}{c} & -\frac{E^2}{c} & -\frac{E^3}{c} \\ \cosh \eta \frac{E^1}{c} & -\sinh \eta \frac{E^1}{c} & -B^3 & B^2 \\ \cosh \eta \frac{E^2}{c} - \sinh \eta B^3 & -\sinh \eta \frac{E^2}{c} + \cosh \eta B^3 & 0 & -B^1 \\ \cosh \eta \frac{E^3}{c} + \sinh \eta B^2 & -\sinh \eta \frac{E^3}{c} - \cosh \eta B^2 & B^1 & 0 \end{pmatrix} =$$

$$\begin{pmatrix} 0 & -\frac{E^1}{c} & -\cosh \eta \frac{E^2}{c} + \sinh \eta B^3 & -\cosh \eta \frac{E^3}{c} - \sinh \eta B^2 \\ \frac{E^1}{c} & 0 & \sinh \eta \frac{E^2}{c} - \cosh \eta B^3 & \sinh \eta \frac{E^3}{c} + \cosh \eta B^2 \\ \cosh \eta \frac{E^2}{c} - \sinh \eta B^3 & -\sinh \eta \frac{E^2}{c} + \cosh \eta B^3 & 0 & -B^1 \\ \cosh \eta \frac{E^3}{c} + \sinh \eta B^2 & -\sinh \eta \frac{E^3}{c} - \cosh \eta B^2 & B^1 & 0 \end{pmatrix}.$$

As the rapidity η is related to the relative speed v via $\tanh \eta = v/c$, hence

$$\cosh \eta = \frac{1}{\sqrt{1 - \frac{v^2}{c^2}}}, \quad \sinh \eta = \frac{v}{c \sqrt{1 - \frac{v^2}{c^2}}}, \quad (105)$$

we find the following transformation rules for \vec{E} and \vec{B} :

$$\tilde{E}^1 = E^1, \quad \tilde{B}^1 = B^1, \quad (106)$$

$$\tilde{E}^2 = \frac{E^2 - v B^3}{\sqrt{1 - \frac{v^2}{c^2}}}, \quad \tilde{B}^2 = \frac{\frac{v}{c^2} E^3 + B^2}{\sqrt{1 - \frac{v^2}{c^2}}}, \quad (107)$$

$$\tilde{E}^3 = \frac{E^3 + v B^2}{\sqrt{1 - \frac{v^2}{c^2}}}, \quad \tilde{B}^3 = \frac{-\frac{v}{c^2} E^2 + B^3}{\sqrt{1 - \frac{v^2}{c^2}}}. \quad (108)$$

Note that electric and magnetic components are mixed; what is an electrostatic field in the untwiddled inertial system ($\vec{B} = \vec{0}$), is an electromagnetic field with $\vec{E} \neq \vec{0}$ and $\vec{B} \neq \vec{0}$ in the twiddled inertial system.

It is not difficult to verify that under an arbitrary Lorentz transformation the two scalar quantities

$$I_1 = F_{\mu\nu} F^{\mu\nu} \quad \text{and} \quad I_2 = \epsilon^{\mu\nu\sigma\tau} F_{\mu\nu} F_{\sigma\tau} \quad (109)$$

remain unchanged. Here $\epsilon^{\mu\nu\sigma\tau}$ denotes the totally antisymmetric epsilon symbol, see p. 33. If expressed in terms of \vec{E} and \vec{B} , these two scalar invariants read

$$I_1 = F_{\mu\nu} F^{\mu\nu} = 2 F_{0i} F^{0i} + F_{jk} F^{jk} = 2 \left(-\frac{|\vec{E}|^2}{c^2} + |\vec{B}|^2 \right), \quad (110)$$

$$I_2 = \epsilon^{\mu\nu\sigma\tau} F_{\mu\nu} F_{\sigma\tau} = 4 F_{01} F_{23} + 4 F_{02} F_{31} + 4 F_{03} F_{12} = -\frac{4}{c} \vec{E} \cdot \vec{B}. \quad (111)$$

Plane harmonic waves have $I_1 = I_2 = 0$, i.e., \vec{E} and \vec{B} are perpendicular and the magnitude of \vec{E} equals the magnitude of $c\vec{B}$, in any inertial system.

The energy-momentum tensor of an electromagnetic field in vacuum reads

$$T_{\rho\sigma} = \frac{1}{\mu_0} \left(F_{\rho\alpha} F_{\sigma}^{\alpha} - \frac{1}{4} \eta_{\rho\sigma} F_{\alpha\beta} F^{\alpha\beta} \right). \quad (112)$$

and will be discussed in Worksheet 4.

Maxwell's equations determine the dynamics of the electromagnetic field. This must be supplemented with the Lorentz force equation which determines the dynamics of a charged particle in an electromagnetic field. We want to write the Lorentz force as a four-force using the index notation of special relativity.

Recall eq. (40): The four-force that acts on a particle with constant (rest) mass m is given as

$$F^{\mu} = \frac{dp^{\mu}}{d\tau} = \frac{d}{d\tau} (m u^{\mu}) = m \frac{du^{\mu}}{d\tau} = m \frac{d^2 x^{\mu}}{d\tau^2}. \quad (113)$$

If F^{μ} is known, this equation together with initial conditions determines the worldline $x^{\mu}(\tau)$.

We postulate that, for a particle with electric charge q in an electromagnetic field $F^{\mu\nu}$, the four-force is given by

$$F^\mu = q \eta_{\nu\sigma} u^\nu F^{\sigma\mu} . \quad (114)$$

This expression is known as the *relativistic Lorentz force*.

To motivate this postulate, we observe that F^μ satisfies the following two properties.

(T1) F^μ transforms according to $\tilde{F}^\mu = L^\mu_\gamma F^\gamma$ under a Lorentz transformation.

Proof: $\tilde{F}^\mu = q \eta_{\nu\sigma} \tilde{u}^\nu \tilde{F}^{\sigma\mu} = q \eta_{\nu\sigma} L^\nu_\alpha u^\alpha L^\sigma_\beta L^\mu_\gamma F^{\beta\gamma} = q \eta_{\alpha\beta} L^\mu_\gamma F^{\beta\gamma} = L^\mu_\gamma F^\gamma$.

(T2) For $v = 0$ one recovers the non-relativistic Lorentz force.

Proof: If $v = 0$, we have $F^0 = q \eta_{00} u^0 F^{00} = 0$ and $F^i = q \eta_{00} u^0 F^{0i} = q(-1)c(-E^i/c) = qE^i$ which is the familiar non-relativistic Lorentz force on a charge q with $v = 0$.

These two properties fix the relativistic Lorentz force uniquely.

The 0-component of the relativistic Lorentz force reads

$$F^0 = q \delta_{ij} u^i F^{j0} = q \delta_{ij} \frac{v^i}{\sqrt{1 - \frac{v^2}{c^2}}} \frac{E^j}{c} = \frac{q}{c} \frac{\vec{v} \cdot \vec{E}}{\sqrt{1 - \frac{v^2}{c^2}}} . \quad (115)$$

It gives the power (work per time) exerted by the electromagnetic field onto the particle,

$$F^0 = \frac{dp^0}{d\tau} = \frac{1}{\sqrt{1 - \frac{v^2}{c^2}}} \frac{dE}{dt} = \frac{q \vec{v} \cdot \vec{E}}{c \sqrt{1 - \frac{v^2}{c^2}}} \implies \frac{dE}{dt} = q \vec{v} \cdot \vec{E} . \quad (116)$$

Note that the magnetic field \vec{B} is doing no work.

The i -components of the relativistic Lorentz force equation read

$$F^1 = q \left(-u^0 F^{01} + u^2 F^{21} + u^3 F^{31} \right) = q \left(\frac{\not{c}}{\sqrt{1 - \frac{v^2}{c^2}}} \frac{E^1}{\not{c}} + \frac{v^2 B^3}{\sqrt{1 - \frac{v^2}{c^2}}} - \frac{v^3 B^2}{\sqrt{1 - \frac{v^2}{c^2}}} \right) ,$$

$$F^2 = q \left(-u^0 F^{02} + u^1 F^{12} + u^3 F^{32} \right) = q \left(\frac{\not{c}}{\sqrt{1 - \frac{v^2}{c^2}}} \frac{E^2}{\not{c}} - \frac{v^1 B^3}{\sqrt{1 - \frac{v^2}{c^2}}} + \frac{v^3 B^1}{\sqrt{1 - \frac{v^2}{c^2}}} \right) ,$$

$$F^3 = q \left(-u^0 F^{03} + u^1 F^{13} + u^2 F^{23} \right) = q \left(\frac{\not{c}}{\sqrt{1 - \frac{v^2}{c^2}}} \frac{E^3}{\not{c}} + \frac{v^1 B^2}{\sqrt{1 - \frac{v^2}{c^2}}} - \frac{v^2 B^1}{\sqrt{1 - \frac{v^2}{c^2}}} \right) .$$

They give the equation of motion of the particle,

$$\vec{F} = m \frac{d^2 \vec{x}}{d\tau^2} = \frac{q}{\sqrt{1 - \frac{v^2}{c^2}}} \left(\vec{E} + \vec{v} \times \vec{B} \right) \quad \text{where} \quad \vec{v} = \frac{d\vec{x}}{dt} . \quad (117)$$

After expressing τ -derivatives in terms of t -derivatives, one finds

$$\frac{m}{\sqrt{1 - \frac{v^2}{c^2}}} \frac{d}{dt} \left(\frac{1}{\sqrt{1 - \frac{v^2}{c^2}}} \frac{d\vec{x}}{dt} \right) = \frac{q}{\sqrt{1 - \frac{v^2}{c^2}}} \left(\vec{E} + \vec{v} \times \vec{B} \right). \quad (118)$$

For $v \ll c$ we may write, as a valid approximation,

$$\frac{1}{\sqrt{1 - \frac{v^2}{c^2}}} = 1 + \frac{1}{2} \frac{v^2}{c^2} + \dots \approx 1. \quad (119)$$

Then we recover the non-relativistic Lorentz force equation

$$\frac{d^2\vec{x}}{dt^2} = \frac{q}{m} \left(\vec{E} + \vec{v} \times \vec{B} \right). \quad (120)$$

3 Heuristic approach to general relativity

Soon after Einstein had established special relativity in 1905, he started thinking about how to include gravity. The obvious idea would be to modify Newtonian gravity in such a way that it becomes Lorentz invariant. However, all such attempts failed. After a struggle of 10 years, Einstein found the solution to this problem: One has to modify the underlying spacetime theory, i.e., one has to replace special relativity by general relativity. In this section we sketch the heuristic ideas that were essential for this insight. We begin with a discussion of why Newtonian gravity does not fit into special relativity.

Newtonian gravity is based on two equations, i.e., the field equation

$$\Delta\phi = 4\pi G\mu, \quad (121)$$

(ϕ = gravitational potential, μ = mass density, $\Delta = \partial/\partial(x^1)^2 + \partial/\partial(x^2)^2 + \partial/\partial(x^3)^2$ and G = Newton's gravitational constant) and the equation of motion

$$m \frac{d^2\vec{x}}{dt^2} = -m_S \nabla\phi, \quad (122)$$

($\vec{x}(t)$ = trajectory of a particle, $\nabla = (\partial/\partial x^1, \partial/\partial x^2, \partial/\partial x^3)$, m = inertial mass, m_S = gravitational mass).

Experiment shows that the quotient of inertial and gravitational mass is a constant of Nature, i.e., that we can choose the units such that $m = m_S$. In Newtonian gravity the equality of inertial and gravitational mass seems to be a coincidence; the theory would work equally well if it were not true.

Clearly, neither (121) nor (122) is Lorentz invariant. This is an immediate consequence of the fact that the operators Δ and ∇ involve only spatial derivatives. So, in contrast to Maxwell's electrodynamics, Newtonian gravity does not fit into special relativity. This is also quite clear

from the fact that (121) implies an action-at-a-distance: Juggling a mass here would change the gravitational field there without any delay, in contrast to the requirement from special relativity that superluminal signals should not be possible.

To remedy this, one could try to modify Newtonian gravity in such a way that it becomes Lorentz invariant. A fairly obvious suggestion is

$$\square\phi = 4\pi G\mu, \quad (123)$$

$$m \frac{d^2 x^\sigma}{d\tau^2} = -m_S \eta^{\sigma\nu} \partial_\nu \phi, \quad (124)$$

where $\square = \Delta - c^{-2} \partial_t^2$ is the wave operator. These equations are, indeed, Lorentz invariant provided that ϕ and μ are Lorentz invariant,

$$\tilde{\phi}(\tilde{x}^0, \tilde{x}^1, \tilde{x}^2, \tilde{x}^3) = \phi(x^0, x^1, x^2, x^3), \quad \tilde{\mu}(\tilde{x}^0, \tilde{x}^1, \tilde{x}^2, \tilde{x}^3) = \mu(x^0, x^1, x^2, x^3). \quad (125)$$

If one interprets μ as the mass density (mass divided by volume) in the chosen inertial system, this is of course not a reasonable assumption, because the volume undergoes length contraction. This could be remedied by the assumption that μ always denotes the mass density in the rest system. However, a problem remains with (124). Its 0-component

$$m \frac{d^2 x^0}{d\tau^2} = -\eta^{00} m_S \partial_0 \phi \quad \Longleftrightarrow \quad m \frac{d}{d\tau} \left(\frac{c}{\sqrt{1 - \frac{v^2}{c^2}}} \right) = m_S \frac{1}{c} \partial_t \phi \quad (126)$$

is in utter contradiction with experiments: For a time-independent gravitational field the right-hand side equals zero, so the equation would require v to be constant. This is of course nonsensical as planets and comets clearly move with nonconstant v in the Solar system. A possible modification of (124) would be

$$m \frac{d^2 x^\sigma}{d\tau^2} = -m_S \left(\eta^{\sigma\nu} - \frac{1}{c^2} \frac{dx^\sigma}{d\tau} \frac{dx^\nu}{d\tau} \right) \partial_\nu \phi. \quad (127)$$

The Lorentz invariant gravity theory based on (123) and (127) is known as *Nordström's first theory*. It was considered for a while but finally turned out to be in contradiction with experiments. As the gravitational field is described by a scalar quantity, ϕ , such theories are called “Lorentz invariant scalar theories of gravity”. Other variants of such theories were suggested, e.g., by Einstein, Mie and Nordström. All of them either have conceptual problems or are in contradiction with experiments.

As a possible remedy, theories were tried where the gravitational field is described by a more complicated mathematical object than a scalar. Actually, this seems quite natural: From special relativity we know that mass is but one form of energy and that it can be converted into other forms of energy. So it seems natural to assume that *any* sort of energy can be the source of a gravitational field. As we know from Section 2.6 that the energy density ε is a quadratic form in the four-velocity of the observer, $c^2 \varepsilon = T_{\rho\sigma} u^\rho u^\sigma$, this would mean that we have the energy-momentum tensor $T_{\rho\sigma}$ on the right-hand side of the field equation. But

then the gravitational field should also be described by a “quantity with two indices”, i.e., by a second-rank tensor field. Such “Lorentz invariant tensor theories of gravity” have been suggested by Einstein and others, but again they have either conceptual problems or are in contradiction with experiments.

Einstein tried to work out a relativistic theory of gravity from 1905 until 1915. During this ten-year-long struggle he became more and more convinced that gravity cannot be Lorentz invariant; instead of looking for a new gravity theory on spacetime as one knows it from special relativity, one has to change the theory of spacetime itself. Of course, then one needs new guiding principles of how to find such a new theory of spacetime. Einstein was led by three such principles which he called *equivalence principle*, *general relativity principle* and *Mach’s principle*. We will now discuss the equivalence principle in detail as it is of crucial relevance for general relativity. It will lead us to the conclusion that special relativity is valid only as a good approximation in “sufficiently small” spacetime regions, i.e., that it has to be replaced by a new spacetime theory. The quest for a Lorentz invariant theory of gravity will be given up. The equivalence principle starts out from the idea that the equality of inertial mass and gravitational mass is not just a coincidence but rather a fundamental law of nature:

Weak equivalence principle (first version): “inertial mass = gravitational mass”.

This can be rephrased in the following way:

Weak equivalence principle (second version): “The trajectory of a freely falling particle is uniquely determined by its initial position and its initial velocity”.

In this version, the weak equivalence principle is also known as the “universality of free fall” (UFF).

Another equivalent formulation is the following.

Weak equivalence principle (third version): “In a box that is freely falling in a homogeneous gravitational field all free-fall experiments are undistinguishable from free-fall experiments in a box that is at rest with respect to an inertial system.”

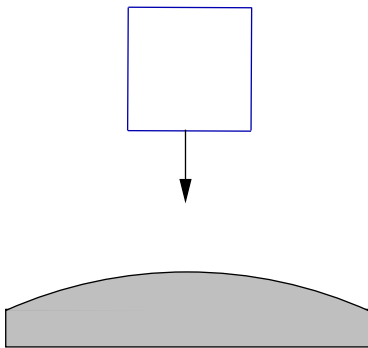


Figure 23: Freely falling box in a homogeneous gravitational field

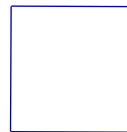


Figure 24: Box at rest with respect to an inertial system

In other words, as long as only freely falling objects are observed, an experimentalist cannot distinguish if he is in rectilinear uniform motion, far away from all gravitating masses, in a spaceship or in a freely falling elevator in a homogeneous gravitational field.

Finally, the following reformulation is of interest.

Weak equivalence principle (fourth version): “In a box that is standing in a homogeneous gravitational field all free-fall experiments are undistinguishable from free-fall experiments in a box that is uniformly accelerated with respect to an inertial system.”

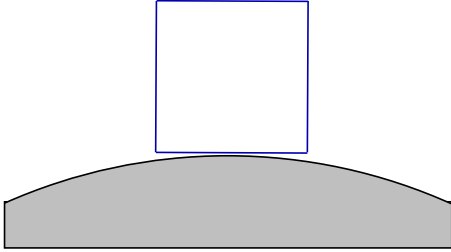


Figure 25: Box at rest in a homogeneous gravitational field

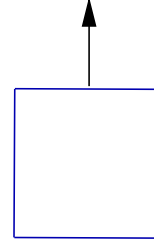


Figure 26: Box uniformly accelerated with respect to an inertial system

This means that, as far as free-fall experiments are concerned, a homogeneous gravitational field in a box can be mimicked by “pulling the box with constant acceleration through the universe”, far away from all gravitating masses. The acceleration must be of the same magnitude as the (constant) gravitational acceleration and directed in the opposite sense.

For the last two versions of the equivalence principle it is essential that the gravitational field can be viewed as homogeneous. The gravitational field around a celestial body, like the Earth or the Sun, is of course not homogeneous. However, we may apply this principle, e.g., to the gravitational field of the Earth if we choose the box sufficiently small; then the gravitational field inside the box can be viewed, to within a good approximation, as homogeneous. This is the situation shown in the diagrams. Note that the gravitational field of the Earth varies vertically; therefore, not only the spatial dimension of the freely falling box but also the duration of the experiment must be sufficiently small.

The equality of inertial and gravitational mass is experimentally well established. It was found by Galileo Galilei who allegedly performed free-fall experiments on the Leaning Tower of Pisa, and then re-established with higher accuracy, e.g., by Issac Newton and Friedrich Bessel. More precise measurements were made later:

- Eötvös, relative accuracy 10^{-7} (1889) ,
- Eöt-Wash, relative accuracy 10^{-13} (2001) .

A satellite experiment aiming at a relative accuracy of 10^{-15} was launched in April 2016. It is a project under French leadership, with participation from ZARM, Bremen, called MICROSCOPE (MICRO-Satellite à traînée Compensée pour l’Observation du Principe d’Equivalence). The satellite was decommissioned in October 2018. A first evaluation demonstrated that the weak equivalence principle was verified to within an accuracy of almost 10^{-15} . Further evaluations of the data taken may even improve this a bit. A NASA project called STEP (Satellite Test of the Equivalence Principle), aiming at a relative accuracy of 10^{-18} , was developed since the 1970s but has been cancelled, for the foreseeable future, because of funding cuts.

Because of Eötvös's measurements, the universality of free fall was fairly well established experimentally at the time of Einstein. However, people did not think that it would go beyond free-fall experiments. So one thought that, with the help of other experiments (from optics, electrodynamics, thermodynamics, etc.) the two situations could be distinguished. In contrast to this, Einstein formulated in 1907 the “strong equivalence principle” which he later called the “happiest thought of my life”.

Strong equivalence principle (first version): “In a box that is freely falling in a homogeneous gravitational field all experiments are undistinguishable from experiments in a box that is at rest with respect to an inertial system.”

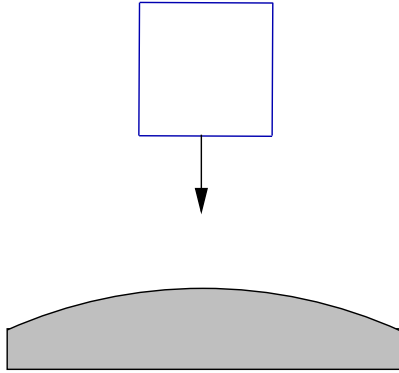


Figure 27: Freely falling box in a homogeneous gravitational field

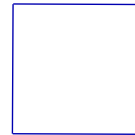


Figure 28: Box at rest with respect to an inertial system

This means that, in view of any experiment one could think of, a homogeneous gravitational field can be transformed away by going into a freely falling reference system. – If we consider the fourth version of the weak equivalence principle, the corresponding strong version reads as follows.

Strong equivalence principle (second version): “In a box that is standing in a homogeneous gravitational field all experiments are undistinguishable from experiments in a box that is uniformly accelerated with respect to an inertial system.”

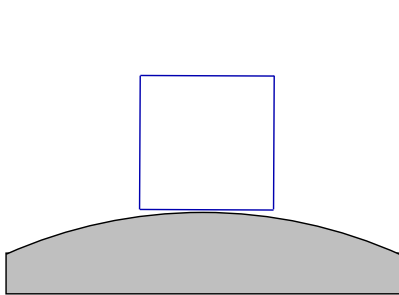


Figure 29: Box at rest in a homogeneous gravitational field

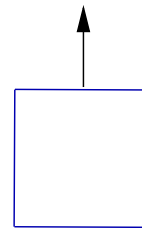


Figure 30: Box uniformly accelerated with respect to an inertial system

This is the most fruitful version of the strong equivalence principle. It says that, with respect to all experiments, a homogeneous gravitational field can be mimicked by an acceleration.

In a later modification of the strong equivalence principle (historically incorrectly called “Einstein’s equivalence principle”) one restricted to non-gravitational experiments (i.e., one excluded experiments where the gravitational attraction of two bodies inside the box played a role), and one divided the principle into *universality of free fall*, *local position invariance* and *local Lorentz invariance*. We will not discuss this modification here .

The second version of the strong equivalence principle allows to calculate all effects in a homogeneous gravitational field, on the basis of special relativity. One just has to transform from an inertial system to a uniformly accelerated system.

We will now illustrate this method by applying it to the motion of a classical photon. This will allow us to derive formulas for (i) the light deflection and (ii) the redshift in a homogeneous gravitational field.

To that end we have to consider an inertial system and then to introduce observers that move, relative to this inertial system, with constant acceleration a ($a^2 = \eta_{\mu\nu} a^\mu a^\nu$). We have already calculated the four-velocity of these *Rindler observers*, see (24) and (30),

$$(u^\mu(\tau)) = \left(\frac{dx^\mu(\tau)}{d\tau} \right) = \begin{pmatrix} c \cosh\left(\frac{a\tau}{c}\right) \\ c \sinh\left(\frac{a\tau}{c}\right) \\ 0 \\ 0 \end{pmatrix}. \quad (128)$$

We have chosen the x^1 -direction as the direction of relative motion, i.e., the gravitational field that is to be mimicked points into the negative x^1 -direction.

If we integrate the expression for $dx^\mu/d\tau$ over τ with initial conditions

$$(x^\mu(0)) = \begin{pmatrix} 0 \\ X \\ Y \\ Z \end{pmatrix}, \quad (129)$$

we get the worldlines of the accelerated observers, labeled by their spatial coordinates (X, Y, Z) in the inertial system at $t = 0$,

$$(x^\mu(\tau)) = \begin{pmatrix} \frac{c^2}{a} \sinh\left(\frac{a\tau}{c}\right) \\ \frac{c^2}{a} \cosh\left(\frac{a\tau}{c}\right) + X - \frac{c^2}{a} \\ Y \\ Z \end{pmatrix}. \quad (130)$$

(X, Y, Z) can be viewed as Cartesian coordinates of the points in the accelerated system.

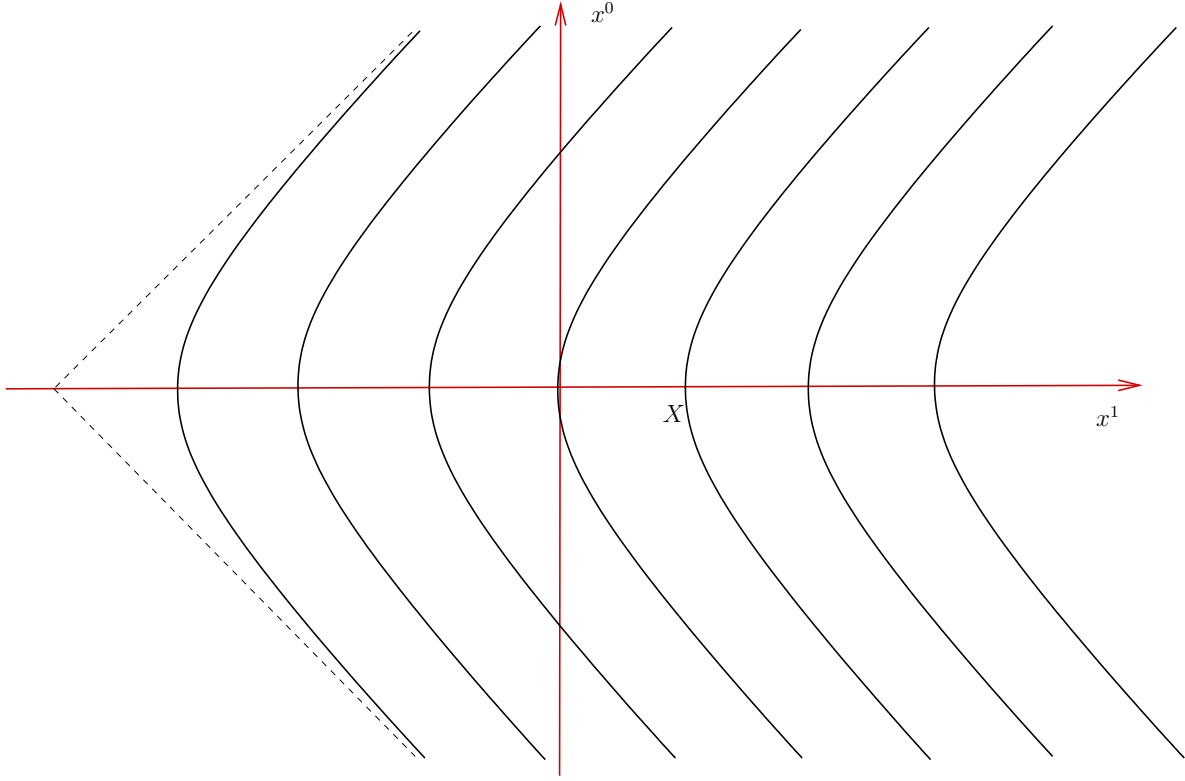


Figure 31: Worldlines of Rindler observers

We consider a classical photon moving, without loss of generality, in the x^1 - x^2 -plane,

$$(x_p^\mu(s)) = \begin{pmatrix} s \\ s \cos \vartheta \\ s \sin \vartheta \\ 0 \end{pmatrix}. \quad (131)$$

We have chosen the parameter s such that it coincides with the x^0 -coordinate. (Recall that there is no proper time for photons!) The trajectory of the photon in the accelerated system, i.e. X, Y and Z as functions of s , is found by equating $x^\mu(\tau)$ with $x_p^\mu(s)$,

$$s = \frac{c^2}{a} \sinh\left(\frac{a\tau}{c}\right), \quad (132)$$

$$s \cos \vartheta = \frac{c^2}{a} \cosh\left(\frac{a\tau}{c}\right) + X - \frac{c^2}{a}, \quad (133)$$

$$s \sin \vartheta = Y, \quad 0 = Z, \quad (134)$$

and then eliminating τ ,

$$X = \frac{c^2}{a} \left(1 - \sqrt{1 + \frac{s^2 a^2}{c^4}}\right) + s \cos \vartheta, \quad Y = s \sin \vartheta, \quad Z = 0.$$

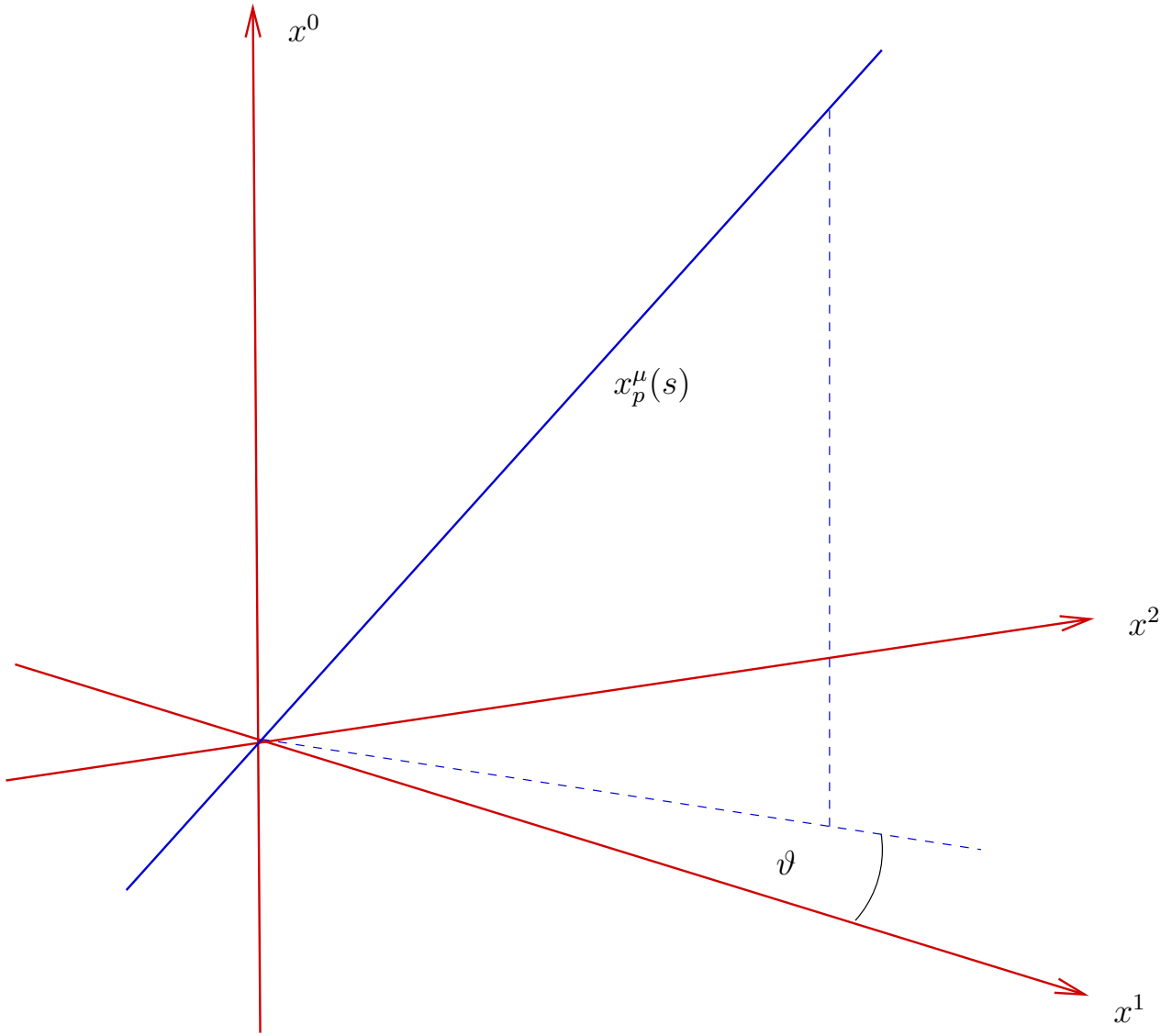


Figure 32: Worldline of a light ray

(i) We first calculate the light deflection, restricting to the case $\vartheta = \pi/2$:

$$X = \frac{c^2}{a} \left(1 - \sqrt{1 + \frac{s^2 a^2}{c^4}} \right), \quad Y = s \quad Z = 0. \quad (135)$$

This is the equation of a hyperbola, see Fig. 33,

$$\left(X - \frac{c^2}{a} \right)^2 - Y^2 = \frac{c^4}{a^2}. \quad (136)$$

In Fig. 33 we have chosen the X -axis vertical, to have the gravitational field to be mimicked pointing downward.

If $a^2 Y^2 \ll c^4$ the hyperbola can be approximated by a parabola,

$$X = \frac{c^2}{a} \left(1 - \sqrt{1 + \frac{a^2 Y^2}{c^4}} \right) \approx \frac{c^2}{a} \left(1 - 1 - \frac{a^2 Y^2}{2c^4} \right) = -\frac{a Y^2}{2c^2}. \quad (137)$$

If we want to mimic the gravitational field inside a (sufficiently small) laboratory on Earth, we have to choose

$$a = g = 9.81 \text{ m/s}^2. \quad (138)$$

Then the path of the photon deviates on a distance of $|Y| = 10 \text{ m}$ from a straight line by only

$$|X| \approx \frac{g Y^2}{2 c^2} \approx 5 \times 10^{-15} \text{ m}. \quad (139)$$

This is not more than about three times the diameter of a proton.

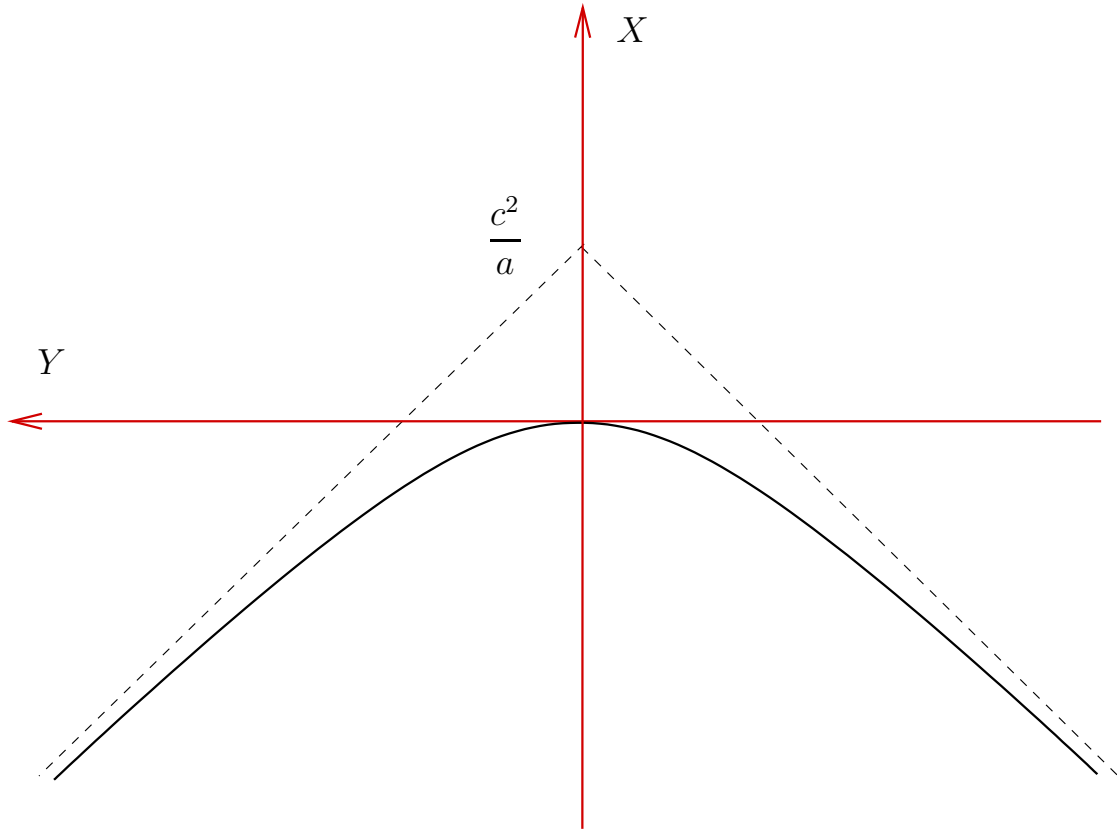


Figure 33: Trajectory of a light ray in an accelerated box

(ii) We calculate the redshift for $\vartheta = 0$:

$$s = \frac{c^2}{a} \sinh\left(\frac{a\tau}{c}\right), \quad s = \frac{c^2}{a} \cosh\left(\frac{a\tau}{c}\right) + X - \frac{c^2}{a}, \quad 0 = Y, \quad 0 = Z. \quad (140)$$

The four-momentum of the photon is of the form

$$(p^\mu) = k \begin{pmatrix} 1 \\ 1 \\ 0 \\ 0 \end{pmatrix}, \quad (141)$$

with a factor k that is to be determined later.

Recall that the four-velocity of the accelerated observers is

$$(u^\mu(\tau)) = \left(\frac{dx^\mu(\tau)}{d\tau}\right) = \begin{pmatrix} c \cosh\left(\frac{a\tau}{c}\right) \\ c \sinh\left(\frac{a\tau}{c}\right) \\ 0 \\ 0 \end{pmatrix}. \quad (142)$$

This implies

$$\eta_{\mu\nu} u^\mu(\tau) p^\nu = c k \left(-\cosh\left(\frac{a\tau}{c}\right) + \sinh\left(\frac{a\tau}{c}\right) \right) = c k \left(-\cancel{\frac{a}{c^2}} + \frac{aX}{c^2} - 1 + \cancel{\frac{a}{c^2}} \right). \quad (143)$$

On the other hand, p^μ can be decomposed into a part parallel to $u^\mu(\tau)$ and a part perpendicular to $u^\mu(\tau)$, recall (48),

$$p^\mu = \frac{E(\tau)}{c^2} \left(u^\mu(\tau) - c n^\mu(\tau) \right). \quad (144)$$

Here $E(\tau)$ is the energy of the photon with respect to an observer with four-velocity $u^\mu(\tau)$. This yields

$$\eta_{\mu\nu} u^\mu(\tau) p^\nu = \frac{E(\tau)}{c^2} \left(\underbrace{\eta_{\mu\nu} u^\mu(\tau) u^\nu(\tau)}_{=-c^2} - c \underbrace{\eta_{\mu\nu} u^\mu(\tau) n^\nu(\tau)}_{=0} \right) = -E(\tau). \quad (145)$$

Equating the two expressions for $\eta_{\mu\nu} u^\mu(\tau) p^\nu$ results in

$$E(\tau) = c k \left(1 - \frac{aX}{c^2} \right). \quad (146)$$

As the accelerated observer with $X = 0$ meets the photon at $\tau = 0$, we must have $E(0) = ck$ and hence

$$E(\tau) = E(0) - E(0) \frac{aX}{c^2}. \quad (147)$$

This gives us the desired redshift formula

$$\frac{\Delta E}{E} = \frac{E(\tau) - E(0)}{E(0)} = -\frac{aX}{c^2} . \quad (148)$$

For the gravitational field of the Earth ($a = g = 9.81 \text{ m/s}^2$) we find that a photon that travels upwards over a distance of $|X| = 22.5 \text{ m}$ undergoes a redshift of

$$\left| \frac{\Delta E}{E} \right| \approx 2 \times 10^{-15} . \quad (149)$$

This gravitational redshift was measured by Pound and Rebka in a building of 22.5 m height in the year 1959 with γ particles.

We have thus calculated two important effects – the light deflection and the redshift – in a homogeneous gravitational field, just with the help of the strong equivalence principle. We will discuss a third effect in the 5th Worksheet: We will find that an observer who compares two standard clocks, one directly next to him and another one at a lower position in a homogeneous gravitational field, will see the clock at the lower position go slower. This effect can be viewed as equivalent to the gravitational redshift, taking into account that frequency (\sim energy) and time are just inverse to each other. Therefore, it should not come as a surprise that the factor by which the two standard clocks differ is just the inverse of the redshift factor $E(\tau)/E(0) = 1 - aX/c^2$ calculated above.

For inhomogeneous gravitational fields, the strong equivalence principle alone does not allow us to calculate effects like the light deflection or the redshift; this will require the full apparatus of general relativity. However, the strong equivalence principle can serve as a guideline to the correct mathematical formalism of general relativity. The strong equivalence principle can be rephrased in the following way.

In a sufficiently small region of spacetime, the gravitational field can be approximated by a homogeneous gravitational field. It can then be “transformed away” by passing to a “freely falling elevator”. This means that, in a sufficiently small region of spacetime, special relativity holds with arbitrarily good accuracy.

This leads us to the following geometric idealisation, based on (the four-dimensional analogue of) the idea that a sufficiently small portion of a curved surface can be approximated arbitrarily well by its tangent plane.

A spacetime with a gravitational field is to be described by a curved “manifold”. At each event, the tangent space to this manifold looks like the spacetime of special relativity.

“The gravitational field” is the map that assigns to each point in spacetime the Minkowski metric on the tangent space attached to this point; in particular, this map determines the orientation of the light cone in each tangent space.

In order to translate this idea into precise mathematics, we need the definition of a “pseudo-Riemannian manifold”. The corresponding mathematical notions will be introduced in the next section.

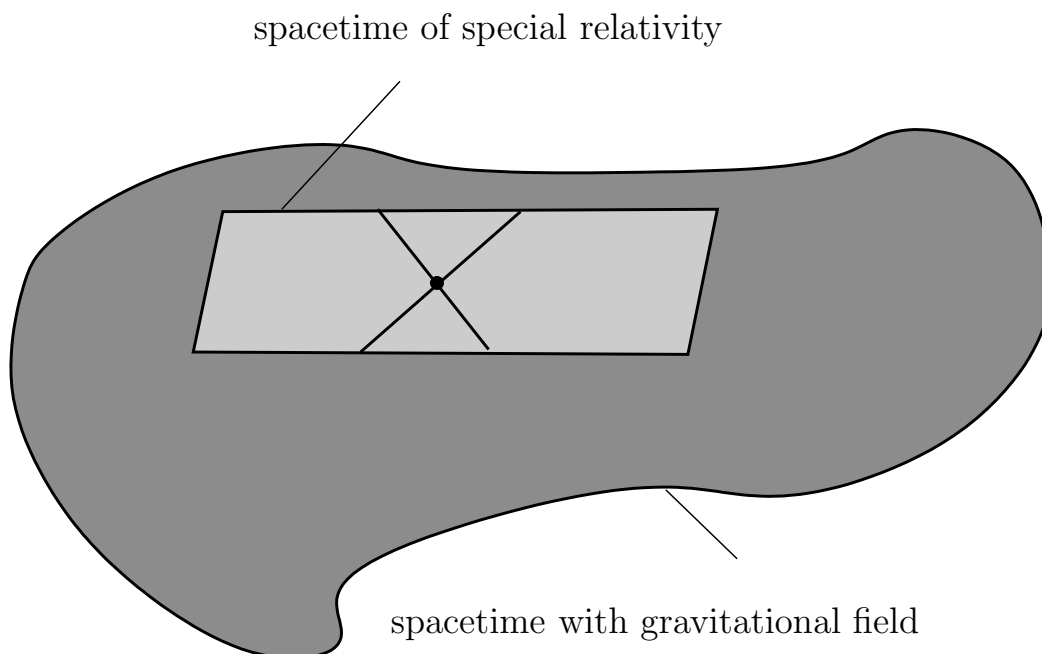


Figure 34: The spacetime of general relativity may be approximated by the spacetime of special relativity in sufficiently small spacetime regions

We have already mentioned that, in addition to the equivalence principle, Einstein was led by two other “principles”.

Principle of general relativity (Allgemeines Relativitätsprinzip): “All laws of Nature preserve their form under arbitrary coordinate changes.”

Mach’s principle: “The inertia of a body is determined by its relation to all other masses in the universe..”

We will discuss later to what extent these principles are actually realised in general relativity.

4 Basic concepts of differential geometry

4.1 Manifolds

Our first goal is to give a precise definition of a “manifold”, which will need a bit of preparation. Roughly speaking, a manifold is something on which the notion of differentiability is defined. Differentiability is introduced in terms of coordinate systems (“charts”). We begin with some preliminaries.

Definition: A *topological space* is a set M with a collection \mathcal{T} of subsets of M , such that the following holds.

- (a) $\emptyset \in \mathcal{T}$ and $M \in \mathcal{T}$.
- (b) If $U_\alpha \in \mathcal{T}$ for all $\alpha \in I$, then $\bigcup_{\alpha \in I} U_\alpha \in \mathcal{T}$. Here I denotes an arbitrary index set.
- (c) If $U_1 \in \mathcal{T}$ and $U_2 \in \mathcal{T}$, then $U_1 \cap U_2 \in \mathcal{T}$.

The elements of \mathcal{T} are called “open sets”.

\mathbb{R}^n , with the open sets defined as usual, is a topological space.

Definition: Let M be a topological space. An n -dimensional *local chart* for M is a map

$$\begin{aligned} \phi : U &\longrightarrow \mathcal{O} \\ p &\longmapsto \phi(p) = (x^1(p), \dots, x^n(p)) \end{aligned} \tag{150}$$

with the following properties.

- (a) U is an open subset of M .
- (b) \mathcal{O} is an open subset of \mathbb{R}^n .
- (c) ϕ maps every open subset of U bijectively onto an open subset of \mathcal{O} .

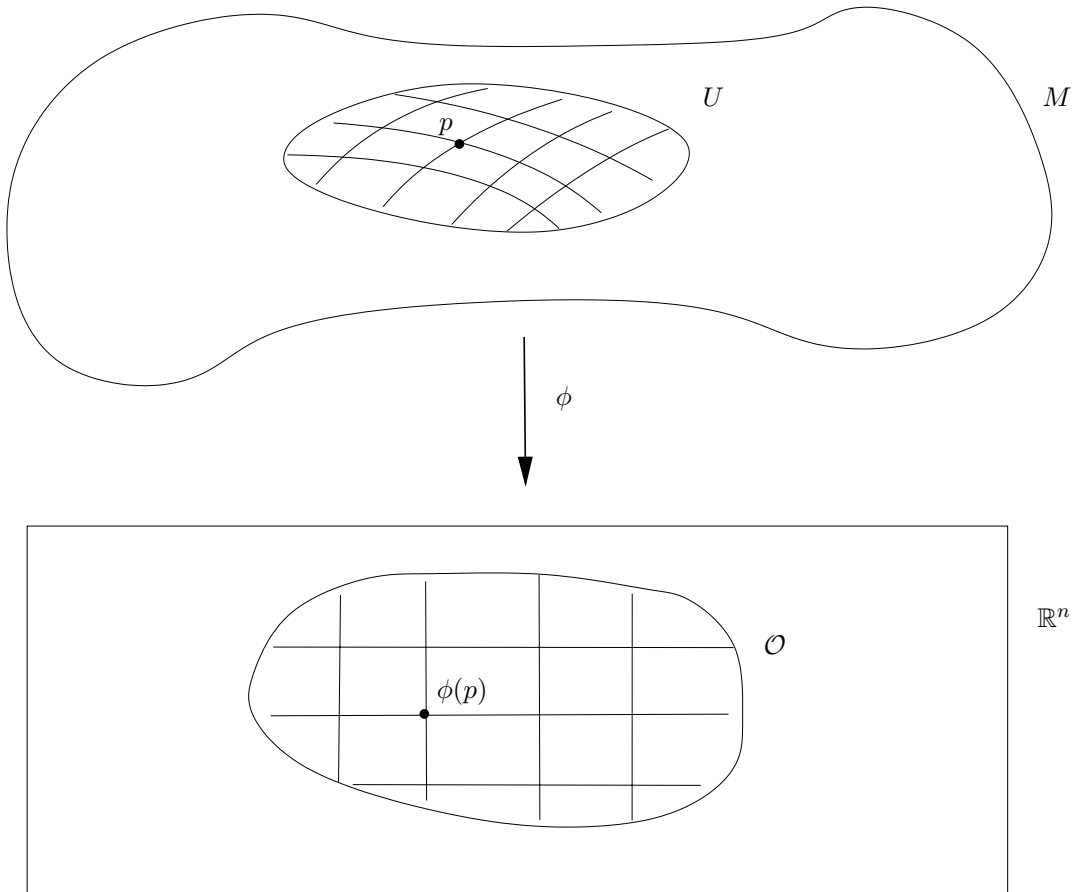


Figure 35: Definition of a local chart

We may visualise a local chart as a grid of coordinates that covers the set U . The grid is made up of the coordinate lines, i.e., of those lines that are mapped by ϕ onto the natural coordinate lines in \mathbb{R}^n .

Every map in an atlas or in a guide-book is a local chart for the surface of the Earth.

Definition: Two n -dimensional charts $\phi_1 : U_1 \longrightarrow \mathcal{O}_1$ and $\phi_2 : U_2 \longrightarrow \mathcal{O}_2$ for a topological space M are C^k -compatible, if the map

$$\phi_1 \circ \phi_2^{-1} : \phi_2(U_1 \cap U_2) \longrightarrow \phi_1(U_1 \cap U_2) , \quad (151)$$

which is bijective by assumption, is a C^k -map (i.e., k times continuously differentiable) in either direction. This condition is considered as being satisfied if $U_1 \cap U_2 = \emptyset$.

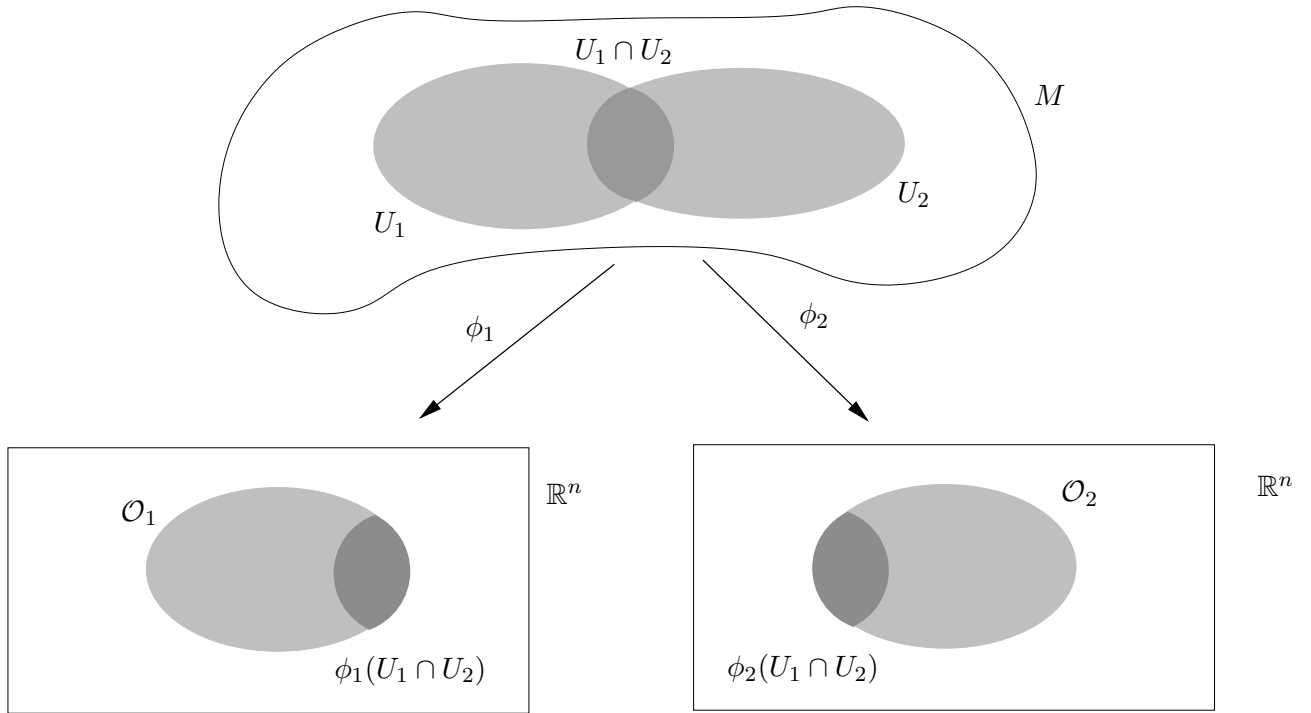


Figure 36: Compatibility of two charts

Definition: An n -dimensional C^k atlas for a topological space M is a set of n -dimensional local charts $\{\phi_\alpha : U_\alpha \longrightarrow \mathcal{O}_\alpha \mid \alpha \in I\}$ that are pairwise C^k -compatible and satisfy the condition $\bigcup_{\alpha \in I} U_\alpha = M$.

Definition: An n -dimensional C^k manifold is a topological space M with a maximal n -dimensional C^k atlas.

If one has an n -dimensional C^k atlas for M , this defines a unique manifold structure for M ; the maximal atlas is found by adding all n -dimensional charts that are C^k -compatible with the ones in the given atlas. (Strictly speaking, a proof that any atlas is a subset of a maximal atlas requires Zorn's lemma and, thus, the axiom of choice.)

Examples:

- For $M = \mathbb{R}^n$ the identity map

$$\begin{aligned} \text{id} : \mathbb{R}^n &\longrightarrow \mathbb{R}^n \\ (x^1, \dots, x^n) &\longmapsto (x^1, \dots, x^n) \end{aligned} \tag{152}$$

defines an n -dimensional C^∞ atlas consisting of only one (global) chart. Adding all local C^∞ charts that are C^∞ -compatible with id makes \mathbb{R}^n into an n -dimensional C^∞ manifold.

- For the 2-sphere $S^2 = \{ (x^1, x^2, x^3) \in \mathbb{R}^3 \mid (x^1)^2 + (x^2)^2 + (x^3)^2 = 1 \}$ there is no global chart. We can construct two local charts with the help of stereographic projection,

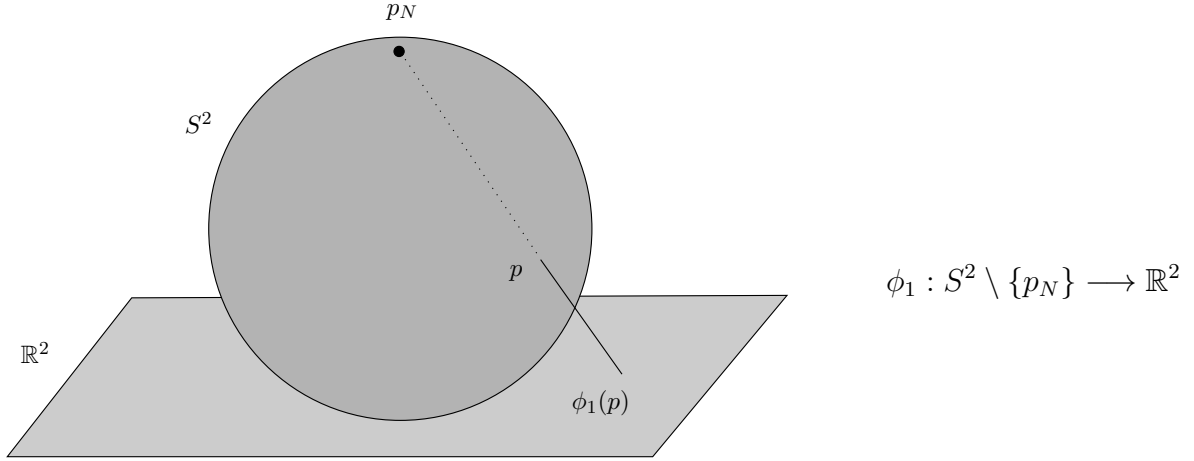


Figure 37: Stereographic projection from the north pole

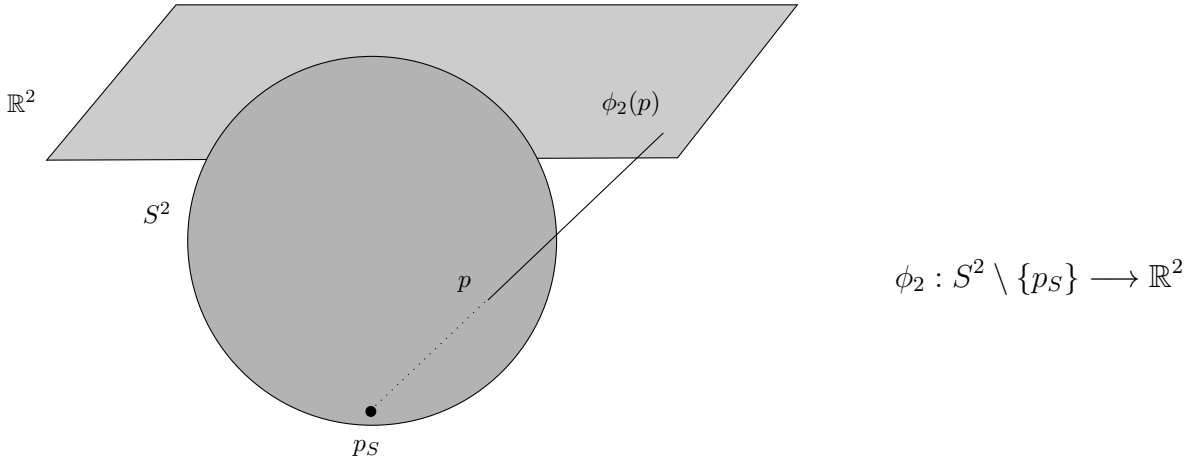


Figure 38: Stereographic projection from the south pole

which together are a C^∞ atlas for S^2 . By adding all other C^∞ -compatible 2-dimensional local charts one makes S^2 into a 2-dimensional C^∞ manifold

Similarly, the n -sphere $S^n = \{ (x^1, \dots, x^{n+1}) \in \mathbb{R}^{n+1} \mid (x^1)^2 + \dots + (x^{n+1})^2 = 1 \}$ can be made into an n -dimensional C^∞ manifold.

Examples for manifolds in physics:

- The spacetime of general relativity is a 4-dimensional manifold, with coordinates (x^0, x^1, x^2, x^3) .
- The phase space of classical mechanics is a $2k$ -dimensional manifold, with coordinates $(q^1, \dots, q^k, p_1, \dots, p_k)$.
- The state space of phenomenological equilibrium thermodynamics is a manifold, with coordinates $(S, V, M, \dots) = (\text{entropy, volume, magnetisation, } \dots)$.

It is usual to include two additional requirements into the definition of a manifold:

(A1) Hausdorff's axiom: For any two points p_1 and p_2 in M with $p_1 \neq p_2$ there are open sets U_1 and U_2 such that $p_1 \in U_1$, $p_2 \in U_2$ and $U_1 \cap U_2 = \emptyset$.

(A2) Second countability axiom: There are countably many open sets $\{U_\alpha \mid \alpha \in \mathbb{N}\}$ such that any open set U can be written as $U = \bigcup_{\alpha \in I} U_\alpha$ with $I \subseteq \mathbb{N}$.

(A1) and (A2) together imply paracompactness and, thus, the existence of a partition of unity, which is important, e.g., for doing integration theory on a manifold.

For $M = \mathbb{R}^n$ (with the standard topology) (A1) is obviously true. (A2) is less obvious, but it is true as well: For the sets U_α one may choose all open balls with rational radii and rational centre coordinates.

We agree on the following conventions.

- From now on, the term “ n -dimensional manifold” is understood as meaning “ n -dimensional C^∞ manifold that satisfies (A1) and (A2)”.
- In Section 4, where we deal with manifolds of unspecified dimension, we adopt the summation convention for greek indices running from 1 to $\dim(M)$.

We now define differentiability for maps from one manifold to another.

Definition: Let M be an n -dimensional manifold and let \hat{M} be an \hat{n} -dimensional manifold. A map $\psi : M \rightarrow \hat{M}$ is called a C^∞ map if the following holds: For every $p \in M$ there exist charts

$$\phi : U \subseteq M \rightarrow \mathcal{O} \subseteq \mathbb{R}^n \quad \text{und} \quad \hat{\phi} : \hat{U} \subseteq \hat{M} \rightarrow \hat{\mathcal{O}} \subseteq \mathbb{R}^{\hat{n}} \quad (153)$$

with $p \in U$ and $\psi(p) \in \hat{U}$ such that

$$\hat{\phi} \circ \psi \circ \phi^{-1} : \mathcal{O} \rightarrow \hat{\mathcal{O}} \quad (154)$$

is a C^∞ map (i.e., arbitrarily often differentiable) at the point p , see Fig. 39.

The set of all C^∞ maps from M to \hat{M} is denoted $C^\infty(M, \hat{M})$.

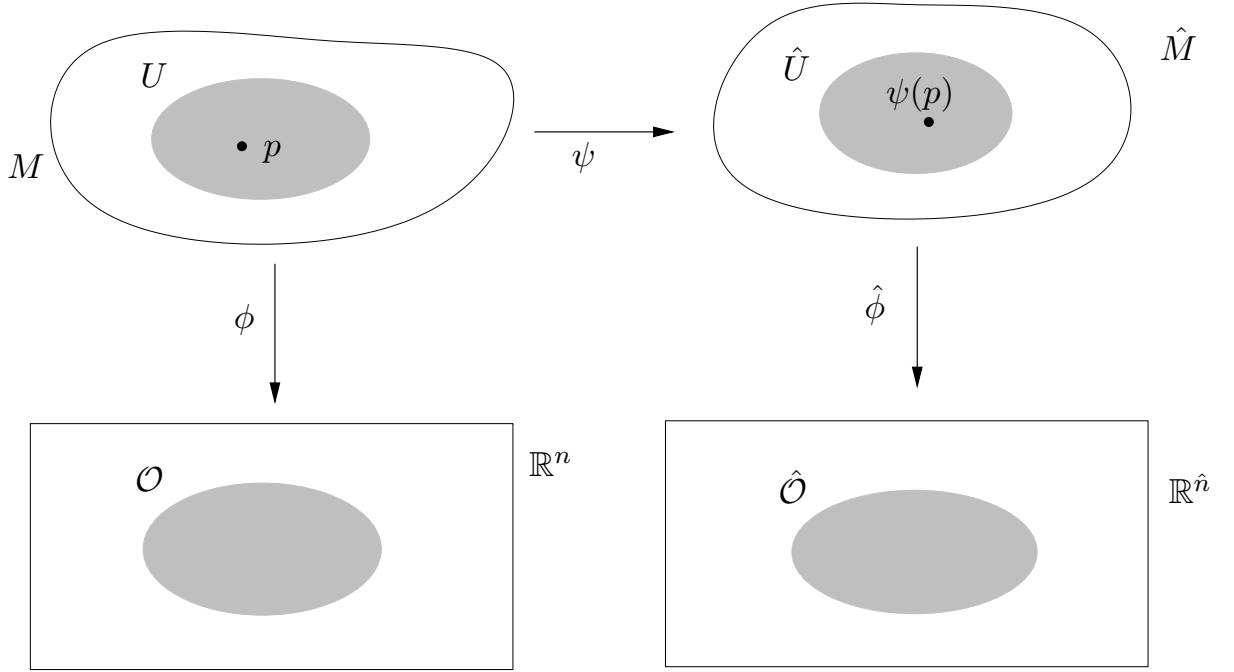


Figure 39: Differentiability of a map from M to \hat{M}

Definition: $\psi : M \longrightarrow \hat{M}$ is called a *diffeomorphism* if ψ is bijective and if both ψ and ψ^{-1} are C^∞ maps.

If there exists a diffeomorphism from M to \hat{M} , then the two manifolds M and \hat{M} are considered as equivalent. Such an equivalence class is called a *differentiable structure*. The question of how many non-equivalent differentiable structures exist on a given topological space is highly non-trivial. It is known since several decades that on \mathbb{R}^n with $n \neq 4$ there is only one differentiable structure. The case $n = 4$ was solved only in the 1990s. It was found that there are more than countably many different differentiable structures on \mathbb{R}^4 . In physics we only use the standard differentiable structure which is generated by the identity map. If the other ones, the so-called *exotic* differentiable structures on \mathbb{R}^4 , are of any relevance for physics, e.g. as spacetime models, is not clear until now. Another surprising example is the 7-dimensional sphere, S^7 , which admits precisely 15 different differentiable structures.

If we think of a surface, i.e. of a 2-dimensional manifold, we usually assume that it can be embedded into \mathbb{R}^3 , and we visualise it in this way. Also for $n > 2$ it is often possible to embed an n -dimensional manifold into \mathbb{R}^{n+1} , and several manifolds are even defined in this way, e.g. the n -dimensional sphere S^n . This raises the question of whether or not *any* n -dimensional manifold can be embedded into \mathbb{R}^{n+1} . For a thorough discussion of this question we have to define the notion of an “embedding” precisely.

Definition: An *embedding* of a manifold M into a manifold \hat{M} is a map $\psi \in C^\infty(M, \hat{M})$ such that (a) ψ is injective, and (b) $\psi^{-1} : \psi(M) \longrightarrow M$ is continuous.

The following theorem was proven in the 1930s by H. Whitney. It demonstrates that an n -dimensional manifold can always be embedded into some higher-dimensional \mathbb{R}^m , though not, in general, into \mathbb{R}^{n+1} . The topological axioms (A1) and (A2) are essential for this theorem.

Whitney's embedding theorem: Any n -dimensional manifold M can be embedded into \mathbb{R}^{2n} . Any two embeddings of M into \mathbb{R}^{2n+1} are *isotopic*, i.e., they can be continuously deformed into each other.

Although embeddings into some \mathbb{R}^m exist for any manifold, they are not usually considered in physics. The reason is that the embedding space has no physical meaning. If M is a spacetime, measurements can be made only within M , but not in some embedding space that exists only as a mathematical construction. Properties of M are called *extrinsic* if they refer to an embedding space, and they are called *intrinsic* if they refer only to M itself. For M being a spacetime, only intrinsic properties of M have a physical meaning.

Note, however, that there are some (speculative) theories according to which the universe has more than 4 spacetime dimensions. E.g., in the so-called *braneworld theory* our 4-dimensional visible spacetime is a boundary (“(mem)brane”) in a higher-dimensional (“bulk”) manifold.

Now we define the tangent space to a manifold. We want to do this on the basis of intrinsic concepts only. Therefore, we cannot define tangent vectors as “arrows that point into an embedding space”. We define tangent vectors as “derivations”.

Definition: Let M be an n -dimensional manifold and $p \in M$. A *derivation* at the point p is a map $X_p : C^\infty(M, \mathbb{R}) \longrightarrow \mathbb{R}$, such that for all $f_1, f_2 \in C^\infty(M, \mathbb{R})$ the following properties hold.

- (a) Locality: If f_1 and f_2 coincide on an open neighbourhood of p , then $X_p f_1 = X_p f_2$.
- (b) Linearity: $X_p(c_1 f_1 + c_2 f_2) = c_1 X_p f_1 + c_2 X_p f_2$ for all $c_1, c_2 \in \mathbb{R}$.
- (c) Leibniz rule: $X_p(f_1 f_2) = f_1(p) X_p f_2 + f_2(p) X_p f_1$.

The set of all derivations at the point p is called the *tangent space* at p . It is denoted $T_p M$.

Obviously, $T_p M$ is a vector space. It is less obvious that the dimension of the vector space $T_p M$ equals the dimension, n , of the underlying manifold. We will give a basis for this vector space later.

The definition of $T_p M$ in terms of derivations becomes a bit more intuitive by the following consideration. Given a curve $\gamma \in C^\infty(\mathbb{R}, M)$, one can assign at each point $\gamma(s)$ a tangent vector $\dot{\gamma}(s) \in T_{\gamma(s)} M$ to this curve, by the following prescription:

$$\begin{aligned} \dot{\gamma}(s) : C^\infty(M, \mathbb{R}) &\longrightarrow \mathbb{R} \\ f &\longmapsto \dot{\gamma}(s)f := \frac{d}{ds}f(\gamma(s)) = \lim_{\varepsilon \rightarrow 0} \frac{f(\gamma(s + \varepsilon)) - f(\gamma(s))}{\varepsilon} \end{aligned} \quad (155)$$

Here d/ds denotes the ordinary derivative of the function $f \circ \gamma : \mathbb{R} \rightarrow \mathbb{R}$, $s \mapsto f(\gamma(s))$. It is easy to show that, indeed, $\dot{\gamma}(s)$ satisfies the defining properties (a), (b) and (c) of a derivation. Also, one can show that any derivation can be written as a tangent vector to a curve. For this reason, one can define a tangent vector as an equivalence class of curves. This definition, which is mathematically equivalent to the one in terms of derivatives, could be considered as geometrically more intuitive. For calculations, however, this alternative definition is rather awkward. Therefore, we will always view a tangent vector as a derivation.

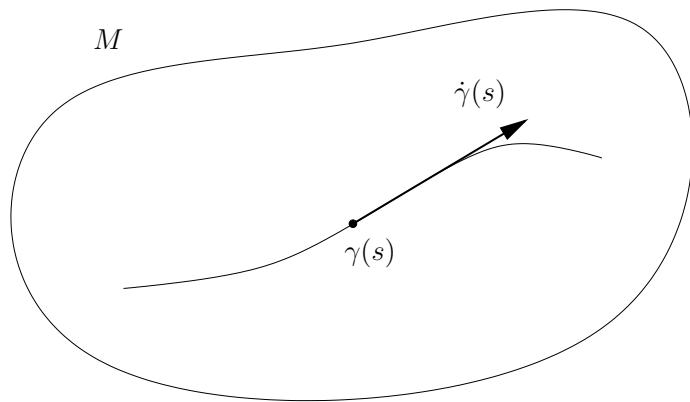


Figure 40: Tangent vector of a curve

Definition: The set $TM := \bigcup_{p \in M} T_p M$ is called the *tangent bundle* of M .

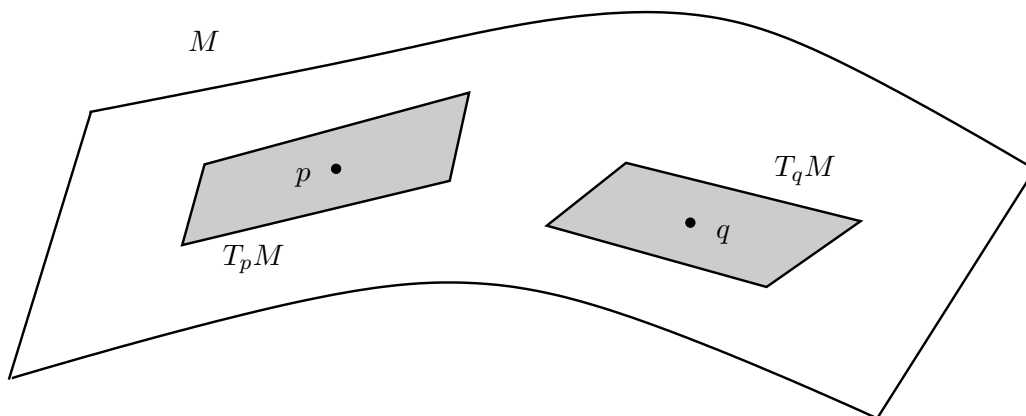


Figure 41: Tangent bundle

Definition: A *vector field* on M is a map $X : M \rightarrow TM$ that assigns to each $p \in M$ a vector $X_p \in T_p M$.

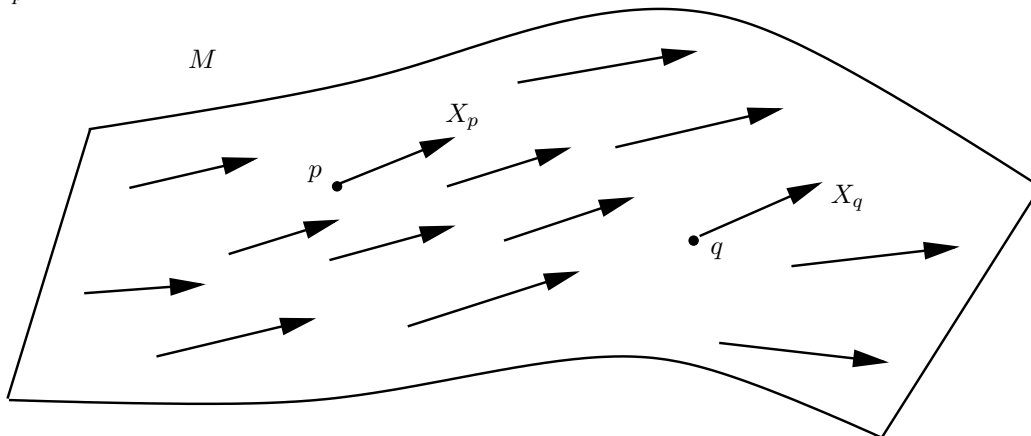


Figure 42: A vector field X

A vector field $X : p \mapsto X_p$ is called a C^∞ vector field if for any $f \in C^\infty(M, \mathbb{R})$ the function Xf is, again, in $C^\infty(M, \mathbb{R})$. Here Xf denotes the function that takes the value $X_p f$ at $p \in M$.

A local chart

$$\begin{aligned} \phi : U \subseteq M &\longrightarrow \mathcal{O} \subseteq \mathbb{R}^n \\ p &\longmapsto \phi(p) = (x^1(p), \dots, x^n(p)) \end{aligned} \quad (156)$$

defines, at each point $p \in U$, the so-called “Gaussian basis”

$$\left\{ \left. \frac{\partial}{\partial x^1} \right|_p, \dots, \left. \frac{\partial}{\partial x^n} \right|_p \right\} \quad (157)$$

of the vector space $T_p M$; this basis is constructed by taking, at p , the tangent vector to each coordinate curve

$$\left. \frac{\partial}{\partial x^\mu} \right|_p f = \left. \frac{d}{ds} \left((f \circ \phi^{-1})(x^1(p), \dots, x^\mu(p) + s, \dots, x^n(p)) \right) \right|_{s=0}. \quad (158)$$

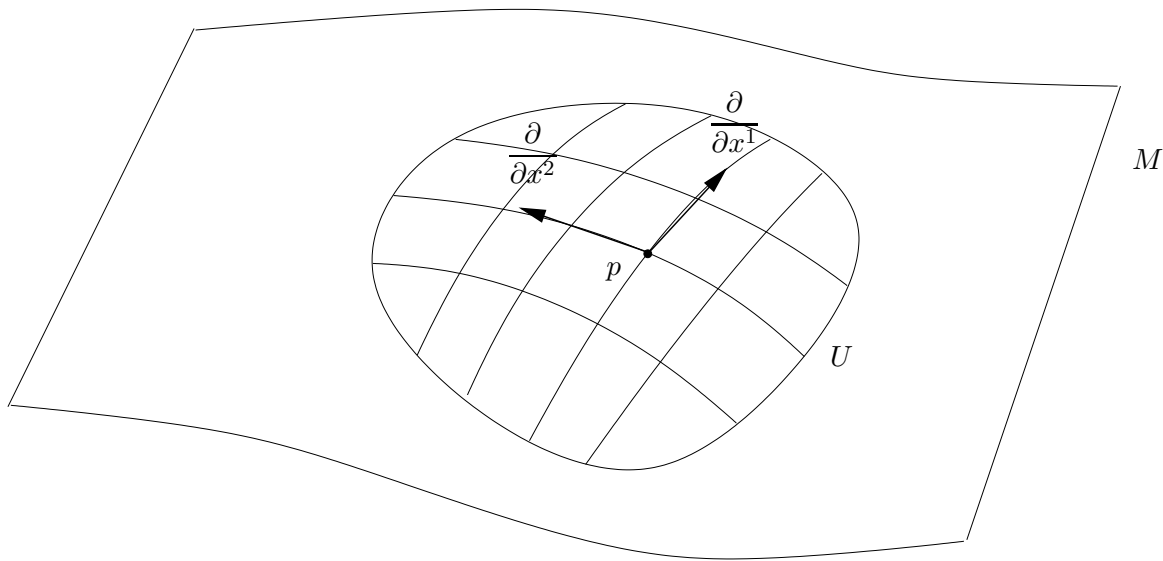


Figure 43: The Gaussian basis vector fields

As a short-hand, we often write ∂_μ instead of $\partial/\partial x^\mu$.

As the $\partial/\partial x^\mu|_p$ form a basis for $T_p M$, every vector field X on U can be written as

$$X = X^\mu \frac{\partial}{\partial x^\mu}, \quad (159)$$

with coefficients $X^\mu : U \longrightarrow \mathbb{R}$. The X^μ are called the *components* of X in the chosen chart. X is a C^∞ vector field if and only if its components are C^∞ functions, in any chart.

We want to determine the transformation behaviour of the components of a vector field under a change of coordinates, i.e., under a change from one chart $\phi = (x^1, \dots, x^n)$ to another chart $\tilde{\phi} = (\tilde{x}^1, \dots, \tilde{x}^n)$. On the overlap of the two charts, we can define the Jacobi matrix

$$J^\mu{}_\nu = \frac{\partial \tilde{x}^\mu}{\partial x^\nu} \quad (160)$$

and its inverse

$$(J^{-1})^\nu{}_\mu = \frac{\partial x^\nu}{\partial \tilde{x}^\mu} . \quad (161)$$

By the chain rule, the basis vector fields transform according to

$$\frac{\partial}{\partial \tilde{x}^\mu} = (J^{-1})^\nu{}_\mu \frac{\partial}{\partial x^\nu} . \quad (162)$$

As a consequence, we find

$$X = X^\nu \frac{\partial}{\partial x^\nu} = \tilde{X}^\mu \frac{\partial}{\partial \tilde{x}^\mu} = \tilde{X}^\mu (J^{-1})^\nu{}_\mu \frac{\partial}{\partial x^\nu} \quad (163)$$

$$\implies X^\nu = (J^{-1})^\nu{}_\mu \tilde{X}^\mu, \quad \tilde{X}^\mu = J^\mu{}_\nu X^\nu . \quad (164)$$

This transformation behaviour is called *contravariant*. In particular in the older literature, it is quite common to *define* vector fields by this property: A vector field is determined by a quantity with an upper index, X^μ , with a contravariant transformation behaviour.

Vector fields are special cases of tensor fields. We will now define tensor fields of arbitrary rank. To that end we first have to introduce the cotangent space T_p^*M and then, by repeated application of tensor products, tensor spaces of arbitrary rank.

Given an n -dimensional vector space V , one defines the *dual vector space* V^* as the set of all linear maps $V \rightarrow \mathbb{R}$. The dual space V^* is a vector space of the same dimension as V . The dual space of the tangent space T_pM is denoted T_p^*M ; it is called the *cotangent space* of M at the point p . Any element $\alpha_p \in T_p^*M$ is a linear map

$$\begin{aligned} \alpha_p : T_pM &\longrightarrow \mathbb{R} \\ X_p &\longmapsto \alpha_p(X_p) . \end{aligned} \quad (165)$$

Note that the bidual space of a vector space can be identified with the vector space itself, $(T_p^*M)^* = T_pM$, by identifying $X_p \in T_pM$ with

$$\begin{aligned} \hat{X}_p : T_p^*M &\longrightarrow \mathbb{R} \\ \alpha_p &\longmapsto \alpha_p(X_p) . \end{aligned} \quad (166)$$

Definition: The set $T^*M := \bigcup_{p \in M} T_p^*M$ is called the *cotangent bundle* of M . A *covector field* is a map $\alpha : M \rightarrow T^*M$ that assigns to each $p \in M$ an $\alpha_p \in T_p^*M$.

To any function $f \in C^\infty(M, \mathbb{R})$ one can assign a covector field df by the prescription

$$\begin{aligned} (df)_p : T_p M &\longrightarrow \mathbb{R} \\ X_p &\longmapsto (df)_p(X_p) := X_p f . \end{aligned} \quad (167)$$

df is called the *differential* of f .

A local chart

$$\begin{aligned} \phi : U \subseteq M &\longrightarrow \mathcal{O} \subseteq \mathbb{R}^n \\ p &\longmapsto \phi(p) = (x^1(p), \dots, x^n(p)) \end{aligned} \quad (168)$$

defines at each point $p \in U$ a basis

$$\{ dx^1|_p, \dots, dx^n|_p \} \quad (169)$$

of the vector space $T_p^* M$. Here dx^μ denotes the differential of the function $x^\mu : U \longrightarrow \mathbb{R}$.

As the dx^μ form a basis, any covector field α on U can be written as

$$\alpha = \alpha_\mu dx^\mu \quad (170)$$

with coefficients $\alpha_\mu : U \longrightarrow \mathbb{R}$. The α_μ are called the *components* of α in the chosen chart.

Under a change of coordinates, the basis covector fields dx^μ transform according to the chain rule,

$$d\tilde{x}^\mu = J^\mu{}_\nu dx^\nu, \quad \text{where} \quad J^\mu{}_\nu = \frac{\partial \tilde{x}^\mu}{\partial x^\nu}$$

denotes the Jacobi matrix, as before. This allows us to calculate the transformation behaviour of the components α_μ of a covector field,

$$\alpha = \alpha_\nu dx^\nu = \tilde{\alpha}_\mu d\tilde{x}^\mu = \tilde{\alpha}_\mu J^\mu{}_\nu dx^\nu \implies \alpha_\nu = \tilde{\alpha}_\mu J^\mu{}_\nu, \quad \tilde{\alpha}_\mu = \alpha_\nu (J^{-1})^\nu{}_\mu. \quad (171)$$

This transformation behaviour is called *covariant*. In comparison with the contravariant transformation behaviour, the Jacobi matrix, J , has been replaced by its inverse, J^{-1} . In analogy to vector fields, covector fields can be defined by the transformation behaviour of their components which is common in particular in the older literature.

We are now ready to define tensor fields of arbitrary rank. To that end we need the definition of the tensor product: For any two finite-dimensional vector spaces V and W one defines the *tensor product* $V \otimes W$ as the set of all bilinear maps $V^* \times W^* \longrightarrow \mathbb{R}$. For $v \in V$ and $w \in W$ one defines $v \otimes w \in V \otimes W$ by the prescription

$$\begin{aligned} v \otimes w : V^* \times W^* &\longrightarrow \mathbb{R} \\ (\alpha, \beta) &\longmapsto (v \otimes w)(\alpha, \beta) := \alpha(v)\beta(w). \end{aligned} \quad (172)$$

$V \otimes W$ is a vector space with the dimension $\dim(V \otimes W) = \dim(V)\dim(W)$. If $\{a_\mu | \mu = 1, \dots, \dim(V)\}$ is a basis in V , and $\{b_i | i = 1, \dots, \dim(W)\}$ is a basis in W , then $\{a_\mu \otimes b_i | \mu = 1, \dots, \dim(V), i = 1, \dots, \dim(W)\}$ is a basis in $V \otimes W$.

Using this notation, we can now define for any manifold M the tensor space of rank (r, s) at $p \in M$ as

$$(T_s^r)_p M := \underbrace{T_p M \otimes \dots \otimes T_p M}_{r \text{ times}} \otimes \underbrace{T_p^* M \otimes \dots \otimes T_p^* M}_{s \text{ times}}. \quad (173)$$

(As the tensor product is associative, repeated tensor products may be written without brackets.) Note that $(T_0^0)_p M \simeq \mathbb{R}$, $(T_0^1)_p M \simeq T_p M$ und $(T_1^0)_p M \simeq T_p^* M$.

Definition: The set $T_s^r M := \bigcup_{p \in M} (T_s^r)_p M$ is called the *tensor bundle* of rank (r, s) of M . A *tensor field* of rank (r, s) on M is a map $A : M \longrightarrow T_s^r M$ that assigns to each point $p \in M$ a tensor $A_p \in (T_s^r)_p M$.

A tensor field of rank (r, s) is also called an “ r times contravariant and s times covariant tensor field”.

In a local chart, a tensor field of rank (r, s) is represented in the form

$$A = A^{\mu_1 \dots \mu_r}_{\nu_1 \dots \nu_s} \frac{\partial}{\partial x^{\mu_1}} \otimes \dots \otimes \frac{\partial}{\partial x^{\mu_r}} \otimes dx^{\nu_1} \otimes \dots \otimes dx^{\nu_s}. \quad (174)$$

Under a change of coordinates, the components transform according to

$$\tilde{A}^{\rho_1 \dots \rho_r}_{\sigma_1 \dots \sigma_s} = A^{\mu_1 \dots \mu_r}_{\nu_1 \dots \nu_s} J^{\rho_1}_{\mu_1} \dots J^{\rho_r}_{\mu_r} (J^{-1})^{\nu_1}_{\sigma_1} \dots (J^{-1})^{\nu_s}_{\sigma_s}, \quad (175)$$

which can be verified easily, using the above-mentioned transformation behaviour of the basis vector fields $\partial/\partial x^\mu$ and of the basis covector fields dx^ν .

With this coordinate representation, the tensor bundle $T_s^r M$ becomes an $(n + n^{r+s})$ -dimensional manifold. (Here n coordinates determine the point $p \in M$ and the remaining n^{r+s} coordinates determine the tensor in $(T_s^r)_p M$.) Hence, it is well-defined what we mean by a C^∞ tensor field. The following definition is equivalent: A tensor field is a C^∞ tensor field if its components $A^{\mu_1 \dots \mu_r}_{\nu_1 \dots \nu_s}$ are C^∞ functions, in any chart.

In the following we denote by $\mathcal{T}_s^r M$ the set of all C^∞ tensor fields of rank (r, s) . Note that

$$\begin{aligned} \mathcal{T}_0^0 M &\simeq C^\infty(M, \mathbb{R}) = C^\infty \text{ functions}, \\ \mathcal{T}_0^1 M &\simeq C^\infty \text{ vector fields}, \\ \mathcal{T}_1^0 M &\simeq C^\infty \text{ covector fields}. \end{aligned} \quad (176)$$

Every $A \in \mathcal{T}_s^r M$ is to be viewed as map

$$\begin{aligned} A : \underbrace{\mathcal{T}_1^0 M \times \dots \times \mathcal{T}_1^0 M}_{r \text{ times}} \times \underbrace{\mathcal{T}_0^1 M \times \dots \times \mathcal{T}_0^1 M}_{s \text{ times}} &\longrightarrow \mathcal{T}_0^0 M \\ (\alpha_1, \dots, \alpha_r, X_1, \dots, X_s) &\longmapsto A(\alpha_1, \dots, \alpha_r, X_1, \dots, X_s), \end{aligned} \quad (177)$$

that is linear in each slot. Here linearity is meant not only with respect to coefficients $\in \mathbb{R}$ but even for coefficients $f_1, f_2 \in C^\infty(M, \mathbb{R})$, e.g.

$$\begin{aligned} A(\alpha_1, \dots, \alpha_r, X_1, \dots, X_{s-1}, f_1 Y_1 + f_2 Y_2) &= \\ = f_1 A(\alpha_1, \dots, \alpha_r, X_1, \dots, X_{s-1}, Y_1) + f_2 A(\alpha_1, \dots, \alpha_r, X_1, \dots, X_{s-1}, Y_2). \end{aligned} \quad (178)$$

So if one wants to check if a map of the form (177) actually is a tensor field, one has to check this linearity property with respect to coefficients in $C^\infty(M, \mathbb{R})$

As an alternative, one may identify a tensor field $A \in \mathcal{T}_s^r M$ with the map

$$\begin{aligned} \hat{A} : \underbrace{\mathcal{T}_1^0 M \times \cdots \times \mathcal{T}_1^0 M}_{\hat{r} \text{ times}} \times \underbrace{\mathcal{T}_0^1 M \times \cdots \times \mathcal{T}_0^1 M}_{\hat{s} \text{ times}} &\longrightarrow \mathcal{T}_{s-\hat{s}}^{r-\hat{r}} M \\ (\alpha_1, \dots, \alpha_{\hat{r}}, X_1, \dots, X_{\hat{s}}) &\longmapsto A(\alpha_1, \dots, \alpha_{\hat{r}}, \cdot, \dots, \cdot, X_1, \dots, X_{\hat{s}}, \cdot, \dots, \cdot) \end{aligned} \quad (179)$$

which is defined by leaving open the remaining $r - \hat{r} + s - \hat{s}$ slots of A . When using local coordinates and index calculus, this map \hat{A} is indeed represented by exactly the same array of components as the original map A .

For tensor fields, the following algebraic operations can be defined.

- (a) Two tensor fields of the same rank can be added together: For $A, B \in \mathcal{T}_s^r M$ we define $C = A + B \in \mathcal{T}_s^r M$ pointwise in the natural way; i.e., in local coordinates $C^{\mu_1 \cdots \mu_r}_{\nu_1 \cdots \nu_s} = A^{\mu_1 \cdots \mu_r}_{\nu_1 \cdots \nu_s} + B^{\mu_1 \cdots \mu_r}_{\nu_1 \cdots \nu_s}$
- (b) Two tensor fields of arbitrary, in general different, rank can be multiplied together in the sense of the tensor product: For $A \in \mathcal{T}_s^r M$ and $B \in \mathcal{T}_{\hat{s}}^{\hat{r}} M$ this defines $D = A \otimes B \in \mathcal{T}_{s+\hat{s}}^{r+\hat{r}} M$; in local coordinates $D^{\mu_1 \cdots \mu_{r+\hat{r}}}_{\nu_1 \cdots \nu_{s+\hat{s}}} = A^{\mu_1 \cdots \mu_r}_{\nu_1 \cdots \nu_s} B^{\mu_{r+1} \cdots \mu_{r+\hat{r}}}_{\nu_{s+1} \cdots \nu_{s+\hat{s}}}$.
- (c) From a tensor field $A \in \mathcal{T}_s^r M$ with $r \geq 1$ and $s \geq 1$ one can construct a new tensor field E of rank $(r-1, s-1)$ by contraction; in coordinates, contraction means equating an upper and a lower index, e.g. $E^{\mu_1 \cdots \mu_{r-1}}_{\nu_1 \cdots \nu_{s-1}} = A^{\mu_1 \cdots \mu_{r-1} \rho}_{\nu_1 \cdots \nu_{s-1} \rho}$. In general, the result depends of course on which index pair the contraction is done.

4.2 Covariant derivatives and curvature

We will now discuss how to differentiate a tensor field. The simplest method is to apply, in any chart, the operator ∂_μ to the components of a tensor field. However, this notion of differentiation has the unwanted property that the result is not a tensor field. This will be demonstrated in Worksheet 6, by way of example, where we show that $\partial_\mu A_\rho dx^\rho \otimes dx^\mu \neq \tilde{\partial}_\mu \tilde{A}_\rho d\tilde{x}^\rho \otimes d\tilde{x}^\mu$ for a covector field $A_\rho dx^\rho = \tilde{A}_\rho d\tilde{x}^\rho$. We need an additional mathematical structure on M to differentiate tensor fields in such a way that the result is again a tensor field. Such an additional structure can be defined in the following way.

Definition: A *covariant derivative* or a *linear connection* on a manifold M is a map

$$\begin{aligned} \nabla : \mathcal{T}_0^1 M \times \mathcal{T}_0^1 M &\longrightarrow \mathcal{T}_0^1 M \\ (X, Y) &\longmapsto \nabla_X Y \end{aligned} \quad (180)$$

with the following properties.

- (a) $\nabla_{X_1+X_2} Y = \nabla_{X_1} Y + \nabla_{X_2} Y$, $\nabla_{fX} Y = f \nabla_X Y$,
- (b) $\nabla_X (Y_1 + Y_2) = \nabla_X Y_1 + \nabla_X Y_2$, $\nabla_X (fY) = f \nabla_X Y + (Xf)Y$,

for all $X, Y, X_1, X_2, Y_1, Y_2 \in \mathcal{T}_0^1 M$ and $f \in \mathcal{T}_0^0 M$.

Remarks:

- Because of (b) ∇ is *not* a tensor field.
- Covariant derivatives exist on any manifold. (The topological requirements (A1) and (A2) are essential for the existence proof.)

By definition, the operator ∇_X acts on vector fields

$$\nabla_X : \mathcal{T}_0^1 M \longrightarrow \mathcal{T}_0^1 M . \quad (181)$$

We extend it to an operator acting on tensor fields of arbitrary rank,

$$\nabla_X : \mathcal{T}_s^r M \longrightarrow \mathcal{T}_s^r M , \quad (182)$$

by the following rules.

(i) For $f \in \mathcal{T}_0^0 M$ it is $\nabla_X f = X f$.

(ii) For $\alpha \in \mathcal{T}_1^0 M$ it is $(\nabla_X \alpha)(Y) = X(\alpha(Y)) - \alpha(\nabla_X Y)$.

(iii) For $A_1, A_2 \in \mathcal{T}_s^r M$ it is $\nabla_X(A_1 + A_2) = \nabla_X A_1 + \nabla_X A_2$.

For $A \in \mathcal{T}_s^r M$ and $B \in \mathcal{T}_s^{\hat{r}} M$ it is $\nabla_X(A \otimes B) = A \otimes (\nabla_X B) + (\nabla_X A) \otimes B$.

In a chart, a covariant derivative is characterised by its *connection coefficients* or *Christoffel symbols*, defined by

$$\nabla_{\partial_\nu} \partial_\sigma = \Gamma^\mu_{\nu\sigma} \partial_\mu . \quad (183)$$

The Christoffel symbols satisfy the following two equations.

- $\Gamma^\rho_{\nu\sigma} = dx^\rho(\nabla_{\partial_\nu} \partial_\sigma)$.

Proof: $dx^\rho(\nabla_{\partial_\nu} \partial_\sigma) = dx^\rho(\Gamma^\mu_{\nu\sigma} \partial_\mu) = \Gamma^\mu_{\nu\sigma} dx^\rho(\partial_\mu) = \Gamma^\mu_{\nu\sigma} \delta^\rho_\mu = \Gamma^\rho_{\nu\sigma}$.

- $\nabla_{\partial_\nu} dx^\sigma = -\Gamma^\sigma_{\nu\rho} dx^\rho$.

Proof: $(\nabla_{\partial_\nu} dx^\sigma)(\partial_\tau) = \partial_\nu(dx^\sigma(\partial_\tau)) - dx^\sigma(\nabla_{\partial_\nu} \partial_\tau) = \partial_\nu(\delta^\sigma_\tau) - dx^\sigma(\Gamma^\mu_{\nu\tau} \partial_\mu) = 0 - \Gamma^\mu_{\nu\tau} \delta^\sigma_\mu = -\Gamma^\sigma_{\nu\tau} = -\Gamma^\sigma_{\nu\rho} \delta^\rho_\tau = -\Gamma^\sigma_{\nu\rho} dx^\rho(\partial_\tau)$.

With the help of these rules we can now differentiate, with respect to a covariant derivative, tensor fields of any rank. For writing this out in local coordinates, we begin with vector fields.

For $X \in \mathcal{T}_0^1 M$ we find

$$\begin{aligned} \nabla_{\partial_\mu} X &= \nabla_{\partial_\mu} (X^\nu \partial_\nu) = (\nabla_{\partial_\mu} X^\nu) \partial_\nu + X^\nu \nabla_{\partial_\mu} \partial_\nu = \\ &= (\partial_\mu X^\nu) \partial_\nu + X^\nu \Gamma^\sigma_{\mu\nu} \partial_\sigma = (\partial_\mu X^\sigma + \Gamma^\sigma_{\mu\nu} X^\nu) \partial_\sigma =: \nabla_\mu X^\sigma \partial_\sigma . \end{aligned}$$

From this expression we read that, in local coordinates, the covariant derivative of $X \in \mathcal{T}_0^1 M$ is given by

$$\nabla_\mu X^\sigma = \partial_\mu X^\sigma + \Gamma^\sigma_{\mu\nu} X^\nu . \quad (184)$$

Some authors write

$$\partial_\mu X^\sigma = X^\sigma_{, \mu} \quad \text{and} \quad \nabla_\mu X^\sigma = X^\sigma_{; \mu} \quad (185)$$

or

$$\partial_\mu X^\sigma = X^\sigma_{| \mu} \quad \text{and} \quad \nabla_\mu X^\sigma = X^\sigma_{|| \mu} . \quad (186)$$

In particular the comma-semicolon notation is used in many text-books on General Relativity, but we will not use it here.

In analogy to the covariant derivative of a vector field, we find the coordinate representation of the covariant derivative of a covector field $\alpha \in \mathcal{T}_1^0 M$:

$$\begin{aligned}\nabla_{\partial_\mu} \alpha &= \nabla_{\partial_\mu} (\alpha_\sigma dx^\sigma) = (\nabla_{\partial_\mu} \alpha_\sigma) dx^\sigma + \alpha_\sigma \nabla_{\partial_\mu} dx^\sigma = \\ &= (\partial_\mu \alpha_\sigma) dx^\sigma - \alpha_\sigma \Gamma^\sigma_{\mu\rho} dx^\rho = (\partial_\mu \alpha_\rho - \Gamma^\sigma_{\mu\rho} \alpha_\sigma) dx^\rho =: \nabla_\mu \alpha_\rho dx^\rho .\end{aligned}\quad (187)$$

So, in local coordinates, the covariant derivative of $\alpha \in \mathcal{T}_1^0 M$ is given by

$$\nabla_\mu \alpha_\rho = \partial_\mu \alpha_\rho - \Gamma^\sigma_{\mu\rho} \alpha_\sigma . \quad (188)$$

Again, some authors write

$$\partial_\mu \alpha_\rho = \alpha_{\rho,\mu} \quad \text{and} \quad \nabla_\mu \alpha_\rho = \alpha_{\rho;\mu} , \quad (189)$$

or

$$\partial_\mu \alpha_\rho = \alpha_{\rho|\mu} \quad \text{and} \quad \nabla_\mu \alpha_\rho = \alpha_{\rho||\mu} . \quad (190)$$

Analogously one can calculate the coordinate expressions for the covariant derivatives of higher-rank tensor fields. For $A \in \mathcal{T}_s^r M$ one finds

$$\begin{aligned}\nabla_\sigma A^{\mu_1 \dots \mu_r}_{\nu_1 \dots \nu_s} &= \partial_\sigma A^{\mu_1 \dots \mu_r}_{\nu_1 \dots \nu_s} \\ &+ \Gamma^{\mu_1}_{\sigma\rho} A^{\rho\mu_2 \dots \mu_r}_{\nu_1 \dots \nu_s} + \dots + \Gamma^{\mu_r}_{\sigma\rho} A^{\mu_1 \dots \mu_{r-1}\rho}_{\nu_1 \dots \nu_s} \\ &- \Gamma^\rho_{\sigma\nu_1} A^{\mu_1 \dots \mu_r}_{\rho\nu_2 \dots \nu_s} - \dots - \Gamma^\rho_{\sigma\nu_s} A^{\mu_1 \dots \mu_r}_{\nu_1 \dots \nu_{s-1}\rho} .\end{aligned}\quad (191)$$

So, as a general rule, we get a term with a Christoffel symbol with a positive sign for any upper index and with a negative sign for any lower index. This formula is the most relevant one for practical calculations of covariant derivatives in local coordinates.

In contrast to the partial derivatives $\partial_\sigma A^{\mu_1 \dots \mu_r}_{\nu_1 \dots \nu_s}$, the covariant derivatives transform tensorially, i.e., like the components of a tensor field. This is clear from the way we introduced covariant derivatives. As a check, one could verify it by direct computation. For that, one needs the transformation behaviour of the Christoffel symbols under a change of coordinates. In Worksheet 6 we will see that this transformation behaviour is given by

$$\tilde{\Gamma}^\rho_{\tau\lambda} = \frac{\partial x^\mu}{\partial \tilde{x}^\tau} \frac{\partial x^\nu}{\partial \tilde{x}^\lambda} \frac{\partial \tilde{x}^\rho}{\partial x^\sigma} \Gamma^\sigma_{\mu\nu} + \frac{\partial^2 x^\sigma}{\partial \tilde{x}^\tau \partial \tilde{x}^\lambda} \frac{\partial \tilde{x}^\rho}{\partial x^\sigma} . \quad (192)$$

The second-derivative term in (192) makes sure that under a change of the coordinate system in (191) the non-tensorial terms cancel out.

From (191) we see that, on the domain of a local chart, a covariant derivative is uniquely characterised by the Christoffel symbols. So we can *define* a covariant derivative, on the domain of a local chart, by prescribing any functions $\Gamma^\mu_{\nu\sigma}$ of the coordinates. In particular, we can define a covariant derivative on \mathbb{R}^n , considering the latter as a manifold given by the identity map as a global chart, by prescribing $\Gamma^\mu_{\nu\sigma} = 0$. The resulting covariant derivative is known as the *canonical covariant derivative* on \mathbb{R}^n . Note that in curvilinear coordinates the canonical covariant derivative is characterised by non-zero Christoffel symbols. E.g., if one uses polar coordinates on \mathbb{R}^3 one gets non-zero Christoffel symbols for the canonical covariant derivative, see Worksheet 6. It is important to keep in mind that the Christoffel symbols transform non-tensorially, because of the second term on the right-hand side of (192): If the Christoffel symbols are zero in one chart, they are, in general, non-zero in another chart.

With the help of a covariant derivative ∇ one can define parallel transport of vectors (and tensors) along curves. Given a vector field X , we call a curve $\gamma : \mathbb{R} \rightarrow M$ an *integral curve* of X if it satisfies the condition $\dot{\gamma}(s) = X_{\gamma(s)}$ for all $s \in \mathbb{R}$. Then Y is called *parallel* (with respect to ∇) along γ if

$$(\nabla_X Y)_{\gamma(s)} = 0$$

for all $s \in \mathbb{R}$. For this property to hold only the restriction of Y to γ matters.

For expressing the condition for parallel transport in local coordinates we calculate

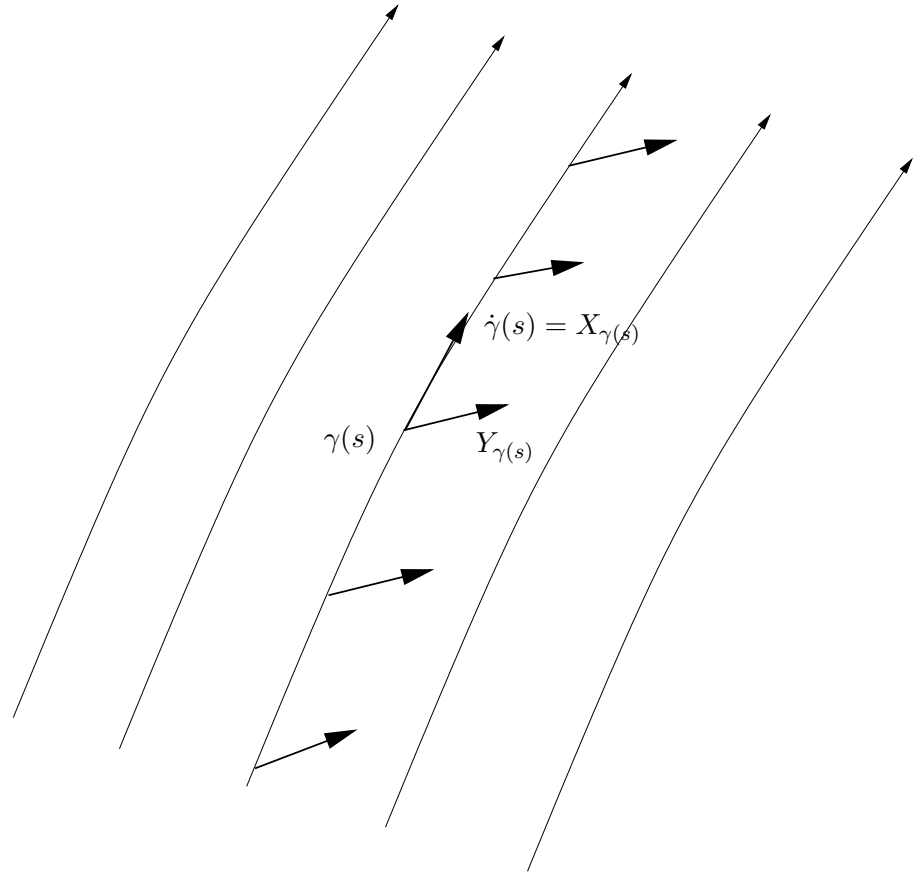


Figure 44: Parallel transport of vector fields

$$\begin{aligned} \nabla_X Y &= \nabla_{(X^\mu \partial_\mu)} (Y^\nu \partial_\nu) = X^\mu \nabla_{\partial_\mu} (Y^\nu \partial_\nu) \\ &= X^\mu (\nabla_{\partial_\mu} Y^\nu) \partial_\nu + X^\mu Y^\nu \nabla_{\partial_\mu} \partial_\nu = X^\mu (\partial_\mu Y^\sigma) \partial_\sigma + X^\mu Y^\nu \Gamma^\sigma_{\mu\nu} \partial_\sigma \\ &= X^\mu (\partial_\mu Y^\sigma + Y^\nu \Gamma^\sigma_{\mu\nu}) \partial_\sigma = X^\mu \nabla_\mu Y^\sigma \partial_\sigma. \end{aligned}$$

This demonstrates that Y is parallel along an integral curve of X if and only if the equation

$$X^\mu (\partial_\mu Y^\sigma + Y^\nu \Gamma_{\mu\nu}^\sigma) = 0 \quad (193)$$

holds along this curve. This has the following important consequence: If the Christoffel symbols are zero on the whole domain U of a chart, then a vector field $Y^\sigma \partial_\sigma$ is parallel along a curve if and only if the coefficients Y^σ are constant along this curve. Hence, a vector field Y with constant coefficients Y^σ is parallel along *any* curve. In this case we have an absolute parallelism (or teleparallelism), while in general parallel-transport from one point to another depends on the path. We may thus say: The existence of a chart in which the Christoffel symbols are equal to zero is a criterion for the path-independence of parallel-transport.

Recall that we have defined the canonical covariant derivative on \mathbb{R}^n by the property that, in the chart given by the identity map on \mathbb{R}^n , the Christoffel symbols vanish. The above argument demonstrates that the canonical covariant derivative on \mathbb{R}^n defines a parallel transport that is path-independent, i.e., that it defines a teleparallelism.

With the help of parallel-transport, we can define curves which are “as straight as possible”, in the sense that the tangent vector field is parallel along the curve:

Definition: A curve γ is called a *geodesic* or an *autoparallel* (with respect to ∇) if $\dot{\gamma}$ is parallel along γ (with respect to ∇), i.e., if there exists a vector field X such that $\dot{\gamma}(s) = X_{\gamma(s)}$ and $(\nabla_X X)_{\gamma(s)} = 0$ for all s .

We will discuss this notion in more detail in the following subsection, when we have introduced a metric on M . Geodesics will play a crucial role in general relativity.

For every covariant derivative ∇ we define

- the *torsion* $T(X, Y) = \nabla_X Y - \nabla_Y X - [X, Y]$,
- the *curvature* $R(X, Y, Z) = \nabla_X \nabla_Y Z - \nabla_Y \nabla_X Z - \nabla_{[X, Y]} Z$,

where $X, Y \in \mathcal{T}_0^1 M$, and $[X, Y]$ is the *commutator* (or the *Lie bracket*) of the derivations X and Y , defined by $[X, Y]f = X(Yf) - Y(Xf)$, see Worksheet 6.

Claim: T and R are tensor fields, $T \in \mathcal{T}_2^1 M$ and $R \in \mathcal{T}_3^1 M$.

Proof: We have to show that T and R are linear in each slot, where linear combinations with coefficients in $C^\infty(M, \mathbb{R})$ are to be considered. As additivity, $T(X_1 + X_2, Y) = T(X_1, Y) + T(X_2, Y)$ etc., is obvious, we only have to show that $T(fX, Y) = fT(X, Y)$ etc. holds. To that end we first calculate

$$\begin{aligned} [fX, Y]h &= fX(Yh) - Y(fXh) = fX(Yh) - (Yf)(Xh) - fY(Xh) = \\ &= f[X, Y]h - (Yf)(Xh) = (f[X, Y] - (Yf)X)h, \end{aligned}$$

hence $[fX, Y] = f[X, Y] - (Yf)X$. This results in

$$\begin{aligned} T(fX, Y) &= \nabla_{fX} Y - \nabla_Y (fX) - [fX, Y] = \\ &= f\nabla_X Y - (Yf)X - f\nabla_Y X - f[X, Y] + (Yf)X = fT(X, Y). \end{aligned}$$

For the other four slots of T and R the calculation is quite analogous.

In local coordinates the torsion tensor field is represented as

$$\begin{aligned}
T(\partial_\mu, \partial_\nu) &= \nabla_{\partial_\mu} \partial_\nu - \nabla_{\partial_\nu} \partial_\mu - [\partial_\mu, \partial_\nu] \\
&= \Gamma^\sigma_{\mu\nu} \partial_\sigma - \Gamma^\sigma_{\nu\mu} \partial_\sigma - 0 \\
&= (\Gamma^\sigma_{\mu\nu} - \Gamma^\sigma_{\nu\mu}) \partial_\sigma =: T^\sigma_{\mu\nu} \partial_\sigma .
\end{aligned}$$

The components of the torsion tensor field are, thus,

$$T^\sigma_{\mu\nu} = \Gamma^\sigma_{\mu\nu} - \Gamma^\sigma_{\nu\mu} . \quad (194)$$

This implies that the torsion vanishes if and only if the Christoffel symbols are symmetric, $\Gamma^\sigma_{\mu\nu} = \Gamma^\sigma_{\nu\mu}$, in any chart. For this reason, one says that a covariant derivative is *symmetric* if it has vanishing torsion.

For the curvature tensor field one finds, analogously,

$$\begin{aligned}
R(\partial_\mu, \partial_\nu, \partial_\sigma) &= \nabla_{\partial_\mu} \nabla_{\partial_\nu} \partial_\sigma - \nabla_{\partial_\nu} \nabla_{\partial_\mu} \partial_\sigma - \nabla_{[\partial_\mu, \partial_\nu]} \partial_\sigma \\
&= \nabla_{\partial_\mu} (\Gamma^\rho_{\nu\sigma} \partial_\rho) - \nabla_{\partial_\nu} (\Gamma^\rho_{\mu\sigma} \partial_\rho) - 0 \\
&= (\partial_\mu \Gamma^\rho_{\nu\sigma}) \partial_\rho + \Gamma^\rho_{\nu\sigma} \nabla_{\partial_\mu} \partial_\rho - (\partial_\nu \Gamma^\rho_{\mu\sigma}) \partial_\rho - \Gamma^\rho_{\mu\sigma} \nabla_{\partial_\nu} \partial_\rho \\
&= (\partial_\mu \Gamma^\tau_{\nu\sigma}) \partial_\tau + \Gamma^\rho_{\nu\sigma} \Gamma^\tau_{\mu\rho} \partial_\tau - (\partial_\nu \Gamma^\tau_{\mu\sigma}) \partial_\tau - \Gamma^\rho_{\mu\sigma} \Gamma^\tau_{\nu\rho} \partial_\tau \\
&= (\partial_\mu \Gamma^\tau_{\nu\sigma} - \partial_\nu \Gamma^\tau_{\mu\sigma} + \Gamma^\rho_{\nu\sigma} \Gamma^\tau_{\mu\rho} - \Gamma^\rho_{\mu\sigma} \Gamma^\tau_{\nu\rho}) \partial_\tau =: R_{\mu\nu\sigma}{}^\tau \partial_\tau .
\end{aligned}$$

So the components of the curvature tensor field are

$$R_{\mu\nu\sigma}{}^\tau = \partial_\mu \Gamma^\tau_{\nu\sigma} - \partial_\nu \Gamma^\tau_{\mu\sigma} + \Gamma^\rho_{\mu\rho} \Gamma^\tau_{\nu\sigma} - \Gamma^\rho_{\nu\rho} \Gamma^\tau_{\mu\sigma} . \quad (195)$$

Now we consider the special case that there is a chart such that the Christoffel symbols vanish on the entire domain U of the chart, $\Gamma^\sigma_{\mu\nu} = 0$. We know already that this characterises the situation that parallel transport in U is path-independent, i.e. that we have a teleparallelism. Our last calculation demonstrates that then $R_{\mu\nu\sigma}{}^\tau = 0$ in the chosen chart. However, as R is a tensor field, this means that $R_{\mu\nu\sigma}{}^\tau = 0$ in *any* chart. We have thus shown that the condition of vanishing curvature, $R = 0$, is necessary for the parallel transport to be path-independent. One can show that, on a simply connected domain U , it is also sufficient; for a proof see, e.g., N. Straumann [*General Relativity and Relativistic Astrophysics*, Springer (1984)], p.69. So, on a simply connected domain, the curvature tensor field vanishes if and only if the parallel transport is path-independent. Roughly speaking, the curvature tensor of a connection ∇ is a measure for the path-dependence of the parallel-transport defined by ∇ .

One says that a covariant derivative ∇ is *flat* if the curvature tensor of ∇ vanishes. Obviously, a covariant derivative is flat on the domain of a local chart if the Christoffel symbols vanish in this local chart. This demonstrates that, in particular, the canonical covariant derivative on \mathbb{R}^n is a flat connection. It is often said, more concisely, that “ \mathbb{R}^n is flat”. If one uses this terminology, one should be aware of the fact that it tacitly refers to the canonical covariant derivative on \mathbb{R}^n . Of course, there are many (non-canonical) covariant derivatives on \mathbb{R}^n with non-vanishing curvature.

Torsion and curvature satisfy the following identities.

- $T(X, Y) = -T(Y, X)$ or, in local coordinates, $T^\mu{}_{\nu\sigma} = -T^\mu{}_{\sigma\nu}$.
- $R(X, Y, Z) = -R(Y, X, Z)$ or, in local coordinates, $R_{\mu\nu\sigma}{}^\tau = -R_{\nu\mu\sigma}{}^\tau$.
- If the torsion vanishes, $T = 0$, the curvature tensor field satisfies, in addition, the so-called *Bianchi identities*:

$$(B1) \quad R(X, Y, Z) + R(Y, Z, X) + R(Z, X, Y) = 0$$

$$\text{or, in local coordinates, } R_{\mu\nu\sigma}{}^\tau + R_{\nu\sigma\mu}{}^\tau + R_{\sigma\mu\nu}{}^\tau = 0,$$

$$(B2) \quad (\nabla_X R)(Y, Z, U) + (\nabla_Y R)(Z, X, U) + (\nabla_Z R)(X, Y, U) = 0$$

$$\text{or in local coordinates: } \nabla_\mu R_{\nu\sigma\rho}{}^\tau + \nabla_\nu R_{\sigma\mu\rho}{}^\tau + \nabla_\sigma R_{\mu\nu\rho}{}^\tau = 0.$$

The first two identities are obvious. The Bianchi identities are less obvious, but the proof is straight-forward, just by writing out the expressions on the left-hand sides. Therefore, we will not work out the details here.

There are also versions of the Bianchi identities for covariant derivatives with non-vanishing torsion. We will not give them here because we will not need them in the following: In general relativity one works with a torsion-free (symmetric) covariant derivative, see below.

By contraction we get from the curvature tensor field $R \in \mathcal{T}_3^1 M$ the *Ricci* tensor field $\text{Ric} = R_{\mu\nu} dx^\mu \otimes dx^\nu \in \mathcal{T}_2^0 M$, defined by

$$R_{\mu\nu} = R_{\tau\mu\nu}{}^\tau. \quad (196)$$

Contraction over another index can be expressed by the Ricci tensor (and the torsion): From $R_{\mu\nu\sigma}{}^\tau = -R_{\nu\mu\sigma}{}^\tau$ we find

$$R_{\mu\tau\nu}{}^\tau = -R_{\mu\nu}. \quad (197)$$

For a torsion-free connection, we find from the first Bianchi identity

$$R_{\mu\nu\tau}{}^\tau = R_{\nu\mu} - R_{\mu\nu}. \quad (198)$$

Note that some authors use other conventions for the order of indices on $R_{\mu\nu\sigma}{}^\tau$ and for the sign of $R_{\mu\nu}$. This is a major source for sign mistakes: When taking formulas which involve the curvature tensor or its contractions from text-books or articles, one has to be very careful to check the conventions used.

The following argument gives a geometric interpretation to Lie bracket, torsion and curvature.

- If two vector fields X and Y can be represented in a chart as $X = \partial_1$ and $Y = \partial_2$, they must satisfy $[X, Y] = 0$ (because partial derivatives commute). If $[X, Y] \neq 0$, such a representation is impossible. Hence, $[X, Y] = 0$ is a condition that guarantees that the integral curves of X and Y form a closed two-dimensional grid, like the x^1 - and x^2 -lines in a coordinate system. If $[X, Y]$ is a linear combination of X and Y , the integral curves of X and Y form two-dimensional surfaces, but the integral curves do not necessarily close.

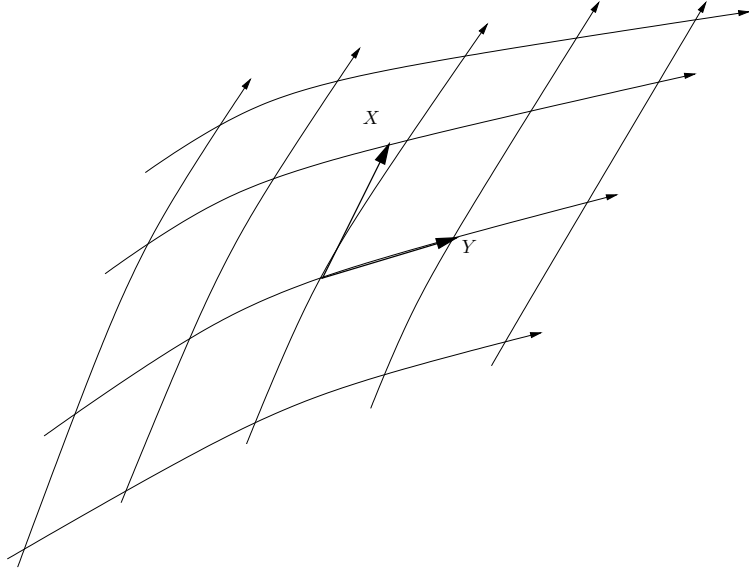


Figure 45: Two vector fields with vanishing Lie bracket

- Obviously, the conditions $\nabla_X Y = 0$ and $\nabla_Y X = 0$ are compatible with $[X, Y] = 0$ if and only if the torsion vanishes. This has the following consequence.

If Y is parallel in the direction of X and X is parallel in the direction of Y , then the integral curves of X and Y can form a closed grid if and only if $T = 0$. Hence, the torsion measures the failure of closure for integral curves that result from parallel transport of their tangent vector fields.

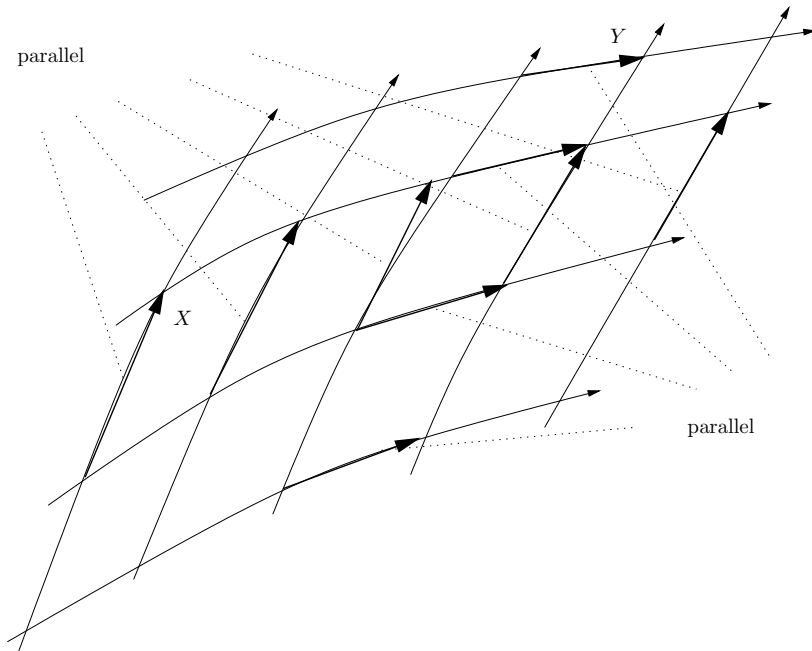


Figure 46: Two parallel-transported vector fields with vanishing Lie bracket in the case of vanishing torsion

- We have already mentioned that the curvature is a measure for the path-dependence of parallel-transport. Another geometric interpretation can be given to curvature if the torsion vanishes, $T = 0$. In this case the curvature determines the relative motion of neighbouring geodesics: Consider two vector fields X and Y such that (i) $\nabla_X X = 0$ (i.e., the integral curves of X are geodesics), (ii) $\nabla_X Y = 0$ (i.e., Y is parallel along each integral curve of X), and (iii) $[X, Y] = 0$ (i.e., the integral curves of X and Y form a closed grid). Then we have

$$R(X, Y, X) = \nabla_X \nabla_Y X - \underbrace{\nabla_Y \nabla_X X}_{=0} - \underbrace{\nabla_{[X, Y]} X}_{=0}. \quad (199)$$

As $T(X, Y) = 0$ and $[X, Y] = 0$, we must have $\nabla_Y X = \nabla_X Y$, hence

$$\nabla_X \nabla_X Y - R(X, Y, X) = 0. \quad (200)$$

This equation is known as the *equation of geodesic deviation* or *Jacobi equation*. Along each integral curve $s \mapsto \gamma(s)$ of X we can interpret “the tip of the arrow $Y_{\gamma(s)}$ ” as an “infinitesimally close neighbouring geodesic”. The Jacobi equation is a differential equation of second order that tells how this neighbouring geodesic moves relative to γ .

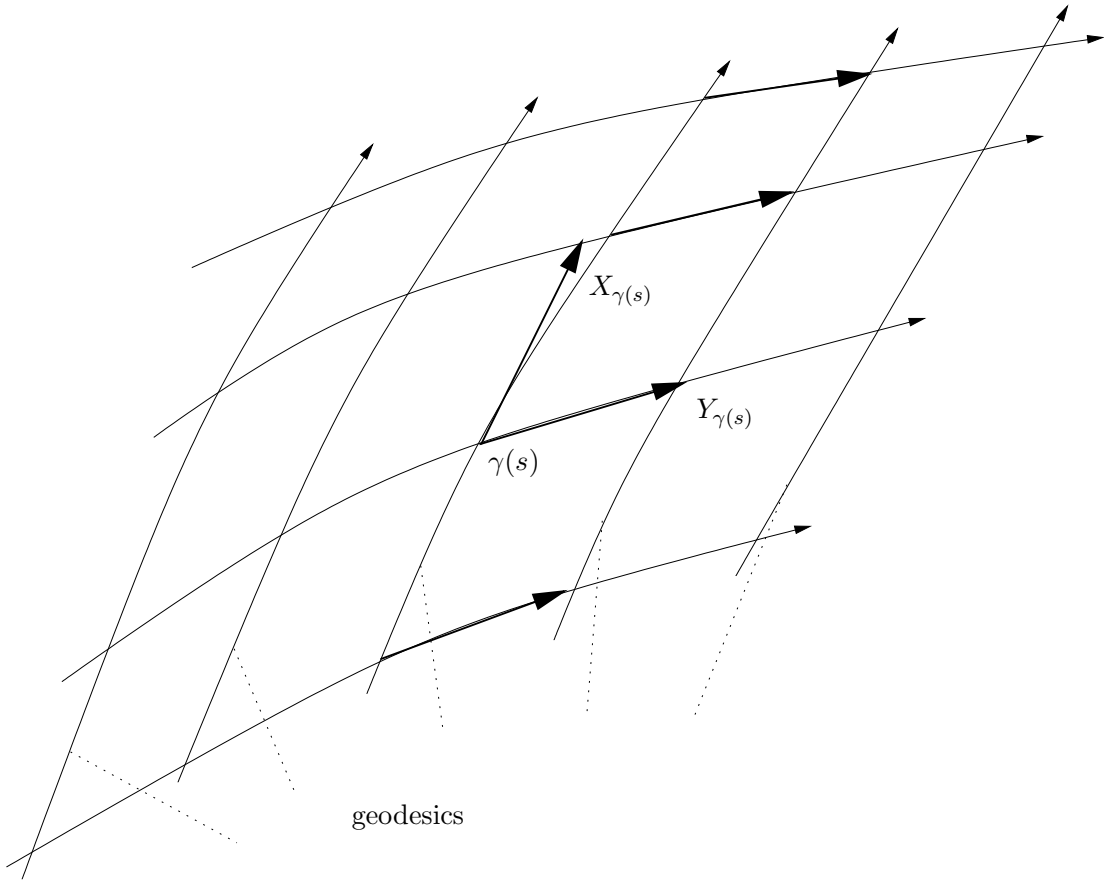


Figure 47: Relative motion of neighbouring geodesics

4.3 Pseudo-Riemannian metrics

We now introduce a notion that will play the central role in general relativity.

Definition: A *pseudo-Riemannian metric* on a manifold M is a tensor field $g \in \mathcal{T}_2^0 M$ with the following properties:

- (a) g is symmetric, i.e., for all $p \in M$ and $X_p, Y_p \in T_p M$ we have

$$g_p(X_p, Y_p) = g_p(Y_p, X_p);$$

- (b) g is non-degenerate, i.e. for all $p \in M$ and $X_p \in T_p M$ the following implication is true:

$$g_p(X_p, \cdot) = 0 \implies X_p = 0.$$

Then (M, g) is called a *pseudo-Riemannian manifold*.

Some authors say “semi-Riemannian” instead of “pseudo-Riemannian”.

The following observations follow from the definition.

- If we represent a pseudo-Riemannian metric in a coordinate system, $g = g_{\mu\nu} dx^\mu \otimes dx^\nu$, we have $g_{\mu\nu} = g_{\nu\mu}$ (because of (a)) and $\det(g_{\mu\nu}) \neq 0$ (because of (b)). This guarantees that the inverse matrix $(g^{\nu\tau})$ exists,

$$g_{\mu\nu} g^{\nu\tau} = \delta_\mu^\tau = g^{\tau\rho} g_{\rho\mu}, \quad (201)$$

and that it is again symmetric, $g^{\nu\tau} = g^{\tau\nu}$. This defines an inverse metric which will be denoted $g^{-1} = g^{\nu\tau} \partial_\nu \otimes \partial_\tau \in \mathcal{T}_0^2 M$.

- $g_{\mu\nu}$ and $g^{\nu\tau}$ can be used for lowering and raising indices, e.g.

$$g_{\mu\nu} X^\nu = X_\mu, \quad X^\nu = g^{\nu\tau} X_\tau, \quad (202)$$

$$g_{\mu\nu} R_{\sigma\tau\rho}{}^\nu = R_{\sigma\tau\rho\mu}, \quad R_{\sigma\tau\rho}{}^\mu = g^{\mu\nu} R_{\sigma\tau\rho\nu}. \quad (203)$$

In this way we can identify, with the help of a pseudo-Riemannian metric, any tensor field in $\mathcal{T}_s^r M$ with a tensor field in $\mathcal{T}_{\hat{s}}^{\hat{r}} M$, whenever $(r + s) = (\hat{r} + \hat{s})$.

- The *orthocomplement* of $X_p \in T_p M$ (with respect to g),

$$X_p^\perp = \{ Y_p \in T_p M \mid g_p(X_p, Y_p) = 0 \}, \quad (204)$$

is for $X_p \neq 0$ an $(n - 1)$ -dimensional subspace of $T_p M$ (because of (b)).

- Any symmetric matrix can be diagonalised. Hence, we can choose the coordinates such that at any one point $p \in M$ the matrix $(g_{\mu\nu})$ is diagonal (because of (a)). As $\det(g_{\mu\nu}) \neq 0$ (because of (b)), all diagonal elements must be different from zero; we can then make them equal to ± 1 by stretching or compressing the coordinate axes. As a consequence, a pseudo-Riemannian metric can be put into the form $(g_{\mu\nu}) = \text{diag}(-1, \dots, -1, 1, \dots, 1)$ at any one point. The sequence $(-1, \dots, -1, 1, \dots, 1)$ (or the number of plus signs minus the number of minus signs) is called the *signature* of the metric. As we require g to be continuous (by our assumption that $g \in \mathcal{T}_2^0 M$), the signature cannot change from point to point, so any pseudo-Riemannian metric has a unique signature.

Two types of signature are particularly important:

- A pseudo-Riemannian metric of signature $(1, \dots, 1)$ is called a *Riemannian metric*. In this case, $g_p(X_p, X_p) > 0$ for all $X_p \neq 0$ and $\sqrt{g_p(X_p, X_p)}$ can be interpreted as the *length* of the vector X_p (as measured with the metric g).

For any $X_p \neq 0$ it follows that $X_p \notin X_p^\perp$, so a vector together with its orthocomplement spans the whole tangent space. A *Riemannian manifold* is a manifold with a Riemannian metric, (M, g) .

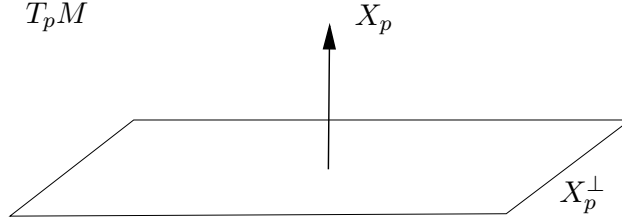


Figure 48: Orthocomplement of a non-lightlike vector

- A pseudo-Riemannian metric with signature $(-1, 1, \dots, 1)$ is called a *Lorentzian metric* (or a *pseudo-Riemannian metric with Lorentzian signature*). Also in this case, one often calls $g_p(X_p, X_p)$ the “length squared”; however, this is an abuse of terminology, because $g_p(X_p, X_p)$ can be negative. A vector $X_p \neq 0$ is called

spacelike $\iff g_p(X_p, X_p) > 0$,

lightlike $\iff g_p(X_p, X_p) = 0$,

timelike $\iff g_p(X_p, X_p) < 0$.

Instead of “lightlike” many authors say “null”. To avoid confusion of a null vector (in this sense) with the zero vector, we will always say “lightlike” and not “null”. The zero vector is usually considered as being spacelike; this is convenient because then it is true that a vector must be spacelike if it is orthogonal to a timelike one. – A curve $\gamma : \mathbb{R} \rightarrow M$ is called spacelike, lightlike or timelike if its tangent vector $\dot{\gamma}(s)$ has this property for all $s \in \mathbb{R}$.

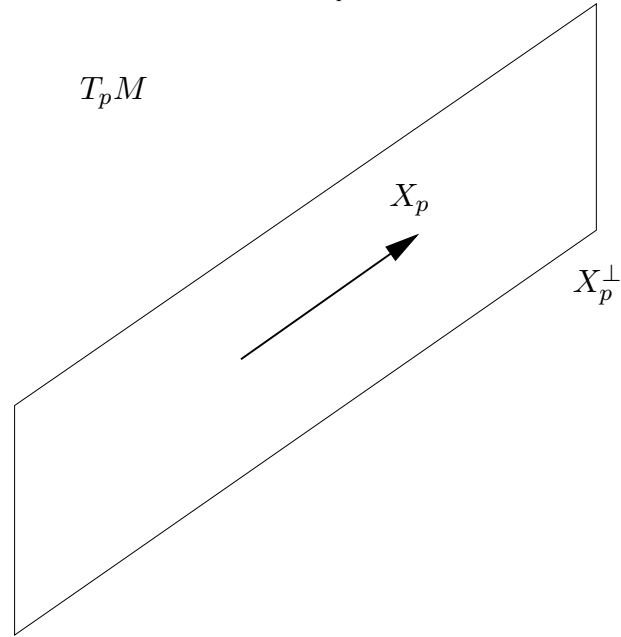


Figure 49: Orthocomplement of a lightlike vector

A lightlike vector is contained in its own orthocomplement, $X_p \in X_p^\perp$, so a lightlike vector and its orthocomplement do *not* span the whole tangent space.

A *Lorentzian manifold* is a manifold with a Lorentzian metric, (M, g) . For a 4-dimensional Lorentzian manifold, the tangent space $(T_p M, g_p)$ has the same mathematical structure as the spacetime of special relativity.

We had seen that on a manifold we need an additional structure, i.e. a covariant derivative ∇ , if we want to differentiate tensor fields in such a way that the result is again a tensor field. The following theorem demonstrates that on a pseudo-Riemannian manifold (M, g) of any signature there is a distinguished covariant derivative.

Theorem: On a pseudo-Riemannian manifold (M, g) there is precisely one covariant derivative ∇ with the following properties:

- (a) ∇ is torsion-free, $T = 0$,
- (b) ∇ is metric, i.e. $\nabla_X g = 0$ for all $X \in \mathcal{T}_0^1 M$.

This covariant derivative ∇ is called the *Levi-Civita derivative* (or *Levi-Civita connection*) of g .

Proof: If ∇ has the properties (a) and (b), we have for all $X, Y, Z \in \mathcal{T}_0^1 M$:

$$\begin{aligned} Xg(Y, Z) &= g(\nabla_X Y, Z) + g(Y, \nabla_X Z) = g(\nabla_X Y, Z) + g(Y, \nabla_Z X) + g(Y, [X, Z]) , \\ Yg(Z, X) &= g(\nabla_Y Z, X) + g(Z, \nabla_Y X) + g(Z, [Y, X]) , \\ Zg(X, Y) &= g(\nabla_Z X, Y) + g(X, \nabla_Z Y) + g(X, [Z, Y]) . \end{aligned}$$

Subtracting the last equation from the other two results in

$$\begin{aligned} Xg(Y, Z) + Yg(Z, X) - Zg(X, Y) &= \\ 2g(\nabla_X Y, Z) + g(Y, [X, Z]) + g(Z, [Y, X]) - g(X, [Z, Y]) \end{aligned}$$

and hence

$$\begin{aligned} g(\nabla_X Y, Z) &= \\ \frac{1}{2} \left(Xg(Y, Z) + Yg(Z, X) - Zg(X, Y) - g(Y, [X, Z]) - g(Z, [Y, X]) + g(X, [Z, Y]) \right) . \end{aligned} \tag{205}$$

As g is non-degenerate, this equation determines $\nabla_X Y$, i.e., it uniquely defines an operator $\nabla : \mathcal{T}_0^1 M \times \mathcal{T}_0^1 M \longrightarrow \mathcal{T}_0^1 M$. It is easy to verify that the operator ∇ which is defined by (205) satisfies all the defining properties of a covariant derivative and that it *necessarily* satisfies (a) and (b). This proves the unique existence of a ∇ with the desired properties.

The metricity condition $\nabla_X g = 0$ means that the ∇ -parallel transport along an integral curve of X preserves the “length squared” $g(Y, Y)$:

$$\nabla_X Y = 0 \implies Xg(Y, Y) = \underbrace{(\nabla_X g)(Y, Y)}_{=0} + \underbrace{g(\nabla_X Y, Y)}_{=0} + \underbrace{g(Y, \nabla_X Y)}_{=0} = 0 . \tag{206}$$

If we consider the case $Y = X$, this observation implies the following important result: If a ∇ -geodesic is timelike, lightlike or spacelike at one point, then it has this property at every point.

The proof of the theorem provides us with an explicit representation of the Levi-Civita derivative; in particular, (205) gives us an explicit representation of the Christoffel symbols of the Levi-Civita derivative: For $X = \partial_\mu$, $Y = \partial_\nu$ und $Z = \partial_\sigma$ equation (205) takes the following form:

$$\begin{aligned} g(\underbrace{\nabla_{\partial_\mu} \partial_\nu}_{=\Gamma^\rho{}_{\mu\nu} \partial_\rho}, \partial_\sigma) &= \frac{1}{2} \left(\partial_\mu g(\partial_\nu, \partial_\sigma) + \partial_\nu g(\partial_\rho, \partial_\mu) - \partial_\sigma g(\partial_\mu, \partial_\nu) + 0 \right), \\ \Gamma^\rho{}_{\mu\nu} g_{\rho\sigma} &= \frac{1}{2} \left(\partial_\mu g_{\nu\sigma} + \partial_\nu g_{\sigma\mu} - \partial_\sigma g_{\mu\nu} \right), \quad |g^{\tau\sigma} \\ \Gamma^\tau{}_{\mu\nu} &= \frac{1}{2} g^{\tau\sigma} \left(\partial_\mu g_{\sigma\nu} + \partial_\nu g_{\sigma\mu} - \partial_\sigma g_{\mu\nu} \right). \end{aligned} \quad (207)$$

This formula allows to calculate the Christoffel symbols of the Levi-Civita derivative from the metric components $g_{\mu\nu}$. As a consistency check, one may verify that the covariant derivative defined by these Christoffel symbols is, indeed, torsion-free,

$$\Gamma^\tau{}_{\mu\nu} = \Gamma^\tau{}_{\nu\mu}, \quad (208)$$

and metric,

$$\nabla_\sigma g_{\mu\nu} = \partial_\sigma g_{\mu\nu} - \Gamma^\tau{}_{\sigma\mu} g_{\tau\nu} - \Gamma^\tau{}_{\sigma\nu} g_{\mu\tau} = 0. \quad (209)$$

The metricity property $\nabla_\sigma g_{\mu\nu} = 0$ has the following important consequence: Together with the equation $\nabla_\sigma g^{\rho\mu} = 0$ (which follows immediately from differentiating the identity $g^{\nu\rho} g_{\rho\mu} = \delta^\nu_\mu$) it guarantees that indices can be raised and lowered with the metric even if they are under a covariant derivative, e.g.

$$\nabla_\mu X_\nu = S_{\mu\nu} \iff \nabla_\mu X^\sigma = S_\mu{}^\sigma. \quad (210)$$

Note that indices must not be raised or lowered under a partial derivative.

We will now investigate if it is possible that the $g_{\mu\nu}$ are constant on the whole domain U of a chart. From (207) we read that then we have $\Gamma^\mu{}_{\nu\sigma} = 0$ on U . We know already from Section 4.2 that a chart with this property exists only if the curvature tensor R vanishes on U . This demonstrates that, unless in the flat case, it is impossible to have $(g_{\mu\nu}) = \text{diag}(-1, \dots, -1, 1, \dots, 1)$ on an open neighbourhood.

In Section 4.2 we have introduced geodesics as the autoparallels of a covariant derivative ∇ , i.e., we have said that a curve $x(s)$ is a geodesic if its tangent field X satisfies the condition $\nabla_X X = 0$. In local coordinates, the latter condition reads

$$0 = X^\mu \nabla_\mu X^\tau = X^\mu \partial_\mu X^\tau + \Gamma^\tau{}_{\mu\nu} X^\mu X^\nu$$

where $X^\mu = \dot{x}^\mu$. Here the overdot means differentiation with respect to the curve parameter s . By the chain rule, the last equation can be rewritten as

$$\frac{d}{ds} X^\tau + \Gamma^\tau{}_{\mu\nu} X^\mu X^\nu = 0,$$

hence

$$\ddot{x}^\tau + \Gamma^\tau{}_{\mu\nu} \dot{x}^\mu \dot{x}^\nu = 0 \quad (211)$$

which is the general form of the geodesic equation in local coordinates. For an arbitrary covariant derivative, it is not possible to characterise the geodesics by a variational principle. For the geodesics of the Levi-Civita connection, however, this can be done, as the following theorem demonstrates.

Theorem: Let g be a pseudo-Riemannian metric of arbitrary signature. The geodesics of the Levi-Civita derivative are the solutions to the Euler-Lagrange equations

$$\frac{d}{ds} \frac{\partial L}{\partial \dot{x}^\mu} - \frac{\partial L}{\partial x^\mu} = 0 \quad (212)$$

with the Lagrange function

$$L(x, \dot{x}) = \frac{1}{2} g_{\mu\nu}(x) \dot{x}^\mu \dot{x}^\nu . \quad (213)$$

Proof: With the Lagrangian from (213), the Euler-Lagrange equations (212) read

$$\begin{aligned} \frac{d}{ds} (g_{\mu\sigma} \dot{x}^\mu) - \frac{1}{2} (\partial_\sigma g_{\mu\nu}) \dot{x}^\mu \dot{x}^\nu &= 0 \quad \Longleftrightarrow \\ g_{\sigma\mu} \ddot{x}^\mu + (\partial_\nu g_{\sigma\mu}) \dot{x}^\nu \dot{x}^\mu - \frac{1}{2} (\partial_\sigma g_{\mu\nu}) \dot{x}^\mu \dot{x}^\nu &= 0 \quad \Longleftrightarrow \\ g_{\sigma\mu} \ddot{x}^\mu + \frac{1}{2} (\partial_\mu g_{\sigma\nu} + \partial_\nu g_{\sigma\mu}) \dot{x}^\mu \dot{x}^\nu - \frac{1}{2} (\partial_\sigma g_{\mu\nu}) \dot{x}^\mu \dot{x}^\nu &= 0 . \end{aligned}$$

By multiplication with $g^{\tau\sigma}$ and comparison with (207) we see that the last equation is indeed equivalent to the geodesic equation (211).

This theorem demonstrates that a curve with coordinate representation $x^\mu(s)$ is a geodesic (i.e., an autoparallel) of the Levi-Civita connection of g if and only if it is a stationary point of the action functional

$$W = \int_a^b L(x(s), \dot{x}(s)) ds \quad (214)$$

with respect to variations that keep the endpoints fixed, $\delta W = 0$.

As the curvature tensor of the Levi-Civita connection is constructed from a metric tensor, it satisfies some special properties, in addition to the properties shared by all curvature tensors.

- With the help of the metricity condition $\nabla \cdot g = 0$ one can show that the identity

$$g(U, R(X, Y, Z)) = -g(Z, R(X, Y, U)) \quad (215)$$

holds, which can be written in local coordinates as $g_{\tau\rho} R_{\mu\nu\sigma}{}^\rho = -g_{\sigma\rho} R_{\mu\nu\tau}{}^\rho$, i.e.,

$$R_{\tau\mu\nu\sigma} = -R_{\sigma\mu\nu\tau} . \quad (216)$$

- Using this additional curvature identity and the first Bianchi identity, as it holds for the curvature tensor of any torsion-free covariant derivative, we find that the Ricci tensor is symmetric,

$$\text{Ric}(X, Y) = \text{Ric}(Y, X) , \quad (217)$$

or, in local coordinates,

$$R_{\nu\sigma} = R_{\sigma\nu} \quad (218)$$

where $R_{\nu\sigma} = R_{\tau\nu\sigma}{}^{\tau}$.

- With the help of the metric we can contract the Ricci tensor. The resulting scalar field

$$R = g^{\mu\nu} R_{\mu\nu} = R^{\nu}{}_{\nu} = R_{\mu}{}^{\mu} \quad (219)$$

is called the *scalar curvature* or the *Ricci scalar*.

The curvature tensor R of the Levi-Civita connection of a metric g is often called the *Riemannian curvature tensor* or the *Riemann tensor* of g .

At the end of this section we collect the most important formulas of pseudo-Riemannian geometry in local coordinates. If the metric $g = g_{\mu\nu}(x)dx^{\mu} \otimes dx^{\nu}$ is given, all relevant geometric quantities can be calculated from the $g_{\mu\nu}$.

Inverse metric:

$$g^{\mu\nu} g_{\nu\sigma} = \delta_{\sigma}^{\mu} = g_{\sigma\tau} g^{\tau\mu} . \quad (220)$$

Christoffel symbols of the Levi-Civita connection:

$$\Gamma^{\tau}{}_{\mu\nu} = \frac{1}{2} g^{\tau\sigma} \left(\partial_{\mu} g_{\sigma\nu} + \partial_{\nu} g_{\sigma\mu} - \partial_{\sigma} g_{\mu\nu} \right) . \quad (221)$$

Curvature tensor:

$$R_{\mu\nu\sigma}{}^{\tau} = \partial_{\mu} \Gamma^{\tau}{}_{\nu\sigma} - \partial_{\nu} \Gamma^{\tau}{}_{\mu\sigma} + \Gamma^{\tau}{}_{\mu\rho} \Gamma^{\rho}{}_{\nu\sigma} - \Gamma^{\tau}{}_{\nu\rho} \Gamma^{\rho}{}_{\mu\sigma} . \quad (222)$$

Ricci tensor:

$$R_{\nu\sigma} = R_{\mu\nu\sigma}{}^{\mu} \quad (223)$$

Scalar curvature (= Ricci scalar):

$$R = R_{\nu\sigma} g^{\nu\sigma} \quad (224)$$

Geodesic equation:

$$\ddot{x}^{\tau} + \Gamma^{\tau}{}_{\mu\nu} \dot{x}^{\mu} \dot{x}^{\nu} = 0 . \quad (225)$$

Lagrangian for the geodesic equation:

$$L(x, \dot{x}) = \frac{1}{2} g_{\mu\nu}(x) \dot{x}^{\mu} \dot{x}^{\nu} . \quad (226)$$

5 Foundations of general relativity

5.1 General-relativistic spacetimes

Motivated by the equivalence principle we postulate:

A general-relativistic *spacetime* is a 4-dimensional Lorentzian manifold (M, g) , i.e., a 4-dimensional manifold M with a pseudo-Riemannian metric g of signature $(-1, +1, +1, +1)$.

According to this postulate, the tangent space $T_p M$ to a general-relativistic spacetime looks like the spacetime of special relativity. We may thus say that, on a sufficiently small neighbourhood of any point $p \in M$, a general-relativistic spacetime differs arbitrarily little from the spacetime of special relativity.

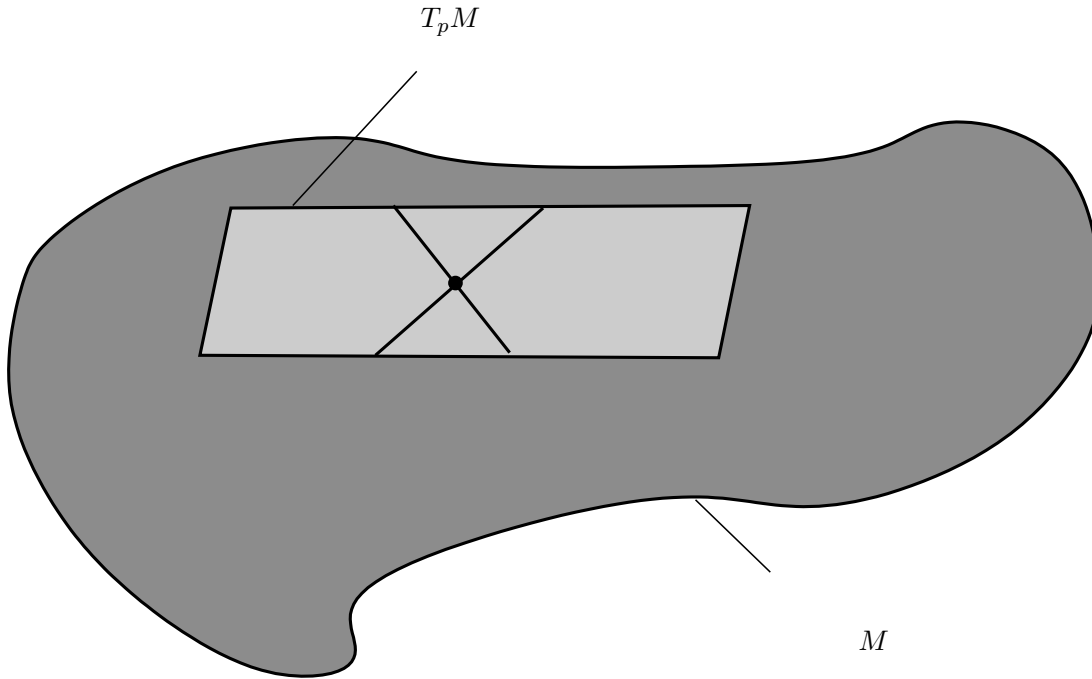


Figure 50: A general-relativistic spacetime

As suggested by the name, special relativity is indeed a special case of general relativity. The spacetime of special relativity is a special case of a general-relativistic spacetime, namely a Lorentzian manifold that admits a global chart

$$M \longrightarrow \mathbb{R}^4$$

$$p \longmapsto (x^0(p), x^1(p), x^2(p), x^3(p))$$

such that $g_{\mu\nu} = \eta_{\mu\nu}$ everywhere, $(\eta_{\mu\nu}) = \text{diag}(-1, 1, 1, 1)$. This requires the curvature tensor of the Levi-Civita connection to be zero. The spacetime of special relativity is known as *Minkowski spacetime*. The coordinate systems in which $g_{\mu\nu} = \eta_{\mu\nu}$ are the inertial systems; they are interrelated by Lorentz transformations.

In the following by a “spacetime” we always mean a general-relativistic spacetime. If a spacetime is assumed given, ∇ always denotes the Levi-Civita connection, and $\Gamma^\mu_{\nu\sigma}$ always denotes the Christoffel symbols of the Levi-Civita connection.

Coordinates on a spacetime will be denoted (x^0, x^1, x^2, x^3) . From now on we will use the summation convention, again, for greek indices $\mu, \nu, \sigma, \dots = 0, 1, 2, 3$ and for latin indices $i, j, k, \dots = 1, 2, 3$.

In many cases, but not always, one uses local coordinates on a spacetime such that the x^0 -lines are timelike, $g_{00} = g(\partial_0, \partial_0) < 0$, as it is shown in Figure 51.

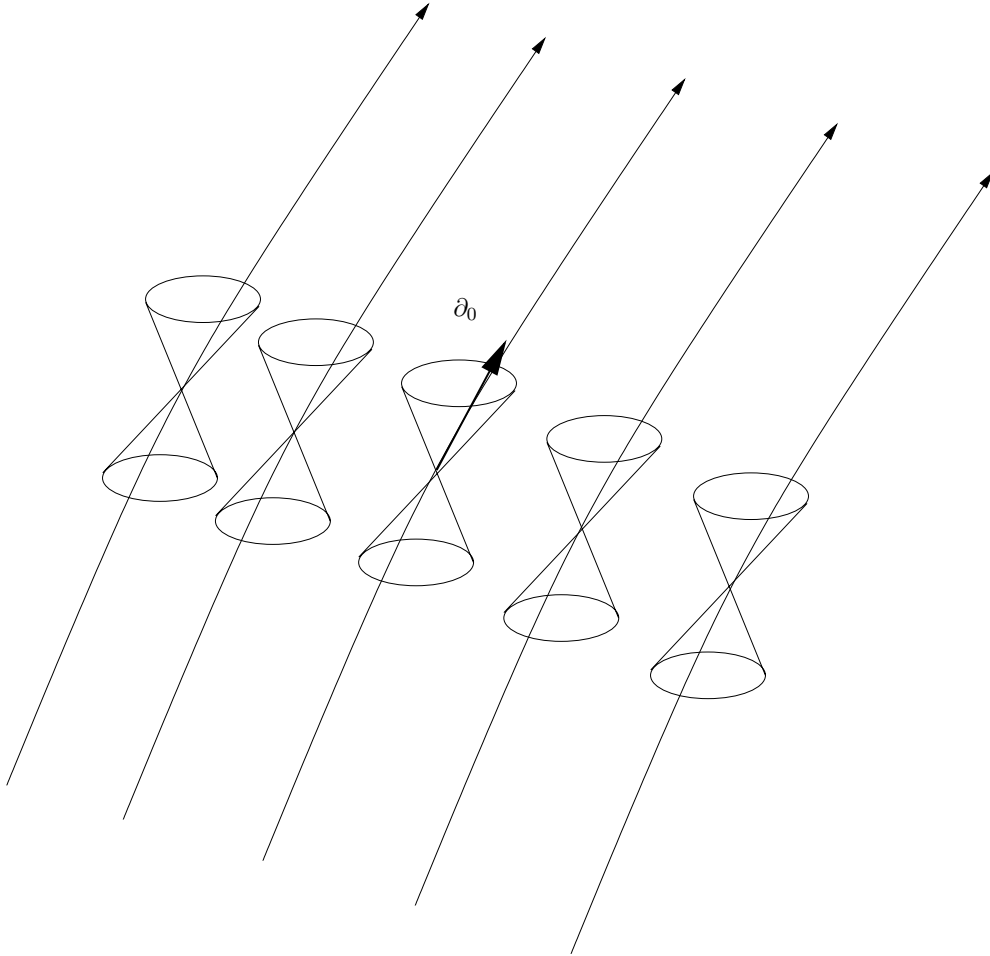


Figure 51: A coordinate system with ∂_0 timelike

We cannot make the $g_{\mu\nu}$ equal to $\eta_{\mu\nu}$ everywhere, unless the spacetime is flat, but we can always do this at any one point. At the same time, it is possible to make the Christoffel symbols equal to zero at this chosen point, i.e., the following theorem holds.

Theorem: Let (M, g) be a spacetime and $p \in M$. Then there is a coordinate system, defined on a neighbourhood of p , such that

$$g_{\mu\nu}|_p = \eta_{\mu\nu} \quad \text{und} \quad \Gamma^\mu_{\nu\sigma}|_p = 0 . \quad (227)$$

Proof: As the Levi-Civita connection is torsion-free, we can find a coordinate system such that $\Gamma^\mu_{\nu\sigma}|_p = 0$, see Worksheet 7. By another coordinate transformation $x^\mu \mapsto \bar{x}^\mu = A^\mu_{\sigma} x^\sigma$ with a *constant* matrix A^ρ_{σ} we can then make $\bar{g}_{\mu\nu}|_p = \eta_{\mu\nu}$; as the Christoffel symbols transform homogeneously under such a *linear* transformation, we have $\bar{\Gamma}^\mu_{\nu\sigma}|_p = 0$.

If we want to connect our mathematical spacetime model of a Lorentzian manifold (M, g) with experiments or observations, we have to know which physical interpretation can be given to geometric objects in (M, g) . This is done in the following list which is motivated throughout by the equivalence principle.

- Points in M are events.
- Timelike curves are worldlines of massive particles or, more generally, of objects that move at subluminal speed. In local coordinates, any such worldline can be written as $x(\tau) = (x^0(\tau), x^1(\tau), x^2(\tau), x^3(\tau))$, with

$$g_{\mu\nu}(x(\tau))\dot{x}^\mu(\tau)\dot{x}^\nu(\tau) < 0 . \quad (228)$$

The parameter τ is to be interpreted as the reading of a clock. In the following we choose the parametrisation such that

$$g_{\mu\nu}(x(\tau))\dot{x}^\mu(\tau)\dot{x}^\nu(\tau) = -c^2 . \quad (229)$$

If the orientation (“from the past to the future”) has been fixed, the parameter τ is then determined uniquely up to a transformation $\tau \mapsto \tau + \tau_0$, i.e., up to “choosing the zero on the dial”. This parameter is called *proper time*, and a clock that shows proper time is called a *standard clock*. These notions are straight-forward generalisations from special relativity.

- Timelike geodesics are worldlines of *freely falling* massive particles, i.e., of massive particles that are influenced only by gravity. For such worldlines we have, in coordinate language,

$$g_{\mu\nu}(x(\tau))\dot{x}^\mu(\tau)\dot{x}^\nu(\tau) = -c^2 \quad \text{and} \quad \ddot{x}^\mu(\tau) + \Gamma^\mu_{\nu\sigma}(x(\tau))\dot{x}^\nu(\tau)\dot{x}^\sigma(\tau) = 0 . \quad (230)$$

As the geodesic equation describes the motion of a particle under the influence of gravity alone, it can be viewed as the general-relativistic analogue of the Newtonian equation of motion for a particle in a gravitational potential, $\ddot{x}^i(t) = -\partial_i\phi(x(t))$.

- Lightlike geodesics are worldlines of classical photons. In coordinate language, they satisfy

$$g_{\mu\nu}(x(s))\dot{x}^\mu(s)\dot{x}^\nu(s) = 0 \quad \text{and} \quad \ddot{x}^\mu(s) + \Gamma^\mu_{\nu\sigma}(x(s))\dot{x}^\nu(s)\dot{x}^\sigma(s) = 0 . \quad (231)$$

In this case the parametrisation cannot be fixed by a normalisation of the tangent vector. (We know already from special relativity that there is no proper time for classical photons.) The parameter s is determined uniquely up to affine transformations,

$$s \mapsto \hat{s} = k s + s_0 \quad (232)$$

with a non-zero constant k and an arbitrary constant s_0 , see Worksheet 7. Any such parametrisation of a lightlike geodesics is called an *affine parametrisation*.

- In a coordinate system with $g_{\mu\nu}|_p = \eta_{\mu\nu}$ and $\Gamma^\sigma_{\mu\nu}|_p = 0$ any geodesic is a straight line up to *second* order, i.e., if the geodesic passes at the parameter value $\tau = 0$ through the point p , then

$$x^\mu(\tau) = x^\mu(0) + \dot{x}^\mu(0)\tau + \ddot{x}^\mu(0)\frac{\tau^2}{2} + O(\tau^3) =$$

$$x^\mu(0) + \dot{x}^\mu(0)\tau - \underbrace{\Gamma^\mu_{\nu\sigma}|_p}_{=0}\dot{x}^\nu(0)\dot{x}^\sigma(0)\frac{\tau^2}{2} + O(\tau^3) = x^\mu(0) + \dot{x}^\mu(0)\tau + O(\tau^3). \quad (233)$$

Such a coordinate system differs from an inertial system as little as possible. We may think of such a coordinate system as being attached to Einstein's freely falling elevator; the elevator must be so small that, inside the elevator box, terms of third and higher order can be neglected.

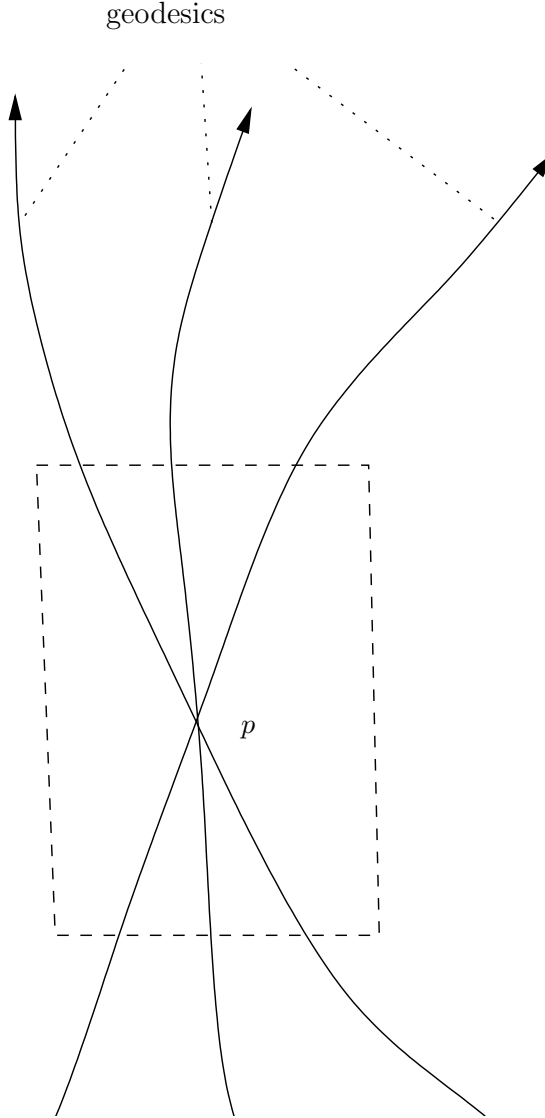


Figure 52: A coordinate system attached to Einstein's elevator

The geodesic equation is of particular physical relevance. It tells us how a spacetime can be probed with the help of freely falling massive particles and photons.

5.2 The rule of minimal coupling

In addition to the motion of massive particles and classical photons we also need to know how to describe fields on a general-relativistic spacetime. This includes

- the electromagnetic field,
- fields from continuum mechanics, e.g. the four-velocity, the energy density and the pressure of perfect fluids
- the Dirac field,
- the Klein-Gordon field,

and others. We emphasise that the gravitational field is *not* to be treated as a field on a general-relativistic spacetime; the gravitational field is coded into the geometry of the spacetime itself.

If one knows for a particular field the special-relativistic equations, then the equivalence principle severely restricts the possible generalisations to general relativity. However, the equivalence principle does not determine the general-relativistic equations uniquely. This is true because there are many different equations, formulated on an unspecified general-relativistic spacetime, that all take the same form if we specialise to the spacetime of special relativity, i.e., to Minkowski spacetime. The *simplest* method to transfer a special-relativistic equation into general relativity is the following.

Rule of minimal coupling: Write the special-relativistic version of a field equation in an inertial system. Then replace $\eta_{\mu\nu}$ with $g_{\mu\nu}$ and replace all partial derivatives ∂_μ with covariant derivatives ∇_μ . This gives the general-relativistic form of the field equation in arbitrary coordinates.

The rule of minimal coupling is also known as the “comma-goes-to-semicolon rule”, referring to the alternative notation of using a comma for partial derivatives and a semicolon for covariant derivatives, $\partial_\mu(\cdot) = (\cdot)_{,\mu} \mapsto \nabla_\mu(\cdot) = (\cdot)_{;\mu}$.

The rule of minimal coupling can be understood as a rule of how to couple a certain field to gravity in the simplest possible way. (The passage from special relativity to general relativity can be viewed as “switching on gravity”.)

The rule of minimal coupling is but a rule of thumb; in some cases it does not give the correct physical law. Two observations are important.

- In some cases the rule is ambiguous, as $\partial_\mu\partial_\nu = \partial_\nu\partial_\mu$ but $\nabla_\mu\nabla_\nu \neq \nabla_\nu\nabla_\mu$. If the special-relativistic version of a field equation involves second partial derivatives in a non-symmetrised form, the rule of minimal coupling gives different general-relativistic laws, depending on the order in which the partial derivatives are written.
- It is always possible to add curvature terms to a general-relativistic equation without violating the equivalence principle. This is true because curvature terms vanish when passing from general to special relativity. The question of whether or not the correct version of a general-relativistic field equation involves curvature terms has to be investigated by comparison with experiments.

To illustrate the rule of minimal coupling with two examples, we consider the electromagnetic field and a perfect fluid.

- In special relativity, Maxwell's equations in inertial coordinates read

$$(MI) \quad \partial_\mu F_{\nu\sigma} + \partial_\nu F_{\sigma\mu} + \partial_\sigma F_{\mu\nu} = 0 ,$$

$$(MII) \quad \partial_\mu G^{\mu\rho} = J^\rho .$$

The law of charge conservation, $\partial_\rho J^\rho = 0$, is a consequence of (MII).

The energy-momentum tensor of the electromagnetic field in vacuum is

$$T_{\rho\sigma} = \frac{1}{\mu_0} \left(F_{\rho\alpha} F_\sigma^\alpha - \frac{1}{4} \eta_{\rho\sigma} F_{\alpha\beta} F^{\alpha\beta} \right) , \quad (234)$$

recall Problem 2 of Worksheet 4. If the system is closed, the conservation law $\partial_\rho T^{\rho\sigma} = 0$ holds. Here indices are lowered and raised with $\eta_{\mu\nu}$ and $\eta^{\rho\sigma}$, respectively.

We now translate these equations into general relativity with the rule of minimal coupling, i.e., we replace everywhere $\eta_{\mu\nu}$ with $g_{\mu\nu}$ and ∂_μ with ∇_μ ; correspondingly, indices are now lowered and raised with $g_{\mu\nu}$ and $g^{\rho\sigma}$, respectively.

$$(MI) \quad \nabla_\mu F_{\nu\sigma} + \nabla_\nu F_{\sigma\mu} + \nabla_\sigma F_{\mu\nu} = 0 ,$$

$$(MII) \quad \nabla_\mu G^{\mu\rho} = J^\rho .$$

The law of charge conservation becomes $\nabla_\rho J^\rho = 0$.

The energy-momentum tensor of the electromagnetic field in vacuum reads

$$T_{\rho\sigma} = \frac{1}{\mu_0} \left(F_{\rho\alpha} F_\sigma^\alpha - \frac{1}{4} g_{\rho\sigma} F_{\alpha\beta} F^{\alpha\beta} \right) . \quad (235)$$

If the system is closed, it satisfies $\nabla_\rho T^{\rho\sigma} = 0$. Here, in general relativity, the system is “closed” if the electromagnetic field interacts only with the gravitational field (which is coded into the geometry of spacetime), and not with any other fields such as charges, currents, material media etc.

In this case the rule of minimal coupling yields the correct general-relativistic equations, as verified by all experiments to date. In Worksheet 8 we will show that

- the first Maxwell equation $\nabla_\mu F_{\nu\sigma} + \nabla_\nu F_{\sigma\mu} + \nabla_\sigma F_{\mu\nu} = 0$ is equivalent to the equation $\partial_\mu F_{\nu\sigma} + \partial_\nu F_{\sigma\mu} + \partial_\sigma F_{\mu\nu} = 0$ in any coordinate system;
- the law of charge conservation $\nabla_\rho J^\rho = 0$ follows from the second Maxwell equation $\nabla_\mu G^{\mu\rho} = J^\rho$.

- In special relativity in inertial coordinates, a perfect fluid has the energy-momentum tensor

$$T_{\rho\sigma} = \left(\mu + \frac{p}{c^2} \right) U_\rho U_\sigma + p \eta_{\rho\sigma} ; \quad (236)$$

for a closed system, $\partial_\rho T^{\rho\sigma} = 0$, the relativistic Euler equation

$$\left(\mu + \frac{p}{c^2} \right) U^\rho \partial_\rho U^\sigma + \partial_\tau p \left(\eta^{\tau\sigma} + \frac{1}{c^2} U^\tau U^\sigma \right) = 0 \quad (237)$$

holds, recall Problem 3 from Worksheet 3.

According to the rule of minimal coupling, in general relativity the energy-momentum tensor of a perfect fluid reads

$$T_{\rho\sigma} = \left(\mu + \frac{p}{c^2} \right) U_\rho U_\sigma + p g_{\rho\sigma} \quad (238)$$

in any coordinate system. If the system is closed, the equation $\nabla_\rho T^{\rho\sigma} = 0$ holds and the fluid satisfies the Euler equation

$$\left(\mu + \frac{p}{c^2} \right) U^\rho \nabla_\rho U^\sigma + \nabla_\tau p \left(g^{\tau\sigma} + \frac{1}{c^2} U^\tau U^\sigma \right) = 0. \quad (239)$$

(For the scalar function p we have of course $\nabla_\tau p = \partial_\tau p$.) Also in this case, the rule of minimal coupling gives the correct general-relativistic equations.

If in special relativity the energy-momentum tensor of a certain field satisfies in inertial coordinates the continuity equation $\partial_\mu T^{\mu\nu} = 0$, and if the rule of minimal coupling is applied, the resulting general-relativistic energy-momentum tensor satisfies in any coordinates the equation $\nabla_\mu T^{\mu\nu} = 0$. The latter equation is *not* a continuity equation: It does *not* imply that the temporal change of the energy content of a spatial volume equals the energy flux over its boundary. Energy conservation in this sense holds only in “infinitesimally small spacetime regions”, i.e., in regions that are so small that, in an appropriately chosen chart, the Christoffel symbols are negligibly small so that the covariant derivative may be replaced by a partial derivative. To put this another way, in general relativity energy conservation holds only in regions that are so small that, according to the equivalence principle, the gravitational field can be transformed away. In larger regions energy of the matter fields may be converted into gravitational waves. Therefore, an energy conservation law *cannot* hold for the matter fields in the presence of a gravitational field, i.e., on a curved spacetime. Note that it is impossible to ascribe an energy-momentum tensor to the gravitational field: the latter is coded into the spacetime geometry in a way that it can be transformed away at any one point (i.e., approximately on any sufficiently small neighbourhood); if a tensor at some point is zero in one coordinate system, then it is zero in any coordinate system.

5.3 Einstein’s field equation

In Section 5.1 we have established the geometric framework of general relativity (Lorentzian manifolds) and the equations of motion for freely falling particles and for classical photons. In Section 5.2 we have discussed how to describe fields on a general-relativistic spacetime. What is still missing is the field equation for the gravitational field, i.e., the general-relativistic analogue of the Poisson equation.

Newtonian theory of gravity:

$$\frac{d^2}{dt^2} \vec{r} + \vec{\nabla} \phi = 0$$

$$\frac{1}{4\pi G} \Delta \phi = \mu$$

Einstein’s theory of gravity:

$$\ddot{x}^\mu + \Gamma^\mu_{\nu\sigma} \dot{x}^\nu \dot{x}^\sigma = 0,$$

???

Comparison of the Newtonian equation of motion for a particle in a gravitational field with the geodesic equation shows that the Christoffel symbols are analogous to the gradient of the Newtonian potential ϕ . As the Christoffel symbols are built from first-order derivatives of the metric, this suggests that the metric is analogous to ϕ . This is of course in perfect agreement with the fundamental idea of general relativity that the gravitational field is coded into the geometry, i.e., that all the information about the gravitational field is given by the metric tensor field $g \in \mathcal{T}_2^0 M$.

We have already discussed in Chapter 3 that the mass density μ has to be replaced by the energy-momentum tensor $T \in \mathcal{T}_2^0 M$. We are thus led to the conclusion that, when passing from Newtonian to Einsteinian gravity, the following replacements should be made.

$$\phi \longmapsto g \in \mathcal{T}_2^0 M \text{ (the spacetime metric)} \quad (240)$$

$$\mu \longmapsto T \in \mathcal{T}_2^0 M \text{ (the energy-momentum tensor field)} \quad (241)$$

$$\frac{1}{4\pi G} \Delta \longmapsto \mathcal{D} \text{ (a differential operator)} \quad (242)$$

Hence, the desired field equation should be of the form

$$\mathcal{D}g = T . \quad (243)$$

We require that the operator \mathcal{D} should satisfy the following two conditions.

(L1) $\mathcal{D}g$ contains derivatives of g up to second order;

(L2) $\mathcal{D}g$ is a tensor field of rank $(0, 2)$, $\mathcal{D}g = (\mathcal{D}g)_{\mu\nu} dx^\mu \otimes dx^\nu \in \mathcal{T}_2^0 M$, that satisfies

$$\nabla^\mu (\mathcal{D}g)_{\mu\nu} = 0 . \quad (244)$$

The first condition is motivated by comparison with the Newtonian theory; the second condition comes from the observation that, by the rule of minimal coupling, the energy-momentum tensor of a closed system satisfies the condition $\nabla^\mu T_{\mu\nu} = 0$; if we accept the idea that *all* fields on the spacetime act as the source of gravity, the energy-momentum tensor on the right-hand side of the field equation should certainly refer to a closed system.

It is a remarkable mathematical result that the two properties (L1) and (L2) fix the differential operator \mathcal{D} uniquely:

Theorem (Lovelock, 1971): (L1) and (L2) are satisfied if and only if $\mathcal{D}g$ has the following form:

$$(\mathcal{D}g)_{\mu\nu} = \frac{1}{\kappa} \left(R_{\mu\nu} - \frac{R}{2} g_{\mu\nu} + \Lambda g_{\mu\nu} \right) . \quad (245)$$

Here $R_{\mu\nu}$ is the Ricci tensor field, R is the Ricci scalar, and κ and Λ are constants.

Proof: The “if” part is easy to verify: (L1) is obvious and (L2) follows from the contracted second Bianch identity, as will be proven in Worksheet 8. The “only if” part is highly non-trivial. The proof, which is rather long, was given by David Lovelock in two papers [J. Math. Phys. 12, 498 (1971), J. Math. Phys. 13, 874 (1972)]. In the first paper Lovelock assumed that the operator \mathcal{D} satisfies, in addition to (L2), the symmetry property $(\mathcal{D}g)_{\mu\nu} = (\mathcal{D}g)_{\nu\mu}$; in the second paper he showed that this symmetry property can be dropped because it follows automatically. The Lovelock theorem is true only in four dimensions.

Hence the gravitational field equation (“Einstein’s field equation”) takes the following form:

$$R_{\mu\nu} - \frac{R}{2} g_{\mu\nu} + \Lambda g_{\mu\nu} = \kappa T_{\mu\nu} . \quad (246)$$

The curvature quantity

$$G_{\mu\nu} = R_{\mu\nu} - \frac{R}{2} g_{\mu\nu} \quad (247)$$

is called the *Einstein tensor field*, Λ is called the *cosmological constant*, and κ is called *Einstein’s gravitational constant*. The relation between κ and the Newtonian gravitational constant G will be derived in Section 5.4 below when we discuss the Newtonian limit of general relativity.

When Einstein established his field equation in 1915, after a long struggle with various problems, the Lovelock theorem was of course not yet known. Einstein arrived at this equation on the basis of rather strong additional assumptions that were heuristically motivated. In the first version of his field equation there was no cosmological constant; he introduced it later “by hand” when he saw that without this term he could not get static cosmological solutions. After evidence for a cosmic expansion (i.e., the Lemaître-Hubble law) had come about in the late 1920s, Einstein according to George Gamow called the introduction of the cosmological constant his “biggest blunder”. Actually, on the basis of the Lovelock theorem, there is no reason why the cosmological constant should be equal to zero.

Note that $\Lambda^{-1/2}$ has the dimension of a length. In the next section we will see that this length must be large in comparison to dimensions for which the Newtonian limit has been verified, i.e., that Λ plays a role only at a cosmological scale. According to the present concordance model of cosmology, known as the Λ Cold Dark Matter (Λ CDM) model, we believe that we live in a universe with a (small but non-zero) positive cosmological constant.

By transvecting Einstein’s field equation with $g^{\mu\nu}$ we find

$$\begin{aligned} R - \frac{R}{2} 4 + \Lambda 4 &= \kappa T_{\mu\nu} g^{\mu\nu} , \\ R &= 4 \Lambda - \kappa T_{\mu\nu} g^{\mu\nu} . \end{aligned} \quad (248)$$

This demonstrates that the field equation can be equivalently rewritten as

$$R_{\mu\nu} = \Lambda g_{\mu\nu} + \kappa \left(T_{\mu\nu} + \frac{1}{2} T_{\rho\sigma} g^{\rho\sigma} g_{\mu\nu} \right) . \quad (249)$$

According to Einstein’s field equation the distribution of energy and momentum on the space-time manifold (i.e. $T_{\mu\nu}$) gives us a second-order non-linear partial differential equation for the

metric tensor field and, thus, for the gravitational field. The solution is uniquely determined only after boundary conditions or initial conditions have been fixed. Note that it is meaningless to say that a certain metric “satisfies Einstein’s field equation” unless the energy-momentum tensor has been specified.

The most important cases are:

- Vacuum: $T_{\mu\nu} = 0$.

In this case, Einstein’s field equation (249) reads

$$R_{\mu\nu} = \Lambda g_{\mu\nu} . \quad (250)$$

A pseudo-Riemannian manifold whose Ricci tensor is of this form is called an *Einstein manifold*. For local considerations, e.g. for determining the gravitational field near an isolated celestial body, we may consider Einstein’s vacuum equation without a cosmological constant

$$R_{\mu\nu} = 0 . \quad (251)$$

The Minkowski metric $g_{\mu\nu} = \eta_{\mu\nu}$, i.e., the spacetime metric of special relativity, is a (trivial) solution of (251). The most famous non-trivial solution of this equation is the Schwarzschild solution which will be discussed in the next chapter. It describes the vacuum spacetime around a spherically symmetric matter distribution and also the spacetime of a spherically symmetric (i.e., non-rotating) black hole. Other important solutions to the vacuum field equation without a cosmological constant are the Kerr solution (spacetime of a rotating black hole), the Neugebauer-Meinell disc (spacetime around a rigidly rotating disc of dust) and spacetimes describing gravitational waves. Vacuum solutions with a cosmological constant are, e.g., the Kottler solution (which generalises the Schwarzschild solution by allowing for a non-zero Λ), the deSitter solution ($\Lambda > 0$) and the anti-deSitter solution ($\Lambda < 0$); the latter two play a role in cosmology.

- Perfect fluid:

With the energy-momentum tensor field of a perfect fluid on the right-hand side, Einstein’s field equation (246) reads

$$R_{\rho\sigma} - \frac{R}{2} g_{\rho\sigma} + \Lambda g_{\rho\sigma} = \kappa \left(\left(\mu + \frac{p}{c^2} \right) U_\rho U_\sigma + p g_{\rho\sigma} \right) . \quad (252)$$

By (248), the Ricci scalar can be replaced by $R = 4\Lambda - \kappa(3p - \mu c^2)$ and written on the right-hand side to get the field equation in the form of (249). For $p = 0$ we have the more special case of a dust.

Perfect fluid solutions without a cosmological constant are of interest as models for the interior of stars. The interior Schwarzschild solution, which will be discussed below, is an example; it describes a spherically symmetric static star with constant energy density $\varepsilon = \mu c^2$. The Friedmann-Lemaître solutions, which are the simplest cosmological models of our universe, are perfect fluid solutions with a cosmological constant. The rather pathological Goedel universe (Kurt Goedel’s birthday present to Einstein on occasion of his 70th birthday in 1949) is a dust solution with a non-vanishing cosmological constant.

- Electrovacuum:

With the energy-momentum tensor of a vacuum electromagnetic field (no charges, no medium) on the right-hand side, Einstein's field equation (246) reads

$$R_{\mu\nu} - \frac{R}{2} g_{\mu\nu} + \Lambda g_{\mu\nu} = \frac{\kappa}{\mu_0} \left(F_{\mu\alpha} F_{\nu}{}^{\alpha} - \frac{1}{4} g_{\mu\nu} F_{\alpha\beta} F^{\alpha\beta} \right). \quad (253)$$

As the energy-momentum tensor is trace-free, $T_{\mu\nu} g^{\mu\nu} = 0$, by (248) the Ricci scalar must be a constant, $R = 4\Lambda$, just as in vacuum. The best-known electrovacuum solutions without a cosmological constant are the Reissner-Nordström solution (field outside of a charged spherically symmetric static object) and the Kerr-Newman solution (field of a charged and rotating black hole). There are also solutions describing coupled electromagnetic and gravitational waves.

We conclude this section with three remarks.

- Einstein's field equation can be derived from a variational principle. This variational formulation of the field equation was found, independently of Einstein, by David Hilbert in 1915. The variational principle can be written in the following way.

$$0 = \delta\mathcal{W} = \delta \int_{\Omega} \left(\frac{R}{2} - \kappa \mathcal{L}_{\text{mat}} \right) \sqrt{|\det(g_{\mu\nu})|} dx^0 dx^1 dx^2 dx^3. \quad (254)$$

\mathcal{W} is called the *Einstein-Hilbert action*. Here the symbols have the following meaning.

$$R = R_{\mu\nu} g^{\mu\nu},$$

κ = Einstein's gravitational constant,

$$\mathcal{L}_{\text{mat}} = \text{matter Lagrangian}, \quad T_{\mu\nu} = \frac{-2}{\sqrt{|\det(g_{\mu\nu})|}} \frac{\partial(\sqrt{|\det(g_{\mu\nu})|} \mathcal{L}_{\text{mat}})}{\partial g^{\mu\nu}},$$

$$\Omega \subseteq M,$$

δ = variation keeping the metric on $\partial\Omega$ fixed.

- Einstein's field equation has the same form, given by (246), in any coordinate system. In contrast to special relativity, there are no distinguished coordinate systems in general relativity. This can be interpreted as saying that the “principle of general relativity” is satisfied, recall p. 49.
- If the distribution of matter (i.e., the energy-momentum tensor) is known, the metric and hence the geodesics are not yet determined uniquely by the field equation; in addition, boundary conditions – or initial conditions – are needed. It is thus true that the distribution of matter does *not* determine the motion of freely falling particles uniquely. In this sense, “Mach's principle” is *not* satisfied in general relativity, recall. p. 49.

5.4 The Newtonian limit

Now we want to show that Einstein's gravitational theory reproduces Newton's gravitational theory in a certain limit, i.e., if certain approximative assumptions are satisfied. As Newton's gravitational theory works well (in its domain of validity), this is crucial for the acceptance of Einstein's gravitational theory.

Newton's theory relies on two equations (recall Chapter 3 and Section 5.3), i.e., the equation of motion for a particle in a gravitational potential and the field equation for the gravitational potential. In a certain limit, the first equation must follow from the geodesic equation and the second equation must follow from Einstein's field equation. In other words, it is our goal to demonstrate that

$$\frac{d^2 x^\mu}{d\tau^2} + \Gamma_{\nu\sigma}^\mu \frac{dx^\nu}{d\tau} \frac{dx^\sigma}{d\tau} = 0 \quad \xrightarrow{\text{approximation}} \quad \frac{d^2 x^i}{dt^2} + \delta^{ij} \partial_j \phi = 0 , \quad (255)$$

$$R_{\mu\nu} - \frac{R}{2} g_{\mu\nu} + \Lambda g_{\mu\nu} = \kappa T_{\mu\nu} \quad \xrightarrow{\text{approximation}} \quad \Delta \phi = 4\pi G \mu . \quad (256)$$

Now we list the approximative assumptions that are necessary for the Newtonian limit.

- (N1) The gravitational field is weak in the sense that the metric differs but little from the metric of special relativity,

$$g_{\mu\nu} = \eta_{\mu\nu} + h_{\mu\nu} . \quad (257)$$

Here it is assumed that $h_{\mu\nu}$ is so small that only terms of first order in $h_{\mu\nu}$ and $\partial_\sigma h_{\mu\nu}$ have to be taken into account. The inverse metric is then of the form

$$g^{\nu\rho} = \eta^{\nu\rho} - \eta^{\nu\tau} \eta^{\rho\lambda} h_{\tau\lambda} . \quad (258)$$

(Proof: $g_{\mu\nu} g^{\nu\rho} = (\eta_{\mu\nu} + h_{\mu\nu})(\eta^{\nu\rho} - \eta^{\nu\tau} \eta^{\rho\lambda} h_{\tau\lambda}) = \eta_{\mu\nu} \eta^{\nu\rho} + h_{\mu\nu} \eta^{\nu\rho} - \eta_{\mu\nu} \eta^{\nu\tau} \eta^{\rho\lambda} h_{\tau\lambda} = \delta_\mu^\rho + h_{\mu\lambda} \eta^{\lambda\rho} - \delta_\mu^\tau \eta^{\rho\lambda} h_{\tau\lambda}$, where we have dropped all terms of higher than first order.)

- (N2) The gravitational field varies so slowly that it can be approximated as being time-independent, i.e.

$$\partial_0 h_{\mu\nu} = 0 . \quad (259)$$

- (N3) The particle velocity is small in comparison to the speed of light, i.e., its proper time τ differs but little from coordinate time t ,

$$\left| \frac{dx^0}{d\tau} \right| = \left| \frac{c dt}{d\tau} \right| \approx c , \quad \left| \frac{dx^i}{d\tau} \right| \approx \left| \frac{dx^i}{dt} \right| \ll c . \quad (260)$$

- (N4) Matter moves so slowly that it can be approximated as being in rest and only the mass density μ acts as the source of gravity,

$$T_{00} = c^2 \mu , \quad T_{0i} = 0 , \quad T_{ik} = 0 . \quad (261)$$

To calculate the Newtonian limit we begin with the spatial components ($\mu = i$) of the geodesic equation for a freely falling particle with proper time τ ,

$$\frac{d^2 x^i}{d\tau^2} + \Gamma^i_{\nu\sigma} \frac{dx^\nu}{d\tau} \frac{dx^\sigma}{d\tau} = 0 . \quad (262)$$

The sums over ν and σ are split into temporal and spatial parts,

$$\frac{d^2 x^i}{d\tau^2} + \Gamma^i_{00} \frac{dx^0}{d\tau} \frac{dx^0}{d\tau} + 2 \Gamma^i_{j0} \frac{dx^j}{d\tau} \frac{dx^0}{d\tau} + \Gamma^i_{jk} \frac{dx^j}{d\tau} \frac{dx^k}{d\tau} = 0 . \quad (263)$$

Owing to (N3) the third and the fourth term can be neglected in comparison to the second term,

$$\frac{d^2 x^i}{d\tau^2} = - \Gamma^i_{00} \frac{dx^0}{d\tau} \frac{dx^0}{d\tau} . \quad (264)$$

This can be rewritten, again because of (N3), to within a good approximation as

$$\frac{d^2 x^i}{dt^2} = - \Gamma^i_{00} c^2 . \quad (265)$$

Γ^i_{00} can be calculated with the help of (N1) and (N2):

$$\begin{aligned} \Gamma^i_{00} &= \frac{1}{2} g^{i\mu} (\partial_0 g_{\mu 0} + \partial_0 g_{\mu 0} - \partial_\mu g_{00}) \\ &= \frac{1}{2} \eta^{i\mu} (2 \underbrace{\partial_0 h_{\mu 0}}_{=0} - \partial_\mu h_{00}) = - \frac{1}{2} \delta^{ij} \partial_j h_{00} . \end{aligned} \quad (266)$$

This puts the equation of motion (265) into the following form.

$$\frac{d^2 x^i}{dt^2} = \frac{1}{2} \delta^{ij} \partial_j h_{00} c^2 . \quad (267)$$

With the identification

$$h_{00} = - \frac{2\phi}{c^2} , \quad g_{00} = - \left(1 + \frac{2\phi}{c^2} \right) , \quad (268)$$

this is indeed the equation of motion of Newtonian theory.

Note that ϕ is defined only up to an additive constant. Here we have fixed this constant in such a way that g_{00} takes the same value as in special relativity if $\phi = 0$.

Now we consider Einstein's field equation in the form of (249). With (N4), the 00-component of this equation can be written as

$$R_{00} = \Lambda g_{00} + \kappa \left(T_{00} - \frac{1}{2} T_{00} g^{00} g_{00} \right) = \Lambda g_{00} + \kappa c^2 \mu \left(1 - \frac{1}{2} g^{00} g_{00} \right). \quad (269)$$

Because of (N1) we have

$$g_{00} = \eta_{00} + h_{00} = -1 + h_{00} \quad (270)$$

and

$$g^{00} g_{00} = (\eta^{00} - \eta^{0\mu} \eta^{0\nu} h_{\mu\nu}) (\eta_{00} + h_{00}) = (-1 - h_{00})(-1 + h_{00}) = 1. \quad (271)$$

Inserting this result into (269) shows that

$$R_{00} = \Lambda (-1 + h_{00}) + \frac{1}{2} \kappa c^2 \mu. \quad (272)$$

On the other hand, R_{00} can be calculated with the help of (N1) and (N2):

$$R_{00} = R_{\mu 00}{}^\mu = \partial_\mu \Gamma^\mu{}_{00} - \partial_0 \Gamma^\mu{}_{\mu 0} + \dots \quad (273)$$

Here the ellipses stand for terms that can be neglected because of (N1). From (N2) we get $\partial_0 \Gamma^\mu{}_{\rho\sigma} = 0$, hence

$$R_{00} = \partial_\mu \Gamma^\mu{}_{00} = \partial_i \Gamma^i{}_{00}. \quad (274)$$

Together with (266) this yields

$$R_{00} = -\frac{1}{2} \delta^{ij} \partial_i \partial_j h_{00} = -\frac{1}{2} \Delta h_{00}. \quad (275)$$

By comparison of (272) and (275),

$$\Delta h_{00} = 2\Lambda (-1 + h_{00}) - \kappa c^2 \mu. \quad (276)$$

As we know already that h_{00} has to be identified with $-2\phi/c^2$, recall (268), our last result implies that

$$\Delta \phi = -\Lambda (c^2 + 2\phi) + \frac{1}{2} \kappa c^4 \mu. \quad (277)$$

This is indeed the Poisson equation of Newton's gravitational theory if

$$\Lambda = 0 \quad (278)$$

and

$$\kappa = \frac{8\pi G}{c^4}. \quad (279)$$

We have thus proven that, if these two equations are true, in all cases where the approximative assumptions (N1) to (N4) are justified, Einstein’s gravitational theory reproduces Newton’s gravitational theory. This makes sure that Newton’s theory can still be viewed as a viable physical theory within a large domain of validity.

It is important to realise that Einstein’s theory admits the correct Newtonian limit only if the cosmological constant is set equal to zero, $\Lambda = 0$. With a non-zero cosmological constant, the approximative assumptions (N1) to (N4) do not lead to the Poisson equation but rather to a modified Newtonian field equation of gravity (277).

Note that in the case $\Lambda \neq 0$ the Minkowski metric is no longer a solution to the vacuum field equation. The maximally symmetric solution of the field equation $R_{\mu\nu} = \Lambda g_{\mu\nu}$ is called the *deSitter metric* for $\Lambda > 0$ and the *anti-deSitter metric* for $\Lambda < 0$. Therefore, when dealing with $\Lambda \neq 0$, it would be more natural to replace in the ansatz $g_{\mu\nu} = \eta_{\mu\nu} + h_{\mu\nu}$ the Minkowski metric with the (anti-)deSitter metric.

To date there is no experimental evidence that the standard Newtonian gravitational theory has to be modified, within its domain of validity. This indicates that the cosmological constant must be so small that it can be neglected for all experiments where the Newtonian theory gives a good approximation. This includes all experiments in the Solar system. At a cosmological scale, however, the situation is different. Observations indicate an *accelerated* expansion of the universe, as was demonstrated with the help of Type Ia Supernovae. (This earned Saul Perlmutter, Brian Schmidt and Adam Riess the Physics Nobel Prize in 2011.) A positive cosmological constant is needed to explain this accelerated expansion. Λ acts like a “medium”, called “dark energy”, that fills the universe homogeneously and drives the galaxies apart. To fit the observations, one has to assume that $\Lambda^{-1/2} \approx 10^{26}\text{m}$ (which corresponds to $\Lambda \approx 10^{-122}$ in Planck units). Λ can be safely ignored in regions that are small in comparison to $\Lambda^{-1/2}$. Note that the diameter of our Galaxy is about 10^{20}m , i.e., the cosmological constant plays a role only at length scales that are several orders of magnitude bigger than the size of our Galaxy.

6 Schwarzschild solution

One of the most important solutions to Einstein’s vacuum field equation was found by Karl Schwarzschild in 1916 (and independently by Johann Droste, a PhD student of Hendrik Antoon Lorentz, a few months later). It describes the gravitational field outside of a spherically symmetric body, e.g. the gravitational field of the Sun.

The analogous problem in Newtonian theory has the solution $\phi(r) = -GM/r$, which can be derived in a few minutes by solving the equation $\Delta\phi = 0$ under the assumption that ϕ depends on r only. This leads to $\phi(r) = A/r + B$, and the Gauss theorem yields $A = -GM$ where M is the mass of the central body. (B can be set equal to zero without loss of generality.) In general relativity, the analogous problem is much more complicated and requires a fairly long calculation. As in Newtonian theory, it turns out that the solution is necessarily time-independent, i.e. that, as long as spherical symmetry is preserved, a pulsating star has the

same gravitational field in the exterior region as a static star with the same mass. In other words, spherically symmetric gravitational waves do not exist. Schwarzschild did not know this; he assumed that the field is time-independent from the beginning. It was shown by George Birkhoff in 1923 that a spherically symmetric solution to the vacuum field equation $R_{\mu\nu} = 0$ is *necessarily* time-independent. Actually, the same result had been found in a little known paper by the Norwegian author Jørg Jebsen already two years earlier. In the following we will derive the Schwarzschild solution from the assumption of spherical symmetry, without assuming time-independence from the outset. We will prove the Jebsen-Birkhoff theorem during the derivation.

6.1 Derivation of the Schwarzschild solution

We want to solve the vacuum field equation without a cosmological constant, $R_{\mu\nu} = 0$, in the exterior region of a spherically symmetric star of radius $r_*(t)$ and mass M . We first have to determine the general form of a metric that is spherically symmetric.

To that end we begin by writing the Minkowski metric, i.e. the spacetime metric of special relativity, in its standard form using inertial coordinates,

$$g = \eta_{\mu\nu} dx^\mu \otimes dx^\nu = -c^2 dt \otimes dt + dx \otimes dx + dy \otimes dy + dz \otimes dz . \quad (280)$$

We agree to write from now on

$$\alpha \beta = \frac{1}{2}(\alpha \otimes \beta + \beta \otimes \alpha) \quad (281)$$

for the symmetrised tensor product of any two covector fields α and β . Then (280) becomes

$$g = -c^2 dt^2 + dx^2 + dy^2 + dz^2 . \quad (282)$$

Switching to spherical polar coordinates,

$$x = r \cos \varphi \sin \vartheta , \quad y = r \sin \varphi \sin \vartheta , \quad z = r \cos \vartheta , \quad (283)$$

results in

$$g = -c^2 dt^2 + dr^2 + r^2 (\sin^2 \vartheta d\varphi^2 + d\vartheta^2) . \quad (284)$$

This metric is obviously spherically symmetric, in the sense that any rotation of the coordinate system leaves the metric invariant. We want to determine the most general deformation of this metric such that spherical symmetry is preserved. We can certainly multiply each term with a function that depends on t and r only. We choose the signs such that the t -lines remain timelike and the r -, ϑ - and φ -lines remain spacelike. The only possible mixed term that does not violate spherical symmetry is an rt -term. The general spherically symmetric metric is thus of the form

$$g = -c^2 e^{\nu(t,r)} dt^2 + e^{\lambda(t,r)} dr^2 + 2 \sigma(t,r) dr dt + r^2 e^{\mu(t,r)} (\sin^2 \vartheta d\varphi^2 + d\vartheta^2) \quad (285)$$

where $dr dt$ denotes the symmetrised tensor product according to (281). We can simplify this expression by introducing a new radius coordinate

$$\tilde{r} = r e^{\mu(t,r)/2} . \quad (286)$$

Then the differential of \tilde{r} is given by

$$d\tilde{r} = e^{\mu(t,r)/2} \left(\frac{r}{2} \frac{\partial \mu(t,r)}{\partial t} dt + \left(1 + \frac{r}{2} \frac{\partial \mu(t,r)}{\partial r} \right) dr \right). \quad (287)$$

Here we assume that the map $(t, r, \vartheta, \varphi) \mapsto (t, \tilde{r}, \vartheta, \varphi)$ is an allowed coordinate transformation, i.e., that it is bijective and in both directions (infinitely often) continuously differentiable. (Here is a subtlety which is glossed over in several text-books: There are certainly examples where the transformation is not bijective, e.g. if $e^{\mu(t,r)} = r^{-2}$ which gives a constant \tilde{r} . For the derivation of the Schwarzschild solution, however, this subtlety is of no relevance because it can be shown that the vacuum field equation $R_{\sigma\rho} = 0$ does not admit spherically symmetric solutions (285) where μ cannot be transformed to zero.) If we replace r and dr in (285) accordingly, we get an expression of the form

$$g = -c^2 e^{\hat{\nu}(t,\tilde{r})} dt^2 + e^{\hat{\lambda}(t,\tilde{r})} d\tilde{r}^2 + 2\hat{\sigma}(t,\tilde{r}) d\tilde{r} dt + \tilde{r}^2 \left(\sin^2 \vartheta d\varphi^2 + d\vartheta^2 \right). \quad (288)$$

Here we assume that the factors in front of dt^2 and $d\tilde{r}^2$ have the desired signs such that they can be written as exponentials. By completing the square we can rewrite the metric as

$$\begin{aligned} g = & -c^2 \left(e^{\hat{\nu}(t,\tilde{r})/2} dt - \frac{\hat{\sigma}(t,\tilde{r})}{c^2} e^{-\hat{\nu}(t,\tilde{r})/2} d\tilde{r} \right)^2 \\ & + \left(\frac{\hat{\sigma}(t,\tilde{r})^2}{c^2} e^{-\hat{\nu}(t,\tilde{r})} + e^{\hat{\lambda}(t,\tilde{r})} \right) d\tilde{r}^2 + \tilde{r}^2 \left(\sin^2 \vartheta d\varphi^2 + d\vartheta^2 \right). \end{aligned} \quad (289)$$

We introduce a new time coordinate \tilde{t} by

$$e^{\hat{\nu}(t,\tilde{r})/2} dt - \frac{\hat{\sigma}(t,\tilde{r})}{c^2} e^{-\hat{\nu}(t,\tilde{r})/2} d\tilde{r} = e^{\tilde{\nu}(\tilde{t},\tilde{r})/2} d\tilde{t}, \quad (290)$$

where $e^{\tilde{\nu}(\tilde{t},\tilde{r})/2}$ is an integrating factor. By writing

$$e^{\tilde{\lambda}(\tilde{t},\tilde{r})} = \frac{\hat{\sigma}(t,\tilde{r})^2}{c^2} e^{-\hat{\nu}(t,\tilde{r})} + e^{\hat{\lambda}(t,\tilde{r})} \quad (291)$$

and then dropping the tildas, the metric reads

$$g = g_{\mu\nu} dx^\mu dx^\nu = -c^2 e^{\nu(t,r)} dt^2 + e^{\lambda(t,r)} dr^2 + r^2 \left(\sin^2 \vartheta d\varphi^2 + d\vartheta^2 \right). \quad (292)$$

We have shown that any spherically symmetric metric can be put into this form, provided that the transformation from r to \tilde{r} is possible and the factors have the correct signs such that they can be written as exponentials. In a more systematic manner, this result could be derived from the assumption that the spacetime admits an algebra of Killing vector fields that is isometric to the Lie algebra of the rotation group $\text{SO}(3)$ and that the orbits spanned by these Killing vector fields are spacelike 2-spheres. For the notion of Killing vector fields see Problem 4 of Worksheet 7.

Eq. (292) is the form of the metric that will be assumed as the starting point for deriving the Schwarzschild metric. The range of the coordinates is, as in Newtonian theory,

$$-\infty < t < \infty, \quad r_*(t) < r < \infty, \quad 0 < \vartheta < \pi, \quad 0 < \varphi < 2\pi \quad (293)$$

where $r_*(t)$ is the physical radius of the spherically symmetric body considered. In most cases it will be a constant, but in principle it may depend on time.

We now want to determine the functions ν and λ such that Einstein's vacuum field equation $R_{\mu\nu} = 0$ is satisfied. Before we can calculate the components of the Ricci tensor we have to determine the Christoffel symbols. From the metric coefficients $g_{\mu\nu}$, which can be read from (292) we could calculate the Christoffel symbols with the help of the formula (207). A more convenient way is to write the geodesic equation in the form of the Euler-Lagrange equations (212) and to get the Christoffel symbols as the coefficients of the $\dot{x}^\mu \dot{x}^\nu$ terms. For the spherically symmetric metric (292), the Lagrangian (213) reads

$$L(x, \dot{x}) = \frac{1}{2} \left(- e^{\nu(t,r)} c^2 \dot{t}^2 + e^{\lambda(t,r)} \dot{r}^2 + r^2 (\sin^2 \vartheta \dot{\varphi}^2 + \dot{\vartheta}^2) \right). \quad (294)$$

Here the overdot means derivative with respect to the curve parameter s which should not be confused with the coordinate time t .

We now write the t -, r -, ϑ - and φ -components of the Euler-Lagrange equation (212).

$$\begin{aligned} 0 &= \frac{d}{ds} \left(\frac{\partial L}{\partial \dot{t}} \right) - \frac{\partial L}{\partial t} = \frac{d}{ds} \left(- e^\nu c^2 \dot{t} \right) + \frac{1}{2} e^\nu \frac{\partial \nu}{\partial t} c^2 \dot{t}^2 - \frac{1}{2} e^\lambda \frac{\partial \lambda}{\partial t} \dot{r}^2 \\ &= - e^\nu c^2 \left(\ddot{t} + \frac{\partial \nu}{\partial r} \dot{r} \dot{t} + \frac{1}{2} \frac{\partial \nu}{\partial t} \dot{t}^2 \right) - \frac{1}{2} e^\lambda \frac{\partial \lambda}{\partial t} \dot{r}^2, \end{aligned} \quad (295)$$

$$\begin{aligned} 0 &= \frac{d}{ds} \left(\frac{\partial L}{\partial \dot{r}} \right) - \frac{\partial L}{\partial r} = \frac{d}{ds} \left(e^\lambda \dot{r} \right) + \frac{1}{2} e^\nu \frac{\partial \nu}{\partial r} c^2 \dot{t}^2 - \frac{1}{2} e^\lambda \frac{\partial \lambda}{\partial r} \dot{r}^2 - r (\sin^2 \vartheta \dot{\varphi}^2 + \dot{\vartheta}^2) \\ &= e^\lambda \left(\ddot{r} + \frac{1}{2} \frac{\partial \lambda}{\partial r} \dot{r}^2 + \frac{\partial \lambda}{\partial t} \dot{t} \dot{r} \right) + \frac{1}{2} e^\nu \frac{\partial \nu}{\partial r} c^2 \dot{t}^2 - r (\sin^2 \vartheta \dot{\varphi}^2 + \dot{\vartheta}^2), \end{aligned} \quad (296)$$

$$\begin{aligned} 0 &= \frac{d}{ds} \left(\frac{\partial L}{\partial \dot{\vartheta}} \right) - \frac{\partial L}{\partial \vartheta} = \frac{d}{d\tau} \left(r^2 \dot{\vartheta} \right) - r^2 \sin \vartheta \cos \vartheta \dot{\varphi}^2 \\ &= r^2 \ddot{\vartheta} + 2 r \dot{r} \dot{\vartheta} - r^2 \sin \vartheta \cos \vartheta \dot{\varphi}^2, \end{aligned} \quad (297)$$

$$\begin{aligned} 0 &= \frac{d}{ds} \left(\frac{\partial L}{\partial \dot{\varphi}} \right) - \frac{\partial L}{\partial \varphi} = \frac{d}{d\tau} \left(r^2 \sin^2 \vartheta \dot{\varphi} \right) \\ &= r^2 \sin^2 \vartheta \ddot{\varphi} + 2 r^2 \sin \vartheta \cos \vartheta \dot{\vartheta} \dot{\varphi} + 2 r \sin^2 \vartheta \dot{r} \dot{\varphi}. \end{aligned} \quad (298)$$

Solving for the second derivatives and equating with the corresponding component of the geodesic equation (225) yields:

$$\ddot{t} = - \frac{\partial \nu}{\partial r} \dot{r} \dot{t} - \frac{1}{2} \frac{\partial \nu}{\partial t} \dot{t}^2 - \frac{1}{2 c^2} e^{\lambda-\nu} \frac{\partial \lambda}{\partial t} \dot{r}^2 = - \Gamma_{\mu\nu}^t \dot{x}^\mu \dot{x}^\nu, \quad (299)$$

$$\ddot{r} = -\frac{1}{2} \frac{\partial \lambda}{\partial r} \dot{r}^2 - \frac{\partial \lambda}{\partial t} \dot{t} \dot{r} - \frac{1}{2} e^{\nu-\lambda} \frac{\partial \nu}{\partial r} c^2 \dot{t}^2 + r e^{-\lambda} (\sin^2 \vartheta \dot{\varphi}^2 + \dot{\vartheta}^2) = -\Gamma^r_{\mu\nu} \dot{x}^\mu \dot{x}^\nu, \quad (300)$$

$$\ddot{\vartheta} = -\frac{2}{r} \dot{r} \dot{\vartheta} + \sin \vartheta \cos \vartheta \dot{\varphi}^2 = -\Gamma^\vartheta_{\mu\nu} \dot{x}^\mu \dot{x}^\nu, \quad (301)$$

$$\ddot{\varphi} = -2 \cot \vartheta \dot{\vartheta} \dot{\varphi} - \frac{2}{r} \dot{r} \dot{\varphi} = -\Gamma^\varphi_{\mu\nu} \dot{x}^\mu \dot{x}^\nu. \quad (302)$$

From these equations we read that the Christoffel symbols are:

$$\begin{aligned} \Gamma^t_{rt} = \Gamma^t_{tr} &= \frac{1}{2} \frac{\partial \nu}{\partial r}, \quad \Gamma^t_{tt} = \frac{1}{2} \frac{\partial \nu}{\partial t}, \quad \Gamma^t_{rr} = \frac{1}{2c^2} e^{\lambda-\nu} \frac{\partial \lambda}{\partial t}, \\ \Gamma^r_{rr} &= \frac{1}{2} \frac{\partial \lambda}{\partial r}, \quad \Gamma^r_{tr} = \Gamma^r_{rt} = \frac{1}{2} \frac{\partial \lambda}{\partial t}, \quad \Gamma^r_{tt} = \frac{c^2}{2} e^{\nu-\lambda} \frac{\partial \nu}{\partial r}, \quad \Gamma^r_{\varphi\varphi} = -r e^{-\lambda} \sin^2 \vartheta, \quad \Gamma^r_{\vartheta\vartheta} = -r e^{-\lambda}, \\ \Gamma^\vartheta_{r\vartheta} &= \Gamma^\vartheta_{\vartheta r} = \frac{1}{r}, \quad \Gamma^\vartheta_{\varphi\varphi} = -\sin \vartheta \cos \vartheta, \\ \Gamma^\varphi_{\vartheta\varphi} &= \Gamma^\varphi_{\varphi\vartheta} = \cot \vartheta, \quad \Gamma^\varphi_{r\varphi} = \Gamma^\varphi_{\varphi r} = \frac{1}{r}. \end{aligned} \quad (303)$$

All the other Christoffel symbols are zero.

With the Christoffel symbols known, we can now calculate the components of the Ricci tensor (223). We find

$$R_{rt} = R_{tr} = \partial_\rho \Gamma^\rho_{tr} - \partial_t \Gamma^\rho_{\rho r} + \Gamma^\rho_{\rho\sigma} \Gamma^\sigma_{tr} - \Gamma^\rho_{t\sigma} \Gamma^\sigma_{\rho r} = \cancel{\partial_t \Gamma^t_{tr}} + \partial_r \Gamma^r_{tr} - \cancel{\partial_t (\Gamma^t_{tr} + \Gamma^r_{rr} + \Gamma^\vartheta_{\vartheta r} + \Gamma^\varphi_{\varphi r})}$$

$$+ (\cancel{\Gamma^t_{tt}} + \cancel{\Gamma^r_{rt}}) \Gamma^t_{tr} + (\Gamma^t_{tr} + \cancel{\Gamma^r_{rr}} + \Gamma^\vartheta_{\vartheta r} + \Gamma^\varphi_{\varphi r}) \Gamma^r_{tr} - \cancel{\Gamma^t_{tt} \Gamma^t_{tr}} - \Gamma^r_{tt} \Gamma^t_{rr} - \cancel{\Gamma^t_{tr} \Gamma^r_{tr}} - \cancel{\Gamma^r_{tr} \Gamma^r_{rr}}$$

$$= \partial_r \left(\frac{1}{2} \frac{\partial \lambda}{\partial t} \right) - \partial_t \left(\frac{1}{2} \frac{\partial \lambda}{\partial r} + \frac{2}{r} \right) + \left(\frac{1}{2} \frac{\partial \lambda}{\partial r} + \frac{2}{r} \right) \frac{1}{2} \frac{\partial \lambda}{\partial t} - \cancel{\frac{c^2}{2} e^{\nu-\lambda} \frac{\partial \nu}{\partial r} \frac{1}{2c^2} e^{\lambda-\nu} \frac{\partial \lambda}{\partial t}} = \frac{1}{r} \frac{\partial \lambda}{\partial t},$$

$$R_{\vartheta t} = R_{t\vartheta} = \partial_\rho \Gamma^\rho_{t\vartheta} - \partial_t \Gamma^\rho_{\rho\vartheta} + \Gamma^\rho_{\rho\sigma} \Gamma^\sigma_{t\vartheta} - \Gamma^\rho_{t\sigma} \Gamma^\sigma_{\rho\vartheta} = 0,$$

$$R_{\varphi t} = R_{t\varphi} = \partial_\rho \Gamma^\rho_{t\varphi} - \partial_t \Gamma^\rho_{\rho\varphi} + \Gamma^\rho_{\rho\sigma} \Gamma^\sigma_{t\varphi} - \Gamma^\rho_{t\sigma} \Gamma^\sigma_{\rho\varphi} = 0,$$

$$R_{\vartheta r} = R_{r\vartheta} = \partial_\rho \Gamma^\rho_{r\vartheta} - \partial_r \Gamma^\rho_{\rho\vartheta} + \Gamma^\rho_{\rho\sigma} \Gamma^\sigma_{r\vartheta} - \Gamma^\rho_{r\sigma} \Gamma^\sigma_{\rho\vartheta} = \Gamma^\varphi_{\varphi\vartheta} \Gamma^\vartheta_{r\vartheta} - \Gamma^\varphi_{\varphi r} \Gamma^\varphi_{\varphi\vartheta} = \frac{\cot \vartheta}{r} - \frac{\cot \vartheta}{r} = 0,$$

$$R_{\varphi r} = R_{r\varphi} = \partial_\rho \Gamma^\rho_{r\varphi} - \partial_r \Gamma^\rho_{\rho\varphi} + \Gamma^\rho_{\rho\sigma} \Gamma^\sigma_{r\varphi} - \Gamma^\rho_{r\sigma} \Gamma^\sigma_{\rho\varphi} = 0 ,$$

$$R_{\varphi\vartheta} = R_{\vartheta\varphi} = \partial_\rho \Gamma^\rho_{\vartheta\varphi} - \partial_\vartheta \Gamma^\rho_{\rho\varphi} + \Gamma^\rho_{\rho\sigma} \Gamma^\sigma_{\vartheta\varphi} - \Gamma^\rho_{\vartheta\sigma} \Gamma^\sigma_{\rho\varphi} = 0 ,$$

$$\begin{aligned} R_{tt} &= \partial_\rho \Gamma^\rho_{tt} - \partial_t \Gamma^\rho_{\rho t} + \Gamma^\rho_{\rho\sigma} \Gamma^\sigma_{tt} - \Gamma^\rho_{t\sigma} \Gamma^\sigma_{\rho t} = \cancel{\partial_t \Gamma^t_{tt}} + \partial_r \Gamma^r_{tt} - \partial_t (\cancel{\Gamma^t_{tt}} + \Gamma^r_{rt}) \\ &+ (\cancel{\Gamma^t_{tt}} + \Gamma^r_{rt}) \Gamma^t_{tt} + (\cancel{\Gamma^t_{tr}} + \Gamma^r_{rr} + \Gamma^\vartheta_{\vartheta r} + \Gamma^\varphi_{\varphi r}) \Gamma^r_{tt} - \cancel{\Gamma^t_{tt} \Gamma^t_{tt}} - \cancel{\Gamma^t_{tr} \Gamma^r_{tt}} - \Gamma^r_{tr} \Gamma^r_{rt} \\ - \Gamma^r_{tt} \Gamma^t_{rt} &= \partial_r \left(\frac{c^2}{2} e^{\nu-\lambda} \frac{\partial \nu}{\partial r} \right) - \partial_t \left(\frac{1}{2} \frac{\partial \lambda}{\partial t} \right) + \frac{1}{2} \frac{\partial \lambda}{\partial t} \frac{1}{2} \frac{\partial \nu}{\partial t} + \left(\frac{1}{2} \frac{\partial \lambda}{\partial r} + \frac{2}{r} \right) \frac{c^2}{2} e^{\nu-\lambda} \frac{\partial \nu}{\partial r} \\ &- \frac{1}{4} \left(\frac{\partial \lambda}{\partial t} \right)^2 - \frac{c^2}{2} e^{\nu-\lambda} \frac{\partial \nu}{\partial r} \frac{1}{2} \frac{\partial \nu}{\partial r} = \frac{c^2}{2} e^{\nu-\lambda} \frac{\partial^2 \nu}{\partial r^2} + \left(\frac{\partial \nu}{\partial r} - \frac{\partial \lambda}{\partial r} \right) \frac{c^2}{2} e^{\nu-\lambda} \frac{\partial \nu}{\partial r} \\ &- \frac{1}{2} \frac{\partial^2 \lambda}{\partial t^2} + \frac{1}{4} \frac{\partial \lambda}{\partial t} \frac{\partial \nu}{\partial t} + \left(\frac{\partial \lambda}{\partial r} + \frac{4}{r} - \frac{\partial \nu}{\partial r} \right) \frac{c^2}{4} e^{\nu-\lambda} \frac{\partial \nu}{\partial r} - \frac{1}{4} \left(\frac{\partial \lambda}{\partial t} \right)^2 \\ &= \left(\frac{1}{2} \frac{\partial^2 \nu}{\partial r^2} + \frac{1}{4} \left(\frac{\partial \nu}{\partial r} \right)^2 - \frac{1}{4} \frac{\partial \lambda}{\partial r} \frac{\partial \nu}{\partial r} + \frac{1}{r} \frac{\partial \nu}{\partial r} \right) c^2 e^{\nu-\lambda} - \frac{1}{2} \frac{\partial^2 \lambda}{\partial t^2} + \frac{1}{4} \frac{\partial \lambda}{\partial t} \frac{\partial \nu}{\partial t} - \frac{1}{4} \left(\frac{\partial \lambda}{\partial t} \right)^2 , \end{aligned}$$

$$\begin{aligned} R_{rr} &= \partial_\rho \Gamma^\rho_{rr} - \partial_r \Gamma^\rho_{\rho r} + \Gamma^\rho_{\rho\sigma} \Gamma^\sigma_{rr} - \Gamma^\rho_{r\sigma} \Gamma^\sigma_{\rho r} = \partial_t \Gamma^t_{tr} + \cancel{\partial_r \Gamma^r_{rr}} \\ &- \partial_r (\Gamma^t_{tr} + \cancel{\Gamma^r_{rr}} + \Gamma^\vartheta_{\vartheta r} + \Gamma^\varphi_{\varphi r}) + (\Gamma^t_{tt} + \cancel{\Gamma^r_{rt}}) \Gamma^t_{rr} + (\Gamma^t_{tr} + \cancel{\Gamma^r_{rr}} + \Gamma^\vartheta_{\vartheta r} + \Gamma^\varphi_{\varphi r}) \Gamma^r_{rr} \\ &- \Gamma^t_{rt} \Gamma^t_{tr} - \Gamma^t_{rr} \Gamma^r_{tr} + \cancel{\Gamma^r_{rt} \Gamma^t_{rr}} - \cancel{\Gamma^r_{rr} \Gamma^r_{rr}} - \Gamma^\vartheta_{r\vartheta} \Gamma^\vartheta_{\vartheta r} - \Gamma^\varphi_{r\varphi} \Gamma^\varphi_{\varphi r} = \partial_t \left(\frac{1}{2c^2} e^{\lambda-\nu} \frac{\partial \lambda}{\partial t} \right) \\ &- \partial_r \left(\frac{1}{2} \frac{\partial \nu}{\partial r} + \frac{2}{r} \right) + \left(\frac{1}{2} \frac{\partial \nu}{\partial t} + \frac{1}{2} \frac{\partial \lambda}{\partial t} \right) \frac{1}{2c^2} e^{\lambda-\nu} \frac{\partial \lambda}{\partial t} + \left(\frac{1}{2} \frac{\partial \nu}{\partial r} + \frac{2}{r} \right) \frac{1}{2} \frac{\partial \lambda}{\partial r} - \frac{1}{4} \left(\frac{\partial \nu}{\partial r} \right)^2 \\ &- \frac{\partial \lambda}{\partial t} \frac{1}{2c^2} e^{\lambda-\nu} \frac{\partial \lambda}{\partial t} - \frac{2}{r^2} = \frac{1}{2c^2} e^{\lambda-\nu} \left(\frac{\partial^2 \lambda}{\partial t^2} + \left(\frac{\partial \lambda}{\partial t} \right)^2 - \frac{\partial \nu}{\partial t} \frac{\partial \lambda}{\partial t} + \frac{1}{2} \frac{\partial \nu}{\partial t} \frac{\partial \lambda}{\partial t} + \frac{1}{2} \left(\frac{\partial \lambda}{\partial t} \right)^2 - \left(\frac{\partial \lambda}{\partial t} \right)^2 \right) \\ &- \frac{1}{2} \frac{\partial^2 \nu}{\partial r^2} + \cancel{\frac{2}{r^2}} + \frac{1}{4} \frac{\partial \lambda}{\partial r} \frac{\partial \nu}{\partial r} + \frac{1}{r} \frac{\partial \lambda}{\partial r} - \frac{1}{4} \left(\frac{\partial \nu}{\partial r} \right)^2 - \cancel{\frac{2}{r^2}} = \\ &= - \frac{1}{2} \frac{\partial^2 \nu}{\partial r^2} - \frac{1}{4} \left(\frac{\partial \nu}{\partial r} \right)^2 + \frac{1}{4} \frac{\partial \lambda}{\partial r} \frac{\partial \nu}{\partial r} + \frac{1}{r} \frac{\partial \lambda}{\partial r} + \frac{1}{2c^2} e^{\lambda-\nu} \left(\frac{\partial^2 \lambda}{\partial t^2} + \frac{1}{2} \left(\frac{\partial \lambda}{\partial t} \right)^2 - \frac{1}{2} \frac{\partial \nu}{\partial t} \frac{\partial \lambda}{\partial t} \right) , \end{aligned}$$

$$\begin{aligned}
R_{\vartheta\vartheta} &= \partial_\rho \Gamma^\rho_{\vartheta\vartheta} - \partial_\vartheta \Gamma^\rho_{\rho\vartheta} + \Gamma^\rho_{\rho\sigma} \Gamma^\sigma_{\vartheta\vartheta} - \Gamma^\rho_{\vartheta\sigma} \Gamma^\sigma_{\rho\vartheta} \\
&= \partial_r \Gamma^r_{\vartheta\vartheta} - \partial_\vartheta \Gamma^\varphi_{\varphi\vartheta} + (\Gamma^t_{tr} + \Gamma^r_{rr} + \cancel{\Gamma^\vartheta_{\vartheta r}} + \Gamma^\varphi_{\varphi r}) \Gamma^r_{\vartheta\vartheta} - \Gamma^\vartheta_{\vartheta r} \Gamma^r_{\vartheta\vartheta} - \cancel{\Gamma^r_{\vartheta\vartheta} \Gamma^\vartheta_{r\vartheta}} - \Gamma^\varphi_{\vartheta\varphi} \Gamma^\varphi_{\varphi\vartheta} \\
&= \partial_r(-r e^{-\lambda}) - \partial_\vartheta(\cot \vartheta) - \left(\frac{1}{2} \frac{\partial \nu}{\partial r} + \frac{1}{2} \frac{\partial \lambda}{\partial r} + \frac{1}{r} \right) r e^{-\lambda} + \frac{1}{r} r e^{-\lambda} - \cot^2 \vartheta \\
&= \cancel{e^{-\lambda}} + r e^{-\lambda} \frac{\partial \lambda}{\partial r} + 1 + \cancel{e \cot^2 \vartheta} - r e^{-\lambda} \left(\frac{1}{2} \frac{\partial \nu}{\partial r} + \frac{1}{2} \frac{\partial \lambda}{\partial r} + \frac{1}{r} \right) + \cancel{e^{-\lambda}} - \cancel{e \cot^2 \vartheta} \\
&= 1 - e^{-\lambda} - \frac{r}{2} e^{-\lambda} \left(\frac{\partial \nu}{\partial r} - \frac{\partial \lambda}{\partial r} \right),
\end{aligned}$$

$$\begin{aligned}
R_{\varphi\varphi} &= \partial_\rho \Gamma^\rho_{\varphi\varphi} - \partial_\varphi \Gamma^\rho_{\rho\varphi} + \Gamma^\rho_{\rho\sigma} \Gamma^\sigma_{\varphi\varphi} - \Gamma^\rho_{\varphi\sigma} \Gamma^\sigma_{\rho\varphi} = \partial_r \Gamma^r_{\varphi\varphi} + \partial_\vartheta \Gamma^\vartheta_{\varphi\varphi} + (\Gamma^t_{tr} + \Gamma^r_{rr} + \Gamma^\vartheta_{\vartheta r} + \cancel{\Gamma^\varphi_{\varphi r}}) \Gamma^r_{\varphi\varphi} \\
&+ \cancel{\Gamma^\varphi_{\varphi\vartheta} \Gamma^\vartheta_{\varphi\varphi}} - \Gamma^\varphi_{\varphi r} \Gamma^r_{\varphi\varphi} - \cancel{\Gamma^r_{\varphi\varphi} \Gamma^\varphi_{r\varphi}} - \cancel{\Gamma^\vartheta_{\varphi\varphi} \Gamma^\varphi_{\vartheta\varphi}} - \Gamma^\varphi_{\varphi\vartheta} \Gamma^\vartheta_{\varphi\varphi} = -\partial_r(r e^{-\lambda} \sin^2 \vartheta) - \partial_\vartheta(\sin \vartheta \cos \vartheta) \\
&- \left(\frac{1}{2} \frac{\partial \nu}{\partial r} + \frac{1}{2} \frac{\partial \lambda}{\partial r} + \frac{1}{r} \right) r e^{-\lambda} \sin^2 \vartheta + \cancel{\frac{1}{r} r e^{-\lambda} \sin^2 \vartheta} + \cot \vartheta \sin \vartheta \cos \vartheta \\
&= r e^{-\lambda} \frac{\partial \lambda}{\partial r} \sin^2 \vartheta - e^{-\lambda} \sin^2 \vartheta - \cancel{e \sin^2 \vartheta} + \sin^2 \vartheta - \frac{r}{2} e^{-\lambda} \sin^2 \vartheta \left(\frac{\partial \nu}{\partial r} + \frac{\partial \lambda}{\partial r} \right) + \cancel{e \sin^2 \vartheta} \\
&= \sin^2 \vartheta \left\{ 1 - e^{-\lambda} - \frac{r}{2} e^{-\lambda} \left(\frac{\partial \nu}{\partial r} - \frac{\partial \lambda}{\partial r} \right) \right\} = \sin^2 \vartheta R_{\vartheta\vartheta}. \tag{304}
\end{aligned}$$

The vacuum field equation $R_{\mu\nu} = 0$ gives us a system of four independent partial differential equations for the functions $\nu(t, r)$ and $\lambda(t, r)$:

$$R_{tr} = 0 \implies \frac{\partial \lambda}{\partial t} = 0, \tag{305}$$

$$R_{tt} = 0 \implies \frac{\partial^2 \nu}{\partial r^2} + \frac{1}{2} \left(\frac{\partial \nu}{\partial r} \right)^2 - \frac{1}{2} \frac{\partial \nu}{\partial r} \frac{\partial \lambda}{\partial r} + \frac{2}{r} \frac{\partial \nu}{\partial r} = 0, \tag{306}$$

$$R_{rr} = 0 \implies \frac{\partial^2 \nu}{\partial r^2} + \frac{1}{2} \left(\frac{\partial \nu}{\partial r} \right)^2 - \frac{1}{2} \frac{\partial \nu}{\partial r} \frac{\partial \lambda}{\partial r} - \frac{2}{r} \frac{\partial \lambda}{\partial r} = 0, \tag{307}$$

$$R_{\vartheta\vartheta} = 0 \implies 1 - e^{-\lambda} - \frac{r}{2} e^{-\lambda} \left(\frac{\partial \nu}{\partial r} - \frac{\partial \lambda}{\partial r} \right) = 0. \tag{308}$$

Here we omitted all terms in (306) and (307) that contained time derivatives of λ , because such terms vanish by (305).

To solve this system of coupled differential equations we subtract (307) from (306):

$$\frac{\partial \nu}{\partial r} + \frac{\partial \lambda}{\partial r} = 0 . \quad (309)$$

Differentiating with respect to t gives, with the help of (305),

$$\frac{\partial^2 \nu}{\partial t \partial r} = - \frac{\partial^2 \lambda}{\partial t \partial r} = 0 \implies \nu(t, r) = \tilde{\nu}(r) + f(t) . \quad (310)$$

Upon inserting into (309) we find

$$\frac{d}{dr} \left(\tilde{\nu}(r) + \lambda(r) \right) = 0 \implies \tilde{\nu}(r) + \lambda(r) = k = \text{const.} \quad (311)$$

$$\implies \nu(t, r) = -\lambda(r) + k + f(t) . \quad (312)$$

The tt -component of the metric is thus of the form

$$e^{\nu(t, r)} dt^2 = e^{-\lambda(r)} e^k e^{f(t)} dt^2 . \quad (313)$$

By a transformation of the time coordinate,

$$\tilde{t} = e^{k/2} \int e^{f(t)/2} dt , \quad d\tilde{t} = e^{k/2} e^{f(t)/2} dt , \quad (314)$$

we put this expression into the following form:

$$e^{\nu(t, r)} dt^2 = e^{-\lambda(r)} d\tilde{t}^2 . \quad (315)$$

After renaming \tilde{t} into t we have now reached a form where the metric coefficients $g_{\mu\nu}$ are time-independent,

$$g = -e^{-\lambda(r)} c^2 dt^2 + e^{\lambda(r)} dr^2 + r^2 d\Omega^2 . \quad (316)$$

This demonstrates that ∂_t is a Killing vector field, see Problem 4 of Worksheet 7. As the mixed metric components g_{ti} vanish, the timelike Killing vector field ∂_t is orthogonal to the hypersurfaces $t = \text{constant}$. A spacetime is called *static* if it admits a timelike Killing vector field that is orthogonal to hypersurfaces. We have thus proven the *Jebsen-Birkhoff theorem*:

Theorem (J. Jebsen, 1921, G. D. Birkhoff, 1923): A spherically symmetric solution to the vacuum field equation $R_{\mu\nu} = 0$ is static.

Schwarzschild did not know this. He *assumed* that the metric coefficients (i.e. ν and λ in our notation) were independent of t . We have proven, following Jebsen and Birkhoff, that in an appropriately chosen coordinate system they *have to be* independent of t , if the metric is spherically symmetric and satisfies the vacuum field equation $R_{\mu\nu} = 0$. The Jebsen-Birkhoff theorem implies that a spherically symmetric pulsating star does not emit gravitational waves.

With $\lambda(t, r) = \lambda(r)$ and $\nu(t, r) = -\lambda(r)$, our system of differential equations (305) – (308) has been reduced to the following form.

- (305) is identically satisfied.
- (306) requires that

$$-\frac{d^2\lambda}{dr^2} + \left(\frac{d\lambda}{dr}\right)^2 - \frac{2}{r} \frac{d\lambda}{dr} = 0. \quad (317)$$

- (307) reduces to the same equation (317).
- (308) requires that

$$1 - e^{-\lambda} + r e^{-\lambda} \frac{d\lambda}{dr} = 0. \quad (318)$$

We solve (318) and demonstrate that then (317) is automatically satisfied.

(318) is an ordinary differential equation of first order. With the substitution

$$u = e^{-\lambda}, \quad \frac{du}{dr} = -e^{-\lambda} \frac{d\lambda}{dr} \quad (319)$$

it can be integrated in an elementary fashion:

$$1 - u - r \frac{du}{dr} = 0 \implies r \frac{du}{dr} = 1 - u \quad (320)$$

$$\implies \int \frac{du}{1-u} = \int \frac{dr}{r} \implies -\ln(1-u) = \ln(r) - \ln(r_S) \quad (321)$$

where r_S is an integration constant that has the same dimension as the radius coordinate, i.e. the dimension of a length. Upon exponentiating, the solution reads

$$\frac{1}{1-u} = \frac{r}{r_S} \implies u = e^{-\lambda} = 1 - \frac{r_S}{r}. \quad (322)$$

The only thing that remains to be shown is that this λ also satisfies (317). With

$$\lambda = -\ln\left(1 - \frac{r_S}{r}\right), \quad \frac{d\lambda}{dr} = -\frac{r_S}{\left(1 - \frac{r_S}{r}\right)r^2} = -\frac{r_S}{r^2 - r_S r}, \quad \frac{d^2\lambda}{dr^2} = \frac{r_S(2r - r_S)}{(r^2 - r_S r)^2} \quad (323)$$

the left-hand side of (317) can be rewritten as

$$\begin{aligned} -\frac{d^2\lambda}{dr^2} + \left(\frac{d\lambda}{dr}\right)^2 - \frac{2}{r} \frac{d\lambda}{dr} &= -\frac{r_S(2r - r_S)}{(r^2 - r_S r)^2} + \frac{r_S^2}{(r^2 - r_S r)^2} + \frac{2r_S}{r(r^2 - r_S r)} = \\ &= \frac{-rr_S(2r - r_S) + rr_S^2 + (r^2 - r_S r)2r_S}{r(r^2 - r_S r)^2} = 0. \end{aligned} \quad (324)$$

Inserting the λ from (322) into the metric (316) gives the general solution to Einstein's vacuum field equation $R_{\mu\nu} = 0$ under the assumption of spherical symmetry. It is known as the *Schwarzschild solution*,

$$g = - \left(1 - \frac{r_S}{r} \right) c^2 dt^2 + \frac{dr^2}{\left(1 - \frac{r_S}{r} \right)} + r^2 (d\vartheta^2 + \sin^2\vartheta d\varphi^2). \quad (325)$$

We recall that the range of the radius coordinate is $r_*(t) < r < \infty$. The geometric meaning of the r -coordinate becomes clear if we consider a circle in the equatorial plane,

$$C : t = \text{constant}, r = \text{constant}, \vartheta = \pi/2, 0 < \varphi < 2\pi. \quad (326)$$

The circumference of this circle, as measured with the metric, is

$$U = \int_C \sqrt{g_{\mu\nu} \frac{dx^\mu}{ds} \frac{dx^\nu}{ds}} ds = \int_C \sqrt{g_{\varphi\varphi} \left(\frac{d\varphi}{ds} \right)^2} ds = \int_C \sqrt{r^2 \left(\frac{d\varphi}{ds} \right)^2} ds = \int_0^{2\pi} r d\varphi = 2\pi r. \quad (327)$$

Hence, the length of a rope laid out along this circle is given by the formula for the circumference of a circle that is familiar from Euclidean geometry. By the same token, the area of the sphere $r = \text{constant}$, $t = \text{constant}$ equals $4\pi r^2$. For this reason, r is sometimes called the *area coordinate*.

By contrast, for a radial line segment

$$S : t = \text{constant}, r_1 < r < r_2, \vartheta = \text{constant}, \varphi = \text{constant}, \quad (328)$$

the length

$$L = \int_S \sqrt{g_{\mu\nu} \frac{dx^\mu}{ds} \frac{dx^\nu}{ds}} ds = \int_S \sqrt{g_{rr} \left(\frac{dr}{ds} \right)^2} ds = \int_{r_1}^{r_2} \sqrt{g_{rr}} dr = \int_{r_1}^{r_2} \frac{dr}{\sqrt{1 - \frac{r_S}{r}}} \quad (329)$$

is different from $r_2 - r_1$. This demonstrates that r cannot be interpreted as a distance from a centre.

We now have to discuss the physical meaning of the integration constant r_S . To that end we use the comparison with the Newtonian theory. We recall that the Newtonian limit is a valid approximation if the four conditions (N1) – (N4) are satisfied, see p. 87. For the Schwarzschild metric (325) condition (N1) is satisfied for r sufficiently large, (N2) and (N4) are everywhere satisfied and (N3) gives no restriction on the metric. The equation

$$g_{00} = - \left(1 + \frac{2\phi}{c^2} \right), \quad (330)$$

which holds in the Newtonian limit, is thus valid for the Schwarzschild metric if r is sufficiently large. With the spherically symmetric Newtonian field

$$\phi(r) = - \frac{GM}{r} \quad (331)$$

we find

$$- \left(1 - \frac{r_S}{r} \right) = - \left(1 - \frac{2GM}{c^2 r} \right) \implies r_S = \frac{2GM}{c^2}. \quad (332)$$

This demonstrates that the integration constant r_S is determined by the mass M of the central body. M can be measured on the basis of the Newtonian theory at a sufficiently large distance from the centre. r_S is called the *Schwarzschild radius* or the *gravitational radius* of the central body.

For positive M , the Schwarzschild radius r_S is positive. If the radius of the central body is smaller than the Schwarzschild radius, $r_* < r_S$, a zero occurs in the denominator of the Schwarzschild metric (325). For normal celestial bodies we have $r_* \gg r_S$; so the Schwarzschild metric is regular in its entire domain of validity. For the Sun, $r_S \approx 3\text{km}$, and for the Earth, $r_S \approx 1\text{cm}$. However, one may think of a hypothetical celestial body that is compressed beyond its Schwarzschild radius. Then the “singularity” at $r = r_S$ becomes relevant. Its physical meaning remained mysterious until the late 1950s. We will discuss below that a body that has collapsed beyond its Schwarzschild radius forms a black hole, with the horizon at $r = r_S$.

At the end of this section we summarise three important properties of the Schwarzschild metric.

- The Schwarzschild metric is *asymptotically flat*: For large values of r it approaches the Minkowski metric, i.e. the metric of special relativity.
- The Schwarzschild metric is *static*: ∂_t is a timelike Killing vector field that is orthogonal to hypersurfaces.
- The Schwarzschild metric is *spherically symmetric*: Every vector field that generates a rotation about a spatial axis is a Killing vector field. For a rotation about the z axis, this is the vector field ∂_φ . The orbit of any point under the action of the rotations is a two-dimensional spacelike sphere, namely the sphere ($t = \text{const.}, r = \text{const.}$).

In the next two sections we will discuss by what observable features one can test if the Schwarzschild metric is a viable model for the spacetime around the Sun (or some other spherically symmetric celestial body). The most important tool is the geodesic equation. The lightlike geodesics are the worldlines of classical photons, i.e., they tell how light propagates in the spacetime. The timelike geodesics are the worldlines of freely falling massive particles; e.g., we may think of planets moving in the gravitational field of the Sun. We will investigate lightlike and timelike geodesics in the Schwarzschild spacetime in the following two sections.

6.2 Lightlike geodesics in the Schwarzschild solution

We use the Lagrange formulation for the geodesic equation. Because of spherical symmetry, any geodesic in the Schwarzschild solution is restricted to a plane through the coordinate centre. (The initial position and the initial velocity of the geodesic determine this plane that is unique, unless the geodesic is radial; because of the symmetry, the geodesic cannot move out of this plane to either side.) Hence, it is no restriction of generality if we restrict to geodesics in the equatorial plane $\vartheta = \pi/2$. Then the Lagrange function reads

$$L(x, \dot{x}) = \frac{1}{2} g_{\mu\nu}(x) \dot{x}^\mu \dot{x}^\nu = \frac{1}{2} \left(- \left(1 - \frac{r_S}{r} \right) c^2 \dot{t}^2 + \frac{\dot{r}^2}{\left(1 - \frac{r_S}{r} \right)} + r^2 \dot{\varphi}^2 \right). \quad (333)$$

The overdot means derivative with respect to the curve parameter s .

We write the t - and φ -components of the Euler-Lagrange equations:

$$0 = \frac{d}{ds} \left(\frac{\partial L}{\partial \dot{t}} \right) - \frac{\partial L}{\partial t} = -c^2 \frac{d}{ds} \left(\left(1 - \frac{r_S}{r} \right) \dot{t} \right), \quad (334)$$

$$0 = \frac{d}{ds} \left(\frac{\partial L}{\partial \dot{\varphi}} \right) - \frac{\partial L}{\partial \varphi} = \frac{d}{ds} \left(r^2 \dot{\varphi} \right). \quad (335)$$

This gives us two constants of motion,

$$\left(1 - \frac{r_S}{r} \right) \dot{t} = E = \text{constant}, \quad (336)$$

$$r^2 \dot{\varphi} = L_z = \text{constant}. \quad (337)$$

These constants of motion exist for timelike, lightlike and spacelike geodesics. For timelike geodesics (i.e., worldlines of freely falling particles), multiplication with the particle mass of E gives the energy and of L_z gives the z -component of the angular momentum of the particle. As the motion is in the $x - y$ -plane, the other two components of the angular momentum are zero. Here we are interested in lightlike geodesics for which E and L_z can also be interpreted, respectively, as measures for energy and angular momentum up to dimensional factors. Recall from Lagrangian mechanics that a constant of motion associated with a time symmetry or with a rotational symmetry is always interpreted, respectively, as an energy or as an angular momentum.

For *lightlike* geodesics we have in addition to (336) and (337)

$$g_{\mu\nu} \dot{x}^\mu \dot{x}^\nu = - \left(1 - \frac{r_S}{r} \right) c^2 \dot{t}^2 + \frac{\dot{r}^2}{\left(1 - \frac{r_S}{r} \right)} + r^2 \dot{\varphi}^2 = 0. \quad (338)$$

The three equations (336), (337) and (338) determine the lightlike geodesics. (The r -component of the Euler-Lagrange equations gives no additional information, as can be verified.)

We first consider *radial* lightlike geodesics, i.e., geodesics with $\dot{\varphi} = 0$ which are equivalently characterised by $L_z = 0$. Then (338) requires

$$- \left(1 - \frac{r_S}{r} \right) c^2 \dot{t}^2 + \frac{\dot{r}^2}{\left(1 - \frac{r_S}{r} \right)} = 0, \quad (339)$$

$$\frac{dr}{dt} = \pm c \left(1 - \frac{r_S}{r} \right).$$

This equation determines the radial lightlike geodesics parametrised by the time coordinate t , with the plus sign for outgoing and the minus sign for ingoing geodesics. We will come back to this equation later.

For non-radial geodesics ($\dot{\varphi} \neq 0$ and $L_z \neq 0$) we may use φ as the curve parameter. To derive an expression for $dr/d\varphi$ and thereby for the shape of the orbit, we divide (338) by $\dot{\varphi}^2$,

$$-\left(1 - \frac{r_S}{r}\right) \frac{c^2 \dot{t}^2}{\dot{\varphi}^2} + \frac{1}{\left(1 - \frac{r_S}{r}\right)} \frac{\dot{r}^2}{\dot{\varphi}^2} + r^2 = 0, \quad (340)$$

and replace \dot{t} and $\dot{\varphi}$ in the first term with the help of (336) and (337):

$$\cancel{-\left(1 - \frac{r_S}{r}\right)} \frac{c^2 E^2 r^4}{\left(1 - \frac{r_S}{r}\right)^2 L_z^2} + \frac{1}{\left(1 - \frac{r_S}{r}\right)} \left(\frac{dr}{d\varphi}\right)^2 + r^2 = 0 \implies$$

$$\left(\frac{dr}{d\varphi}\right)^2 = \frac{c^2 E^2}{L_z^2} r^4 - r^2 + r_S r. \quad (341)$$

Note that the constants of motion enter in this equation only in form of the quantity

$$b = \frac{L_z}{cE} \quad (342)$$

which, for geodesics that come in from infinity, is known as the *impact parameter*. When we introduce an *effective potential*

$$V_b(r) = -\frac{1}{2} \left(\frac{r^4}{b^2} - r^2 + r_S r \right), \quad (343)$$

(341) takes the form of a one-dimensional energy-conservation law,

$$\frac{1}{2} \left(\frac{dr}{d\varphi}\right)^2 + V_b(r) = 0, \quad (344)$$

and taking the derivative with respect to φ gives an equation that looks like a one-dimensional Newtonian equation of motion,

$$\cancel{\frac{d\varphi}{d\varphi}} \frac{d^2 r}{d\varphi^2} = -V'_b(r) \cancel{\frac{d\varphi}{d\varphi}}. \quad (345)$$

Although we divided by $dr/d\varphi$, by continuity the last equation is valid also at points where $dr/d\varphi = 0$. In Worksheet 9 we will use (344) and (345) for demonstrating that at $r = 3r_S/2$ in the Schwarzschild spacetime there is *photon sphere*, i.e., that any lightlike geodesic that starts tangential to this sphere will stay on this sphere. This means that a tunnel built around a great circle on this sphere will appear perfectly straight to an observer who looks into this tunnel and that at the end of the tunnel the observer will see the back of his or her own head. Of course, this photon sphere is present only if the central body has a radius smaller than $3r_S/2$.

Here we will now derive the famous formula for the bending of light in the Schwarzschild spacetime. We first take the square-root of (341) where we have to be careful about the fact that $dr/d\varphi$ may be positive or negative,

$$d\varphi = \frac{\pm dr}{\sqrt{\frac{c^2 E^2}{L_z^2} r^4 - r^2 + r_S r}}. \quad (346)$$

For a photon that comes in from infinity, goes through a minimum radius value at $r = r_m$ and then escapes to infinity, the integral can be decomposed into two symmetric parts. The total interval swept out by the φ -coordinate is then

$$\begin{aligned}\Delta\varphi &= - \int_{\infty}^{r_m} \frac{dr}{\sqrt{\frac{c^2 E^2}{L_z^2} r^4 - r^2 + r_S r}} + \int_{r_m}^{\infty} \frac{dr}{\sqrt{\frac{c^2 E^2}{L_z^2} r^4 - r^2 + r_S r}} \\ &= 2 \int_{r_m}^{\infty} \frac{dr}{\sqrt{\frac{c^2 E^2}{L_z^2} r^4 - r^2 + r_S r}} .\end{aligned}\quad (347)$$

Here r_m is related to the impact parameter $L_z/(cE)$ by the condition

$$0 = \left(\frac{dr}{d\varphi} \right)^2 \Big|_{r=r_m} = \frac{c^2 E^2}{L_z^2} r_m^4 - r_m^2 + r_S r_m , \quad (348)$$

hence

$$\frac{c^2 E^2}{L_z^2} = \frac{1}{r_m^2} - \frac{r_S}{r_m^3} . \quad (349)$$

$\Delta\varphi$ is related to the deflection angle δ by

$$\delta + \pi = \Delta\varphi , \quad (350)$$

as can be read from Fig. 53.

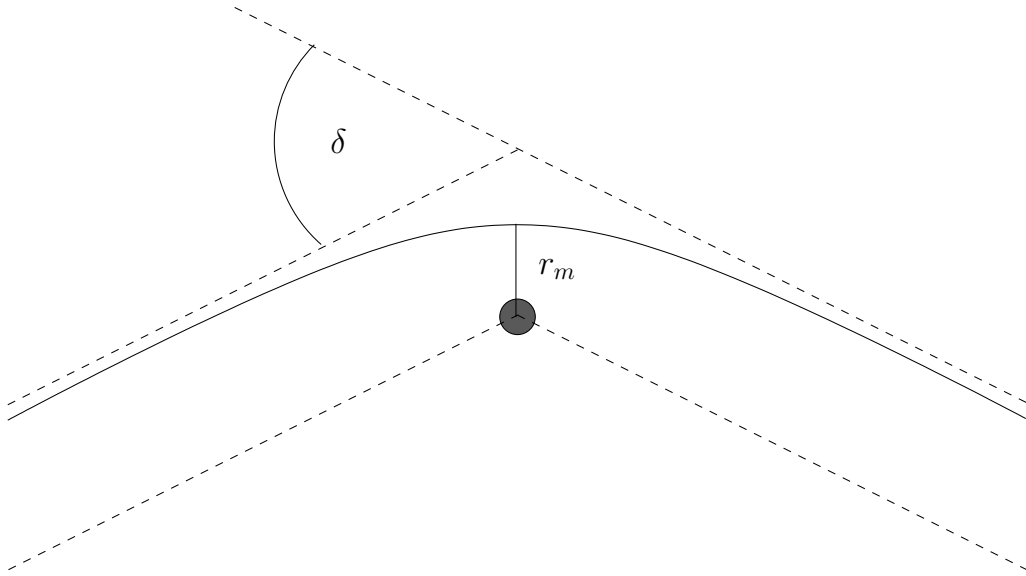


Figure 53: Deflection angle δ of a light ray

If (347) is inserted into (349) we get

$$\delta + \pi = \int d\varphi = 2 \int_{r_m}^{\infty} \frac{dr}{\sqrt{\left(\frac{1}{r_m^2} - \frac{r_S}{r_m^3} \right) r^4 - r^2 + r_S r}} . \quad (351)$$

The expression on the right-hand side is an elliptic integral, which can be numerically calculated for each r_S and for each r_m with arbitrary accuracy. We have thus found an exact formula for the deflection angle of light in the Schwarzschild spacetime.

For ordinary celestial bodies, such as stars or planets, the Schwarzschild radius r_S is very small in comparison to the physical radius r_* . As r_m cannot be smaller than r_* , this means that for light deflection by stars or planets r_S/r_m is very small. We may thus linearise with respect to this quantity. This results in Einstein's deflection formula

$$\delta = 2 \frac{r_S}{r_m} = \frac{4GM}{c^2 r_m}, \quad (352)$$

see Worksheet 9.

For a light ray that grazes the surface of the Sun ($r_m \approx 7 \times 10^5$ km, $r_S \approx 3$ km), we find

$$\delta = 1.75''. \quad (353)$$

This was verified (to within good, though not overwhelming, accuracy) during a Solar eclipse in the year 1919 by an expedition organised by the Royal Astronomical Society and headed by Sir Arthur Eddington. They took photographs of the sky near the Sun during the Solar eclipse, and compared them with photographs of the same area that were taken at a time when the Sun was on the opposite side of the sky. According to the deflection formula, the star positions were displaced radially away from the centre. The result of the Eddington expedition was the most important confirmation of general relativity and made Einstein famous to the general public. Today Einstein's deflection formula has been verified to within a relative accuracy of 0.02 %. Nowadays such observations are made with radio telescopes because then it is not necessary to wait for a Solar eclipse (and because the resolution of radio telescopes, in combination with interferometric methods, is much better than that of optical telescopes).

Such observations are made, in our days, not so much as a test of general relativity but rather in order to get information about the Solar corona; one assumes that Einstein's theory is right, and that any deviation from Einstein's deflection formula is due to a direct influence of the electron density in the Solar corona. (If we deal with the lightlike geodesic equation, we assume of course that light is not influenced by a medium.)

As a historic aside, we mention that light deflection can also be calculated on the basis of the Newtonian theory. One has to assume that light consists of particles that are accelerated by a (Newtonian) gravitational field in exactly the same way as any other particles. If one linearises the Newtonian deflection angle with respect to $2GM/(c^2 r_m)$, one gets just one *half* of Einstein's value, see Worksheet 9, i.e., for a light ray grazing the surface of the Sun,

$$\delta = 0.87''. \quad (354)$$

This Newtonian light deflection was calculated by the Bavarian astronomer Johann von Soldner already in 1801. Even earlier, in 1784, Henry Cavendish had made a sketchy calculation of the Newtonian light deflection on a scrap of paper that was found after his death. At an early stage of his work, Einstein made a calculation of light bending that led to the same formula as Soldner's. (Einstein did not know about Soldner at this time.) In 1915 Einstein calculated the correct value of light deflection on the basis of his linearised field equation.

For deflecting masses that are farther away from us than the Sun (and/or more compact), the relativistic light deflection can lead to multiple images, to strong deformation effects (“Einstein rings”) and to other important observable features. These are summarised under the term “gravitational lensing”. Gravitational lensing is one of the most important tools of astrophysics to get information about “dark” objects, i.e., about objects that do not emit enough light to be directly observable and can, thus, be detected only by their light bending effects. The theoretical basis for the theory of gravitational lensing is the theory of lightlike geodesics.

6.3 Timelike geodesics in the Schwarzschild solution

Also for timelike geodesics we can restrict to the equatorial plane. The equations (334) and (335) hold for this case as well, so we have again the two constants of motion

$$\left(1 - \frac{r_S}{r}\right) \dot{t} = E = \text{constant}, \quad (355)$$

$$r^2 \dot{\varphi} = L_z = \text{constant}. \quad (356)$$

Instead of (338) we have now, for timelike geodesics,

$$g_{\mu\nu} \dot{x}^\mu \dot{x}^\nu = - \left(1 - \frac{r_S}{r}\right) c^2 \dot{t}^2 + \frac{\dot{r}^2}{\left(1 - \frac{r_S}{r}\right)} + r^2 \dot{\varphi}^2 = -c^2. \quad (357)$$

Now the overdot means derivative with respect to proper time τ .

As in the lightlike case, we begin with radial geodesics for which $\dot{\varphi} = 0$ and $L_z = 0$. Then, from (357),

$$\begin{aligned} - \left(1 - \frac{r_S}{r}\right) c^2 \dot{t}^2 + \frac{\dot{r}^2}{\left(1 - \frac{r_S}{r}\right)} &= -c^2, \\ \dot{r}^2 &= \left(1 - \frac{r_S}{r}\right) \left(\left(1 - \frac{r_S}{r}\right) c^2 \dot{t}^2 - c^2 \right). \end{aligned} \quad (358)$$

With (355):

$$\begin{aligned} \dot{r}^2 &= c^2 E^2 - c^2 \left(1 - \frac{r_S}{r}\right), \\ \frac{dr}{d\tau} &= \pm c \sqrt{E^2 - 1 + \frac{r_S}{r}}. \end{aligned} \quad (359)$$

Upon integration, this equation gives us r as a function of proper time τ . The \pm sign distinguishes outgoing from ingoing radial timelike geodesics. E is determined by the initial velocity.

If we want to have the radial geodesics parametrised by coordinate time, rather than by proper time τ , we divide (358) by \dot{t}^2 and use (355):

$$\begin{aligned} \left(\frac{\dot{r}}{\dot{t}}\right)^2 &= \left(1 - \frac{r_S}{r}\right) \left(\left(1 - \frac{r_S}{r}\right) c^2 - \frac{c^2}{E^2} \left(1 - \frac{r_S}{r}\right)^2 \right), \\ \frac{dr}{dt} &= \pm \frac{c}{E} \left(1 - \frac{r_S}{r}\right) \sqrt{E^2 - 1 + \frac{r_S}{r}}. \end{aligned} \quad (360)$$

Having the radial geodesics out of the way, we now consider non-radial timelike geodesics which are characterised by $L_z \neq 0$ and $\dot{\varphi} \neq 0$, i.e., we may use φ for the curve parameter. To that end we divide (357) by $\dot{\varphi}^2$,

$$- \left(1 - \frac{r_S}{r}\right) c^2 \frac{\dot{t}^2}{\dot{\varphi}^2} + \frac{1}{\left(1 - \frac{r_S}{r}\right)} \frac{\dot{r}^2}{\dot{\varphi}^2} + r^2 = - \frac{c^2}{\dot{\varphi}^2}. \quad (361)$$

With the help of (355) and (356), the last equation can be rewritten as:

$$- \frac{\left(1 - \frac{r_S}{r}\right) c^2 E^2 r^4}{\left(1 - \frac{r_S}{r}\right)^2 L_z^2} + \frac{1}{\left(1 - \frac{r_S}{r}\right)} \left(\frac{dr}{d\varphi}\right)^2 + r^2 = - \frac{c^2 r^4}{L_z^2}, \quad (362)$$

$$\left(\frac{dr}{d\varphi}\right)^2 = \frac{c^2 (E^2 - 1) r^4}{L_z^2} + \frac{c^2 r_S r^3}{L_z^2} - r^2 + r_S r =: -2 V_{E,L_z}(r). \quad (363)$$

So similarly as in the lightlike case the orbit equation takes the form of an “energy conservation law”,

$$\frac{1}{2} \left(\frac{dr}{d\varphi}\right)^2 + V_{E,L_z}(r) = 0, \quad (364)$$

but this time with an effective potential $V_{E,L_z}(r)$ that depends on the two constants of motion E and L_z and not only on a particular combination of them.

Differentiation of (364) with respect to φ yields

$$\frac{dr}{d\varphi} \frac{d^2 r}{d\varphi^2} = - V'_{E,L}(r) \frac{dr}{d\varphi}. \quad (365)$$

If $dr/d\varphi \neq 0$, this implies that

$$\frac{d^2 r}{d\varphi^2} = - V'_{E,L}(r). \quad (366)$$

By continuity the Newton-type equation of motion (366) is valid also if $dr/d\varphi = 0$.

By (364), an orbit with constants of motion E and L_z must be confined to the region where $V_{E,L_z}(r) \leq 0$; the boundary points, where $V_{E,L_z}(r) = 0$, are turning points of the orbit where $dr/d\varphi = 0$. So, for each pair of values (E, L_z) , the shape of the potential V_{E,L_z} tells us where orbits can exist. There are *bound orbits*, where the r coordinate oscillates periodically between a minimal value r_1 and a maximal value r_2 , see Fig. 54 and *escape orbits* where the r coordinates

decreases from infinity to a minimal value r_m and then increases again to infinity, see Fig. 55. The same shape of the potential, as shown in Fig. 55, gives also rise to a *plunge orbit*, in the left-hand part of the diagram, where the r coordinate increases to a maximum and then decreases again.

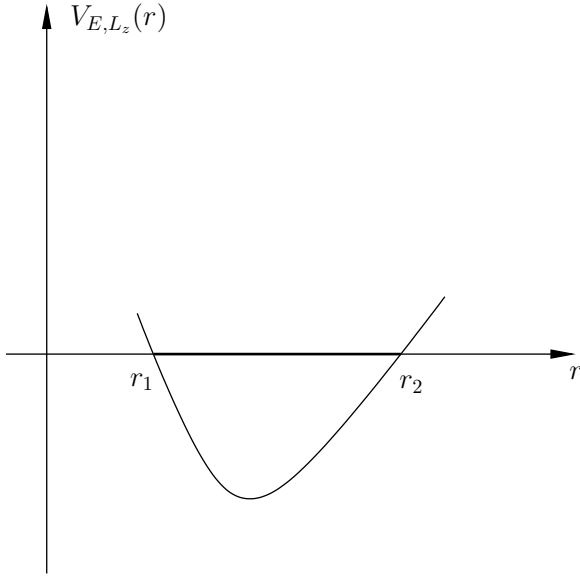


Figure 54: Bound orbit

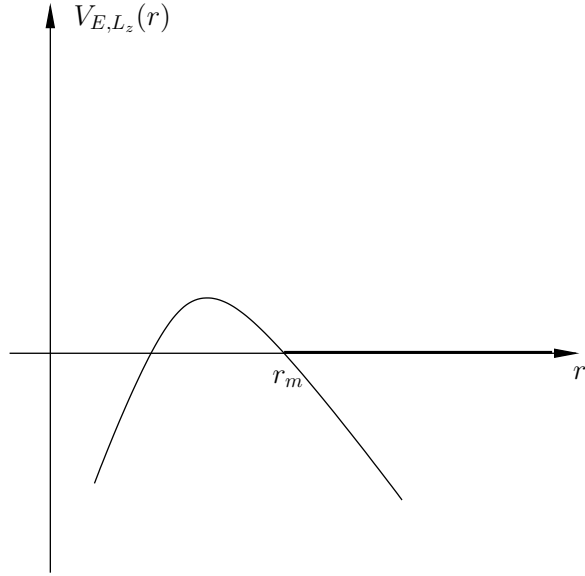


Figure 55: Escape orbit

It is our first goal to investigate for which values of the radius coordinate r circular orbits are possible, and for which values of r these circular orbits are stable. For a circular orbit the equations $dr/d\varphi = 0$ and $d^2r/d\varphi^2 = 0$ have to hold. By (364) and (366), this requires $V_{E,L_z}(r) = 0$ and $V'_{E,L_z}(r) = 0$. Such an orbit is stable if $V''_{E,L_z}(r) > 0$ because then by a small perturbation of E and L_z we get a bound orbit that oscillates about the circular orbit. By contrast, it is unstable if $V''_{E,L_z}(r) < 0$ because then a small perturbation gives an escape or a plunge orbit.

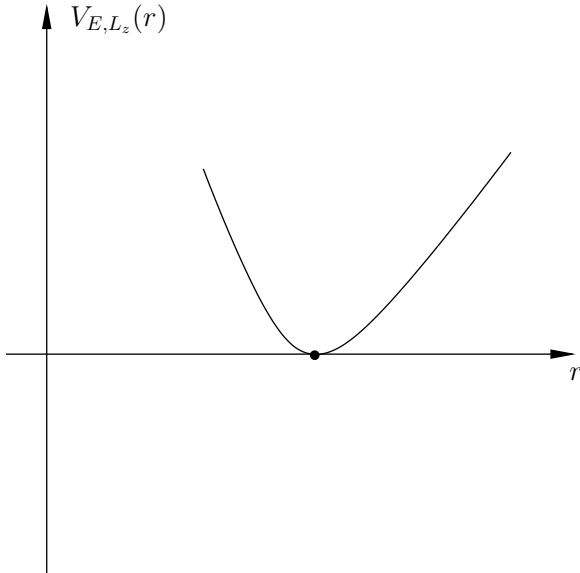


Figure 56: Stable circular orbit

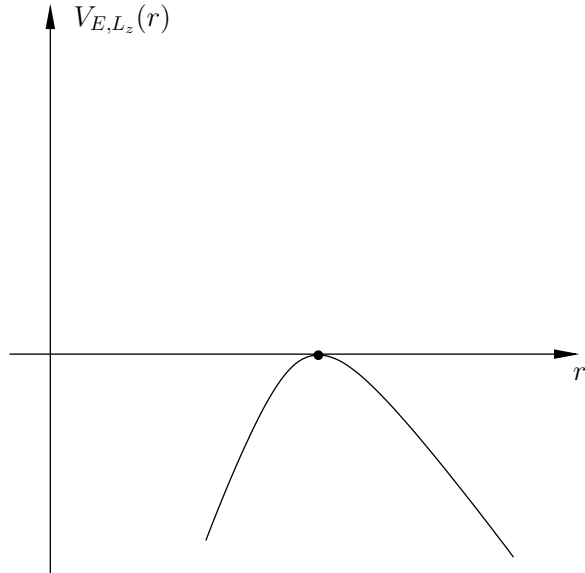


Figure 57: Unstable circular orbit

We calculate the derivatives of our potential V_{E,L_z} :

$$-2 V'_{E,L_z}(r) = \frac{c^2 (E^2 - 1) 4 r^3}{L_z^2} + \frac{c^2 r_S 3 r^2}{L_z^2} - 2 r + r_S , \quad (367)$$

$$-2 V''_{E,L_z}(r) = \frac{c^2 (E^2 - 1) 12 r^2}{L_z^2} + \frac{c^2 r_S 6 r}{L_z^2} - 2 . \quad (368)$$

The conditions for a circular orbit, $V_{E,L_z}(r) = 0$ and $V'_{E,L_z}(r) = 0$, take the following form:

$$\frac{c^2 (E^2 - 1) r^4}{L_z^2} + \frac{c^2 r_S r^3}{L_z^2} - r^2 + r_S r = 0 , \quad (369)$$

$$\frac{c^2 (E^2 - 1) 4 r^3}{L_z^2} + \frac{c^2 r_S 3 r^2}{L_z^2} - 2 r + r_S = 0 . \quad (370)$$

We multiply (369) with $4/r$ and subtract (370):

$$\frac{c^2 r_S r^2}{L_z^2} - 2 r + 3 r_S = 0 . \quad (371)$$

As the first term cannot be negative, circular orbits exist only for those r -values that satisfy the inequality

$$r > \frac{3}{2} r_S . \quad (372)$$

We have already mentioned that at the limiting radius $r = 3r_S/2$ there is a circular *lightlike* geodesic; this will be proven in Problem 3 of Worksheet 9. For $r < 3r_S/2$ the circular orbital velocity is bigger than the velocity of light which means that a circular orbit cannot be realised at such a radius, neither by a freely falling massive particle nor by a photon.

We now insert (371) into (369):

$$\frac{c^2 (E^2 - 1) r^4}{L_z^2} + (2 r - 3 r_S) r - r^2 + r_S r = 0 , \quad (373)$$

$$\frac{c^2 (E^2 - 1) r^2}{L_z^2} = -1 + 2 \frac{r_S}{r} . \quad (374)$$

With (371) and (374) equation (368) gives us the following expression for $V''_{E,L_z}(r)$:

$$-2 V''_{E,L_z}(r) = 12 \left(-1 + 2 \frac{r_S}{r} \right) + 12 - 18 \frac{r_S}{r} - 2 = 6 \frac{r_S}{r} - 2 . \quad (375)$$

The stability condition $V''_{E,L_z}(r) > 0$ is, thus, satisfied for $r > 3r_S$. In the radius interval $3r_S/2 < r < 3r_S$ circular orbits do exist; however, they are unstable which means that practically they cannot be realised, as any small deviation from the initial condition would lead to an escape orbit. The limiting case $r = 3r_S$ is known as the *Innermost Stable Circular Orbit* (ISCO).

We summarise our results on circular orbits of freely falling massive particles in the following table.

$r < 3r_S/2$	circular orbits do not exist
$3r_S/2 < r < 3r_S$	circular orbits do exist, but they are unstable
$3r_S < r$	circular orbits do exist and are stable

Note that here the word “orbit” refers to a timelike geodesic, i.e., to the worldline of a particle in free fall. With the help of a propulsion it is very well possible for an observer to move on a circular path with $r \leq 3r_S/2$.

We will now calculate the perihelion precession of (non-circular) bound orbits. To that end, we have to consider solutions of (363) where the r -coordinate oscillates between a minimum value r_1 (perihelion) and a maximum value r_2 (aphelion). The extremal values r_1 and r_2 are characterised by the property that there the equation $dr/d\varphi = 0$ has to hold, i.e., $V_{E,L_z}(r_1) = 0$ and $V_{E,L_z}(r_2) = 0$. These two equations,

$$\frac{c^2 (E^2 - 1) r_1^4}{L_z^2} + \frac{c^2 r_S r_1^3}{L_z^2} - r_1^2 + r_S r_1 = 0, \quad (376)$$

$$\frac{c^2 (E^2 - 1) r_2^4}{L_z^2} + \frac{c^2 r_S r_2^3}{L_z^2} - r_2^2 + r_S r_2 = 0, \quad (377)$$

allow to express E and L_z in terms of r_1 and r_2 . To work this out, we multiply (376) with r_2^2/r_1 and (377) with r_1^2/r_2 ; then we subtract the second equation from the first:

$$\frac{c^2 (E^2 - 1)}{L_z^2} (r_1^3 r_2^2 - r_2^3 r_1^2) - r_1 r_2^2 + r_2 r_1^2 + r_S (r_2^2 - r_1^2) = 0, \quad (378)$$

$$\frac{c^2 (E^2 - 1)}{L_z^2} r_1^2 r_2^2 (\cancel{r_1 - r_2}) + r_1 r_2 (\cancel{r_1 - r_2}) - r_S (\cancel{r_1 - r_2})(r_1 + r_2) = 0, \quad (379)$$

$$\frac{c^2 (E^2 - 1)}{L_z^2} = \frac{r_S (r_1 + r_2) - r_1 r_2}{r_1^2 r_2^2}. \quad (380)$$

This result inserted into (349) yields

$$\frac{(r_S (r_1 + r_2) - r_1 r_2)}{r_1^2 r_2^2} r_1^4 + \frac{c^2 r_S r_1^3}{L_z^2} - r_1^2 + r_S r_1 = 0, \quad (381)$$

$$\frac{c^2 r_S}{L_z^2} = \frac{r_1^2 r_2 + r_1 r_2^2 - r_S (r_1^2 + r_2 r_1 + r_2^2)}{r_1^2 r_2^2}. \quad (382)$$

This allows us to express E and L_z in (363) in terms of r_1 and r_2 :

$$\left(\frac{dr}{d\varphi}\right)^2 = \frac{r_S(r_1 + r_2) - r_1 r_2}{r_1^2 r_2^2} r^4 + \frac{r_1^2 r_2 + r_1 r_2^2 - r_S(r_1^2 + r_2 r_1 + r_2^2)}{r_1^2 r_2^2} r^3 - r^2 + r_S r = -2V_{E,L}(r). \quad (383)$$

This expression can be rewritten in a more convenient way. We observe that $V_{E,L_z}(r)$ is a fourth-order polynomial with respect to the variable r and that it has a zero at $r = 0$ (which is obvious) and two more zeros at $r = r_1$ and $r = r_2$ (by construction). Hence $V_{E,L_z}(r)$ must be of the form

$$-2V_{E,L_z}(r) = r(r_2 - r)(r - r_1)(Ar + B). \quad (384)$$

If we multiply the right-hand side out and compare with the coefficients in (383) we can determine A and B :

$$A = \frac{r_1 r_2 - r_S(r_1 + r_2)}{r_1^2 r_2^2}, \quad B = -\frac{r_S}{r_1 r_2}. \quad (385)$$

We have, thus, shown that $V_{E,L}(r)$ can be written in the following form:

$$-2V_{E,L_z}(r) = \frac{r^2}{r_1 r_2} (r_2 - r)(r - r_1) \left(1 - \frac{r_S}{r_1 r_2} \left(r_1 + r_2 + \frac{r_1 r_2}{r}\right)\right). \quad (386)$$

From (383) we get the equation

$$d\varphi = \frac{\pm dr}{\sqrt{-2V_{E,L_z}(r)}} \quad (387)$$

which can be integrated over the orbit from one perihelion to the next perihelion. If the result of this integration is equal to 2π , the orbit is closed. The deviation from 2π gives the perihelion precession per revolution. We denote it by Δ , hence

$$2\pi + \Delta = \left(\int_{r_1}^{r_2} - \int_{r_2}^{r_1} \right) \frac{dr}{\sqrt{-2V_{E,L_z}(r)}}. \quad (388)$$

The signs must be chosen such that φ is increasing on both legs of the orbit (from perihelion to aphelion and from aphelion to perihelion). In Fig. 58 four subsequent perihelion passages are indicated by blue dots.

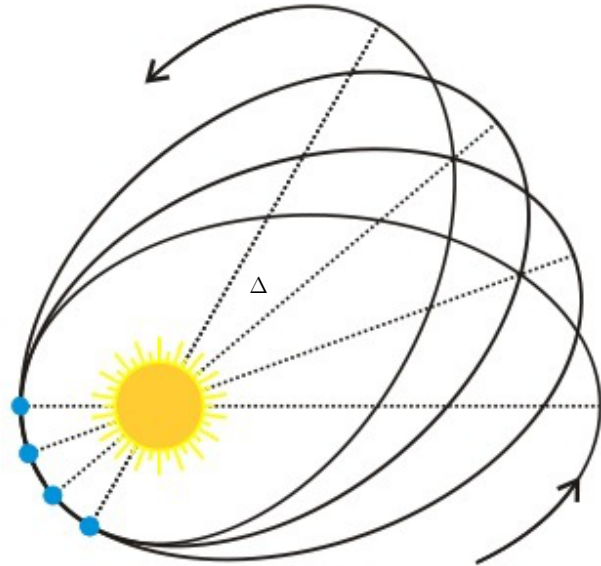


Figure 58: Perihelion precession Δ

With (386) we get the following *exact* formula for the perihelion precession per revolution in terms of an elliptic integral:

$$2\pi + \Delta = 2 \int_{r_1}^{r_2} \frac{\sqrt{r_1 r_2} dr}{r \sqrt{r_2 - r} \sqrt{r - r_1} \sqrt{1 - \frac{r_S}{r_1 r_2} \left(r_1 + r_2 + \frac{r_1 r_2}{r} \right)}} . \quad (389)$$

For applications in the Solar system we get a valid approximation if we linearise this expression with respect to r_S/r_1 :

$$\begin{aligned} 2\pi + \Delta &= 2 \int_{r_1}^{r_2} \left(1 + \frac{r_S}{2r_1 r_2} \left(r_1 + r_2 + \frac{r_1 r_2}{r} \right) \right) \frac{\sqrt{r_1 r_2} dr}{r \sqrt{r_2 - r} \sqrt{r - r_1}} = \\ &= 2 \left(1 + \frac{r_S}{2r_1 r_2} (r_1 + r_2) \right) \underbrace{\sqrt{r_1 r_2} \int_{r_1}^{r_2} \frac{dr}{r \sqrt{-r^2 + (r_1 + r_2)r - r_1 r_2}}}_{=I_1} + \\ &\quad + r_S \sqrt{r_1 r_2} \underbrace{\int_{r_1}^{r_2} \frac{dr}{r^2 \sqrt{-r^2 + (r_1 + r_2)r - r_1 r_2}}}_{=I_2} . \end{aligned} \quad (390)$$

The integrals can be looked up in a table:

$$I_1 = \frac{1}{\sqrt{r_1 r_2}} \arcsin \frac{(r_1 + r_2)r - 2r_1 r_2}{r(r_2 - r_1)} \Big|_{r_1}^{r_2} = \frac{1}{\sqrt{r_1 r_2}} (\arcsin 1 + \arcsin 1) = \frac{\pi}{\sqrt{r_1 r_2}} , \quad (391)$$

$$I_2 = \frac{\sqrt{-r^2 + (r_1 + r_2)r - r_1 r_2}}{\sqrt{r_1 r_2} r} \Big|_{r_1}^{r_2} + \frac{r_1 + r_2}{2r_1 r_2} I_1 = 0 + \frac{(r_1 + r_2)\pi}{2\sqrt{r_1 r_2}^3} . \quad (392)$$

This gives us the following approximative formula for the perihelion precession per revolution:

$$\begin{aligned} \Delta &= 2 \left(1 + \frac{r_S}{2r_1 r_2} (r_1 + r_2) \right) \sqrt{r_1 r_2} I_1 + r_S \sqrt{r_1 r_2} I_2 - 2\pi = \\ &= 2 \left(1 + \frac{r_S}{2r_1 r_2} (r_1 + r_2) \right) \pi + \frac{r_S (r_1 + r_2)}{2r_1 r_2} \pi - 2\pi = \frac{3\pi r_S (r_1 + r_2)}{2r_1 r_2} . \end{aligned} \quad (393)$$

It is common to introduce the following notation, which makes sense for *any* bound orbit (not just for ellipses):

$$a = \frac{r_1 + r_2}{2} = \text{semi-major axis} , \quad \varepsilon = \frac{r_2 - r_1}{r_2 + r_1} = \text{eccentricity} . \quad (394)$$

Solving these two equations for r_1 and r_2 yields $r_1 = a(1 - \varepsilon)$ and $r_2 = a(1 + \varepsilon)$ which gives

$$\Delta = \frac{3\pi r_S \mathcal{Z} \mathcal{A}}{\mathcal{Z} \mathcal{A}^2 (1 - \varepsilon^2)} = \frac{6\pi G M}{c^2 a (1 - \varepsilon^2)} . \quad (395)$$

This formula is correct only up to first order in r_S/a . Note, however, that no approximative assumptions about the eccentricity have been made, i.e., the formula does not require the orbit to be close to a circle. Moreover, note that the perihelion precession does *not* go to zero in the circular limit $\varepsilon \rightarrow 0$.

The perihelion precession is a cumulative effect, meaning that it grows monotonically in the course of time. It is usual to give the quotient Δ/T , where T denotes the (coordinate) time of one revolution. If we insert for M the Solar mass, and for a , ε and T the values of the inner planets, we find the numerical values given in the table. For the outer planets the perihelion precession is negligibly small.

Mercury	$\Delta/T = 43.0$ arcseconds per century
Venus	$\Delta/T = 8.6$ arcseconds per century
Earth	$\Delta/T = 3.8$ arcseconds per century
Mars	$\Delta/T = 1.4$ arcseconds per century

Already in the 19th century it was known that Mercury shows an anomalous perihelion precession, i.e., a perihelion precession that cannot be explained in terms of Newtonian gravity. In 1859 U. Le Verrier found for this anomalous perihelion precession a value of 38 arcseconds per century. Here one has to take into account that the perturbations by the other planets result in a perihelion precession of Mercury that amounts to approximately 530 arcseconds per century. The anomalous perihelion precession is, thus, only a relatively small contribution to the total perihelion precession. As an explanation for the anomalous perihelion precession of Mercury, Le Verrier and others suggested the existence of a hypothetical planet (“Vulcan”) that was supposed to orbit closer to the Sun than Mercury, but it was never found. Einstein gave the correct explanation of the anomalous perihelion precession in 1915, on the basis of his linearised field equation.

6.4 Schwarzschild black holes

We will now discuss what happens to a star whose radius is smaller than r_S . Then the metric in the exterior has a “singularity” at $r = r_S$. The correct interpretation of this singularity was an unsolved problem until the late 1950s.

At $r = r_S$ the metric coefficient $g_{rr} = g(\partial_r, \partial_r)$ diverges to infinity. This does not necessarily indicate a pathology of the metric; it could very well be that the metric is perfectly regular at $r = r_S$, and that it is the coordinate basis vector field ∂_r that causes the divergence. Then we would only have a “coordinate singularity” at $r = r_S$ that could be removed by a coordinate transformation.

In this context it is helpful to calculate curvature invariants (i.e., scalars that are formed out of the curvature tensor). If a curvature invariant becomes infinite, this indicates a “true” singularity, a so-called “curvature singularity”, that cannot be removed by any coordinate transformation. If, however, all curvature invariants remain finite at a point where some metric coefficients diverge, then it might be just a coordinate singularity. As the Ricci tensor is zero, for the Schwarzschild metric the simplest scalar invariant is the so-called Kretschmann scalar which is the contraction of the curvature tensor with itself. One finds that

$$R_{\mu\nu\rho\sigma}R^{\mu\nu\rho\sigma} = \frac{4r_S^2}{r^6}. \quad (396)$$

This demonstrates that there is a curvature singularity at $r = 0$ (if we extend the vacuum Schwarzschild solution that far), but it gives us some hope that at $r = r_S$ we might have only a coordinate singularity.

We will now show that this is, indeed, true. To that end we consider ingoing and outgoing radial lightlike geodesics in the Schwarzschild metric. It is our plan to transform to a new coordinate system in which the ingoing (or outgoing, resp.) radial geodesics are mapped onto straight lines. We will see that in these new coordinates the metric coefficients are regular in the whole domain $0 < r < \infty$.

A radial lightlike curve has to satisfy the equations

$$g_{\mu\nu} \frac{dx^\mu}{ds} \frac{dx^\nu}{ds} = 0, \quad \frac{d\vartheta}{ds} = \frac{d\varphi}{ds} = 0. \quad (397)$$

If we insert the $g_{\mu\nu}$ of the Schwarzschild metric, we get

$$0 = -c^2 \left(1 - \frac{r_S}{r}\right) \left(\frac{dt}{ds}\right)^2 + \frac{1}{\left(1 - \frac{r_S}{r}\right)} \left(\frac{dr}{ds}\right)^2, \quad (398)$$

$$\left(\frac{dr}{ds} \frac{ds}{dt}\right)^2 = c^2 \left(1 - \frac{r_S}{r}\right)^2, \quad \frac{dr}{dt} = \pm c \left(1 - \frac{r_S}{r}\right). \quad (399)$$

In (399) we have shown that this is the equation that holds for radial lightlike *geodesics*, i.e., for classical photons in radial motion. So we see that a radial lightlike *curve* is automatically a radial lightlike *geodesic*. This is, of course, a consequence of the symmetry.

In (399) the upper sign holds for outgoing photons and the lower sign holds for ingoing photons. Integration yields

$$\pm c \int dt = \int \frac{dr}{\left(1 - \frac{r_S}{r}\right)} = \int \frac{(r - r_S + r_S) dr}{r - r_S} = \int dr + r_S \int \frac{dr}{r - r_S}, \quad (400)$$

$$\pm ct = r + r_S \ln|r - r_S| + C. \quad (401)$$

It is convenient to write the integration constant in the form $C = r_S \ln(r_S) + ct_0$. Then the equations for radial lightlike geodesics reads

$$\pm ct = r + r_S \ln \left| \frac{r}{r_S} - 1 \right| + ct_0. \quad (402)$$

This expression is valid in the exterior region $r_S < r < \infty$ and also in the interior region $0 < r < r_S$. Fig. 59 shows ingoing and outgoing radial lightlike geodesics in both regions. In either region the Schwarzschild metric is regular. However, the two regions are separated by the surface $r = r_S$ which shows a singular behaviour in the Schwarzschild coordinates. None of our lightlike geodesics reaches this surface at a finite coordinate time. As the angular coordinates are not shown, any point in this diagram represents a sphere.

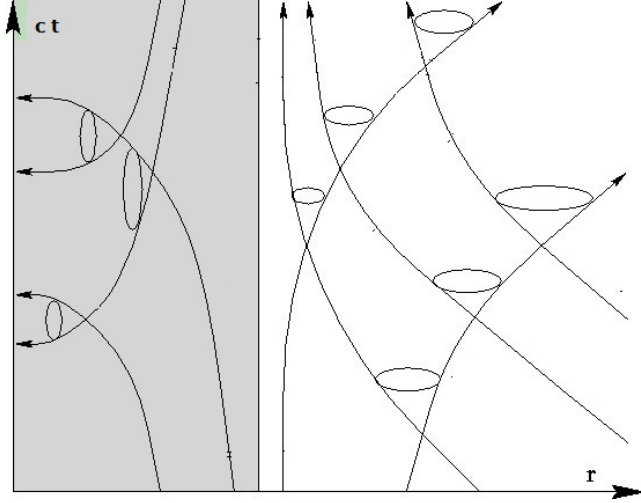


Figure 59: Radial lightlike geodesics in Schwarzschild coordinates

In the interior region r and t have interchanged their causal character: r is a time coordinate, $g_{rr} < 0$, and t is a space coordinate, $g_{tt} > 0$. While in the exterior region t cannot stand still along an observer's worldline, in the interior region r cannot stand still along an observer's worldline. As the Killing vector field ∂_t is not timelike in the interior, in this region the Schwarzschild metric is not static.

	$0 < r < r_S$	$r_S < r < \infty$
∂_r	timelike	spacelike
∂_t	spacelike	timelike

We now transform from Schwarzschild coordinates $(t, r, \vartheta, \varphi)$ to *ingoing Eddington-Finkelstein coordinates* $(t', r, \vartheta, \varphi)$,

$$ct' = ct + r_S \ln \left| \frac{r}{r_S} - 1 \right|, \quad (403)$$

$$cdt' = cdt + \frac{r_S dr}{r - r_S}. \quad (404)$$

This transformation maps ingoing radial lightlike geodesics onto straight lines,

$$-ct' = r + ct_0. \quad (405)$$

By contrast, the outgoing radial lightlike geodesics are now given by the equation

$$ct' = r + 2r_S \ln \left| \frac{r}{r_S} - 1 \right| + ct_0. \quad (406)$$

We will demonstrate now that in the coordinates $(t', r, \vartheta, \varphi)$ the metric coefficients are regular for all values $0 < r < \infty$.

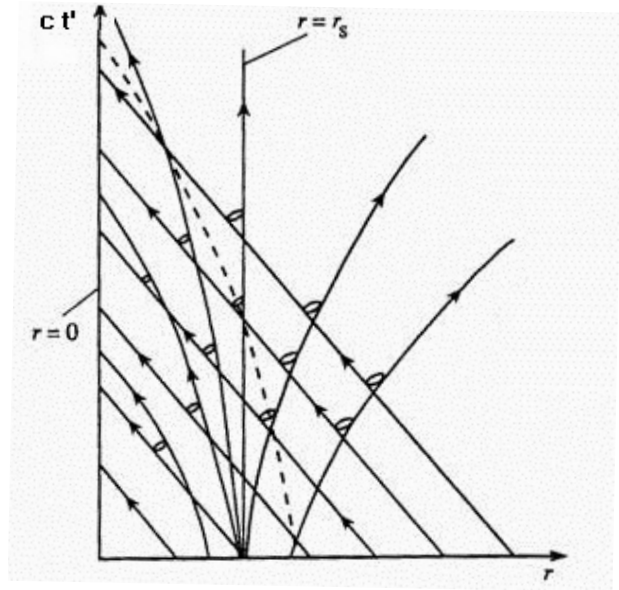


Figure 60: Radial lightlike geodesics in ingoing Eddington-Finkelstein coordinates

$$\begin{aligned}
g - r^2(d\vartheta^2 + \sin^2\vartheta d\varphi^2) &= -\left(1 - \frac{r_S}{r}\right) c^2 dt^2 + \frac{dr^2}{1 - \frac{r_S}{r}} \\
&= -\frac{r - r_S}{r} \left(c dt' - \frac{r_S dr}{r - r_S} \right)^2 + \frac{dr^2}{1 - \frac{r_S}{r}} \\
&= -c^2 \frac{r - r_S}{r} dt'^2 + \frac{2cr_S \cancel{(r - r_S)} dt' dr}{r \cancel{(r - r_S)}} - \frac{r_S^2 \cancel{(r - r_S)} dr^2}{r \cancel{(r - r_S)}^2} + \frac{r dr^2}{r - r_S} \\
&= -c^2 \left(1 - \frac{r_S}{r}\right) dt'^2 + \frac{2cr_S}{r} dt' dr + \frac{\left(1 + \frac{r_S}{r}\right) \cancel{\left(1 - \frac{r_S}{r}\right)} dr^2}{\cancel{\left(1 - \frac{r_S}{r}\right)}}. \tag{407}
\end{aligned}$$

We have no longer a factor of $1 - r_S/r$ in the denominator, so in the new coordinates the Schwarzschild metric is, indeed, regular on the whole domain $0 < r < r_S$. Also the inverse metric exists on this whole domain, as

$$\begin{aligned}
\det(g_{\mu\nu}) &= \det \begin{pmatrix} -c^2 \left(1 - \frac{r_S}{r}\right) & \frac{cr_S}{r} & 0 & 0 \\ \frac{cr_S}{r} & \left(1 + \frac{r_S}{r}\right) & 0 & 0 \\ 0 & 0 & r^2 & 0 \\ 0 & 0 & 0 & r^2 \sin^2\vartheta \end{pmatrix} \\
&= \left(-c^2 \left(1 - \frac{r_S}{r}\right) \left(1 + \frac{r_S}{r}\right) - \frac{c^2 r_S^2}{r^2} \right) r^4 \sin^2\vartheta = -c^2 r^4 \sin^2\vartheta \tag{408}
\end{aligned}$$

is non-zero for all $r > 0$, apart from the familiar coordinate singularity on the axis, where $\sin\vartheta = 0$.

We have thus found an analytical extension of the Schwarzschild spacetime, which was originally given on the domain $r_S < r < \infty$, to the domain $0 < r < \infty$. Fig. 60 shows the radial lightlike geodesics in this extended spacetime.

Eddington-Finkelstein coordinates were introduced by Arthur Eddington already in 1924. However, he did not use them for investigating the behaviour of the Schwarzschild metric at $r = r_S$ but rather for comparing Einstein's general relativity to an alternative gravity theory of Whitehead. The same coordinates were independently rediscovered by David Finkelstein in 1958 who clarified, with their help, the nature of the surface $r = r_S$.

We discuss now the properties of the extended Schwarzschild spacetime that is covered by the ingoing Eddington-Finkelstein coordinates.

- (a) The metric is regular on the whole domain $0 < r < \infty$. It is clear that the spacetime cannot be extended into the domain of negative r -values, as $r = 0$ is a curvature singularity. We have already noticed that the curvature invariant $R_{\mu\nu\sigma\tau}R^{\mu\nu\sigma\tau}$ goes to infinity for $r \rightarrow 0$. As the curvature tensor determines the relative acceleration of neighbouring geodesics (recall the geodesic deviation equation), this means that near $r = 0$ any material body will be torn apart by infinitely strong tidal forces. It is widely believed that a true understanding of what is going on near $r = 0$ requires a (not yet existing) quantum theory of gravity.
- (b) At $r = r_S$ the spacetime is perfectly regular. The tidal forces are finite there. By local experiments near $r = r_S$, an observer would not notice anything unusual. However, the hypersurface $r = r_S$ plays a particular role in view of the global structure of the spacetime: From the $r - ct'$ -diagram one can read that it is an *event horizon* for all observers in the domain $r > r_S$, i.e., that no signal from the domain $r < r_S$ can reach an observer at $r > r_S$. In particular, photons cannot travel from the domain $r < r_S$ to the domain $r > r_S$. For this reason, the spacetime covered by the ingoing Eddington-Finkelstein coordinates is called a *Schwarzschild black hole*. It is usually said that the name “black hole” was introduced by John Wheeler in 1967, although there was some debate recently that actually this name might have been used already a bit earlier. In the Russian literature, it was common for a while to use a term that literally translates as “frozen star”. David Finkelstein called the hypersurface $r = r_S$ a “one-way membrane”. The term “event horizon” goes back to Wolfgang Rindler who had introduced it, in the context of cosmology, already in 1955.
- (c) As the angular coordinates ϑ and φ are suppressed, each point in our spacetime diagram represents a sphere. Correspondingly, in the diagram each light signal represents an ingoing or outgoing spherical wave front. In the domain $r > r_S$ the radius coordinate is increasing for outgoing spheres and decreasing for ingoing spheres, as it should be in accordance with our geometric intuition. In the domain $0 < r < r_S$, however, we read from the diagram that r is decreasing for ingoing and for outgoing spheres. As $4\pi r^2$ gives the area of a sphere, as measured with the metric, this means that both the ingoing and the outgoing spherical wave fronts have decreasing area. In a terminology introduced by Roger Penrose, they are called *closed trapped surfaces*. The existence of closed trapped surfaces is an important indicator for a black hole and plays a major role in the Hawking-Penrose singularity theorems. Penrose called the boundary of the region filled with closed trapped surfaces the *apparent horizon*. For the Schwarzschild spacetime, in the representation used here, the apparent horizon coincides with the event horizon. This is not true for other black-hole spacetimes.
- (d) Along any future-oriented timelike curve in the domain $r < r_S$, the r -coordinate decreases monotonically, as can be read from the $r - ct'$ -diagram. If an observer was foolhardy enough to enter into the region $0 < r < r_S$, he will end up in the singularity at $r = 0$. In Worksheet 11 we will prove that this happens in a finite proper time interval: For the lifetime $\Delta\tau$ (measured in terms of proper time) that an observer can have in the domain $0 < r < r_S$, we will find the bound $c\Delta\tau \leq \pi r_S/2$. We will also prove that the maximal value of $\Delta\tau$ is reached by a freely falling observer; any attempt to escape from the black hole by accelerating away from the singularity, e.g. with a rocket engine, actually shortens one’s lifetime.

- (e) We have emphasised several times that the Schwarzschild metric applies only to the *exterior region* of a spherically symmetric celestial body, $r > r_*(t)$, because only there is the vacuum field equation satisfied. We consider now a star whose radius $r_*(t)$ is bigger than r_S at the beginning and then shrinks beyond r_S . As soon as the radius is smaller than r_S , the star is doomed. It will collapse to a point in a finite time. This follows from the fact that every volume element of the star, in particular every volume element near the surface, moves on a timelike curve. So the argument of item (d) above implies that the radius of the star shrinks to zero in a finite time. This phenomenon, which is known as *gravitational collapse*, is shown in Fig. 61. The dashed line indicates the surface

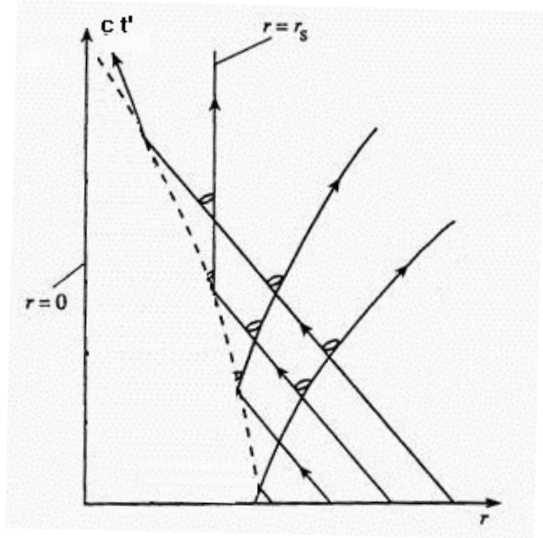


Figure 61: Gravitational collapse

The horizon forms at the moment when the radius of the star becomes smaller than its Schwarzschild radius. This moment is unobservable for an observer in the domain $r > r_S$. For such an observer, the surface of the star approaches the value $r = r_S$ asymptotically, as can be read from the diagram. During this process, the photons from the surface of the star to the observer will be more and more redshifted: We will prove in Worksheet 10 that the redshift goes to infinity if the light source comes closer and closer to $r = r_S$. As every measuring device is sensitive only to a finite frequency range, this means that the star will practically become invisible at a finite time.

For the existence of black holes there is good observational evidence by now. We believe that there are two types of black holes:

- *Stellar black holes* of 1 to 100 Solar masses, which can be observed by way of X rays emitted from matter that is strongly accelerated when falling towards the black hole. The best known example is the X ray source Cyg X1. Until recently, it was thought that stellar black holes could have masses of up to 20 Solar masses. In September 2015, a gravitational-wave signal was received by the LIGO detectors (see next Section) whose analysis indicated that it came from the merger of two stellar black holes of about 30 Solar masses each, so that the resulting black hole had a mass of about 60 Solar masses. This is why we now believe that the masses of stellar black holes may range up to about 100 Solar masses.
- *Supermassive black holes* of 10^6 to 10^{10} Solar masses, which are situated at the centres of galaxies. The best known example is the supermassive black hole at the centre of our own galaxy which is associated with the radio source Sgr A*. Evidence for a black hole comes from infrared observations of stars that orbit the centre of our galaxy. (With optical telescopes, the central region of our galaxy cannot be observed because of too much dust; in the infrared regime, the dust is largely transparent.) From such observations one can estimate the mass of the central object and the volume to which this mass is confined. The results strongly hint to a black hole. Supermassive black holes are believed to sit at the centres of most, if not all, galaxies. A picture of the so-called *shadow* of the supermassive black hole at the centre of the galaxy M87 was released to the public by the Event Horizon Telescope Collaboration in April 2019, see next Subsection.

The existence of black holes whose mass is smaller (mini black holes) or in between (intermediary black holes) is controversial. Also, it is not clear by now if all existing black holes have formed by way of gravitational collapse and subsequent merger, or if some of them came into existence already with the big bang (*premordial* black holes).

Keep in mind that Schwarzschild black holes are spherically symmetric and thus non-rotating. Rotating black holes are described by another solution to Einstein's vacuum field equation that was found by Roy Kerr in 1963. For the stellar and supermassive black holes in Nature, the rotation is probably non-negligible. So one would have to use the Kerr metric, and not the Schwarzschild metric, as a viable mathematical model for them. In comparison to the Schwarzschild metric, the Kerr metric features two interesting new properties. (i) There is a region outside the horizon, known as the *ergoregion* which can be used for extracting energy from the black hole by the so-called *Penrose process*: If a particle enters into the ergoregion and breaks into two particles such that one fragment falls into the black hole and the other fragment escapes to infinity, the energy of the escaping particle may be bigger than the energy of the composed particle in the beginning. (ii) The true singularity at the centre is no longer a point but rather a ring. If the mass and the spin of the black hole are big enough, an observer may pass through this ring unharmed.

In addition to a mass M and spin J , one may also give an electric charge Q to a black hole. Most astrophysicists believe that this is not very relevant because celestial bodies usually have a very small net charge. The solution to Einstein's electrovacuum solution with M and Q different from zero but $J = 0$ is known as the *Reissner-Nordström* solution; with all three parameters different from zero it is called the *Kerr-Newman* solution. The Kerr-Newman solution, which contains the Schwarzschild, the Reissner-Nordström and the Kerr solutions as special cases, is the most general solution to Einstein's field equation with the energy-momentum tensor of an electromagnetic field that describes a time-independent black hole and is asymptotically flat. In other words, such an object is uniquely characterized by the three parameters M , J and Q . This result is known as the *no hair theorem*. If one allows for other energy-momentum tensors, one may construct "hairy" black holes. E.g., one could consider the energy-momentum tensor of a scalar field, i.e., one could give a "scalar charge" to a black hole. Black holes with "scalar hair" are not uniquely characterized by finitely many parameters. In this course we will not discuss any black holes other than the Schwarzschild black holes.

We have constructed Schwarzschild black holes with the help of ingoing Eddington-Finkelstein coordinates whose main property is that they map ingoing radial light rays onto straight lines. We will now briefly discuss what happens if we do the analogous construction with outgoing radial light rays. To that end, we introduce outgoing Eddington-Finkelstein coordinates $(t'', r, \vartheta, \varphi)$, where

$$ct'' = ct - r_S \ln \left| \frac{r}{r_S} - 1 \right|, \quad c dt'' = c dt - \frac{r_S dr}{r - r_S}. \quad (409)$$

In these coordinates the outgoing radial lightlike geodesics are mapped onto straight lines. In complete analogy to the ingoing Eddington-Finkelstein coordinates, also in these coordinates

the metric becomes regular on the whole domain $0 < r < \infty$. In this way we get another analytic extension of the Schwarzschild metric from the domain $r_S < r < \infty$ to the domain $0 < r < \infty$. By construction, it is obvious that it is just the image under time-reflection of the extension we got from the ingoing Eddington-Finkelstein coordinates. Now the hypersurface $r = r_S$ is an event horizon for observers in the region $0 < r < r_S$: Signals can cross this hypersurface only from the inside to the outside, but not from the outside to the inside. For this reason, one speaks of a *Schwarzschild white hole*. Up to now, there is no indication for the existence of white holes in Nature.

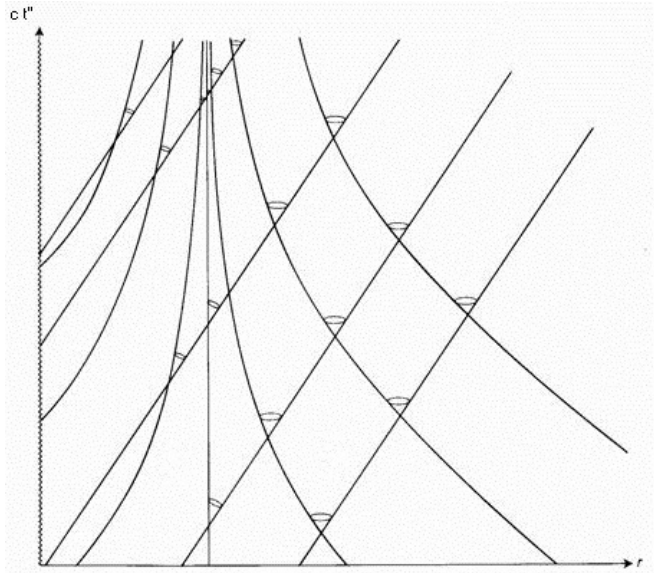


Figure 62: Radial lightlike geodesics in outgoing Eddington-Finkelstein coordinates

The *maximal* analytic extension of the Schwarzschild metric was found independently by Martin Kruskal and by György Szekeres in the late 1950s (and also, with different mathematical techniques, by Christian Frønsdal). This maximal analytic extension, which is probably only of mathematical interest, can be found if one transforms on the domain $r_S < r < \infty$ from Schwarzschild coordinates $(t, r, \vartheta, \varphi)$ to Kruskal(-Szekeres) coordinates $(u, v, \vartheta, \varphi)$ via

$$u = \sqrt{\frac{r}{r_S} - 1} e^{r/(2r_S)} \cosh \frac{ct}{2r_S}, \quad v = \sqrt{\frac{r}{r_S} - 1} e^{r/(2r_S)} \sinh \frac{ct}{2r_S}. \quad (410)$$

On the domain $r_S < r < \infty$, $-\infty < t < \infty$, the map $(t, r) \mapsto (u, v)$ is a diffeomorphism, i.e., an allowed coordinate transformation, although the inverse map cannot be written down in terms of elementary functions. In a $u - v$ -diagram, the lines $t = t_0$ are represented as straight lines,

$$v = \tanh\left(\frac{ct_0}{2r_S}\right) u, \quad (411)$$

while the lines $r = r_0$ are represented as hyperbolas,

$$u + v = \left(\frac{r_0}{r_S} - 1\right) e^{r_0/r_S} \frac{1}{u - v}. \quad (412)$$

In Kruskal(-Szekeres) coordinates the Schwarzschild metric reads

$$g = \frac{4r_S^3}{r} e^{-r/r_S} (du^2 - dv^2) + r^2 d\Omega^2, \quad (413)$$

where r is to be viewed as a function of u and v . The metric is regular on the domain $v^2 - u^2 < 1$. As shown in Fig. 63, this maximal domain covers two copies I and I' of the exterior region $r_S < r < \infty$, a black hole interior region II and a white hole interior region II'. The boundary of the Kruskal-Szekeres extension is given by the equation $v^2 - u^2 = 1$ which corresponds to $r = 0$. In the lettering of the diagram it is $m = GM/c^2$, hence $r_S = 2m$.

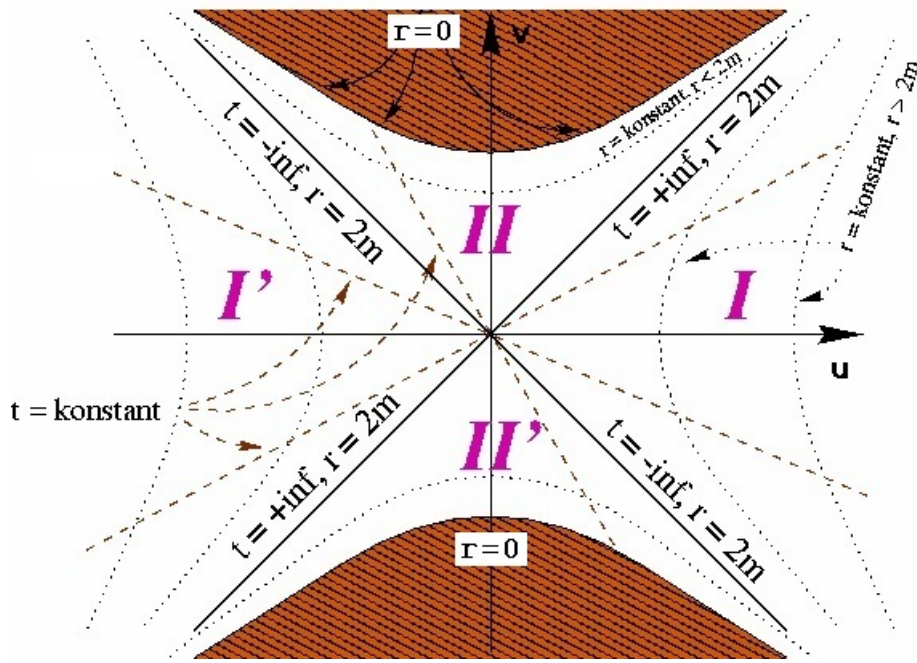


Figure 63: Maximal analytical extension of the Schwarzschild spacetime in Kruskal coordinates

In the $u - v$ -diagram (Kruskal-Szekeres diagram) light signals go under 45 degrees, $du = \pm dv$. Light signals enter into the black-hole interior region by crossing one of the horizons, then they end up in the singularity at $r = 0$. In the white-hole interior region all light signals start at the singularity. They leave the interior white hole region II' over one of the horizons.

The ingoing Eddington-Finkelstein coordinates cover the regions I and II of the Kruskal-Szekeres diagram. Only this part of the diagram is of relevance for the spacetime outside a collapsing star. Correspondingly, the outgoing Eddington-Finkelstein coordinates cover the regions I and II' of the Kruskal-Szekeres diagram.

Note that each point in this diagram represents a sphere, as the coordinates ϑ and φ are not shown. Each straight line $t = \text{constant}$ through the regions I and I' represents a spatial 3-dimensional submanifold of the maximally extended Schwarzschild spacetime all of which together describe the history of a 3-dimensional space that is known as the *Einstein-Rosen bridge*. If we follow a line $t = \text{constant}$ from one end to the other, we pass through a sequence of spheres whose radius decreases from infinity to r_S and then increases again to infinity. This is what one calls a *wormhole* with a *throat* of radius r_S . However, as signals cannot connect a point in the region I with a point in the region I', this wormhole is not traversable. The Einstein-Rosen bridge was discussed in a paper by Einstein and Rosen in the 1930s, at a time when the maximal extension of the Schwarzschild metric was not yet known and the character of $r = r_S$ as a horizon was not yet understood.

We repeat that the maximal extension of the Schwarzschild spacetime is more of mathematical than of physical interest. For a thorough understanding of Schwarzschild black holes the ingoing Eddington-Finkelstein coordinates are quite sufficient.

6.5 Shadow of a Schwarzschild black hole

We fix an observer at radius r_O and consider all light rays that go from the position of this observer into the past. (To put this another way, we consider all light rays that *arrive* at the position of the observer.) They fall into two categories: Category I consists of light rays that go out to infinity, category II consists of light rays that go to the horizon at $r = r_S$. The borderline case that separates the two categories is given by light rays that asymptotically spiral towards the light sphere at $r = 3r_S/2$.

Now assume that there are light sources distributed everywhere in the spacetime but not between the observer and the black hole. Then the initial directions of light rays of category I correspond to points at the observer's sky that are bright, and the initial directions of light rays of category II correspond to points at the observer's sky that are dark, known as the *shadow* of the black hole. The boundary of the shadow corresponds to light rays that spiral towards $r = 3r_S/2$. It is our goal to calculate the angular radius θ_0 of the shadow, in dependence of r_S and r_O .

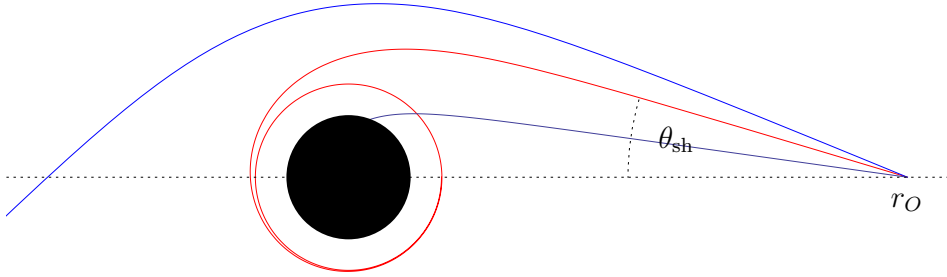


Figure 64: Angular radius θ_{sh} of the shadow

For any light ray, the initial direction makes an angle θ with respect to the axis that is given, according to Fig. 65, by

$$\tan \theta = \lim_{\Delta x \rightarrow 0} \frac{\Delta y}{\Delta x}.$$

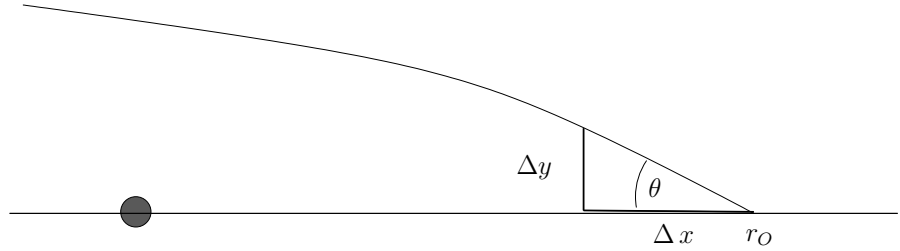


Figure 65: Initial direction of light rays

From the Schwarzschild metric in the equatorial plane,

$$g = - \left(1 - \frac{r_S}{r}\right) c^2 dt^2 + \frac{dr^2}{1 - \frac{r_S}{r}} + r^2 d\varphi^2, \quad (414)$$

we can read the length Δx and Δy in the desired limit,

$$\tan \theta = \left. \frac{r d\varphi}{\left(1 - \frac{r_S}{r}\right)^{-1/2} dr} \right|_{r=r_O}. \quad (415)$$

$dr/d\varphi$ can be expressed with the help of the orbit equation (341), hence

$$\tan^2\theta = \frac{r_O^2\left(1 - \frac{r_S}{r_O}\right)}{\frac{r_O^4}{b^2} - r_O^2 + r_S r_O} = \frac{r_O - r_S}{\frac{r_O^3}{b^2} - r_O + r_S} \quad (416)$$

where, as before,

$$b = \frac{cL_z}{E}. \quad (417)$$

By elementary trigonometry,

$$\begin{aligned} \frac{1}{\tan^2\theta} &= \frac{r_O^3}{b^2(r_O - r_S)} - 1, \\ \frac{\sin^2\theta}{\sin^2\theta} + \frac{\cos^2\theta}{\sin^2\theta} &= \frac{r_O^3}{b^2(r_O - r_S)}, \\ \sin^2\theta &= \frac{b^2(r_O - r_S)}{r_O^3}. \end{aligned} \quad (418)$$

The angular radius θ_{sh} of the shadow is given by the angle θ for a light ray that spirals towards $r = 3r_S/2$. This light ray must have the same constants of motion E and L_z as a circular light ray at $r = 3r_S/2$ (because the tangent vectors of these two light rays come arbitrarily close to each other),

$$b^2 = \frac{c^2 L_z^2}{E^2} = \frac{27}{4} r_S^2 \quad (419)$$

as we have calculated in Problem 3 of Worksheet 9.

This gives us θ_{sh} in dependence of $r_S = 2GM/c^2$ and r_O ,

$$\sin^2\theta_{\text{sh}} = \frac{27 r_S^2 (r_O - r_S)}{4 r_O^3}. \quad (420)$$

This formula was found by J. Synge [Mon. Not. Roy. Astron. Soc. **131**, 463 (1966)]. He did not use the word “shadow”, however, because he considered the time-reversed situation and calculated what he called the “escape cones” of light. If the observer is far away from the black hole, $r_O - r_S \approx r_O$, Synge’s formula can be approximated by

$$\tan\theta_{\text{sh}} \approx \sin\theta_{\text{sh}} \approx \sqrt{3} \times \frac{3r_S}{2r_O}.$$

Up to a factor of $\sqrt{3}$, θ_{sh} is then the angular radius under which a sphere of radius $3r_S/2$ is seen from a distance r_O according to Euclidean geometry. This means that a naive Euclidean estimate correctly gives the order of magnitude of the diameter of the shadow if the observer is far away.

Note that

$r_O \rightarrow \infty$: $\theta_{\text{sh}} \rightarrow 0$ (i.e., the shadow vanishes).

$r_O = 3r_S/2$: $\theta_{\text{sh}} = \pi/2$ (i.e., the shadow covers half of the sky).

$r_O \rightarrow r_S$: $\theta_{\text{sh}} \rightarrow \pi$ (i.e., the shadow covers the whole sky).

The following picture shows, for various observer positions, in red the part of the sky that is bright. Note that our calculation applies to a static observer at the corresponding position. For a moving observer the aberration formula has to be applied. As the aberration formula maps circles onto circles, the shadow of a Schwarzschild black hole is *always* seen circular, independent of the state of motion of the observer. For an observer moving towards the black hole the shadow is smaller than for a static observer, for an observer moving away from the black hole it is bigger.

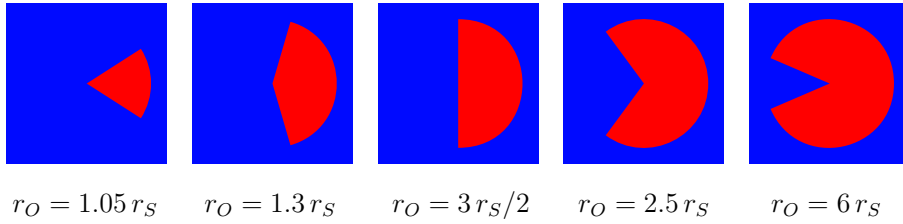


Figure 66: Escape cones of light

We have good evidence that there is a supermassive black hole at the centre of our galaxy, associated with the radio source Sgr A*. For the shadow of this black hole ($M \approx 4 \times 10^6 M_\odot$, $r_O \approx 8.5 \text{ kpc}$) Synge's formula gives an angular diameter of $2\theta_0 \approx 54 \mu\text{as}$. This corresponds to the angle under which a grapefruit on the Moon is seen from Earth. Another promising candidate is the black hole at the centre of the galaxy M87 in the constellation Virgo. In this case ($M \approx 6 \times 10^9 M_\odot$, $r_O \approx 16 \text{ Mpc}$) one finds $2\theta_0 \approx 40 \mu\text{as}$. For all other known black-hole candidates the predicted angular diameter of the shadow is considerably smaller. A picture of the shadow of the object at the centre of M87 was actually made public on 10 April 2019, see below.

Note that the shadow would exist not only for a black hole, but in exactly the same way also for an ultracompact star ($r_S < r_* < 3r_S/2$), provided the star is dark. It is the light sphere at $r = 3r_S/2$ and not the horizon at $r = r_S$ that is relevant for the formation of the shadow. The existence of ultracompact stars is highly speculative. Also, a wormhole would cast a shadow if there is no light coming out of its mouth. However, again, the existence of wormholes is highly speculative.

Our calculation was based on the Schwarzschild metric, so it does not apply to a *rotating* black hole. The latter is to be described by the Kerr metric; then the shadow is not circular but flattened on one side which, however, is not noticeable if we observe from the top or from the bottom. In any case, our calculation with the Schwarzschild metric gives the correct order of magnitude for the size of the shadow.

For observing the shadow we need light sources which provide a bright backdrop against which the shadow can be seen. We need to know how many images each light source produces. To that end we fix a static observer at radius r_O and a static light source at radius r_L . We exclude

the case that observer and light source are exactly aligned (i.e., that they are on a straight line through the origin of the coordinate system) which would give rise to Einstein rings instead of point images. If one thinks of each lightlike geodesic as being surrounded by a thin bundle that is focussed onto the observer's retina (or onto a photographic plate) with a lens, every lightlike geodesic from the light source to the observer gives rise to an image.

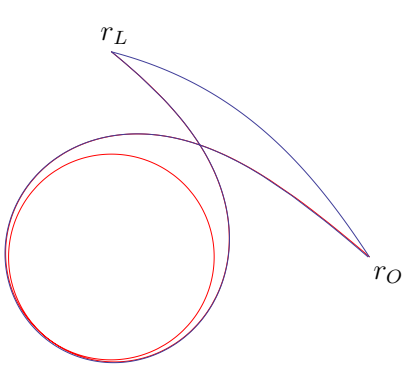


Figure 67: Positively oriented light rays

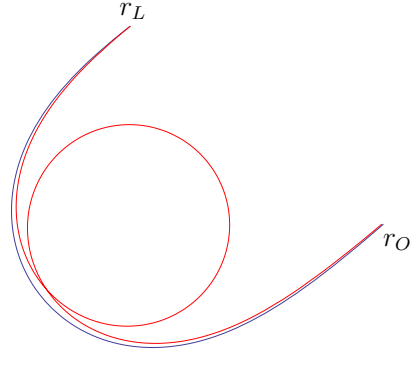


Figure 68: Negatively oriented light rays

The qualitative imaging features follow from the fact that the bending angle grows monotonically to infinity for light rays that approach the photon sphere at $r = 3r_S/2$. As a consequence, for any integer $n = 0, 1, 2, 3, \dots$ there is a light ray from the light source to the observer that makes n full turns in the clockwise sense, and another light ray from the light source to the observer that makes n full turns in the counter-clockwise sense. Hence, there are two infinite sequences of light rays from the light source to the observer, one in the clockwise sense (left picture) and one in the counter-clockwise sense (right picture). Either sequence has as its limit curve a light ray that spirals asymptotically towards $r = 3r_S/2$. The pictures are not just qualitatively correct; they show numerically integrated lightlike geodesics in the Schwarzschild spacetime. One sees that for each sequence the light rays with $n = 1, 2, 3, \dots$ lie practically on top of each other. Correspondingly, the observer sees infinitely many images on either side of the centre. Each sequence rapidly approaches the boundary of the shadow.

In the picture on the right, which is again the result of a calculation, the shadow is shown as a black disc. On either side only the outermost image ($n = 0$) can be isolated, all the other ones clump together and they are very close to the boundary of the shadow. If there are many light sources, their higher-order images form a bright ring around the shadow.

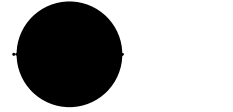


Figure 69: Multiple imaging

It can be shown that the outermost images are brighter than all the other ones combined. Of the two outermost images, the brighter one is called the *primary image* and the other one is called the *secondary image*. All the remaining ones, which correspond to light rays that make at least one full turn around the centre, are known as *higher-order images*.

The first computer simulation of the visual appearance of a Schwarzschild black hole was

produced by J.-P. Luminet in 1979. Here it is assumed that the light comes from a rotating accretion disc. Part of the disc is in front of the black hole, so it covers part of the shadow. The rear part of the disc appears bent upwards because of the light bending. One side of the disc is approaching the observer; because of aberration it appears brighter than the receding side. This is sometimes called *Doppler beaming*. The higher-order images form a thin bright ring around the shadow.

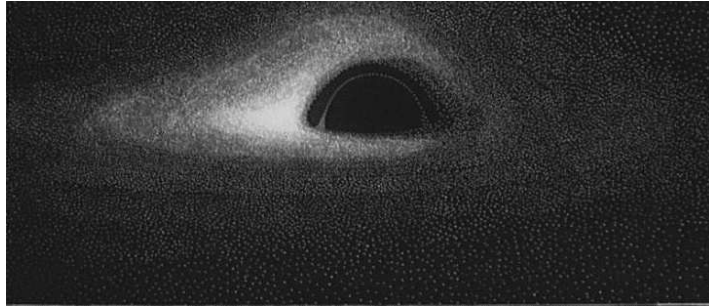


Figure 70: From J.-P. Luminet, *Astron. Astrophys.* 75, 228 (1979)

A similar simulation was shown in the movie “Interstellar”. Here the viewing angle is smaller, i.e., the accretion disc is seen almost exactly edge-on. For this reason one sees both the upper side and the lower side of the rear part of the disc.

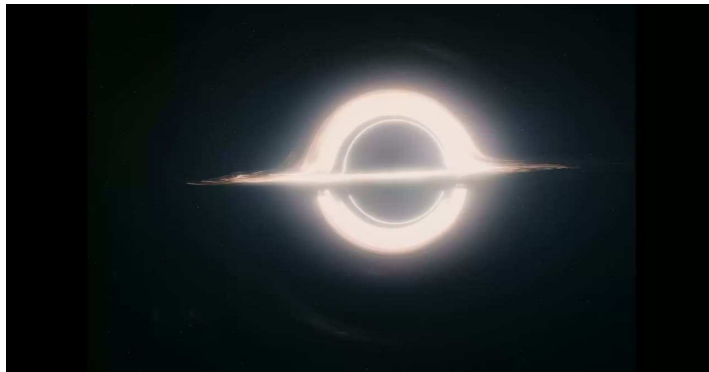


Figure 71: From the movie “Interstellar”

Finally, on 10 April 2019 the first “real picture” of a black hole was presented to the public. The data were taken in April 2017, so the evaluation took two years. The picture was produced by a collaboration of approximately 350 scientists with the so-called *Event Horizon Telescope*. In contrast to what the name suggests, this is not one telescope but it consists of many (radio) telescopes distributed over one hemisphere of the Earth. Each of these telescopes measures the intensity and the phase of the incoming radiation. From these data the Fourier transform of the image can be calculated, from which then a real image is produced. This method is known as *aperture synthesis*. It was invented in the 1950s by Martin Ryle which earned him the physics Nobel Prize in 1974. When used with telescopes on different continents one speaks of *Very Long Baseline Interferometry* (VLBI).



Figure 72: ALMA

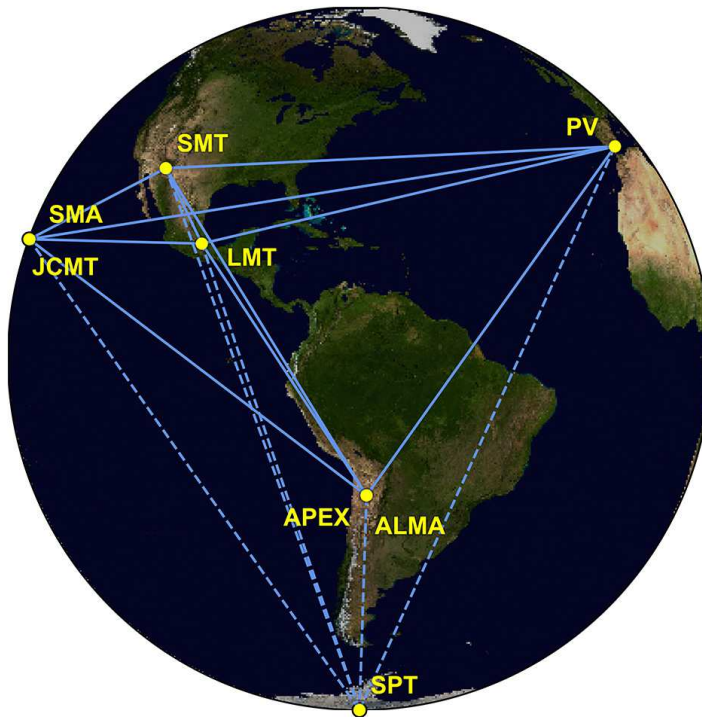


Figure 73: EHT

In 2017, when the successful observations took place, the Event Horizon Telescope included the *Atacama Large Millimeter Array* (ALMA) and the *ALMA Pathfinder Experiment* (APEX) in Chile, the *South Pole Telescope* (SPT), the *Large Millimeter Telescope* (LMT) in Mexico, the *James Clerk Maxwell Telescope* (JCMT) and the *Submillimeter Array* (SMA) on Hawaii, the *Submillimeter Telescope Observatory* (SMT) in Arizona, USA, and the *Pico Veleta Telescope* (PV) in Spain. As scattering would wash out the image at larger wave lengths, the observations were made at a wave length of 1.3 mm which corresponds to a frequency of 230 GHz. At such a small wave length, VLBI is possible only since a few years. As radiation at 1.3 mm is partially blocked by the water vapour in our atmosphere, only telescopes at a high altitude can be used. Although our Sun is not very bright at 1.3 mm, the observations were done during the night

time because then the atmosphere is more stable. At four nights in April 2017, the weather conditions were excellent so that observations were possible at all stations. Both Sgr A* and M87 were observed. However, the environment of Sgr A* turned out to change so rapidly that no clear and stable picture could be produced. In the case of M87 the central black hole is a thousand times heavier, so the orbital periods of particles revolving around the black hole are of the order of days, rather than minutes as for Sgr A*. This is the reason why a surprisingly good picture of this object could be produced.

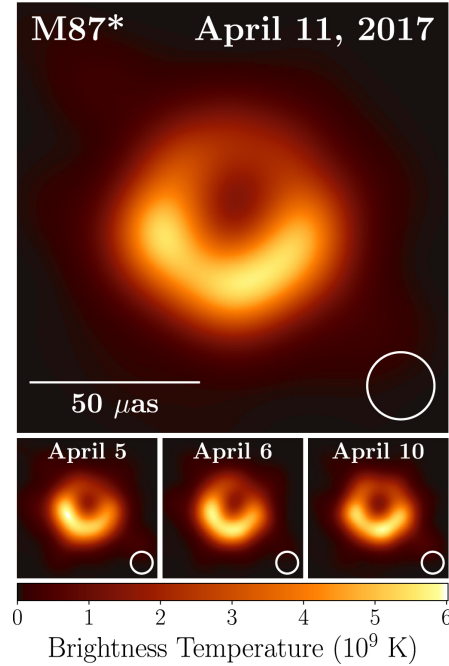


Figure 74: From The Event Horizon Telescope Collaboration, *Astrophys. J. Lett.* 875, L1 (2019)

One clearly sees a black disc in the centre and a bright ring around it. The bright ring is interpreted as radiation coming from an accretion disc. The fact that one side of the ring is considerably brighter than the other indicates that this side is moving towards us. Comparison with simulations indicate that the spin vector of the accretion disc points into the page and a bit to the left. (In the pictures North is up and West is right.) All observations are in agreement with the assumption that the spin of the black hole is aligned with the spin of the accretion disc. The fact that the shadow is practically circular does not mean that the black hole is non-rotating: As we look onto the system almost from the bottom, even for a fast rotating black hole the shadow would be seen as almost circular. The thin ring of higher-order images around the shadow is not visible; this is in agreement with simulations which show that it is too faint. The interpretation of the bright ring as an accretion disc is still under debate. It is also possible that we are looking into the (hollow) jet of M87, or that both an accretion disc and the jet contribute to the ring.

6.6 The interior Schwarzschild solution

The Schwarzschild metric describes the vacuum region outside of a spherically symmetric star (or a black hole). We will now derive a metric that describes the interior region of a spherically symmetric and static star. We use the simplest matter model for the star, i.e. an incompressible perfect fluid. This interior metric was found by K. Schwarzschild in 1916. It is known as the *interior Schwarzschild solution*.

The metric should be spherically symmetric and static,

$$g = -e^{\nu(r)}c^2dt^2 + e^{\lambda(r)}dr^2 + r^2(\sin^2\vartheta d\varphi^2 + d\vartheta^2), \quad (421)$$

and it should satisfy Einstein's field equation (without a cosmological constant)

$$R_{\rho\sigma} - \frac{R}{2}g_{\rho\sigma} = \frac{8\pi G}{c^4}T_{\rho\sigma} \quad (422)$$

with a perfect fluid source,

$$T_{\rho\sigma} = \left(\mu + \frac{p}{c^2}\right)U_\rho U_\sigma + p g_{\rho\sigma}. \quad (423)$$

As the star is static, the four-velocity must be of the form $U^\rho = u\delta_t^\rho$. The factor u follows from the normalisation condition $g_{\rho\sigma}U^\rho U^\sigma = -c^2$,

$$U^\rho = e^{-\nu/2}\delta_t^\rho. \quad (424)$$

We assume that the star has a constant density,

$$\mu = \text{constant}. \quad (425)$$

As the star is static and spherically symmetric, the pressure p can depend on r only. The function $p(r)$ is to be determined.

Einstein's field equation gives us a system of ordinary differential equations for the three unknown functions $\nu(r)$, $\lambda(r)$ and $p(r)$. Before writing out this system of differential equations, we consider the equation $\nabla^\rho T_{\rho\sigma} = 0$ which is a consequence of the field equation (recall Problem 3 of Worksheet 8). We know that, for a perfect fluid, this results in the Euler equation (239)

$$\left(\mu + \frac{p}{c^2}\right)U^\rho \nabla_\rho U^\sigma + \nabla_\tau p \left(g^{\tau\sigma} + \frac{1}{c^2}U^\tau U^\sigma\right) = 0. \quad (426)$$

We will now demonstrate that this equation, which holds necessarily for a solution of the field equation, determines the pressure $p(r)$. (Actually it is always a good idea, when solving Einstein's field equation in matter, to begin with the equation $\nabla^\rho T_{\rho\sigma} = 0$.)

If we express covariant derivatives in terms of partial derivatives, the Euler equation reads

$$\left(\mu + \frac{p}{c^2}\right)U^\rho (\partial_\rho U^\sigma + \Gamma^\sigma_{\rho\nu}U^\nu) + \partial_\tau p \left(g^{\tau\sigma} + \frac{1}{c^2}U^\tau U^\sigma\right) = 0. \quad (427)$$

For $x^\sigma = t, \vartheta, \varphi$, this equation is trivially satisfied. The fourth component, $x^\sigma = r$, however, results in

$$\left(\mu + \frac{p}{c^2}\right)(U^t)^2 \Gamma^r_{tt} + p' g^{rr} = 0.$$

With Γ_{tt}^r from (303) we find

$$\begin{aligned}
\left(\mu + \frac{p}{c^2} \right) e^{\nu-\lambda} \frac{c^2}{2} e^{\nu-\lambda} \nu' + p' e^{\nu-\lambda} &= 0, \quad \left| e^{\nu/2} \right. \\
e^{\nu/2} \frac{\nu'}{2} (\mu c^2 + p) + e^{\nu/2} p' &= 0, \\
\left(e^{\nu/2} (\mu c^2 + p) \right)' &= 0, \\
e^{\nu/2} (\mu c^2 + p) &= B, \\
p(r) &= B e^{-\nu(r)/2} - \mu c^2. \tag{428}
\end{aligned}$$

So the remaining problem is to determine $\nu(r)$ and $\lambda(r)$ from the field equation.

The components of the Ricci tensor for a spherically symmetric and static metric are known, see (304):

$$\begin{aligned}
R_{tt} &= c^2 e^{\nu-\lambda} \left(\frac{\nu''}{2} + \frac{(\nu')^2}{4} - \frac{\lambda' \nu'}{4} + \frac{\nu'}{r} \right), \\
R_{rr} &= -\frac{\nu''}{2} - \frac{(\nu')^2}{4} + \frac{\lambda' \nu'}{4} + \frac{\lambda'}{r}, \\
R_{\vartheta\vartheta} &= \frac{R_{\varphi\varphi}}{\sin^2\vartheta} = 1 - e^{-\lambda} - \frac{r}{2} e^{-\lambda} (\nu' - \lambda'). \tag{429}
\end{aligned}$$

The off-diagonal components of the Ricci tensor are zero. – We now calculate the Ricci scalar:

$$\begin{aligned}
R &= R_{\mu\nu} g^{\mu\nu} = R_{tt} g^{tt} + R_{rr} g^{rr} + R_{\vartheta\vartheta} g^{\vartheta\vartheta} + R_{\varphi\varphi} g^{\varphi\varphi} = \frac{R_{tt}}{g_{tt}} + \frac{R_{rr}}{g_{rr}} + 2 \frac{R_{\vartheta\vartheta}}{g_{\vartheta\vartheta}} \\
&= -\frac{e^{\nu-\lambda}}{c^2} e^{\nu-\lambda} \left(\frac{\nu''}{2} + \frac{(\nu')^2}{4} - \frac{\lambda' \nu'}{4} + \frac{\nu'}{r} \right) + e^{-\lambda} \left(-\frac{\nu''}{2} - \frac{(\nu')^2}{4} + \frac{\lambda' \nu'}{4} + \frac{\lambda'}{r} \right) \\
&+ \frac{2}{r^2} \left(1 - e^{-\lambda} - \frac{r}{2} e^{-\lambda} (\nu' - \lambda') \right) = e^{-\lambda} \left(-\nu'' - \frac{(\nu')^2}{2} + \frac{\lambda' \nu'}{2} + \frac{2(\lambda' - \nu')}{r} - \frac{2}{r^2} \right) + \frac{2}{r^2}.
\end{aligned}$$

This gives us the following non-zero components of the Einstein tensor, i.e., of the left-hand side of the field equation:

$$\begin{aligned}
R_{tt} - \frac{R}{2} g_{tt} &= c^2 e^{\nu-\lambda} \left(\frac{\nu''}{2} + \frac{(\nu')^2}{4} - \frac{\lambda' \nu'}{4} + \frac{\nu'}{r} \right) \\
&+ \frac{c^2}{2} e^{\nu} \left\{ e^{-\lambda} \left(-\cancel{\nu''} - \frac{(\cancel{\nu'})^2}{2} + \frac{\cancel{\lambda'} \cancel{\nu'}}{2} + \frac{2(\lambda' - \nu')}{r} - \frac{2}{r^2} \right) + \frac{2}{r^2} \right\} \\
&= c^2 e^{\nu} \left\{ e^{-\lambda} \left(\frac{\lambda'}{r} - \frac{1}{r^2} \right) + \frac{1}{r^2} \right\},
\end{aligned}$$

$$\begin{aligned}
R_{rr} - \frac{R}{2} g_{rr} &= -\frac{\nu''}{2} - \frac{(\nu')^2}{4} + \frac{\lambda'\nu'}{4} + \frac{\lambda'}{r} \\
-\frac{1}{2} e^\lambda \left\{ e^{-\lambda} \left(-\nu'' - \frac{(\nu')^2}{2} + \frac{\lambda'\nu'}{2} + \frac{2(\lambda' - \nu')}{r} - \frac{2}{r^2} \right) + \frac{2}{r^2} \right\} &= \frac{\nu'}{r} + \frac{1}{r^2} - \frac{e^\lambda}{r^2}, \\
R_{\vartheta\vartheta} - \frac{R}{2} g_{\vartheta\vartheta} &= 1 - e^{-\lambda} - \frac{r}{2} e^{-\lambda} (\nu' - \lambda') - \frac{r^2}{2} \left\{ e^{-\lambda} \left(-\nu'' - \frac{(\nu')^2}{2} + \frac{\lambda'\nu'}{2} + \frac{2(\lambda' - \nu')}{r} - \frac{2}{r^2} \right) + \frac{2}{r^2} \right\} \\
&= \lambda - \cancel{e^\lambda} + e^{-\lambda} \left(-\frac{r\nu'}{2} + \frac{r\lambda'}{2} + \frac{r\nu''}{2} + \frac{r^2(\nu')^2}{4} - \frac{r^2\lambda'\nu'}{4} - r(\lambda' - \nu') + \lambda \right) - \lambda \\
&= r^2 e^{-\lambda} \left(\frac{\nu' - \lambda'}{2r} + \frac{\nu''}{2r} + \frac{(\nu')^2}{4} - \frac{\lambda'\nu'}{4} \right), \\
R_{\varphi\varphi} - \frac{R}{2} g_{\varphi\varphi} &= \sin^2\vartheta \left(R_{\vartheta\vartheta} - \frac{R}{2} g_{\vartheta\vartheta} \right). \tag{430}
\end{aligned}$$

The off-diagonal components of the Einstein tensor are all zero. – We now turn to the right-hand side of the field equation.

$$\begin{aligned}
T_{tt} &= \left(\mu + \frac{p}{c^2} \right) U_t U_t + p g_{tt} = \left(\mu + \frac{p}{c^2} \right) (g_{tt} U^t)^2 + p g_{tt} \\
&= \left(\mu + \frac{p}{c^2} \right) c^4 e^{2\nu} e^{-\nu} - p c^2 e^\nu = \mu c^4 e^\nu, \\
T_{rr} &= \left(\mu + \frac{p}{c^2} \right) U_r U_r + p g_{rr} = p e^\lambda, \\
T_{\vartheta\vartheta} &= \left(\mu + \frac{p}{c^2} \right) U_\vartheta U_\vartheta + p g_{\vartheta\vartheta} = p r^2, \\
T_{\varphi\varphi} &= \left(\mu + \frac{p}{c^2} \right) U_\varphi U_\varphi + p g_{\varphi\varphi} = p r^2 \sin^2\vartheta = T_{\vartheta\vartheta} \sin^2\vartheta. \tag{431}
\end{aligned}$$

Again, all off-diagonal components are zero. So the field equation gives us three independent equations, i.e., the tt -, rr - and $\vartheta\vartheta$ -component:

$$\begin{aligned}
\text{(F1)} \quad \cancel{e^\lambda} \left\{ e^{-\lambda} \left(\frac{\lambda'}{r} - \frac{1}{r^2} \right) + \frac{1}{r^2} \right\} &= \frac{8\pi G}{c^2 \cancel{e^\lambda}} \mu \cancel{e^\lambda} \cancel{e^\lambda}, \\
\text{(F2)} \quad \frac{\nu'}{r} + \frac{1}{r^2} - \frac{e^\lambda}{r^2} &= \frac{8\pi G}{c^4} p e^\lambda, \\
\text{(F3)} \quad \cancel{r^2} e^{-\lambda} \left(\frac{\nu' - \lambda'}{2r} + \frac{\nu''}{2r} + \frac{(\nu')^2}{4} - \frac{\lambda'\nu'}{4} \right) &= \frac{8\pi G}{c^4} p \cancel{r^2}.
\end{aligned}$$

We begin with (F1):

$$\begin{aligned}
e^{-\lambda} \lambda' r - e^{-\lambda} + 1 - \frac{8\pi G}{c^2} \mu r^2 &= 0, \\
\left(-e^{-\lambda} r + r - \frac{8\pi G}{c^2} \mu \frac{r^3}{3} \right)' &= 0, \\
-e^{-\lambda} r + r - \frac{8\pi G}{c^2} \mu \frac{r^3}{3} &= C.
\end{aligned} \tag{432}$$

The metric should be regular everywhere inside the star, in particular at $r = 0$. As this requires $e^{-\lambda(0)}$ to be finite, evaluating (432) at $r = 0$ gives $C = 0$, hence

$$e^{-\lambda(r)} = 1 - \frac{8\pi G}{3c^2} \mu r^2. \tag{433}$$

So the remaining task is to determine $\nu(r)$. We turn to (F2):

$$e^{-\lambda} \left(\frac{\nu'}{r} + \frac{1}{r^2} \right) - \frac{1}{r^2} - \frac{8\pi G}{c^4} p = 0.$$

We insert our earlier results for $p(r)$ and $e^{-\lambda(r)}$, i.e., eqs. (428) and (433):

$$\begin{aligned}
\left(1 - \frac{8\pi G}{3c^2} \mu r^2 \right) \left(\frac{\nu'}{r} + \frac{1}{r^2} \right) - \frac{1}{r^2} - \frac{8\pi G}{c^4} \left(B e^{-\nu/2} - \mu c^2 \right) &= 0, \\
\left(1 - \frac{8\pi G}{3c^2} \mu r^2 \right) \frac{\nu'}{r} + \cancel{\frac{1}{r^2}} - \frac{8\pi G}{3c^2} \mu - \cancel{\frac{1}{r^2}} - \frac{8\pi G}{c^4} B e^{-\nu/2} + \frac{8\pi G}{c^2} \mu &= 0, \\
\left(1 - \frac{8\pi G}{3c^2} \mu r^2 \right) \frac{\nu'}{r} + \frac{2}{3} \frac{8\pi G}{c^2} \mu - \frac{8\pi G}{c^4} B e^{-\nu/2} &= 0, \quad \left| \frac{r e^{\nu/2}}{2 \sqrt{1 - \frac{8\pi G}{3c^2} \mu r^2}} \right|^3 \\
\frac{e^{\nu/2} \nu'}{2 \sqrt{1 - \frac{8\pi G}{3c^2} \mu r^2}} + \frac{8\pi G \mu r e^{\nu/2}}{3c^2 \sqrt{1 - \frac{8\pi G}{3c^2} \mu r^2}^3} - \frac{8\pi G B r}{2c^4 \sqrt{1 - \frac{8\pi G}{3c^2} \mu r^2}^3} &= 0, \\
\left(\frac{e^{\nu/2}}{\sqrt{1 - \frac{8\pi G}{3c^2} \mu r^2}} - \frac{3B}{2\mu c^2 \sqrt{1 - \frac{8\pi G}{3c^2} \mu r^2}} \right)' &= 0, \\
\frac{e^{\nu/2}}{\sqrt{1 - \frac{8\pi G}{3c^2} \mu r^2}} - \frac{3B}{2\mu c^2 \sqrt{1 - \frac{8\pi G}{3c^2} \mu r^2}} &= -D, \\
e^{\nu(r)/2} &= \frac{3B}{2\mu c^2} - D \sqrt{1 - \frac{8\pi G}{3c^2} \mu r^2}.
\end{aligned}$$

We have thus determined the unknown metric functions

$$e^{\nu(r)/2} = \frac{3B}{2\mu c^2} - D \sqrt{1 - \frac{8\pi G}{3c^2} \mu r^2}, \quad e^{-\lambda(r)} = 1 - \frac{8\pi G}{3c^2} \mu r^2, \quad (434)$$

and the pressure

$$\begin{aligned} p(r) &= B e^{-\nu(r)/2} - \mu c^2 = \frac{B - \mu c^2 e^{\nu(r)/2}}{e^{\nu(r)/2}} \\ &= \mu c^2 \frac{\left(-B + 2D \mu c^2 \sqrt{1 - \frac{8\pi G}{3c^2} \mu r^2} \right)}{\left(3B - 2D \mu c^2 \sqrt{1 - \frac{8\pi G}{3c^2} \mu r^2} \right)}. \end{aligned} \quad (435)$$

It can be checked that (F3) gives no further information. The general solution involves three constants μ , B and D which remain undetermined by the field equation.

To have a viable star model, our interior Schwarzschild solution should be matched, at the surface of the star $r = r_*$, to an (exterior, vacuum) Schwarzschild metric with mass M ,

$$e^{\nu(r)} = e^{-\lambda(r)} = 1 - \frac{2GM}{c^2 r}, \quad r_* < r < \infty.$$

We will now show that this allows to express the three constants μ , B and D in terms of r_* and M . The matching conditions (or *junction conditions*) can be derived from the field equation, in a similar fashion as the junction conditions for electromagnetic fields can be derived from Maxwell's equations. We will not derive the general junction conditions here. For the case at hand, they can be motivated directly: An obvious condition is that the metric coefficients must be continuous at $r = r_*$, because otherwise the Christoffel symbols would have Dirac-delta-like singularities which would result in a jump of the geodesics (freely falling particles and light rays) when they pass through the surface of the star. A second condition is that the pressure must go to zero if $r = r_*$ is approached from the inside, because otherwise the star would expand and could not be static. So we have the following junction conditions:

$$(J1) \quad e^{\nu/2} \text{ continuous at } r = r_*: \quad \frac{3B}{2\mu c^2} - D \sqrt{1 - \frac{8\pi G}{3c^2} \mu r_*^2} = \sqrt{1 - \frac{2GM}{c^2 r_*}},$$

$$(J2) \quad e^{-\lambda} \text{ continuous at } r = r_*: \quad 1 - \frac{8\pi G}{3c^2} \mu r_*^2 = 1 - \frac{2GM}{c^2 r_*},$$

$$(J3) \quad p = 0 \text{ at } r = r_*: \quad B = 2D \mu c^2 \sqrt{1 - \frac{8\pi G}{3c^2} \mu r_*^2}.$$

Condition (J2) immediately allows us to express μ in terms of M and r_* :

$$\frac{4}{3} \pi r_*^3 \mu = M. \quad (436)$$

At first sight, this equation seems to be obvious: The total mass of the star is its (constant) mass density multiplied with its volume. Actually, this result is far from obvious: M was defined asymptotically, by comparison with the Newtonian theory, not as an integral over the

mass density. Moreover, we are in a curved geometry, so there is no reason why the Euclidean formula for the volume of a sphere should hold. In fact, it is kind of mystery that this simple formula for μ is true.

Inserting this result into (J1) and (J3) gives:

$$B = \frac{2(D+1)}{3} \mu c^2 \sqrt{1 - \frac{2GM}{c^2 r_*}} ,$$

$$B = 2D \mu c^2 \sqrt{1 - \frac{2GM}{c^2 r_*}} ,$$

hence

$$D = \frac{1}{2} , \quad B = \frac{3 M c^2}{4\pi r_*^3} \sqrt{1 - \frac{2GM}{c^2 r_*}} . \quad (437)$$

We have thus determined the three constants μ , D and B in terms of r_* and M . Finally, we insert these values into the expressions for $\nu(r)$, $\lambda(r)$ and get the interior Schwarzschild solution in comprehensive form:

$$e^{\nu(r)/2} = \frac{1}{2} \left(3 \sqrt{1 - \frac{r_S}{r_*}} - \sqrt{1 - \frac{r_S r^2}{r_*^3}} \right) , \quad e^{-\lambda(r)} = 1 - \frac{r_S r^2}{r_*^3} , \quad (438)$$

where $r_S = 2GM/c^2$ is the Schwarzschild radius. The pressure is

$$p(r) = \frac{3c^4 r_S}{8\pi G r_*^3} \frac{\left(-\sqrt{1 - \frac{r_S}{r_*}} + \sqrt{1 - \frac{r_S r^2}{r_*^3}} \right)}{\left(3 \sqrt{1 - \frac{r_S}{r_*}} - \sqrt{1 - \frac{r_S r^2}{r_*^3}} \right)} . \quad (439)$$

Clearly, we must have $r_* > r_S$ because otherwise the pressure is not real. This should not come as a surprise: We know already that a star with $r_* < r_S$ cannot be static but collapses in a finite proper time interval into a singularity.

However, for a physically reasonable solution, we should also require that the pressure is finite and non-negative everywhere inside the star. From

$$p(0) = \frac{3c^4 r_S}{8\pi G r_*^3} \frac{\left(-\sqrt{1 - \frac{r_S}{r_*}} + 1 \right)}{\left(3 \sqrt{1 - \frac{r_S}{r_*}} - 1 \right)} \quad (440)$$

we read that this requires

$$3 \sqrt{1 - \frac{r_S}{r_*}} > 1 .$$

After squaring both sides, this condition can be rewritten as

$$r_* > \frac{9}{8} r_S . \quad (441)$$

So the radius of the star cannot be arbitrarily close to the Schwarzschild radius, it is bounded away by a factor of 9/8. This is known as the *Buchdahl limit*. We will discuss the r dependence of the pressure inside the star and the Buchdahl limit in Worksheet 12.

We have derived the Buchdahl limit here for an incompressible perfect fluid model only, $\mu = \text{constant}$. Actually, Hans Buchdahl has shown in 1959 that this limit holds for all perfect fluid models provided that the mass density is monotonically non-increasing from the centre to the surface, $d\mu/dr \leq 0$.

A star with a radius that lies between the Schwarzschild radius and the radius of the photon sphere, $2m < r_* < 3m$ in units of $m = GM/c^2$, is called *ultracompact*. If ultracompact stars may exist in Nature is a matter of debate.

7 Gravitational waves

In 1916 Einstein predicted the existence of gravitational waves, based on his linearised vacuum field equation. In 1918 he derived his famous quadrupole formula which relates emitted gravitational waves to the quadrupole moment of the source. Since the 1920s, a number of wave-like exact solutions to the (full non-linear) vacuum Einstein equation were found.

In this chapter we will derive the most important properties of gravitational waves on the basis of the *linearised* Einstein theory. As a consequence, the results are true only for gravitational waves whose amplitudes are small. We will see that, to within this approximation, the theory of gravitational waves is very similar to the theory of electromagnetic waves. On the basis of this simplified theory we will understand how gravitational wave detectors work, in particular the interferometric detectors that have actually successfully detected the first gravitational wave signal in September 2015, and many more since then.

7.1 The linearisation of Einstein's field equation

We consider a metric that takes, in an appropriate coordinate system, the form

$$g_{\mu\nu} = \eta_{\mu\nu} + h_{\mu\nu} . \quad (442)$$

In the following we will linearise Einstein's field equation with respect to the $h_{\mu\nu}$ and their derivatives. This gives a valid approximation of Einstein's theory of gravity if the $h_{\mu\nu}$ and their derivatives are small, i.e., if the spacetime is very close to the spacetime of special relativity. We say that a quantity is small of first order if quadratic and higher-order terms in this quantity and its derivatives can be neglected.

Our assumptions fix the coordinate system up to transformations of the form

$$x^\mu \mapsto \tilde{x}^\mu = a^\mu + \Lambda^\mu{}_\nu x^\nu + f^\mu(x) \quad (443)$$

where $(\Lambda^\mu{}_\nu)$ is a Lorentz transformation, $\Lambda^\mu{}_\nu \Lambda^\rho{}_\sigma \eta_{\mu\rho} = \eta_{\nu\sigma}$, and the f^μ are small of first order.

We agree that, in this chapter, greek indices are lowered and raised with $\eta_{\mu\nu}$ and $\eta^{\mu\nu}$, respectively. As an abbreviation, we write

$$h := h_{\mu\nu} \eta^{\mu\nu} = h_\mu{}^\mu = h^\nu{}_\nu . \quad (444)$$

Then the inverse metric is of the form

$$g^{\nu\rho} = \eta^{\nu\rho} - h^{\nu\rho} . \quad (445)$$

Proof: $(\eta_{\mu\nu} + h_{\mu\nu})(\eta^{\nu\rho} - h^{\nu\rho}) = \eta_{\mu\nu}\eta^{\nu\rho} + h_{\mu\nu}\eta^{\nu\rho} - \eta_{\mu\nu}h^{\nu\rho} + \dots = \delta_\mu^\rho + h_\mu{}^\rho - h_\mu{}^\rho = \delta_\mu^\rho$, where the ellipses stand for a quadratic term that is to be neglected, according to our assumptions. \square

We will now derive the linearised field equation. As a first step, we have to calculate the Christoffel symbols. We find

$$\Gamma^\rho{}_{\mu\nu} = \frac{1}{2} g^{\rho\sigma} (\partial_\mu g_{\sigma\nu} + \partial_\nu g_{\sigma\mu} - \partial_\sigma g_{\mu\nu}) = \frac{1}{2} \eta^{\rho\sigma} (\partial_\mu h_{\sigma\nu} + \partial_\nu h_{\sigma\mu} - \partial_\sigma h_{\mu\nu}) + \dots \quad (446)$$

Thereupon, we can calculate the components of the Ricci tensor:

$$\begin{aligned} R_{\mu\nu} &= \partial_\mu \Gamma^\rho{}_{\rho\nu} - \partial_\rho \Gamma^\rho{}_{\mu\nu} + \dots = \\ &= \frac{1}{2} \eta^{\rho\sigma} \partial_\mu (\partial_\rho h_{\sigma\nu} + \partial_\nu h_{\sigma\rho} - \partial_\sigma h_{\rho\nu}) - \frac{1}{2} \eta^{\rho\sigma} \partial_\rho (\partial_\mu h_{\sigma\nu} + \partial_\nu h_{\sigma\mu} - \partial_\sigma h_{\mu\nu}) = \\ &= \frac{1}{2} (\partial_\mu \partial_\nu h - \partial_\mu \partial^\rho h_{\rho\nu} - \partial^\sigma \partial_\nu h_{\sigma\mu} + \square h_{\mu\nu}) . \end{aligned} \quad (447)$$

Here, \square denotes the wave operator (d'Alembert operator) that is formed with the Minkowski metric,

$$\square = \eta^{\mu\nu} \partial_\mu \partial_\nu = \partial^\nu \partial_\nu = -\partial_0^2 + \delta^{ij} \partial_i \partial_j = -\frac{1}{c^2} \partial_t^2 + \Delta . \quad (448)$$

From (447) we can calculate the scalar curvature:

$$\begin{aligned} R &= g^{\mu\nu} R_{\mu\nu} = \eta^{\mu\nu} R_{\mu\nu} + \dots = \frac{1}{2} \eta^{\mu\nu} (\partial_\mu \partial_\nu h - \partial_\mu \partial^\rho h_{\rho\nu} - \partial^\sigma \partial_\nu h_{\sigma\mu} + \square h_{\mu\nu}) \\ &= \frac{1}{2} (\square h - \partial^\nu \partial^\rho h_{\rho\nu} - \partial^\sigma \partial^\mu h_{\sigma\mu} + \square h) = \square h - \partial^\sigma \partial^\mu h_{\sigma\mu} . \end{aligned} \quad (449)$$

Hence, the linearised version of Einstein's field equation (without a cosmological constant)

$$2 R_{\mu\nu} - R g_{\mu\nu} = 2 \kappa T_{\mu\nu} , \quad \kappa = \frac{8\pi G}{c^4} \quad (450)$$

reads

$$\partial_\mu \partial_\nu h - \partial_\mu \partial^\rho h_{\rho\nu} - \partial^\sigma \partial_\nu h_{\sigma\mu} + \square h_{\mu\nu} - \eta_{\mu\nu} (\square h - \partial^\sigma \partial^\tau h_{\sigma\tau}) = 2 \kappa T_{\mu\nu} . \quad (451)$$

This is a system of linear partial differential equations of second order for the $h_{\mu\nu}$. It can be rewritten in a more convenient form after substituting for $h_{\mu\nu}$ the quantity

$$\gamma_{\mu\nu} = h_{\mu\nu} - \frac{h}{2} \eta_{\mu\nu} . \quad (452)$$

As the relation between $h_{\mu\nu}$ and $\gamma_{\mu\nu}$ is linear, the $h_{\mu\nu}$ are small of first order if and only if the $\gamma_{\mu\nu}$ are small of first order. In order to express the $h_{\mu\nu}$ in terms of the $\gamma_{\mu\nu}$, we calculate the trace,

$$\gamma := \eta^{\mu\nu} \gamma_{\mu\nu} = h - \frac{1}{2} 4 h = -h , \quad (453)$$

$$h_{\mu\nu} = \gamma_{\mu\nu} - \frac{\gamma}{2} \eta_{\mu\nu} . \quad (454)$$

Upon inserting this expression into the linearised field equation (451), we find

$$\begin{aligned} & -\cancel{\partial_\mu \partial_\nu \gamma} - \partial_\mu \partial^\rho \gamma_{\rho\nu} + \cancel{\frac{1}{2} \eta_{\rho\nu} \partial_\mu \partial^\rho \gamma} - \partial^\sigma \partial_\nu \gamma_{\sigma\mu} + \cancel{\frac{1}{2} \eta_{\sigma\mu} \partial^\sigma \partial_\nu \gamma} + \\ & + \square \gamma_{\mu\nu} - \cancel{\frac{1}{2} \eta_{\mu\nu} \square \gamma} - \eta_{\mu\nu} (-\cancel{\square \gamma} - \partial^\sigma \partial^\tau \gamma_{\sigma\tau} + \cancel{\frac{1}{2} \eta_{\sigma\tau} \partial^\sigma \partial^\tau \gamma}) = 2 \kappa T_{\mu\nu} , \end{aligned} \quad (455)$$

$$\square \gamma_{\mu\nu} - \partial_\mu \partial^\rho \gamma_{\rho\nu} - \partial_\nu \partial^\rho \gamma_{\rho\mu} + \eta_{\mu\nu} \partial^\sigma \partial^\tau \gamma_{\sigma\tau} = 2 \kappa T_{\mu\nu} . \quad (456)$$

This equation can be simplified further by a coordinate transformation (443) with $a^\mu = 0$ and $\Lambda^\mu{}_\nu = \delta^\mu_\nu$,

$$x^\mu \mapsto x^\mu + f^\mu(x) \quad (457)$$

where the f^μ are small of first order. For such a coordinate transformation, we have obviously

$$dx^\mu \mapsto dx^\mu + \partial_\rho f^\mu dx^\rho \quad (458)$$

and thus

$$\partial_\sigma \mapsto \partial_\sigma - \partial_\sigma f^\tau \partial_\tau . \quad (459)$$

Proof: $(dx^\mu + \partial_\rho f^\mu dx^\rho) (\partial_\sigma - \partial_\sigma f^\tau \partial_\tau) = dx^\mu (\partial_\sigma) + \partial_\rho f^\mu dx^\rho (\partial_\sigma) - \partial_\sigma f^\tau dx^\mu (\partial_\tau) + \dots = \delta^\mu_\sigma + \cancel{\partial_\rho f^\mu \delta^\rho_\sigma} - \cancel{\partial_\sigma f^\tau \delta^\mu_\tau}$. \square

With the help of these equations, we can now calculate how the $g_{\mu\nu}$, the $h_{\mu\nu}$, and the $\gamma_{\mu\nu}$ behave under such a coordinate transformation:

$$g_{\mu\nu} = g(\partial_\mu, \partial_\nu) \mapsto g(\partial_\mu - \partial_\mu f^\tau \partial_\tau, \partial_\nu - \partial_\nu f^\sigma \partial_\sigma) = g_{\mu\nu} - \partial_\mu f^\tau g_{\tau\nu} - \partial_\nu f^\sigma g_{\mu\sigma} , \quad (460)$$

$$h_{\mu\nu} = g_{\mu\nu} - \eta_{\mu\nu} \mapsto g_{\mu\nu} - \partial_\mu f^\tau g_{\tau\nu} - \partial_\nu f^\sigma g_{\mu\sigma} - \eta_{\mu\nu} = h_{\mu\nu} - \partial_\mu f^\tau \eta_{\tau\nu} - \partial_\nu f^\sigma \eta_{\mu\sigma} + \dots , \quad (461)$$

$$\gamma_{\mu\nu} = h_{\mu\nu} - \frac{1}{2} \eta_{\mu\nu} h \mapsto h_{\mu\nu} - \partial_\mu f^\tau \eta_{\tau\nu} - \partial_\nu f^\sigma \eta_{\mu\sigma} - \frac{1}{2} \eta_{\mu\nu} (h - 2 \partial_\tau f^\tau) = \gamma_{\mu\nu} - \partial_\mu f^\tau \eta_{\tau\nu} - \partial_\nu f^\sigma \eta_{\mu\sigma} + \eta_{\mu\nu} \partial_\tau f^\tau . \quad (462)$$

For the divergence of $\gamma_{\mu\nu}$, which occurs three times in (456), this gives the following transformation behaviour:

$$\partial^\mu \gamma_{\mu\nu} \mapsto \partial^\mu \gamma_{\mu\nu} - \partial^\mu \partial_\mu f_\nu - \cancel{\partial^\mu \partial_\nu f_\mu} + \cancel{\eta_{\mu\nu} \partial^\mu \partial_\tau f^\tau} = \partial^\mu \gamma_{\mu\nu} - \square f_\nu . \quad (463)$$

This shows that, if it is possible to choose the f_ν such that

$$\square f_\nu = \partial^\mu \gamma_{\mu\nu} , \quad (464)$$

then $\partial^\mu \gamma_{\mu\nu}$ is transformed to zero. Such a choice is, indeed, possible as the wave equation on Minkowski spacetime,

$$\square f_\nu = \Phi_\nu , \quad (465)$$

has solutions for any (sufficiently regular) function Φ_ν : If Φ_ν is compactly supported or falls off sufficiently fast, a solution is provided by the retarded potentials, see below. In any case, a solution can be found by prescribing e.g. initial values $f_\nu = 0$ and $\partial_0 f_\nu = 0$ on a hypersurface $x^0 = \text{constant}$ and then solving the Cauchy problem for the inhomogeneous wave equation (465); the fact that such a solution exists (and is even unique) is a consequence of the so-called *Duhamel Principle*.

We have thus shown that, by an appropriate coordinate transformation, we can put the linearised field equation (456) into the following form:

$$\square \gamma_{\mu\nu} = 2\kappa T_{\mu\nu} . \quad (466)$$

Now the $\gamma_{\mu\nu}$ have to satisfy the additional condition

$$\partial^\mu \gamma_{\mu\nu} = 0 \quad (467)$$

which is known as the *Hilbert gauge*. The transformation of $\gamma_{\mu\nu}$ under a change of coordinates is analogous to a gauge transformation of the four-potential A_μ in electrodynamics. Even after imposing the Hilbert gauge condition, there is still the freedom to make coordinate transformations (443) with $\square f^\mu = 0$. In particular, the theory is invariant under Lorentz transformations.

The linearised Einstein theory is a Lorentz invariant theory of the gravitational field on Minkowski spacetime. It is very similar to Maxwell's vacuum electrodynamics, which is a (linear) Lorentz invariant theory of electromagnetic fields on Minkowski spacetime. The table illustrates the analogy. Here “electrodynamics” stands for “electrodynamics on Minkowski spacetime in vacuum, $G_{\mu\nu} = \mu_0^{-1} F_{\mu\nu}$ ”. Roughly speaking, the main difference is in the fact that the gravitational equations have one index more.

lin. Einstein theory	electrodynamics
$\gamma_{\mu\nu}$	A_μ
$T_{\mu\nu}$	J_μ
Hilbert gauge $\partial^\mu \gamma_{\mu\nu} = 0$	Lorenz gauge $\partial^\mu A_\mu = 0$
$\square \gamma_{\mu\nu} = 2\kappa T_{\mu\nu}$	$\square A_\mu = \mu_0^{-1} J_\mu$

Of course, one has to keep in mind that the linearised Einstein theory is only an approximation; an *exact* Lorentz invariant theory of gravity on Minkowski spacetime cannot be formulated, as we have discussed in Chapter 3.

The linearised Einstein theory has been used as the starting point for developing a quantum theory of gravitation, in analogy to quantum electrodynamics which is the fairly well understood quantised version of Maxwell's electrodynamics on Minkowski spacetime. While the quanta associated with the field A_μ are called *photons*, the quanta associated with the field $\gamma_{\mu\nu}$ (or $h_{\mu\nu}$) are called *gravitons*. The fact that A_μ is a tensor field of rank one while $\gamma_{\mu\nu}$ is a tensor field of rank two has the consequence that photons have spin one while gravitons have spin two. Apart from the fact that it is far from clear if quantising the *linearised* theory is a reasonable way of quantising gravity, one encounters technical problems related to the fact that the coupling constant of gravity has a dimension (whereas in the electromagnetic case we have the dimensionless fine structure constant).

Here we are interested only in the classical aspects of the linearised Einstein theory. In the next section we discuss wavelike solutions to the source-free linearised field equation.

7.2 Plane-harmonic-wave solutions to the linearised field equation without sources

In this section we consider the linearised field equation without sources (i.e., in regions where $T_{\mu\nu} = 0$) in the Hilbert gauge,

$$\square \gamma_{\mu\nu} = 0, \quad \partial^\mu \gamma_{\mu\nu} = 0. \quad (468)$$

In analogy to the electrodynamical theory, we can write the general solution as a superposition of plane harmonic waves. In our case, any such plane harmonic wave is of the form

$$\gamma_{\mu\nu}(x) = \text{Re}\{A_{\mu\nu}e^{ik_\rho x^\rho}\} \quad (469)$$

with a real wave covector k_ρ and a complex amplitude $A_{\mu\nu} = A_{\nu\mu}$.

Such a plane harmonic wave satisfies the linearised vacuum field equation if and only if

$$0 = \eta^{\sigma\tau} \partial_\sigma \partial_\tau \gamma_{\mu\nu}(x) = \text{Re}\{\eta^{\sigma\tau} A_{\mu\nu} i k_\sigma i k_\tau e^{ik_\rho x^\rho}\}. \quad (470)$$

This holds for all x , with $(A_{\mu\nu}) \neq (0)$, if and only if

$$\eta^{\sigma\tau} k_\sigma k_\tau = 0. \quad (471)$$

In other words, (k_0, k_1, k_2, k_3) has to be a lightlike covector with respect to the Minkowski metric. This result can be interpreted as saying that, to within the linearised Einstein theory, gravitational waves propagate on Minkowski spacetime at the speed c , just as electromagnetic waves in vacuum.

Our plane harmonic wave satisfies the Hilbert gauge condition if and only if

$$0 = \eta^{\mu\tau} \partial_\tau \gamma_{\mu\nu}(x) = \text{Re}\{\eta^{\mu\tau} A_{\mu\nu} i k_\tau e^{ik_\rho x^\rho}\} \quad (472)$$

which is true, for all $x = (x^0, x^1, x^2, x^3)$, if and only if

$$k^\mu A_{\mu\nu} = 0. \quad (473)$$

For a given k_μ , the Hilbert gauge condition restricts the possible values of the amplitude $A_{\mu\nu}$, i.e., it restricts the possible polarisation states of the gravitational wave. For electromagnetic waves, it is well known that there are two polarisation states (“left-handed and right-handed”, or “linear in x -direction and linear in y -direction”) from which all possible polarisation states can be formed by way of superposition. We will see that also for gravitational waves there are two independent polarisation states; however, they are of a different geometric nature which has its origin in the fact that $\gamma_{\mu\nu}$ has two indices while the electromagnetic four-potential A_μ has only one.

In order to find all possible polarisation states of a gravitational wave, we begin by counting the independent components of the amplitude: The $A_{\mu\nu}$ form a (4×4) -matrix which has 16 entries. As $A_{\mu\nu} = A_{\nu\mu}$, only 10 of them are independent; the Hilbert gauge condition (467) consists of 4 scalar equations, so one might think that there are 6 independent components and thus six independent polarisation states. This, however, is wrong. The reason is that we can impose additional conditions onto the amplitudes, even after the Hilbert gauge has been chosen: The Hilbert gauge condition is preserved if we make a coordinate transformation of the form

$$x^\mu \mapsto x^\mu + f^\mu(x) \quad \text{with} \quad \square f^\mu = 0. \quad (474)$$

We can use this freedom to impose additional conditions onto the amplitudes $A_{\mu\nu}$.

Claim: Assume we have a plane-harmonic-wave solution

$$\gamma_{\mu\nu}(x) = \text{Re}\{A_{\mu\nu}e^{ik_\rho x^\rho}\}$$

of the linearised vacuum field equation in the Hilbert gauge. Let (u^μ) be a constant four-velocity vector, $\eta_{\mu\nu}u^\mu u^\nu = -c^2$. Then we can make a coordinate transformation such that the Hilbert gauge condition is preserved and such that

$$u^\mu A_{\mu\nu} = 0, \quad (475)$$

$$\eta^{\mu\nu} A_{\mu\nu} = 0, \quad (476)$$

in the new coordinates (TT *gauge*, *transverse-traceless gauge*).

Proof: We perform a coordinate transformation

$$x^\mu \mapsto x^\mu + f^\mu(x), \quad f^\mu(x) = \text{Re}\{i C^\mu e^{ik_\rho x^\rho}\}$$

with the wave covector (k_ρ) from our plane harmonic wave solution and with some complex coefficients C^μ . Then we have $\square f^\mu = 0$, i.e., the Hilbert gauge condition is satisfied in the new coordinates as well. We want to choose the C^μ such that in the new coordinates (475) and (476) hold true. As a first step, we calculate how the amplitudes $A_{\mu\nu}$ transform. We start out from the transformation behaviour of the $\gamma_{\mu\nu}$ which was calculated above,

$$\gamma_{\mu\nu} \mapsto \gamma_{\mu\nu} - \partial_\mu f_\nu - \partial_\nu f_\mu + \eta_{\mu\nu} \partial_\rho f^\rho,$$

hence

$$\text{Re}\{A_{\mu\nu}e^{ik_\rho x^\rho}\} \mapsto \text{Re}\{(A_{\mu\nu} - i i k_\mu C_\nu - i i k_\nu C_\mu + \eta_{\mu\nu} i i k_\rho C^\rho) e^{ik_\rho x^\rho}\},$$

$$A_{\mu\nu} \mapsto A_{\mu\nu} + k_\mu C_\nu + k_\nu C_\mu - \eta_{\mu\nu} k_\rho C^\rho.$$

We want to choose the C_μ such that the equations (475) and (476) hold,

$$0 = u^\mu (A_{\mu\nu} + k_\mu C_\nu + k_\nu C_\mu - \eta_{\mu\nu} k_\rho C^\rho) , \quad (\text{T1})$$

$$0 = \eta^{\mu\nu} (A_{\mu\nu} + k_\mu C_\nu + k_\nu C_\mu - \eta_{\mu\nu} k_\rho C^\rho) = \eta^{\mu\nu} A_{\mu\nu} - 2 k_\rho C^\rho . \quad (\text{T2})$$

To demonstrate that such a choice is possible, we choose the coordinates such that

$$(u^\mu) = \begin{pmatrix} c \\ 0 \\ 0 \\ 0 \end{pmatrix} .$$

This can be done by a Lorentz transformation which, as a linear coordinate transformation, preserves all the relevant properties of the coordinate system. Then the spatial part of the desired condition (T1) reads:

$$(\text{T1}) \text{ for } \nu = j : \quad 0 = A_{0j} + k_0 C_j + k_j C_0 \quad \Longleftrightarrow \quad C_j = -k_0^{-1} (A_{0j} + k_j C_0) .$$

These equations show that the C_j are determined by C_0 . We have thus to show that C_0 can be determined such that the temporal part of (T1) and condition (T2) hold:

$$(\text{T1}) \text{ for } \nu = 0 : \quad 0 = A_{00} + 2 k_0 C_0 + \eta^{\rho\sigma} k_\rho C_\sigma = A_{00} + 2 k_0 C_0 - \cancel{k_0 C_0} + \eta^{ij} k_i C_j$$

$$= A_{00} + k_0 C_0 - \eta^{ij} k_i k_0^{-1} (A_{0j} + k_j C_0) = A_{00} + k_0 C_0 - \eta^{ij} k_i k_0^{-1} A_{0j} + \eta^{00} k_0 \cancel{k_0^{-1} C_0}$$

$$\Longleftrightarrow \quad 0 = -k_0 A_{00} + \eta^{ij} k_i A_{0j} = \eta^{\mu\nu} k_\mu A_{0\nu} .$$

The last expression vanishes, because of the Hilbert gauge condition (473) that is satisfied by assumption, so the $\nu = 0$ component of (475) is identically satisfied if the C^j are chosen as required by the $\nu = j$ components of (475). This leaves C_0 arbitrary. We now turn to the second desired condition (476).

$$(\text{T2}) : \quad 0 = \eta^{\mu\nu} A_{\mu\nu} + 2 k_0 C_0 - 2 \eta^{ij} k_i C_j = A_\mu{}^\mu + 2 k_0 C_0 + 2 \eta^{ij} k_i k_0^{-1} (A_{0j} + k_j C_0)$$

$$= A_\mu{}^\mu + 2 k_0 C_0 + 2 \eta^{ij} k_i k_0^{-1} A_{0j} - 2 \eta^{00} k_0 \cancel{k_0^{-1} C_0} = A_\mu{}^\mu + 4 k_0 C_0 + 2 \eta^{ij} k_i k_0^{-1} A_{0j}$$

$$\Longleftrightarrow \quad C_0 = \frac{-A_\mu{}^\mu k_0 - 2 \eta^{ij} k_i A_{0j}}{4 k_0^2} .$$

If we choose C_0 according to this equation, and then the C_j as required above, (475) and (476) are indeed satisfied in the new coordinates. \square

In the TT gauge we have $\gamma = 0$ and thus $h_{\mu\nu} = \gamma_{\mu\nu}$. As a consequence, the metric is of the form

$$g_{\mu\nu} = \eta_{\mu\nu} + \gamma_{\mu\nu}, \quad \gamma_{\mu\nu} = \text{Re}\{A_{\mu\nu}e^{ik_\rho x^\rho}\} \quad (477)$$

and the amplitudes are restricted by the conditions

$$k^\mu A_{\mu\nu} = 0, \quad u^\mu A_{\mu\nu} = 0, \quad \eta^{\mu\nu} A_{\mu\nu} = 0. \quad (478)$$

If we choose the coordinates such that

$$(u^\mu) = \begin{pmatrix} c \\ 0 \\ 0 \\ 0 \end{pmatrix}, \quad (k^\rho) = \begin{pmatrix} \omega/c \\ 0 \\ 0 \\ \omega/c \end{pmatrix} \quad (479)$$

which can be reached by a Lorentz transformation, equations (473), (475) and (476) read, respectively,

$$0 = k^\mu A_{\mu\nu} = \frac{\omega}{c} (A_{0\nu} + A_{3\nu}), \quad (480)$$

$$0 = u^\mu A_{\mu\nu} = c A_{0\nu}, \quad (481)$$

$$0 = \eta^{\mu\nu} A_{\mu\nu} = -A_{00} + A_{11} + A_{22} + A_{33} \quad (482)$$

in the TT gauge. The first two conditions together imply that $A_{0\nu} = 0$ and $A_{3\nu} = 0$ for all ν . The last condition then requires $A_{22} = -A_{11}$ and the symmetry of the metric requires $A_{12} = A_{21}$. So in this representation there are only two non-zero (complex!) components of $A_{\mu\nu}$,

$$A_{11} = -A_{22} =: A_+ = |A_+|e^{i\varphi}, \quad A_{12} = A_{21} =: A_\times = |A_\times|e^{i\psi}. \quad (483)$$

The fact that only the 1- and the 2-components are non-zero demonstrates that gravitational waves are *transverse*. There are only two independent polarisation states, the *plus mode* (+) and the *cross mode* (\times).

For the physical interpretation of these two modes we need the following result.

Claim: The x^0 -lines, i.e. the worldlines $x^\mu(\tau)$ with $\dot{x}^\mu(\tau) = u^\mu$, are geodesics.

Proof: From $\dot{x}^\mu(\tau) = u^\mu$ we find $\ddot{x}^\mu(\tau) = 0$. The Christoffel symbols read

$$\begin{aligned} \Gamma^\mu_{\nu\sigma} &= \frac{1}{2} g^{\mu\tau} (\partial_\nu g_{\tau\sigma} + \partial_\sigma g_{\tau\nu} - \partial_\tau g_{\nu\sigma}) = \frac{1}{2} \eta^{\mu\tau} (\partial_\nu \gamma_{\tau\sigma} + \partial_\sigma \gamma_{\tau\nu} - \partial_\tau \gamma_{\nu\sigma}) = \\ &= \frac{1}{2} \eta^{\mu\tau} \text{Re}\{ (i k_\nu A_{\tau\sigma} + i k_\sigma A_{\tau\nu} - i k_\tau A_{\nu\sigma}) e^{ik_\rho x^\rho} \}. \end{aligned}$$

This implies that

$$\begin{aligned} &\ddot{x}^\mu + \Gamma^\mu_{\nu\sigma} \dot{x}^\nu \dot{x}^\sigma = \\ &= 0 + \frac{1}{2} \eta^{\mu\tau} \text{Re}\{ (i k_\nu \underbrace{A_{\tau\sigma}}_{=0} u^\sigma u^\nu + i k_\sigma \underbrace{A_{\tau\nu}}_{=0} u^\nu u^\sigma - i k_\tau \underbrace{A_{\nu\sigma}}_{=0} u^\sigma u^\nu) e^{ik_\rho x^\rho} \} = 0. \end{aligned} \quad \square$$

In other words, the x^0 -lines are the worldlines of freely falling particles. For any such particle the (x^1, x^2, x^3) -coordinates remain constant. This does, of course, *not* mean that the gravitational wave has no effect on freely falling particles. The distance, as it is measured with the metric, between neighbouring x^0 -lines is not at all constant. We calculate the square of the distance between an x^0 -line at the spatial origin $(0, 0, 0)$ and at spatial (x^1, x^2, x^3) for the case that the x^i are so small that the metric can be viewed as constant between $(x^0, 0, 0, 0)$ and (x^0, x^1, x^2, x^3) :

$$\begin{aligned} g_{ij}(x^0, 0, 0, 0) x^i x^j \\ = \left(\delta_{ij} + \gamma_{ij}(x^0, 0, 0, 0) \right) x^i x^j . \end{aligned} \quad (484)$$

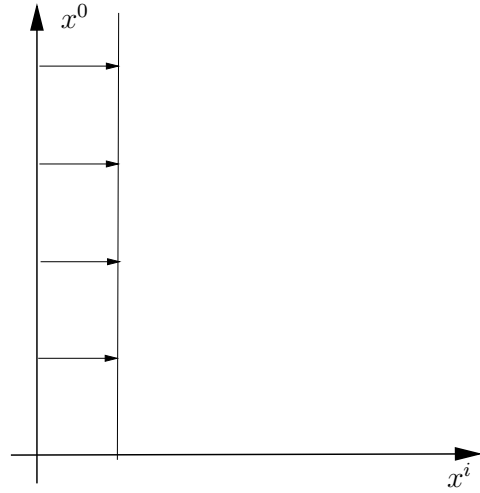


Figure 75: Particles with constant x^i

If we introduce new spatial coordinates

$$y^i = x^i + \frac{1}{2} \gamma^i_k(x^0, 0, 0, 0) x^k, \quad (485)$$

we see that $\delta_{ij} y^i y^j = (\delta_{ij} + \gamma_{ij}(x^0, 0, 0, 0)) x^i x^j$. Comparison with (484) shows that for a particle at constant y^i the distance from the origin remains constant.

We calculate

$$\begin{aligned} \delta_{ij} y^i y^j &= \delta_{ij} x^i x^j + \text{Re}\{A_+((x^1)^2 - (x^2)^2)e^{-i\omega t}\} + \text{Re}\{2A_\times x^1 x^2 e^{-i\omega t}\} = \\ &= \delta_{ij} x^i x^j + |A_+|((x^1)^2 - (x^2)^2) \cos(\varphi - \omega t) + 2|A_\times| x^1 x^2 \cos(\psi - \omega t). \end{aligned} \quad (486)$$

This equation tells how for freely falling particles with constant x^i the distance from the origin changes in dependence of the time t . We demonstrate this in a y^1 - y^2 -diagram, see Fig. 76. The picture illustrates the origin of the names “plus mode” and “cross mode”: In the first case the principal axes form a plus sign, in the second case they form a cross.

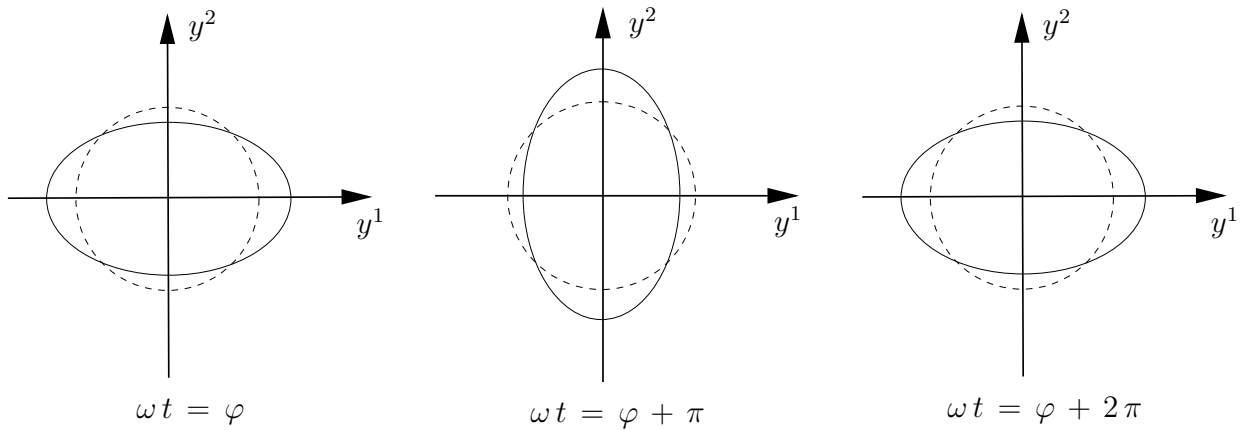
For an animation of the effect of the plus mode and the cross mode on freely falling particles see

https://en.wikipedia.org/wiki/Gravitational_wave

Of course, what is called the plus mode and what is called the cross mode depends on the chosen coordinates. If the coordinate system is rotated by 45° , the two modes interchange. This is in analogy to electromagnetic waves, where there are waves linearly polarised in x direction and waves linearly polarised in y direction; if we rotate the coordinate system by 90° , they interchange their role.

We have thus found, as our main result, that a gravitational wave produces a change of the distances between freely falling particles in the plane perpendicular to the propagation direction. This is what gravitational wave detectors measure, see Section 7.5 below.

Plus mode ($A_+ \neq 0$, $A_\times = 0$):



Cross mode ($A_+ = 0$, $A_\times \neq 0$):

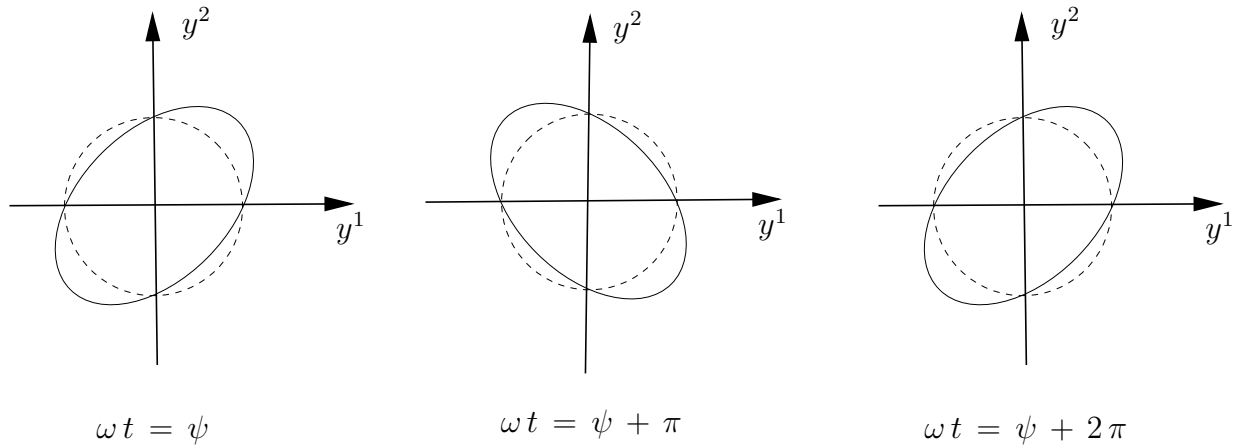


Figure 76: The pictures illustrate what happens to particles that are arranged on a small circle in the plane perpendicular to the propagation direction of the wave and then released to free fall: Both the plus mode and the cross mode produce a time-periodic elliptic deformation. For the plus mode, the main axes of the ellipse coincide with the coordinate axes, for the cross mode they are rotated by 45 degrees. This explains the names “plus mode” and “cross mode”.

7.3 Relating gravitational waves to the source

We will now discuss what sort of sources would produce a gravitational wave. We will see that, in the far-field approximation, the gravitational wave field is determined by the second time-derivative of the quadrupole moment of the source. In other words, gravitational radiation predominantly is quadrupole radiation. By contrast, it is well known that electromagnetic radiation predominantly is dipole radiation.

We now have to consider the linearised field equation with a non-vanishing source term, $T_{\mu\nu} \neq 0$. Again, we choose the Hilbert gauge, so we have to solve the equations

$$\square \gamma^{\mu\nu} = 2\kappa T^{\mu\nu}, \quad \partial_\mu \gamma^{\mu\nu} = 0. \quad (487)$$

Clearly, these two equations require the energy-momentum tensor to satisfy the condition

$$\partial_\mu T^{\mu\nu} = \frac{1}{2\kappa} \partial_\mu \square \gamma^{\mu\nu} = \frac{1}{2\kappa} \square \partial_\mu \gamma^{\mu\nu} = 0. \quad (488)$$

Recall that in the full non-linear theory of general relativity it is the *covariant* divergence of the energy-momentum tensor that vanishes. In the linearised version it is the *ordinary* divergence, formed with the partial derivatives in the chosen coordinates, that vanishes, as in special relativity in inertial coordinates for a closed system. Keep in mind that the coordinates are restricted by the assumptions that in these coordinates the difference $g_{\mu\nu} - \eta_{\mu\nu}$ is small of first order and that the Hilbert gauge condition holds. In contrast to the covariant divergence condition, the one with the partial derivative can be integrated over so that the usual “pill-box argument” gives an integrated conservation law: The temporal change of the energy within a 3-dimensional volume is given by the flow of the energy over the boundary. The conservation law (488) is crucial for the linearised theory of gravitational waves.

For given $T_{\mu\nu}$, the general solution to the inhomogeneous wave equation $\square \gamma^{\mu\nu} = 2\kappa T^{\mu\nu}$ is the general solution to the homogeneous wave equation (superposition of plane harmonic waves) plus a particular solution to the inhomogeneous equation. Such a particular solution can be written down immediately by analogy with the retarded potentials from electrodynamics:

$$\gamma^{\mu\nu}(t, \vec{r}) = \frac{1}{4\pi} \int_{\mathbb{R}^3} \frac{2\kappa T^{\mu\nu}\left(t - \frac{|\vec{r}' - \vec{r}|}{c}, \vec{r}'\right) dV'}{|\vec{r}' - \vec{r}|}. \quad (489)$$

Here and in the following we write

$$x^0 = ct, \quad (x^1, x^2, x^3) = \vec{r}, \quad r = |\vec{r}| \quad (490)$$

and dV' is the volume element with respect to the primed coordinates, $dV' = dx'^1 dx'^2 dx'^3$.

As in electrodynamics one shows by differentiating twice that the $\gamma^{\mu\nu}$ from (489) satisfy, indeed, the equation $\square \gamma^{\mu\nu} = 2\kappa T^{\mu\nu}$ and that the Hilbert gauge condition holds true provided that the energy-momentum tensor satisfies the conservation law (488).

The general solution to the inhomogeneous wave equation is given by adding an arbitrary superposition of plane-harmonic waves that satisfy the homogeneous equation, see Section 7.2. If there are no waves coming in from infinity, (489) alone gives the physically correct solution.

We will now discuss this solution far away from the sources. To that end, we assume that $T^{\mu\nu}$ is different from zero only in a compact region of space. We can then surround this region by a sphere K_R of radius R around the origin, such that

$$T^{\mu\nu}(t, \vec{r}) = 0 \quad \text{if } r \geq R, \quad (491)$$

see Figure 77. We are interested in the field $\gamma^{\mu\nu}$ at a point \vec{r} with $r \gg R$. This is what one calls the *far-field approximation*.

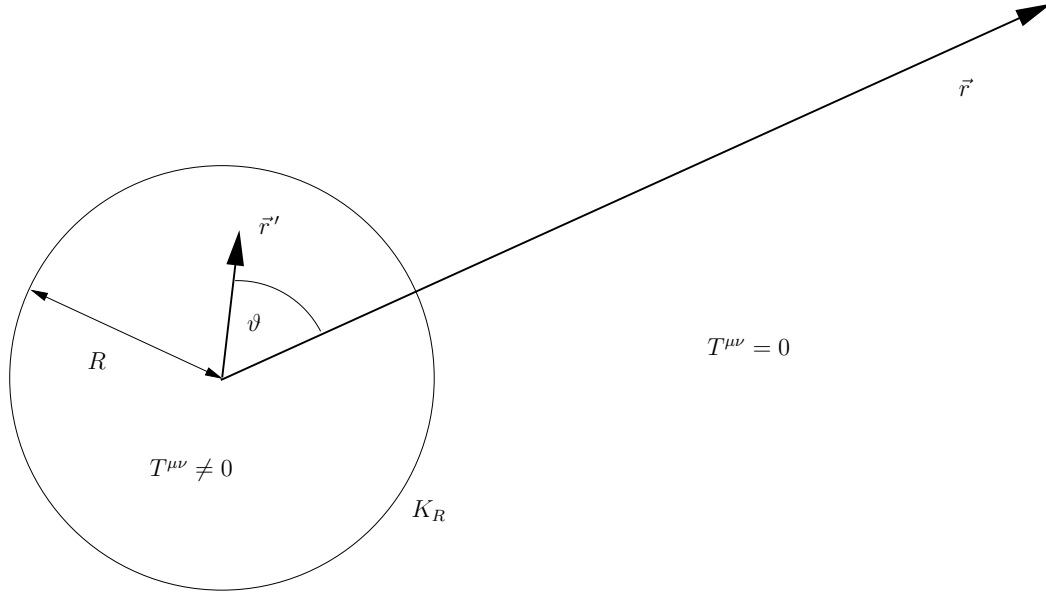


Figure 77: Energy-momentum tensor confined to a sphere K_R

Then

$$\begin{aligned}
 |\vec{r}' - \vec{r}| &= \sqrt{(\vec{r}' - \vec{r}) \cdot (\vec{r}' - \vec{r})} = \sqrt{\vec{r}' \cdot \vec{r}' + \vec{r} \cdot \vec{r} - 2 \vec{r}' \cdot \vec{r}} = \\
 &= \sqrt{r'^2 + r^2 - 2 r' r \cos \vartheta} = r \sqrt{1 - 2 \frac{r'}{r} \cos \vartheta + \frac{r'^2}{r^2}} = r (1 + O(r'/r)). \quad (492)
 \end{aligned}$$

Inserting the result into (489) yields

$$\gamma^{\mu\nu}(t, \vec{r}) = \frac{\kappa}{2\pi} \int_{K_R} \frac{T^{\mu\nu}\left(t - \frac{r}{c} (1 + O(r'/r)), \vec{r}'\right) dV'}{r (1 + O(r'/r))}. \quad (493)$$

In the far-field approximation one assumes that $r \gg R$; then the $O(r'/r)$ -terms can be neglected, as $r' \leq R$ on the whole domain of integration, hence

$$\gamma^{\mu\nu}(t, \vec{r}) = \frac{\kappa}{2\pi r} \int_{K_R} T^{\mu\nu}\left(t - \frac{r}{c}, \vec{r}'\right) dV'. \quad (494)$$

In this approximation, the $\gamma^{\mu\nu}$ depend on \vec{r} only in terms of its modulus $r = |\vec{r}|$, i.e., the wave fronts are spheres, $r = \text{constant}$. As the radii of these spheres are large, they can be approximated as planes on a sufficiently small neighbourhood of any point \vec{r} . This means

that, on any such neighborhood, our gravitational wave resembles a plane wave. If the time-dependence of the source is harmonic, it resembles a plane harmonic wave of the type we have studied in Sec. 7.2.

We will now investigate which properties of the source determine the spatial components γ^{ij} in the far-field approximation. To that end we introduce the multipole moments of the source. They are defined in analogy to electrodynamics, with the charge density replaced by the energy density $T_{00} = -T_0^0 = T^{00}$.

$$M(t) = \int_{K_R} T^{00}(t, \vec{r}) dV \quad (\text{monopole moment}), \quad (495)$$

$$D^k(t) = \int_{K_R} T^{00}(t, \vec{r}) x^k dV \quad (\text{dipole moment}), \quad (496)$$

$$Q^{k\ell}(t) = \int_{K_R} T^{00}(t, \vec{r}) x^k x^\ell dV \quad (\text{quadrupole moment}), \quad (497)$$

...

Instead of $Q^{k\ell}$ one often uses the trace-free part

$$\mathbb{Q}^{k\ell} = Q^{k\ell} - \frac{1}{3} Q_i^i \delta^{k\ell} \quad (498)$$

which is known as the *reduced quadrupole moment*.

We calculate the first and second time derivative of the quadrupole moments. To that end, use the conservation law (488). We find

$$\begin{aligned} \frac{d}{dt} Q^{k\ell}(t) &= \int_{K_R} c \partial_0 T^{00}(t, \vec{r}) x^k x^\ell dV = -c \int_{K_R} \partial_i T^{i0}(t, \vec{r}) x^k x^\ell dV = \\ &= -c \int_{K_R} \left(\partial_i (T^{i0}(t, \vec{r}) x^k x^\ell) - T^{i0}(t, \vec{r}) \delta_i^k x^\ell - T^{i0}(t, \vec{r}) x^k \delta_i^\ell \right) dV. \end{aligned} \quad (499)$$

The first integral can be rewritten, with the Gauss theorem, as a surface integral over the boundary ∂K_R of K_R ,

$$\int_{K_R} \partial_i (T^{i0}(t, \vec{r}) x^k x^\ell) dV = \int_{\partial K_R} T^{i0}(t, \vec{r}) x^k x^\ell dS_i \quad (500)$$

where dS_i is the surface element on ∂K_R . As the sphere K_R surrounds all sources, $T^{\mu\nu}$ is equal to zero on ∂K_R , so the last integral vanishes. Hence

$$\frac{d}{dt} Q^{k\ell}(t) = c \int_{K_R} (T^{k0}(t, \vec{r}) x^\ell + T^{\ell 0}(t, \vec{r}) x^k) dV. \quad (501)$$

Analogously we calculate the second derivative.

$$\begin{aligned}
\frac{d^2}{dt^2} Q^{k\ell}(t) &= c^2 \int_{K_R} \left(\partial_0 T^{k0}(t, \vec{r}) x^\ell + \partial_0 T^{\ell 0}(t, \vec{r}) x^k \right) dV = \\
&= c^2 \int_{K_R} \left(-\partial_i T^{ki}(t, \vec{r}) x^\ell - \partial_i T^{\ell i}(t, \vec{r}) x^k \right) dV = \\
&= c^2 \int_{K_R} \left(-\partial_i (T^{ki}(t, \vec{r}) x^\ell) + T^{ki}(t, \vec{r}) \delta_i^\ell - \partial_i (T^{\ell i}(t, \vec{r}) x^k) + T^{\ell i}(t, \vec{r}) \delta_i^k \right) dV = \\
&= 0 + c^2 \int_{K_R} T^{k\ell}(t, \vec{r}) dV - 0 + c^2 \int_{K_R} T^{\ell k}(t, \vec{r}) dV = 2c^2 \int_{K_R} T^{k\ell}(t, \vec{r}') dV'. \quad (502)
\end{aligned}$$

Upon inserting this result into (494) we find that, in the far-field approximation

$$\gamma^{k\ell}(t, \vec{r}) = \frac{\kappa}{2\pi r} \int_{\mathbb{R}^3} T^{k\ell} \left(t - \frac{r}{c}, \vec{r}' \right) dV' = \frac{\kappa}{2\pi r} \frac{1}{2c^2} \frac{d^2 Q^{k\ell}}{dt^2} \left(t - \frac{r}{c} \right). \quad (503)$$

If Einstein's gravitational constant is expressed with the help of Newton's gravitational constant, $\kappa = 8\pi G/c^4$, the result reads

$$\gamma^{k\ell}(t, \vec{r}) = \frac{2G}{c^6 r} \frac{d^2 Q^{k\ell}}{dt^2} \left(t - \frac{r}{c} \right). \quad (504)$$

In Worksheet 13 we will show that in the far zone $\gamma^{i0}(t, \vec{r}) = 0$ and $\gamma^{00}(t, \vec{r}) = A/r$ with a constant A , so these components give no contribution to the emitted wave.

Recall from Sec. 7.2 that, far away from the sources, a gravitational wave detector responds to the temporal change of the spatial components $\gamma^{k\ell}$ transverse to the propagation direction of the wave. We have just calculated that these are given by the second time derivative of the quadrupole moment at a retarded time. In this sense, gravitational radiation is quadrupole radiation. By contrast, electromagnetic radiation is dipole radiation: A calculation analogous to the above relates the electromagnetic four-potential to the *first* time derivative of the *dipole* moment of the charge distribution at a retarded time. The difference has, of course, its origin in the fact that $\gamma^{\mu\nu}$ and $T^{\mu\nu}$ have two indices, while the analogous quantities A^μ and J^μ in electrodynamics have only one index.

A long and very involved calculation, first carried through by Einstein in 1918, shows that the power radiated away by a source in the form of gravitational waves is given by the *third* derivative of the *reduced* quadrupole moment,

$$P(t, r) = \frac{G}{5c^9} \left\langle \frac{d^3 Q_{mn}}{dt^3} \frac{d^3 Q^{mn}}{dt^3} \right\rangle \left(t - \frac{r}{c} \right). \quad (505)$$

Here the pointed brackets denote a time average over a sufficiently short time interval; e.g., for a binary system one would average over one revolution, so that the long-term time-dependence of the power because of the energy loss of the system is still captured. Eq. (505) is known as *Einstein's quadrupole formula*. We cannot derive it here because the derivation is very long and also conceptually difficult. However, we have completely derived eq. (504) which already clearly indicates that gravitational radiation is predominantly quadrupole radiation.

A time-dependent monopole moment (e.g. a pulsating spherically symmetric star) does not produce gravitational radiation. We knew this already from the Jebsen-Birkhoff theorem of Chapter 6. We have now seen that, moreover, a time-dependent dipole moment does not produce any gravitational radiation in the far-field approximation. We need a time-dependent quadrupole moment. We will now calculate two examples.

Example 1: Rotating cylindrical rod

We consider a homogeneous cylinder of constant mass density $\mu = \frac{M}{\pi a^2 \ell}$, where ℓ is the length and a is the radius of the circular cross-section of the cylinder. We assume that the cylinder rotates with constant angular velocity Ω about an axis that goes perpendicularly through the midpoint of its axis of symmetry, see Fig. 78. For calculating the far field and the radiated power we need the energy quadrupole moment. As the energy stored in such a cylinder is vastly dominated by its rest energy, we can replace the energy quadrupole moment by the mass quadrupole moment multiplied by c^2 . For a rigid body the mass quadrupole moment is the same as the inertia tensor. We first calculate the quadrupole moment, Q'_{ik} , in the rest system of the cylinder,

$$Q'_{ik} = c^2 \int_{\mathcal{V}} \mu x_i x_k dx_1 dx_2 dx_3 \quad (506)$$

where \mathcal{V} is the volume occupied by the cylinder. The integration yields

$$(Q'_{jk}) = c^2 \frac{M}{12} \begin{pmatrix} \ell^2 & 0 & 0 \\ 0 & 3a^2 & 0 \\ 0 & 0 & 3a^2 \end{pmatrix}. \quad (507)$$

Then we transform the quadrupole tensor to the lab frame which is rotated with respect to the rest frame by an angle Ωt about the 3-axis, hence

$$\begin{aligned} (Q_{jk}) &= c^2 \frac{M}{12} \begin{pmatrix} \cos(\Omega t) & -\sin(\Omega t) & 0 \\ \sin(\Omega t) & \cos(\Omega t) & 0 \\ 0 & 0 & 1 \end{pmatrix} \begin{pmatrix} \ell^2 & 0 & 0 \\ 0 & 3a^2 & 0 \\ 0 & 0 & 3a^2 \end{pmatrix} \begin{pmatrix} \cos(\Omega t) & \sin(\Omega t) & 0 \\ -\sin(\Omega t) & \cos(\Omega t) & 0 \\ 0 & 0 & 1 \end{pmatrix} \\ &= c^2 \frac{M}{12} \begin{pmatrix} \cos(\Omega t) & -\sin(\Omega t) & 0 \\ \sin(\Omega t) & \cos(\Omega t) & 0 \\ 0 & 0 & 1 \end{pmatrix} \begin{pmatrix} \ell^2 \cos(\Omega t) & \ell^2 \sin(\Omega t) & 0 \\ -3a^2 \sin(\Omega t) & 3a^2 \cos(\Omega t) & 0 \\ 0 & 0 & 3a^2 \end{pmatrix} \\ &= c^2 \frac{M}{12} \begin{pmatrix} \ell^2 \cos^2(\Omega t) + 3a^2 \sin^2(\Omega t) & (\ell^2 - 3a^2) \sin(\Omega t) \cos(\Omega t) & 0 \\ (\ell^2 - 3a^2) \sin(\Omega t) \cos(\Omega t) & \ell^2 \sin^2(\Omega t) + 3a^2 \cos^2(\Omega t) & 0 \\ 0 & 0 & 3a^2 \end{pmatrix}. \quad (508) \end{aligned}$$

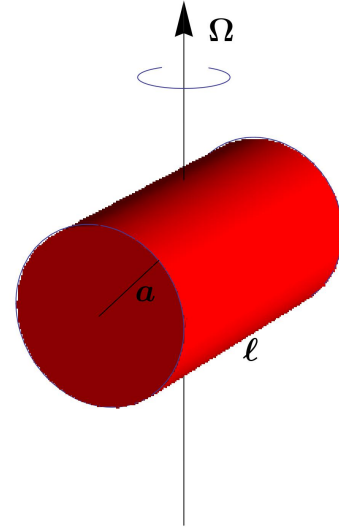


Figure 78: Rotating cylinder

We differentiate this expression with respect to t :

$$\begin{aligned} \left(\frac{dQ_{ik}}{dt}\right) &= c^2 \frac{M\Omega}{12} \begin{pmatrix} -(\ell^2 - 3a^2) 2\sin(\Omega t)\cos(\Omega t) & (\ell^2 - 3a^2)(\cos^2(\Omega t) - \sin^2(\Omega t)) & 0 \\ (\ell^2 - 3a^2)(\cos^2(\Omega t) - \sin^2(\Omega t)) & (\ell^2 - 3a^2)2\sin(\Omega t)\cos(\Omega t) & 0 \\ 0 & 0 & 0 \end{pmatrix} \\ &= c^2 \frac{M\Omega}{12} (\ell^2 - 3a^2) \begin{pmatrix} -\sin(2\Omega t) & \cos(2\Omega t) & 0 \\ \cos(2\Omega t) & \sin(2\Omega t) & 0 \\ 0 & 0 & 0 \end{pmatrix}, \end{aligned} \quad (509)$$

$$\left(\frac{d^2Q_{ik}}{dt^2}\right) = c^2 \frac{M\Omega^2}{6} (\ell^2 - 3a^2) \begin{pmatrix} -\cos(2\Omega t) & -\sin(2\Omega t) & 0 \\ -\sin(2\Omega t) & \cos(2\Omega t) & 0 \\ 0 & 0 & 0 \end{pmatrix}, \quad (510)$$

$$\left(\frac{d^3Q_{ik}}{dt^3}\right) = c^2 \frac{M\Omega^3}{3} (\ell^2 - 3a^2) \begin{pmatrix} \sin(2\Omega t) & -\cos(2\Omega t) & 0 \\ -\cos(2\Omega t) & -\sin(2\Omega t) & 0 \\ 0 & 0 & 0 \end{pmatrix}. \quad (511)$$

Inserting (510) into (503) gives us γ_{ik} in the far-field approximation. As (d^2Q_{ik}/dt^2) is traceless, γ_{ik} coincides with the strain h_{ik} :

$$((h_{ik}(t, \vec{r})) = (\gamma_{ik}(t, \vec{r})) = \frac{G M \Omega^2}{3 c^4 r} (\ell^2 - 3a^2) \begin{pmatrix} -\cos(2\Omega t) & -\sin(2\Omega t) & 0 \\ -\sin(2\Omega t) & \cos(2\Omega t) & 0 \\ 0 & 0 & 0 \end{pmatrix}. \quad (512)$$

Recall that $\gamma_{00}(=h_{00})$ is time-independent and $\gamma_{0i}(=h_{0i})$ is zero in the far-field approximation.

We read from (512) that the frequency of the gravitational wave is

$$\omega = 2\Omega \quad (513)$$

which comes from the symmetry of the cylinder: If it has performed *half* a cycle we are in the same situation as in the beginning. Moreover, we read from (512) that the amplitude of the strain is

$$A = \frac{G M \Omega^2}{3 c^4 r} (\ell^2 - 3a^2). \quad (514)$$

Note that $A = 0$ if $\ell^2 = 3a^2$. In this case the cylinder is a spherical top, i.e., all its principal moments of inertia coincide. Then the quadrupole tensor in the lab frame is constant, i.e., no gravitational waves are emitted.

By inserting (511) into Einstein's quadrupole formula (505) we get the radiated power that passes through a sphere of radius r . As the trace of (d^3Q_{ik}/dt^3) vanishes, we have $d^3Q_{ik}/dt^3 = d^3Q_{ik}/dt^3$, so by multiplying the matrix in (511) with itself and taking the trace we find that

$$\frac{d^3Q^{ik}}{dt^3} \frac{d^3Q_{ik}}{dt^3} = 2 \frac{M^2 c^4 \Omega^6}{9} (\ell^2 - 3a^2)^2. \quad (515)$$

We have assumed throughout our derivation that Ω and, of course, M are constant, so no time-averaging of (515) is necessary. (Because of the energy loss through gravitational radiation,

Ω would actually decrease if the cylinder would be left alone, i.e., our assumption of Ω being constant can be satisfied only if there is an external force by which the cylinder is driven.) For the radiated power we find

$$P = \frac{2 G M^2 \Omega^6}{45 c^4} (\ell^2 - 3a^2)^2. \quad (516)$$

We now insert numerical values to indicate how incredibly small the power of all gravitational waves is that could be produced in the lab: We choose $a = 1$ m, $\ell = 20$ m, $M = 5 \times 10^5$ kg and $\Omega = 30$ Hz. Even with these (quite unrealistic) values we find that the amplitude of the strain (514) gives

$$A \approx \frac{5 \times 10^{-34} \text{ m}}{r}, \quad (517)$$

which means that, if we are 25m away from the cylinder, the distance between two freely falling test masses which are 1m apart changes by only 2×10^{-33} m. Likewise, the radiated power (516) gives $P \approx 4 \times 10^{-29}$ Watts which is unmeasurable for generations to come. And note that this is the power radiated into all of space; only a small fraction will actually hit a detector.

So we have to give up the idea of producing gravitational waves in the lab and then measuring them directly. We need astronomical sources for observing gravitational waves.

Example 2: Binary system in circular orbit

We consider a binary system consisting of two masses $M_1 = M_2 = 1.4 M_\odot = 1.4 \times 1.99 \times 10^{30}$ kg in a circular orbit about their common barycentre. We choose the $x_1 - x_2$ -plane as the orbital plane; the distance of the two stars should be $a = 10^6$ km. (These numbers are similar, as far as the order of magnitude is concerned, to the Hulse-Taylor pulsar and its companion, see next section.) For calculating the quadrupole moment we use again the approximation that the energy density is the mass density multiplied by c^2 and we treat the two stars as Newtonian point masses. Then we have in the rest system of the two masses

$$Q'_{ik} = c^2 \int_{\mathbb{R}^3} \mu(x_1, x_2, x_3) x_i x_k dx_1 dx_2 dx_3 \quad (518)$$

with the mass density

$$\mu(x_1, x_2, x_3) = M (\delta(x_1 - a/2) + \delta(x_1 + a/2)) \delta(x_2) \delta(x_3). \quad (519)$$

This gives

$$(Q'_{ik}) = c^2 \frac{M a^2}{2} \begin{pmatrix} 1 & 0 & 0 \\ 0 & 1 & 0 \\ 0 & 0 & 1 \end{pmatrix}. \quad (520)$$

In the “lab frame” (i.e., in an inertial system where our galaxy is approximately at rest) the stars orbit about their common barycentre with an angular frequency Ω that is given by Kepler’s third law,

$$\Omega^2 = \frac{2GM}{a^3}. \quad (521)$$

So in this system the quadrupole tensor reads

$$\begin{aligned}
(Q_{jk}) &= c^2 \frac{M a^2}{2} \begin{pmatrix} \cos(\Omega t) & -\sin(\Omega t) & 0 \\ \sin(\Omega t) & \cos(\Omega t) & 0 \\ 0 & 0 & 1 \end{pmatrix} \begin{pmatrix} 1 & 0 & 0 \\ 0 & 0 & 0 \\ 0 & 0 & 0 \end{pmatrix} \begin{pmatrix} \cos(\Omega t) & \sin(\Omega t) & 0 \\ -\sin(\Omega t) & \cos(\Omega t) & 0 \\ 0 & 0 & 1 \end{pmatrix} \\
&= c^2 \frac{M a^2}{2} \begin{pmatrix} \cos(\Omega t) & -\sin(\Omega t) & 0 \\ \sin(\Omega t) & \cos(\Omega t) & 0 \\ 0 & 0 & 1 \end{pmatrix} \begin{pmatrix} \cos(\Omega t) & \sin(\Omega t) & 0 \\ 0 & 0 & 0 \\ 0 & 0 & 0 \end{pmatrix} \\
&= c^2 \frac{M a^2}{2} \begin{pmatrix} \cos^2(\Omega t) & \sin(\Omega t) \cos(\Omega t) & 0 \\ \sin(\Omega t) \cos(\Omega t) & \sin^2(\Omega t) & 0 \\ 0 & 0 & 0 \end{pmatrix}. \tag{522}
\end{aligned}$$

We differentiate this expression with respect to t :

$$\begin{aligned}
\left(\frac{dQ_{ik}}{dt}\right) &= c^2 \frac{M a^2 \Omega}{2} \begin{pmatrix} -2 \sin(\Omega t) \cos(\Omega t) & \cos^2(\Omega t) - \sin^2(\Omega t) & 0 \\ \cos^2(\Omega t) - \sin^2(\Omega t) & 2 \sin(\Omega t) \cos(\Omega t) & 0 \\ 0 & 0 & 0 \end{pmatrix} \\
&= c^2 \frac{M a^2 \Omega}{2} \begin{pmatrix} -\sin(2\Omega t) & \cos(2\Omega t) & 0 \\ \cos(2\Omega t) & \sin(2\Omega t) & 0 \\ 0 & 0 & 0 \end{pmatrix}, \tag{523}
\end{aligned}$$

$$\left(\frac{d^2 Q_{ik}}{dt^2}\right) = c^2 M a^2 \Omega^2 \begin{pmatrix} -\cos(2\Omega t) & -\sin(2\Omega t) & 0 \\ -\sin(2\Omega t) & \cos(2\Omega t) & 0 \\ 0 & 0 & 0 \end{pmatrix}, \tag{524}$$

$$\left(\frac{d^3 Q_{ik}}{dt^3}\right) = 2 c^2 M a^2 \Omega^3 \begin{pmatrix} \sin(2\Omega t) & -\cos(2\Omega t) & 0 \\ -\cos(2\Omega t) & -\sin(2\Omega t) & 0 \\ 0 & 0 & 0 \end{pmatrix}. \tag{525}$$

Inserting (524) into (503) gives us γ_{ik} in the far-field approximation. Again, as $(d^2 Q_{ik}/dt^2)$ is traceless, γ_{ik} coincides with the strain h_{ik} :

$$(h_{ik}(t, \vec{r})) = (\gamma^{ik}(t, \vec{r})) = \frac{2 G M a^2 \Omega^2}{c^4 r} \begin{pmatrix} -\cos(2\Omega t) & -\sin(2\Omega t) & 0 \\ -\sin(2\Omega t) & \cos(2\Omega t) & 0 \\ 0 & 0 & 0 \end{pmatrix}. \tag{526}$$

So the frequency of the gravitational wave is

$$\omega = 2 \Omega = \frac{4 G M}{a^3} \tag{527}$$

and the amplitude of the strain is

$$A = \frac{2 G M a^2 \Omega^2}{c^4 r} = \frac{4 G^2 M^2}{c^4 r a}. \tag{528}$$

Inserting (525) into Einstein's quadrupole formula yields

$$P = \frac{8 G M^2 a^4 \Omega^6}{5 c^5} = \frac{64 G^4 M^5}{5 c^5 a^5}. \quad (529)$$

With the numbers given above we find

$$\omega \approx 0.9 \times 10^{-3} \text{ Hz}, \quad A \approx 1.1 \times 10^{-22}, \quad P \approx 1.7 \times 10^{25} \text{ W}. \quad (530)$$

The power is huge, but note that this is what is emitted into all of space; only a very small portion will hit a detector on Earth. The strain is so tiny that at first sight it seems out of the question that such a signal could ever be detected on Earth. However, with the LIGO detectors it was actually possible to measure a strain that was not very much bigger, as we will discuss below.

During the calculation we have assumed that a and, thus, Ω are constants. This would be true only if there were a driving force that keeps the motion of the two stars going on uniformly. Of course, in reality there is no such driving force. Actually, the binary system will lose energy by way of gravitational radiation, so a would decrease in time. We can calculate this change in the *adiabatic approximation*, i.e., by using the formulas which have been derived for constant a and assuming that they will be approximately valid also for slowly varying a . So we assume now that a and, thus, Ω are functions of time.

The energy of our binary system is the sum of kinetic and potential energy,

$$E = 2 \frac{M}{2} \left(\frac{a}{2} \Omega^2 \right)^2 - \frac{G M^2}{a} = \frac{G M^2}{2 a} - \frac{G M}{a} = \frac{-G M^2}{2 a}. \quad (531)$$

Differentiating with respect to t must give the power that is radiated away,

$$\frac{dE}{dt} = -P, \quad (532)$$

hence

$$\begin{aligned} \frac{G M^2}{2 a^2} \frac{da}{dt} &= \frac{64 G^4 M^5}{5 c^5 a^5}, \\ \frac{1}{4} \frac{da^4}{dt} &= a^3 \frac{da}{dt} = \frac{-128 G^3 M^3}{5 c^5}, \\ a(t) &= a_0 \left(1 - \frac{t}{t_{\text{sp}}} \right)^{1/4} \end{aligned} \quad (533)$$

where a_0 is the distance of the stars at time $t = 0$ (for which we insert the above-given value of 10^6 km) and

$$t_{\text{sp}} = \frac{5 c^5 a_0^4}{512 G^3 M^3} \quad (534)$$

is the time when, in our simple model, the stars merge. With the numbers from above, t_{sp} is approximately $3.7 \times 10^{15} \text{ s}$. For the sake of comparison we mention that, in the concordance model of cosmology ("Lambda-Cold-Dark-Matter"), the age of our universe is about 10^{17} s . So we would have to wait for a very long time until the two stars merge.

From (533) we find the temporal change of the frequency of the gravitational wave

$$\omega(t) = 2\Omega(t) = 2\sqrt{\frac{2GM}{a(t)^3}} = 2\sqrt{\frac{2GM}{a_0^3}}\left(1 - \frac{t}{t_{\text{sp}}}\right)^{-3/8} \quad (535)$$

and of the amplitude of the strain

$$\begin{aligned} A(t) &= \frac{4G^2 M^2}{c^4 r a} \\ &= \frac{4G^2 M^2}{c^4 r a_0} \left(1 - \frac{t}{t_{\text{sp}}}\right)^{-1/4}. \end{aligned} \quad (536)$$

So both the frequency and the amplitude go to ∞ for $t \rightarrow t_{\text{sp}}$, see Fig. 79. This is what one calls a “chirp signal”. The name refers to the case of a sound wave where such a signal becomes louder and higher pitched in the course of time.

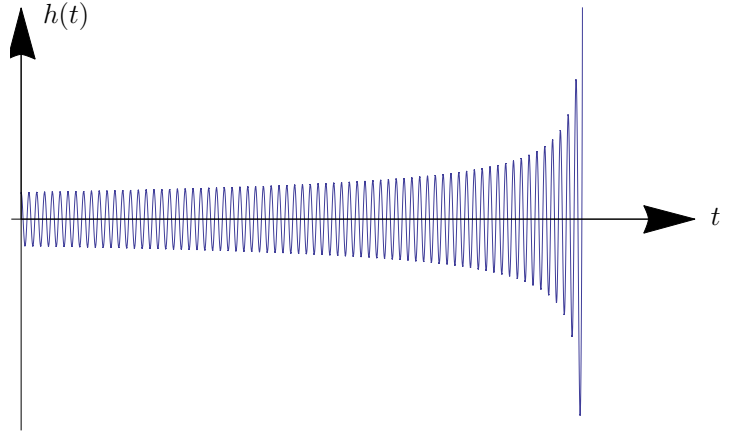


Figure 79: Chirp signal

From the frequency $\Omega(t)$ we get the period $T(t) = 2\pi/\Omega(t)$ of the motion and its time derivative

$$\frac{dT(t)}{dt} = 2\pi\sqrt{\frac{a_0^3}{2GM}} \frac{d}{dt} \left(1 - \frac{t}{t_{\text{sp}}}\right)^{3/8} = -\frac{3\pi}{4t_{\text{sp}}} \sqrt{\frac{a_0^3}{2GM}} \left(1 - \frac{t}{t_{\text{sp}}}\right)^{-5/8}. \quad (537)$$

We see that $dT(t)/dt$ goes to $-\infty$ for $t \rightarrow t_{\text{sp}}$, see Fig. 80. It is this functional behaviour that could be compared with observations from the Hulse-Taylor pulsar, see the next section.

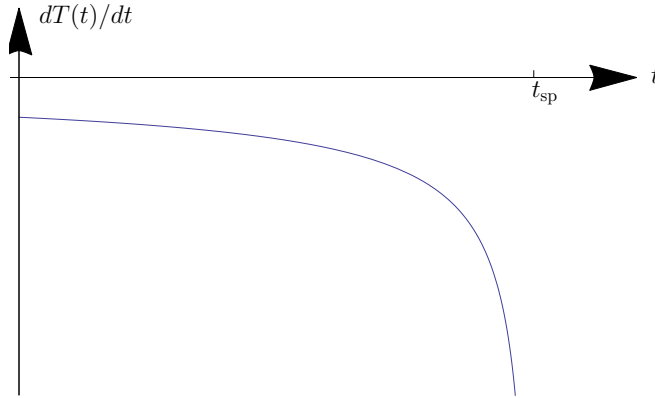


Figure 80: Time derivative of the period in a binary system

Our very simple model of two Newtonian mass points that spiral towards their common barycentre is surprisingly good as long as the two stars are not too close together. In the final stage of the merger this model becomes, of course, unrealistic. E.g., tidal deformations of the stars will play an essential role. It is very difficult to realistically calculate the gravitational wave signal emitted during the merger phase and during the subsequent “ring down”. A combination of analytical approximation methods and of numerical simulations is used for doing this. In these final stages there are significant differences between the merger of two neutron stars, a neutron star and a black hole, and two black holes.

7.4 The Hulse-Taylor pulsar

In 1974, Russell Hulse, then a PhD student of Joe Taylor's, studied a number of pulsars with the Arecibo Telescope. The latter is a radio telescope, embedded in a volcano crater in Puerto Rico with a diameter of 300 m, see Figure 81. A pulsar is an object that emits radio pulses with a very regular frequency. In 1974 it was already known that pulsars are rotating neutron stars which emit a beam of radio rays in a direction not aligned with the rotation axis; the pulses are observed whenever the beam sweeps over the Earth.



Figure 81: Arecibo radio telescope



Figure 82: R. Hulse (1950 -) and J. Taylor (1941 -) celebrating their Nobel Prize in 1993

Hulse's task was to measure the frequencies of several pulsars with high accuracy. One pulsar was very peculiar. Its discovery earned Hulse and Taylor the Nobel Prize in 1993, see Figure 82. This pulsar, with the catalogue name PSR B1913+16, did not have a constant pulse frequency: The frequency was periodically increasing, then decreasing, then increasing again and so on, see Figure 83. This was interpreted by Hulse and Taylor as a Doppler effect. The conclusion was that the pulsar had a companion (which is dark and silent) such that the pulsar and the companion orbit their common barycentre. In the course of this motion the pulsar is periodically moving towards us, then away from us, then again towards us and so on.

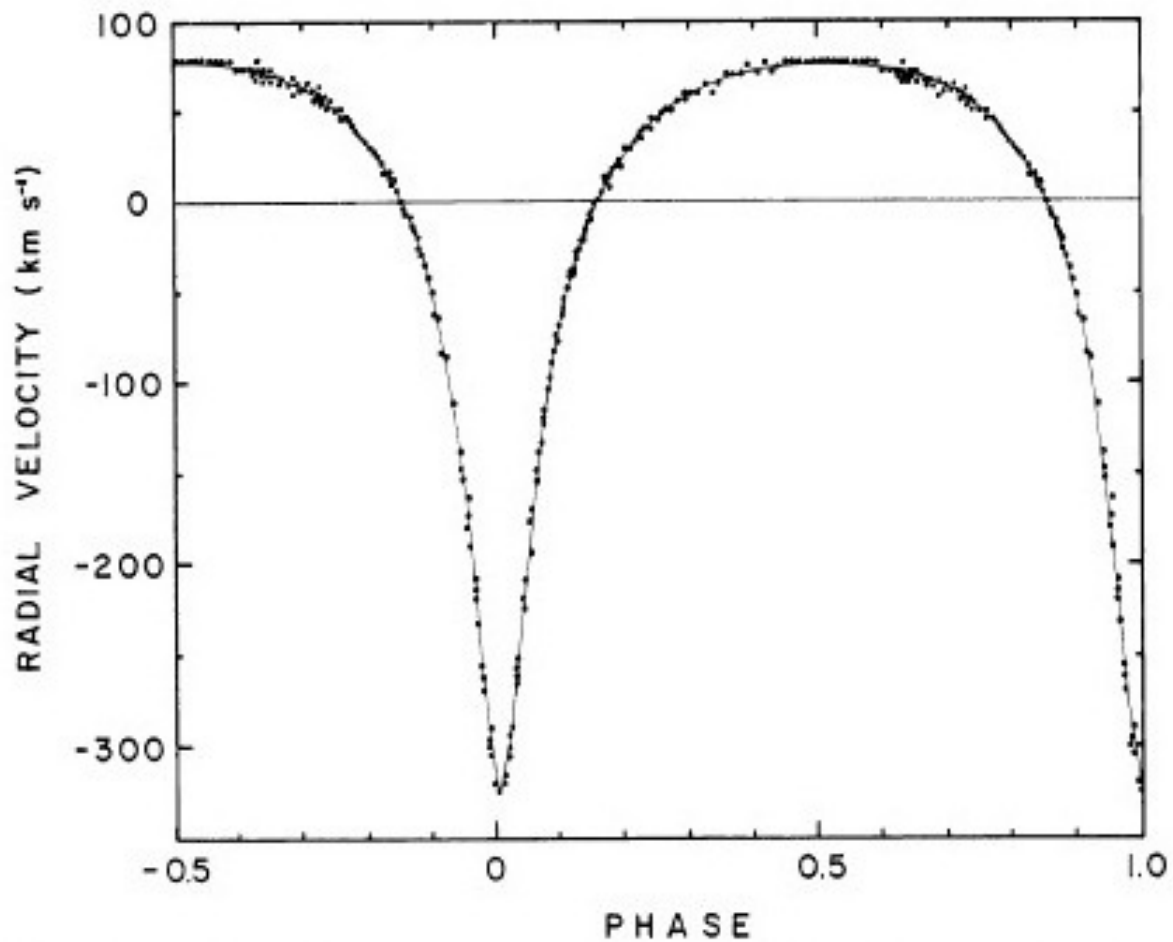


Figure 83: Doppler shift of PSR B1913+16

From the measurement of the Doppler shift one can calculate all the orbital elements of the binary system. (If the calculation is done within the Newtonian theory, there are actually some degeneracies; if, however, post-Newtonian – i.e., relativistic – corrections are taken into account, these degeneracies are completely removed.) With the orbital elements known one could calculate the energy loss as predicted by Einstein’s quadrupole formula. According to this formula the orbital period of the binary system should decrease, see Figure 80 for the simple model of a binary system of two Newtonian point masses. This decay of the orbital period was calculated, at the post-Newtonian level, on the basis of the observed orbital elements. Note that there is no fitting parameter left; the resulting curve is absolutely fixed by the orbital elements and the quadrupole formula. Figure 84 shows the theoretical prediction and the observed values of the decay of the orbital period. The agreement is so convincing that it was generally accepted that this observation is to be considered as an indirect detection of gravitational waves. Note that in Figure 84 it is not directly the decay of the period, dT/dt , that is plotted on the vertical axis, but rather the shift of the periastron time, i.e., of the time when the two stars are closest to each other.

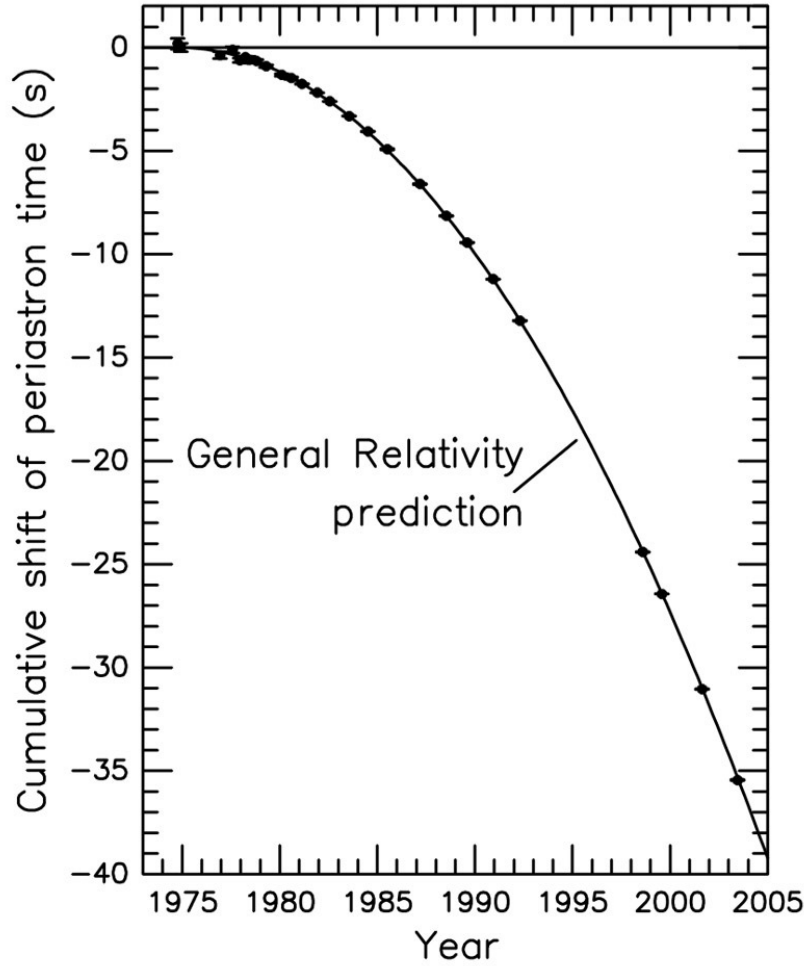


Figure 84: Decay of the orbital period of the Hulse-Taylor pulsar and its companion as calculated on the basis of Einstein’s quadrupole formula (solid curve) and as observed (dots)

We know by now that not only the Hulse-Taylor pulsar but also its companion is a neutron star. The mass of the pulsar is $1.441 M_{\odot}$. The mass of the companion is similar, $\approx 1.4 M_{\odot}$, but not known with very high accuracy. The pulsar rotates with a period of 59 milliseconds about its axis. The semi-major axis of the orbit is $1.9 \times 10^6 \text{ km}$, i.e., the entire system is only a bit too large for fitting inside the Sun. The orbital period $T = 2\pi/\Omega$ is 7.7 h, i.e., the system emits gravitational waves of a frequency $\omega = 2\Omega$ of much less than 1 Hz. As earthbound gravitational wave detectors cannot operate at frequencies below 1 Hz (see next section), there is no chance to observe these gravitational waves directly as long as we have no spaceborn detector.

After the discovery of the Hulse-Taylor pulsar several more binary pulsars (i.e., pulsars in a binary system) were found. In 2003 the first double pulsar (i.e., a binary system where both companions are pulsars) was detected. These systems are the best test-beds of general relativity we have at the moment. Note that the semi-major axis of such systems (typically some 10^6 km) is still large in comparison to the Schwarzschild radius of the neutron stars (typically 4 or 5 km). In this sense, what is tested with binary pulsars is not really “strong gravity”.

7.5 Gravitational wave detectors

Gravitational waves produce an oscillatory motion of free particles in the plane orthogonal to their propagation direction, recall Figure 76. In a solid body, e.g. a piece of metal, the atoms are not free but rather bound by interatomic forces; a gravitational wave has to compete with these forces. Therefore, if a piece of metal is hit by a gravitational wave, this will cause forced oscillations of the atoms whose amplitude could be comparatively large if the gravitational wave comes in with the resonance frequency of the metal.



Figure 85: Joe Weber with a resonant bar detector

Based on this idea, Joe Weber began in the late 1950s to experiment with *resonant bar detectors*, see Figure 85. These detectors, also known as *Weber cylinders*, are aluminium cylinders with a typical weight of 1.5 tons, approximately 150 centimeters long and 60 centimeters in diameter. With the help of piezo crystals glued onto the surface, which are clearly seen in the picture, Weber tried to detect tiny deformations of the cylinder when a gravitational wave hit it. The weakest point of this class of gravitational wave detectors is in the fact that they are sensitive only in a very narrow frequency band around the fundamental resonance frequency which is, for a typical Weber cylinder, at ≈ 1660 Hertz. So with these detectors gravitational waves could be detected only from extremely fast rotating systems or from burst sources (asymmetrical stellar explosions) which contain in their Fourier spectrum high frequencies with sufficiently high amplitudes.

Weber was searching for gravitational waves until his death in 2000. He even claimed that he had detected gravitational waves with his resonant bar detectors, but this was not generally accepted. He also sent a seismometer with the Apollo 17 mission to the moon, but the instrument malfunctioned. The idea was to use the body of the moon as a “resonance detector” of gravitational waves. In this way it would have been possible to detect gravitational waves of much lower frequencies as with the aluminium cylinders. (Several other seismometers have been placed on the surface of the moon but their purpose was to measure seismic activity on the moon, not gravitational waves.)

Some resonant bar detectors are in operation until the present time. The most sophisticated of them, known as Auriga, is an ultracryogenic detector, i.e., it is being operated at extremely low temperatures to minimise thermal noise, see Figure 86. There are also attempts with spherical detectors, e.g. MiniGRAIL, see Figure 87, which have the advantage of being sensitive for gravitational waves from all spatial directions. However, it seems fair to say that in particular in view of the LIGO success the resonant bar detectors have been sidelined by the interferometric detectors.

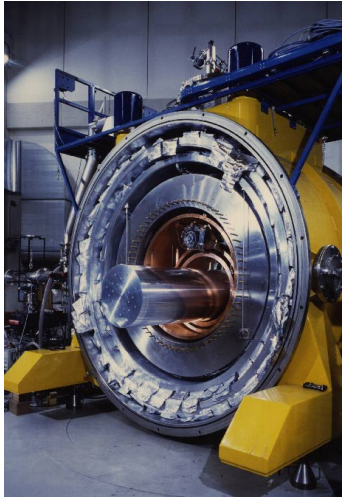


Figure 86: Auriga

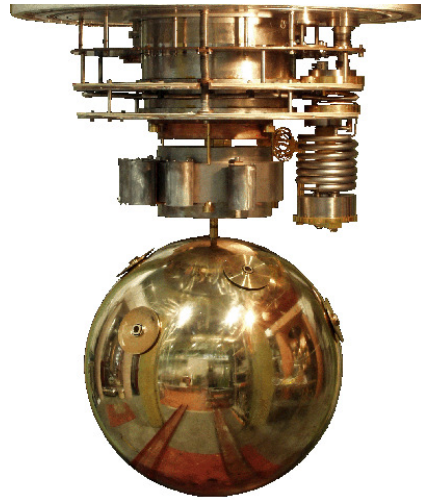


Figure 87: MiniGRAIL

Interferometric gravitational wave detectors are just Michelson interferometers, see Figure 88. The paper plane is to be interpreted as horizontal. The mirrors M_1 and M_2 are suspended on files, so that they can move freely in the horizontal direction. Assume that in the beginning the beam reflected at M_1 and the beam reflected at M_2 give a destructive interference (i.e., darkness) at the detector. If a gravitational wave comes in (ideally travelling perpendicularly to the paper plane), it will periodically change the distances d_1 and d_2 , see Figure 76; as a consequence, we have a signal, periodically changing from darkness to brightness, at the detector.

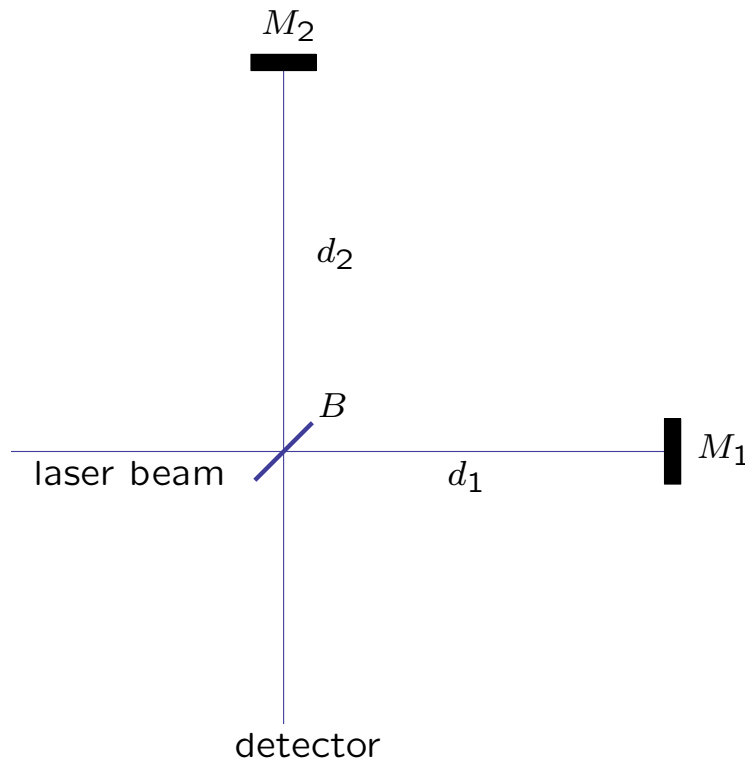


Figure 88: Interferometric gravitational wave detector

The idea of using Michelson interferometers as gravitational wave detectors is almost as old as the idea of using resonant cylinders: It was brought forward by the Soviet physicists M. Gertsenshtein and V. Pustovoit in 1962. However, it took several decades until it was possible to build gravitational wave detectors of this type at a size that had a chance to actually detect gravitational waves. Here is a list of these interferometric gravitational wave detectors.

- TAMA300: This was a Japanese project. The interferometer had an armlength of 300 m. It was operational from 1999 to 2004.
- GEO600: This is a detector in Germany, near Hannover, with a (geometric) armlength of 600 m. It is operational since 2001. Although too small for actually detecting gravitational waves, it was very important for the development of interferometric gravitational wave detectors. Most of the LASER technology and several other parts that went into the LIGO detectors were developed and tested with GEO600.



Figure 89: GEO600

- LIGO: These are the two biggest interferometric gravitational wave detectors that exist to date. They are in the USA, one in Hanford (Washington State) and the other in Livingston (Louisiana). Both have a (geometric) armlength of 4 km. They are operational, with interruptions, since 2002. The interruptions are used for updating the systems. The LIGO detectors were successful in directly detecting a gravitational wave signal for the first time in September 2015, see next section. Rainer Weiss, Kip Thorne and Barry Barish were awarded the Nobel Prize in Physics 2017 “for decisive contributions to the LIGO detector(s) and the observation of gravitational waves”. During the last Science Run, which started in April 2019 and had to be terminated prematurely in March 2020 because of the CoViD-19 pandemic, on average one gravitational wave signal was observed per week.



Figure 90: LIGO

- Virgo: This is an Italian detector which is a little bit smaller than the LIGO instruments, with an armlength of 3 km. It is operational since 2007. When the first gravitational wave signals were detected by the LIGO instruments, Virgo was not online. However, many of the more recent signals were also seen by the Virgo detector.



Figure 91: Virgo

- KAGRA: This is a Japanese instrument, situated in a subterranean cave. The armlength is 3 km. The instrument is cryogenic, i.e., it is operated at a very low temperature to reduce thermal noise. KAGRA was completed in 2019 and the instrument joined the LIGO-Virgo network in January 2020, just a few weeks before it had to be shut down because of the CoViD-19 pandemic in March 2020.

In addition, there are plans for several earthbound future interferometric gravitational wave detectors. Here are two of them.

- LIGO India: This is a third detector of the LIGO type, to be built in India. It is still in the planning stage. The predicted date of commission was 2024, but this will probably be delayed because of the pandemic and other reasons.

- Einstein Telescope: This is a very ambitious European project. It is not clear yet were it will be built (if ever). It is supposed to be a subterranean cryogenic instrument with three arms of 10 km length in a triangular shape. A testing facility is planned to be built in Maastricht in the Netherlands.

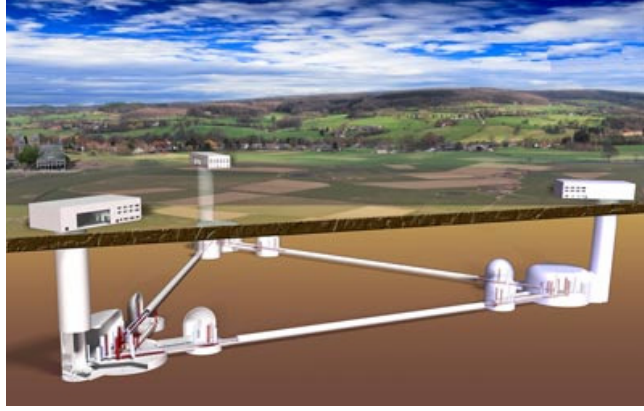


Figure 92: Einstein Telescope

In addition to building new earthbound gravitational wave detectors, there are also plans for constructing a spaceborn interferometric gravitational wave detector. For understanding the motivation we have to look at the so-called *strain sensitivity*, $\sqrt{S_h(\omega)}$, of gravitational wave detectors. The latter is defined in the following way.

For measuring a signal it must be strong enough to come out of the noise. The noise, understood as a non-systematic, random underground of perturbations, is characterised in the following way. Take a sample of pairs of measurements of the strain at times t_1 and t_2 , all with the same time difference $\tau = |t_2 - t_1|$, and average them out. The result is a function of τ which we call κ ,

$$\langle h(t_1)h(t_2) \rangle = \kappa(\tau), \quad \tau = |t_2 - t_1|. \quad (538)$$

Now perform a one-sided Fourier analysis (“one-sided” means that only positive frequencies are taken into account),

$$S_h(\omega) = \begin{cases} \frac{1}{2} \int_0^\infty \kappa(\tau) e^{i\omega\tau} d\tau & \text{if } \omega > 0 \\ 0 & \text{if } \omega < 0. \end{cases} \quad (539)$$

$\sqrt{S_h(\omega)}$ is called the strain sensitivity. It characterises the noise level as a function of the frequency. As the strain (change of distance divided by distance) is dimensionless, the strain sensitivity has the dimension $\text{Hz}^{-1/2}$.

Figure 93 shows the strain sensitivity as a function of the frequency ω . A signal can be detected if its strain has an amplitude bigger than the strain sensitivity. We see that all earthbound detectors are limited to signals above 1 Hz. The reason is seismic noise which at frequencies of less than 1 Hz just drowns all signals. For gravitational waves produced by binary systems this means that they must have a period of less than a second for being detectable which will be true only for the very last moments before the merger. For this reason one wants to build gravitational wave detectors in space.

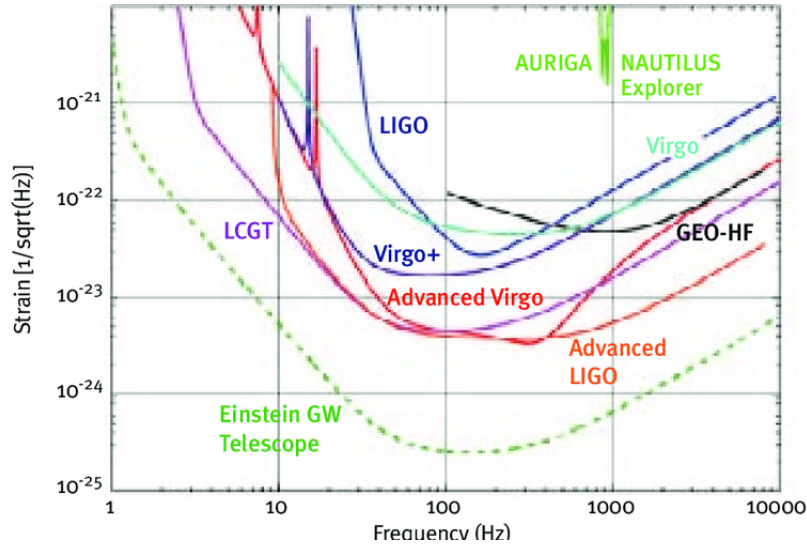


Figure 93: Strain sensitivity of gravitational wave detectors

There are plans for a spaceborn gravitational wave detector since many years. The most promising project is called LISA. It is an ESA project with (on again, off again) participation of NASA. It was several times downscaled, renamed NGO or eLISA, then partly upscaled and renamed LISA again. It consists of three satellites, with LASER beams sent between them. The entire constellation is “rolling” on the orbit of the Earth, trailing the latter by 20° , see Figure 94. Note that this figure is not to scale: The size of the LISA arms is very much exaggerated in comparison to the radii of the orbits of the planets.

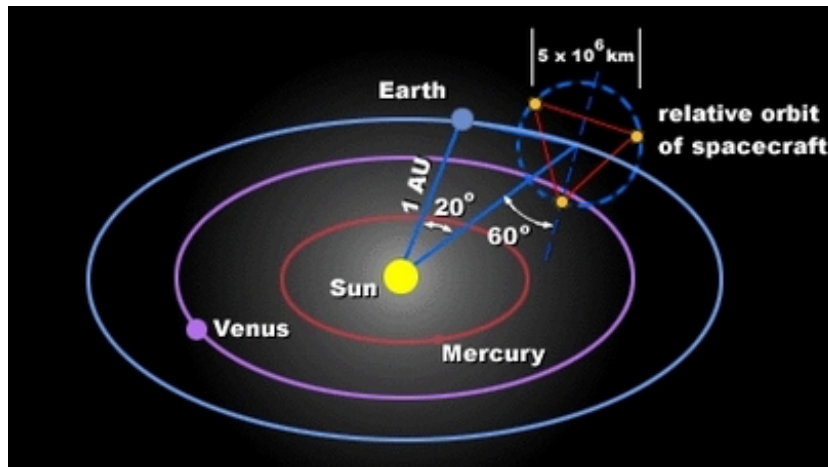


Figure 94: LISA

The armlength is very long (5 Million kilometers according to the original plan). This together with the absence of seismic noise allows the detection of gravitational waves of much lower frequencies than with any earthbound detector, see Figure 95. A test mission, called LISA pathfinder, was very successful. At present there are some hopes that LISA may be launched in the early 2030s. It is expected that LISA will see so many gravitational wave signals that a main problem will be to disentangle them.

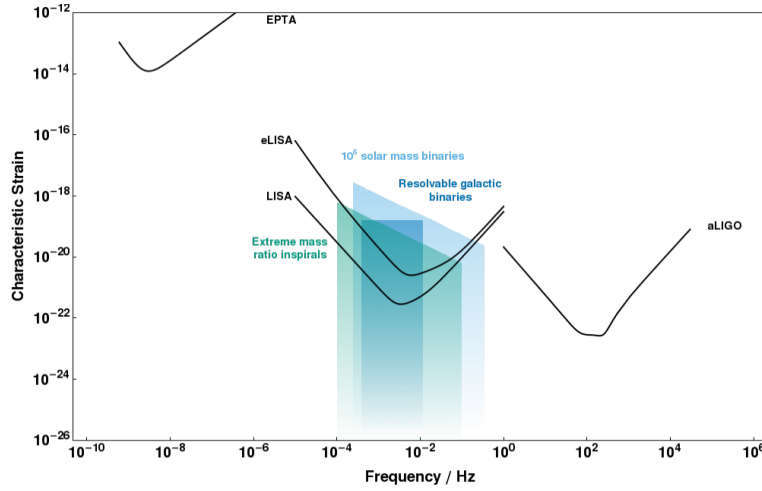


Figure 95: Strain sensitivity of LISA and eLISA

7.6 The LIGO observations

In this section we briefly discuss some of the gravitational wave signals that were detected by the LIGO detectors and partly also by Virgo. They are numbered in the form GWyymmdd. .

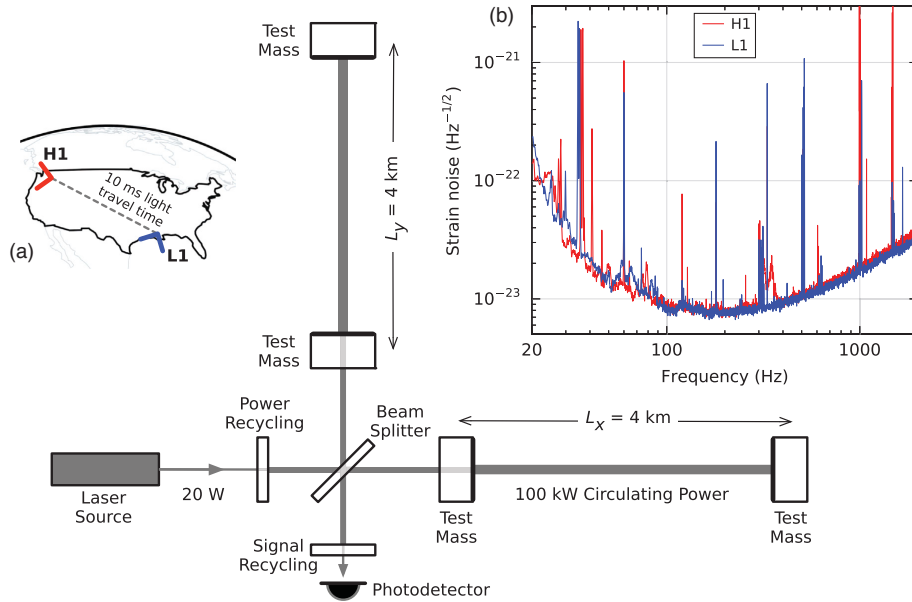


Figure 96: The LIGO detectors

The first event was GW150914, i.e., it was observed on 14 September 2015. At this time Virgo was offline, so the signal was seen only by the two LIGO detectors. The LIGO team announced the observation only in February 2016 because they wanted to be absolutely sure that the signal was real. The results were published in a paper with more than 1000 authors, see B. Abbott et al., Phys. Rev. Lett. 116, 061102 (2016). Figures 96, 97 and 98 are taken from this paper.

As shown in Figure 96, the distance between the two LIGO detectors equals $c \times 10$ ms. Depending on where the gravitational wave comes from, the time at which the signal is detected at one detector should be between 0 and 10 ms after it is detected by the other. Only signals that are registered by both LIGO detectors within 10 ms are considered. In the case of GW150914 the time delay was 6.9 ms. The signal was observed over approximately 0.2 s, see Figure 97.

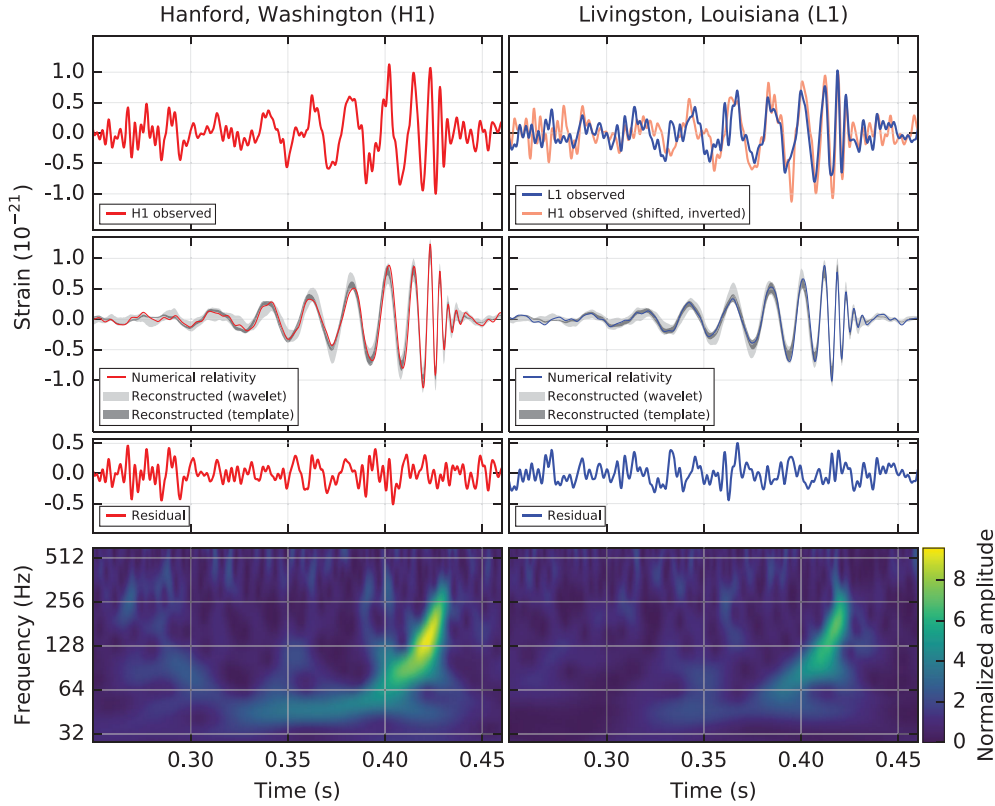


Figure 97: GW150914b

In the first row of this figure, the signals are shown as they were received at Hanford (red) and Livingston (blue). The only manipulation is that frequencies outside of the sensitivity window of the LIGO detectors were filtered away. On the right the Hanford signal is shifted, to account for the time delay, and inverted, because one detector is rotated with respect to the other by 90° . The observed signals were then compared to theoretically calculated wave-forms. Theorists have provided a collection of such wave-forms, for merging black holes and merging neutron stars with a large variety of parameters. The second row of Figure 97 shows the template that fits the observations best. It is a merger of two black holes with masses parameters given in Figure 98. Three phases are to be distinguished: The inspiral (which is periodic with an increasing amplitude), the merger (where the amplitude reaches its maximum) and the ringdown (where the amplitude strongly drops and the system becomes stationary again). The third row of Figure 97 shows the difference between the first and the second row which is to be interpreted as noise. Note that the ringdown is essentially drowned in the noise. As the difference between a merger of black holes (two horizons) and a merger of neutron stars (two surfaces) is significant only in the ringdown phase, one cannot really conclude from the observed wave-form that it is a black-hole merger. The assuredness that this event was indeed a black-hole merger comes mainly from the masses involved which are much too high for neutron stars. The last row in Figure 97 shows the increase in frequency from about 50 Hz to about 250 Hz, i.e., the “chirp”.

From Figure 97 we read that the amplitude of the strain was not more than 10^{-21} . As the armlength of the LIGO detectors is 4 km, this means that the distance between the beam splitter and one of the mirrors changed by approximately 4×10^{-18} m which corresponds to a few thousandths of a proton diameter. Of course, it is totally impossible to measure a *distance* with such an accuracy. However, as demonstrated by the LIGO detectors, it is possible to measure *changes* of a distance with such an accuracy.

Primary black hole mass	$36^{+5}_{-4} M_{\odot}$
Secondary black hole mass	$29^{+4}_{-4} M_{\odot}$
Final black hole mass	$62^{+4}_{-4} M_{\odot}$
Final black hole spin	$0.67^{+0.05}_{-0.07}$
Luminosity distance	410^{+160}_{-180} Mpc
Source redshift z	$0.09^{+0.03}_{-0.04}$

Figure 98: GW150914

The location of the source in the sky is largely unknown: With only two detectors one can locate the source only to within an area that is as big as the constellation Orion. The location is in the Southern sky, i.e., the signal travelled through the body of the Earth, practically without being affected. The more gravitational wave detectors come online, the better the position of a source can be determined by way of triangulation. From Figure 98 we read that the merger took place far outside of our Galaxy, about 1.2×10^9 years ago. The equivalent of 3 Solar masses was converted into gravitational wave energy within less than a second. This corresponds to a radiated power that is more than the power radiated as electromagnetic waves by all visible sources in the Universe.

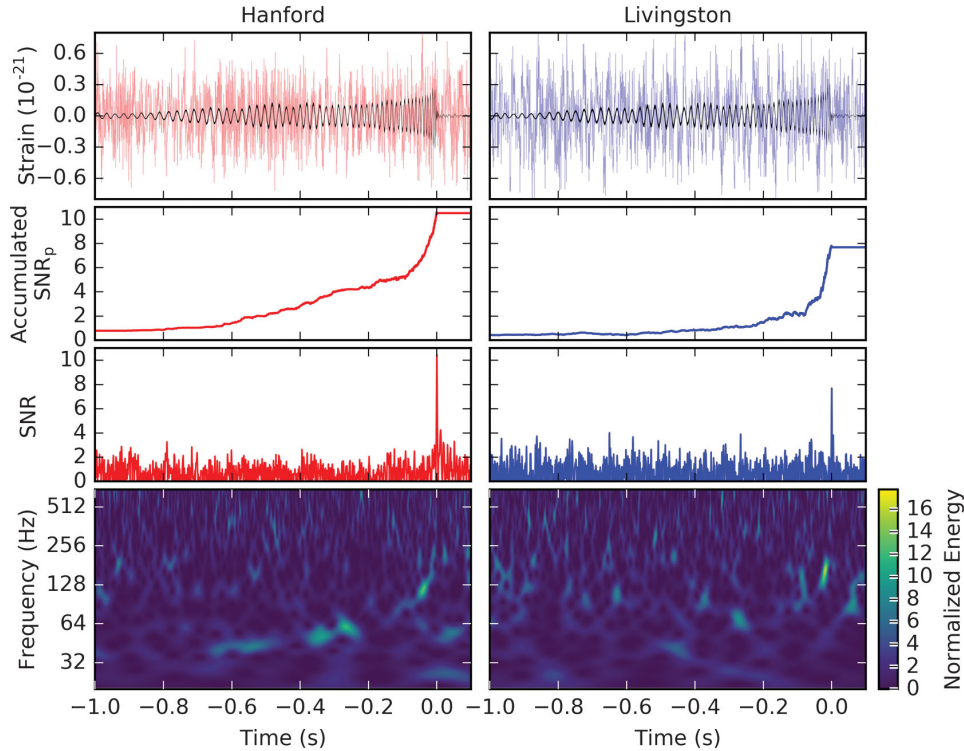


Figure 99: GW151226

Another gravitational wave event was observed on 26 December (Boxing Day) 2015, see B. Abbott et al., Phys. Rev. Lett. 116, 241103 (2016). The inspiral took longer than for the first event which indicates that the masses involved were smaller. The signal-to-noise ratio (SNR) was smaller than in the first event, because the event was farther away. Apart from these differences, the Boxing Day Event GW151226 was similar to GW150914, see Figures 99 and 100.

Primary black hole mass	$14.2^{+8.3}_{-3.7} M_{\odot}$
Secondary black hole mass	$7.5^{+2.3}_{-2.3} M_{\odot}$
Chirp mass	$8.9^{+0.3}_{-0.3} M_{\odot}$
Total black hole mass	$21.8^{+5.9}_{-1.7} M_{\odot}$
Final black hole mass	$20.8^{+6.1}_{-1.7} M_{\odot}$
Radiated gravitational-wave energy	$1.0^{+0.1}_{-0.2} M_{\odot} c^2$
Peak luminosity	$3.3^{+0.8}_{-1.6} \times 10^{56} \text{ erg/s}$
Final black hole spin	$0.74^{+0.06}_{-0.06}$
Luminosity distance	$440^{+180}_{-190} \text{ Mpc}$
Source redshift z	$0.09^{+0.03}_{-0.04}$

Figure 100: GW151226

The first Science Run, O1, of the LIGO detectors terminated in January 2016. A third event, that had been observed in October 2015, was very close to the noise level so the LIGO team hesitated for a while to give it a GW number, but finally it was included in the list. So O1 ended with three gravitational wave observations. All three of them were interpreted as black-hole mergers. The masses involved, in particular in the first event, were surprisingly high. Before the LIGO observations most people had believed that stellar black holes could not be heavier than 25 or at most 30 Solar masses.

The second Science Run, O2, made 8 detections between 30 November 2016 and 25 August 2017. During part of this time also Virgo was online which allowed a better localisation of the sources in the sky. Whereas 7 of the events were black-hole mergers, similar to the ones already known, the 8th one, GW170817, was very different and of particular interest, see B. Abbott et al., Phys. Rev. Lett. 119, 161101 (2017). Firstly, it lasted much longer than the preceding events, indicating that the masses involved were smaller. Secondly, and even more importantly, for the first time electromagnetic counter-parts were observed.

At the time when the signal came in not only the two LIGO detectors but also Virgo was online. However, the signal was so weak that Virgo hardly saw it, see Figure 101. Therefore, the Virgo observations were not used for the determination of the wave-form. However, although very weak the Virgo observation could be used for locating the source in the sky, see the dark green banana in Figure 102.

About 2 s after the merger, a weak gamma-ray burst was detected, see Figure 103. This observation was made with the satellites Fermi and INTEGRAL which allow a very precise localisation in time but only a rather rough localisation on the sky. In any case, with the Gamma-ray Burst Monitor (GBM) on board the Fermi satellite the location could be limited to a certain region (blue disc in Figure 102) which overlaps with the region from where the gravitational-wave signal came (dark green banana in Figure 102).

What is more, a so-called kilonova was observed, first in the optical, in a picture taken 10.9 hours after the gravitational-wave event, then also in the infrared, in the X-ray and in the radio. It faded away after a few weeks. A kilonova is a “new star”, i.e., a star that was not seen before, with an absolute luminosity higher than an ordinary nova but not so high as a supernova. The position of this kilonova could of course be determined with high precision, see again Figure 102; the observations are compatible with the assumption that both the gravitational-wave signal and the gamma-ray burst came from the same spot in the sky where the kilonova was seen. Also, the distance of the host galaxy of the kilonova is in agreement with the distance of the gravitational-wave source (about 40 Mpc). Of course, this is no proof that they are all related to the same physical event, but it is a strong suggestion. The idea is that this event was a merger of two neutron stars, one with a mass between 1.36 and 2.26 M_{\odot} , the other one with a mass between 0.86 and 1.36 M_{\odot} .

In contrast to two black holes, where the two horizons merge rather softly, the merger of two neutron stars with surfaces is believed to be a much more violent process, accompanied by the emission of hard electromagnetic radiation in the form of a gamma-ray burst.

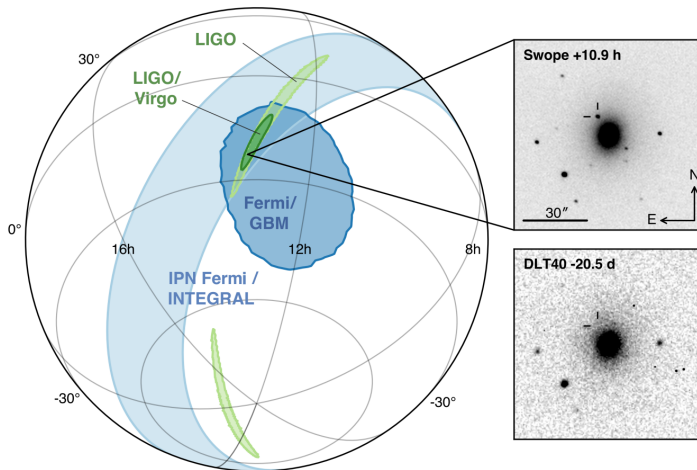


Figure 102: GW170817

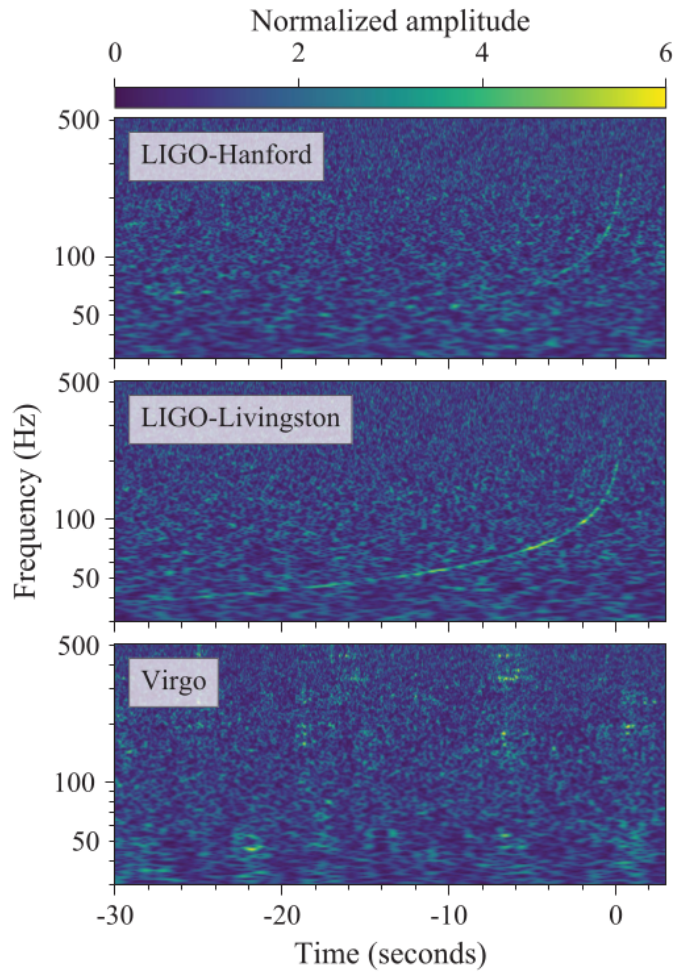


Figure 101: GW170817

As the product of the merger a heavy neutron star is formed which very soon becomes unstable and collapses to a black hole, blowing off a shell of matter in what was seen as the kilonova. It is believed that during this process about 16,000 times the mass of the Earth in heavy elements has been formed, including approximately ten Earth masses just of the two elements gold and platinum.

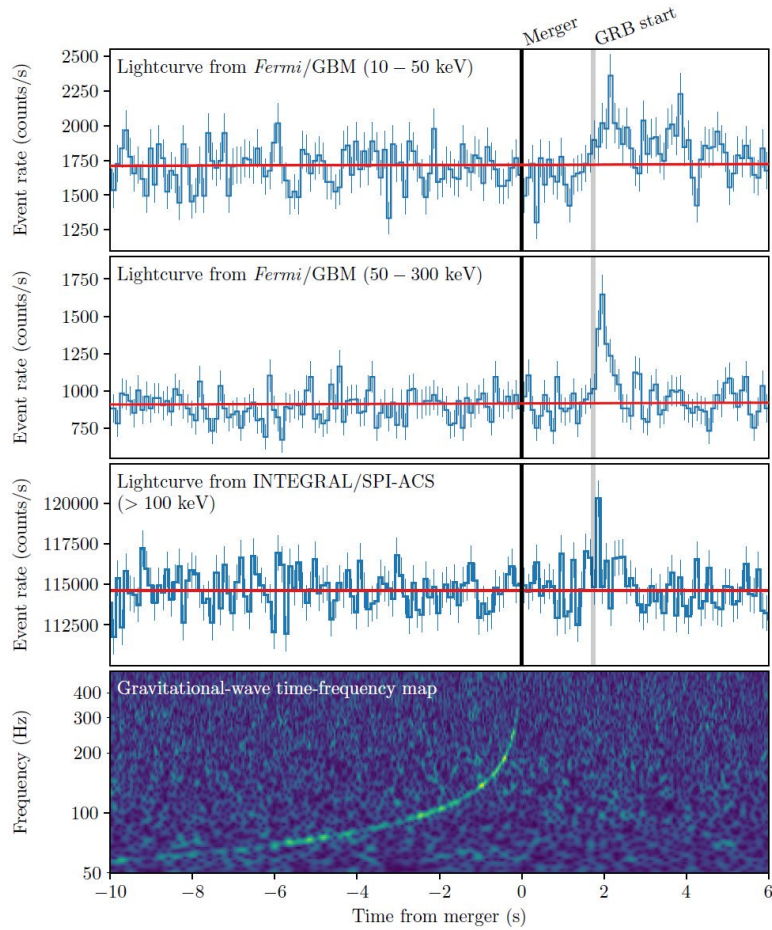


Figure 103: GW170817

The paper on these multi-messenger observations, B. Abbott et al., *Astrophys. J.* 848, L12 (2017), has almost 4000 authors (roughly one third of the astrophysics community) from more than 900 institutions.

Between April 2019 and March 2020, the third Science Run, O3, brought about 33 events that were interpreted as binary black-hole mergers, 5 events that were interpreted as binary neutron-star mergers, and 5 events that were interpreted as mergers of a neutron star with a black hole, together with a few more events where the interpretation is still under debate. One of the black-hole mergers is of particular interest because the resulting black hole had a mass of more than 140 Solar masses, which raises the question of whether this is already an intermediary black hole, rather than a stellar black hole. In one of the binary neutron-star mergers the model parameters suggested that an object with 3.4 Solar masses was formed. As there was no electromagnetic counterpart, i.e., no gamma-ray burst and no kilonova, and as neutron stars of 3.4 Solar masses are not believed to exist, this might suggest that the two neutron stars directly formed a black hole (or that one of the progenitors was actually not a neutron star but a black hole). This observation is still under investigation.

The next Science Run, with both LIGO detectors, Virgo and KAGRA online, will certainly bring many more interesting observations and new insight into the physics of black holes and neutron stars. It is believed that soon the observation of multi-messenger events will become routine, opening a new era of astronomy.